Technische Universität Braunschweig

Metabolic characterisation of the nutritional versatile marine bacterium *Phaeobacter inhibens* DSM 17395 via gas chromatography – mass spectrometry

Von der Fakultät für Lebenswissenschaften

der Technischen Universität Carolo Wilhelmina zu Braunschweig

zur Erlangung des Grades eines

Doktors der Naturwissenschaften

(Dr. rer. nat.)

genehmigte

D i s s e r t a t i o n

von Michael Hensler
aus Lüdenscheid

1. Referent: Professor Dr. Dietmar Schomburg
2. Referent: Professor Dr. Ralf Rabus
3. Referent: Professor Dr. Dieter Jahn
eingereicht am: 24.11.2014
mündliche Prüfung (Disputation) am: 05.03.2015

Druckjahr 2015

Vorveröffentlichungen der Dissertation

Teilergebnisse aus dieser Arbeit wurden mit Genehmigung der Fakultät für Lebenswissenschaften, vertreten durch den Mentor der Arbeit, in folgenden Beiträgen vorab veröffentlicht:

Publikationen

Zech, H., Hensler, M., Koßmehl, S., Drüppel, K., Wöhlbrand, L., Trautwein, K. Hulsch, R., Maschmann, U., Colby, T., Schmidt, J., Reinhardt, R., Schmidt-Hohagen, K., Schomburg, D., Rabus, R. (2013). Adaptation of *Phaeobacter inhibens* DSM 17395 to growth with complex nutrients. *PROTEOMICS* 13, 2851-2868.

Zech, H., Hensler, M., Koßmehl, S., Drüppel, K., Wöhlbrand, L., Trautwein, K., Colby, T., Schmidt, J., Reinhardt, R., Schmidt-Hohagen, K., Schomburg, D., Rabus, R. (2013). Dynamics of amino acid utilization in *Phaeobacter inhibens* DSM 17395. *PROTEOMICS* 13, 2869-2885.

Drüppel, K., Hensler, M., Trautwein, K., Koßmehl, S., Wöhlbrand, L. Schmidt-Hohagen, K., Ulbrich, M., Bergen, N., Meier-Kolthoff, J.P., Göker, M., Klenk, H.P., Schomburg, D., Rabus, R. (2014). Pathways and substrate-specific regulation of amino acid degradation in *Phaeobacter inhibens* DSM 17395 (archetype of the marine *Roseobacter* clade). *Environ. Microbiol.* 16, 218-238.

Wiegmann, K., Hensler M., Wöhlbrand, L., Ulbrich, M., Schomburg, D., Rabus, R. (2014). Carbohydrate Catabolism in *Phaeobacter inhibens* DSM 17395, Member of the Marine *Roseobacter* Clade. *Appl. Environ. Microbiol.* 80, 4725-4737.

Tagungsbeiträge (Vorträge)

Hensler, M., Bill, N., Rex, R. (2011). Metabolome analysis and modelling of the metabolisms of *Dinoroseobacter shibae* and *Phaeobacter gallaeciensis.* 3. Statusseminar des SFB TRR 51, 12. – 13.05.2011, Delmenhorst.

Hensler, M. (2013). Adaptation of *Phaeobacter inhibens* DSM 17395 to nutrient conditions in marine environments. International Symposium of SFB TRR 51, 24. – 26.06.2013, Delmenhorst.

Wiegmann, K., Hensler, M. (2014). Carbohydrate catabolism in *Phaeobacter inhibens* DSM 17395 – Proteomic and Metabolomic analyses. 8. Statusseminar des SFB TRR 51, 08. – 09.05.2014, Oldenburg.

Posterbeiträge

Hensler, M., Zech, H., Koßmehl, S., Drüppel, K., Wöhlbrand, L., Trautwein, K., Schmidt-Hohagen, K., Rabus, R., Schomburg, D. (2013). Dynamics of amino acid utilization by *Phaeobacter gallaeciensis* DSM 17395. Internationale Konferenz der VAAM, 10. – 13.03.2013, Bremen.

Hensler, M., Zech, H., Drüppel, K., Koßmehl, S., Wöhlbrand, L., Trautwein, K., Schmidt-Hohagen, K., Rabus, R., Schomburg, D. (2013). Metabolic and proteomic adaptations of *Phaeobacter inhibens* DSM 17395 to nutrient conditions in marine environment. Metabolomics 2013 – 9th Annual Conference of the Metabolomics Society, 01. – 04.07.2013, Glasgow, United Kingdom.

Hensler, M., Wiegmann, K., Zech, H., Koßmehl, S., Rabus, R., Schomburg, D. (2014). The metabolism of the marine all-rounder *Phaeobacter inhibens* DSM 17395. Trends in Metabolomics – Analytics and Applications. 03. – 05.06.2014, Frankfurt am Main.

Table of Contents

List of figures

List of tables

Abbreviations

Abbreviation	Explanation
2D DIGE	Two-dimensional difference gel electrophoresis
ABC transporter	ATP-binding cassette transporter
ATP	Adenosine-5'-triphosphate
CIP	Collection Institute Pasteur (Paris, France)
CoA	Coenzyme A
DOM	Dissolved organic matter
DSMZ	German Collection for Microorganisms and Cell Cultures (Braunschweig, Germany)
e.g.	Latin: *exempli gratia*, for example
ESI	Electrospray ionisation
et al.	Latin: *et alii*, and others
GC	Gas chromatography
GM medium	Glucose-containing minimal medium
i.e.	Latin: *id est*, that is
ICBM	Institute for Chemistry and Biology of the Marine Environment (Carl von Ossietzky Universität Oldenburg, Germany)
kb, kbp	kilobasepairs
LC	Liquid chromatography
m/z	Mass to charge ratio
MALDI	Matrix assisted laser desorption/ionisation
MB medium	Marine Broth medium
MS	Mass spectrometry
MSTFA	*N*-methyl-*N*-(trimethylsilyl)-trifluoro-acetamide
NAD^+/NADH	Nicotinamide adenine dinucleotide (*oxidised/reduced*)
$NADP^+$/NADPH	Nicotinamide adenine dinucleotide phosphate (*oxidised/reduced*)
$OD_{600\ nm}$	Optical density, measured at 600 nm
OD_{max}	Maximal optical density, measured at 600 nm
PHB	Poly-(*R*)-3-hydroxybutanoate
RI	Retention index
rpm	Rotations per minute
SDS-PAGE	Sodiumdodecylsulfate-polyacrylamide gel electrophoresis
TCA cycle	Tricarboxylic acid cycle, also known as citrate cycle
TMS	Trimethylsilyl

Abbreviation	Explanation
TOF	Time of flight
TRAP transporter	Tripartite ATP-independent periplasmic transporter
t_0, t_{10}, t_{20}, ...	Sampling point, subscript number represents cultivation time in hours.
v/v	Volume per volume
w/v	Weight per volume
× *g*	×-fold acceleration
μ_{max}	maximal specific growth rate

Furthermore, units were abbreviated according to the international unit system (SI, Systéme international d'unités), except for molar concentrations (mol/l), which were abbreviated with the capital letter M. Chemical elements were abbreviated by their symbols of the periodic table of elements.

Summary

Heterotrophic marine bacteria are challenged by versatile and dynamic nutrient conditions, which fluctuate seasonally, as a result of bloom and collapse of algae populations. Due to such conditions, the Roseobacter clade is one of the most abundant and metabolically active bacteria clades in marine environments.

In this thesis, mainly GC-MS-based metabolomic analyses were applied to study how the metabolism of *Phaeobacter inhibens* DSM 17395 is adapted to the nutrient conditions in marine habitats. Collected data were statistically evaluated and interpreted in the context of collaborative performed complementary analyses.

Phenotypic microarray analysis revealed a broad substrate range for carbon and nitrogen sources. Accordingly, cultivation in complex medium led to depletion of most of the provided substrates. Under these cultivation conditions, high abundance of catabolic enzymes and the corresponding intermediates were observed, which revealed simultaneous utilisation of different substrates, especially amino acids. To analyse their utilisation in a detailed study, a defined casamino acid medium was used for a time-dynamic resolution. Although different amino acids were utilised simultaneously, a specific uptake preference was observed. Further, even though sufficient amino acids were still available, cells entered stationary phase. In contrast to this, strains cured from the 262 kbp plasmid showed enhanced growth. Thus, either regulatory factors or the tropodithietic acid biosynthesis, which are encoded on this plasmid, are responsible for growth inhibition.

Based on the original genome annotation, some amino acid (Phe, Lys, His, Met, Leu, Ile, Val, Thr and Trp) and carbohydrate degradation pathways (*N*-acetyl-glucosamine, mannitol, sucrose and xylose) remained unclear. Metabolomic and proteomic analyses, which were conducted in this study, allowed reconstruction of these pathways. Further, these analyses showed that *P. inhibens* DSM 17395 is well adapted to catabolise efficiently single substrates. But replenishment of the TCA cycle for anabolism lacked efficiency, because of usage of the complex ethylmalonyl-CoA pathway. This pathway is widely distributed in the Roseobacter clade and could completely be reconstructed by proteomic and LC-MS-based coenzyme A analysis.

Overall, this thesis revealed many new metabolic features, which explain the adaptation of *P. inhibens* DSM 17395 to marine habitats and improve our understanding of marine bacteria.

Zusammenfassung

Heterotrophe Meeresbakterien müssen vielseitige und dynamische Nährstoffbedingungen bewältigen, die jahreszeitlichen Veränderungen unterliegen, infolge von Blühen und Zusammenbruch von Algenpopulationen. Aufgrund solcher Bedingungen ist die Roseobacter Klade eine der zahlreichsten und metabolisch aktivsten Bakteriengruppen im Meer.

In dieser Arbeit wurde hauptsächlich mittels GC-MS-basierten Metabolomanalysen untersucht, wie der Stoffwechsel von *Phaeobacter inhibens* DSM 17395 an Nährstoffbedingungen in marinen Lebensräumen angepasst ist. Die erhaltenen Daten wurden statistisch ausgewertet und im Kontext von kollaborativ durchgeführten ergänzenden Analysen interpretiert.

Mittels phänotypischer Microarray Analysen wurde ein breites Substrat Spektrum für Kohlenstoff- und Stickstoffquellen festgestellt. Daher führte die Kultivierung im Komplexmedium auch zum Verbrauch der meisten Substrate. Die Fülle an detektierten katabolischen Enzymen und entsprechenden Intermediaten unter diesen Bedingungen zeigte eine gleichzeitige Verwertung verschiedener Substrate, insbesondere von Aminosäuren. Um deren Verwertung genauer zu untersuchen, wurde ein definiertes Medium mit Casaminosäuren für eine Zeit-dynamische Auflösung verwendet. Obwohl verschiedene Aminosäuren gleichzeitig verwendet wurden, wurde eine spezifische Aufnahmepräferenz beobachtet. Trotz noch ausreichend verfügbaren Aminosäuren, traten die Zellen in die stationäre Phase ein. Im Gegensatz dazu wurde bei Stämmen, denen das 262 kbp Plasmid entfernt wurde, erhöhtes Wachstum festgestellt. Daher sind entweder regulatorische Faktoren oder die Biosynthese der Tropodithiensäure, die auf diesem Plasmid kodiert sind, verantwortlich für die Wachstumshemmung.

Basierend auf der Original Genomannotation, blieben einige Aminosäure- (Phe, Lys, His, Met, Leu, Ile, Val, Thr und Trp) und Kohlenhydratabbauwege (*N*-acetyl-glucosamin, Mannitol, Sucrose und Xylose) unklar. Mithilfe von metabolomischen und proteomischen Analysen konnten diese Abbauwege rekonstruiert werden. Weiterhin konnte dabei gezeigt werden, dass *P. inhibens* DSM 17395 gut angepasst ist um individuelle Substrate effizient abzubauen. Allerdings wurde der Citratzyklus für anabolische Zwecke nicht effizient nachgefüllt, wegen der Verwendung des aufwendigen Ethylmalonyl-CoA Stoffwechselwegs. Dieser Stoffwechselweg ist weitverbreitet in der Roseobacter Klade und konnte durch proteomische und LC-MS basierte Coenzym A Analysen rekonstruiert werden.

Insgesamt wurden in dieser Arbeit viele neue metabolische Besonderheiten aufgedeckt, die die Anpassung von *P. inhibens* DSM 17395 an marine Lebensräume erklären und unser Verständnis von Meeresbakterien erweitern.

1 Introduction

1.1 Marine environment as habitat (for bacteria)

The marine environment is the largest and one of the most important ecosystems on earth; it comprises an area of about 3.6×10^8 km^2, which corresponds to more than ⅔ of earth's surface and 97% of available water on earth. Therefore, it contributes to global climate and plays an important role as source for human nutrition. Presently, 239000 different species are known inhabiting this ecosystem; amongst these are 208000 animals, 7600 plants, 1000 different fungi and 1700 bacterial species. Their absolute number, especially for bacteria species, is considerably underestimated (Appeltans *et al.*, 2012). Current estimations assume about 3.6×10^{29} bacterial cells, inhabiting all kinds of different marine environments (Whitman *et al.*, 1998).

These habitats are differentiated first by their distance to coastal regions, second by vertical axis (i.e. sea layers), and third by latitude (e.g. tropic, temperate or polar regions). This results in extreme differences, in regard to temperature, light, pressure, pH, nutrient content and concentration of essential trace elements. However; bacteria are quite adaptive and thus have specialised to the various marine environments. Marine microbial communities are very diverse and complex, showing regional diversity and seasonal dynamics in their composition (Ladau *et al.*, 2013; Sintes *et al.*, 2013; Sogin *et al.*, 2006). Due to high numbers and metabolic activity, marine bacteria contribute to the conversion of dissolved organic matter, and play a major ecological role. Further, secondary metabolites produced by marine bacteria are of particular interest, e.g. as antibiotics or functional foods (Dewapriya and Kim, 2014; Eom *et al.*, 2013; Imhoff *et al.*, 2011). Marine bacteria are also regarded as potential candidates for bioremediation, because of their genetic versatility and adaptivity (Dash *et al.*, 2013).

1.1.1 Characteristics of seawater

Seawater comprises high varieties of physical and chemical parameters, which can be challenging for bacteria. One of the main difficulties for bacteria is the high salinity of seawater, which is in average about 3.5% (w/v), with major regional and monthly

variations on the surface (Maes and O'Kane, 2014; Reul *et al.*, 2014; Subrahmanyam *et al.*, 2013). As protection against osmotic stress, bacteria either accumulate ions (e.g. potassium ions) or compatible solutes, including distinct amino acids (especially glutamate or alanine), sugars (e.g. trehalose), or carboxylates (e.g. ectoine) (Costa *et al.*, 1998). These compatible solutes can interact with protein surfaces and stabilise them. However, such mechanisms are extremely energy-demanding (Vauclare *et al.*, 2014). Seawater is slightly alkaline, with a pH range from about 7.7 to 8.6, in average about 8 in the upper sea layer (0 to 15 m depth). Still, pH can fluctuate daily up to 0.1, and even up to 0.5 in a larger time scale (Duarte *et al.*, 2013). The solubility of organic and inorganic compounds, including trace elements, is influenced by salinity, pH and temperature and thus affects directly the primary production, which is limited to the euphotic zone, i.e. the upper 200 m of the water column. Beneath that zone, light for photosynthesis is not available.

The three most important elements for primary production are nitrogen, phosphor and iron. In oceans, gaseous N_2 is fixed by selected heterotrophic bacteria, or cyanobacteria, especially by cyanobacterium *Trichodesmium* spp. (Karl *et al.*, 1997). The resulting product, nitrate (NO_3^-) is the main inorganic nitrogen source for phytoplankton and bacterioplankton in upper sea layers, whereas ammonium (NH_4^+) is strongly limited and more abundant in deep sea layers; the nitrogen cycle in the ocean is simplified in figure 1.

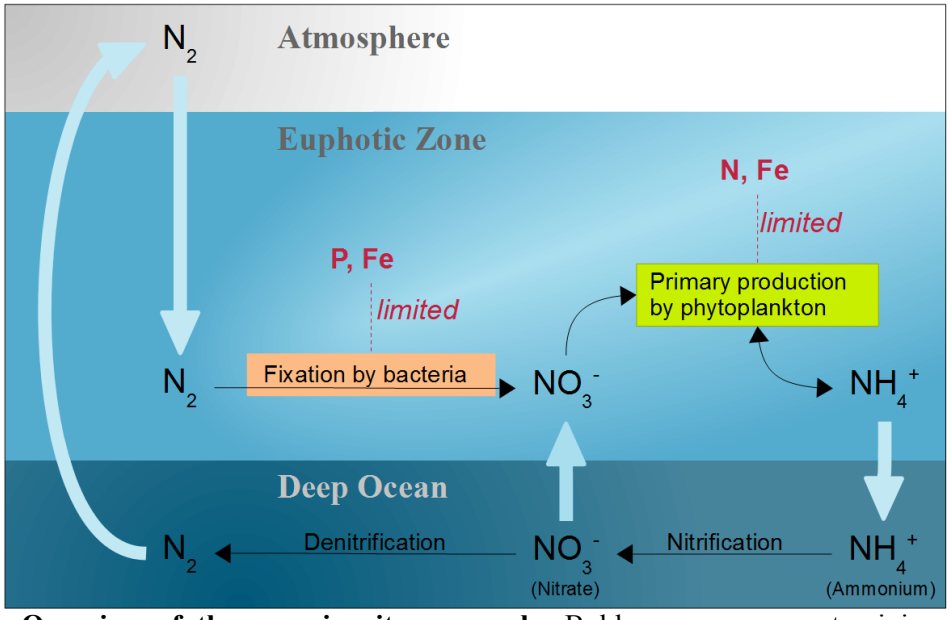

Figure 1: Overview of the oceanic nitrogen cycle. Bold arrows represent mixing of water columns. Nitrogen fixation is mainly limited by low phosphor and iron concentrations; the primary production is limited by nitrogen and iron. Figure was adapted from Gruber and Galloway (2008).

The overall N:P molar ratio for organic matter production in algae is about 16:1 (Karl *et al.*, 1997), indicating higher relevance of nitrogen. But, as phosphor cannot be fixed from atmosphere sources and enters the ocean mainly by rivers, oceanic phosphor concentrations are significantly lower than nitrogen and thus are strongly limited (Tyrrell, 1999). As Mills *et al.* (2004) have shown, primary productivity is nitrogen limited; whereas N_2-fixation is co-limited by iron and phosphor. Iron as a key element for many molecular processes is essential for phytoplankton growth and production of biomass, serving as carbon source for heterotrophs (Sunda and Huntsman, 1997). Photosynthesis is only possible in the euphotic zone. This is why this zone is inhabited by cyanobacteria and algae and is generally rich in nutrients. Organisms inhabiting deeper sea layers have to generate energy from dead cell material, that sank from upper sea layers, and have to sustain higher pressure.

Further, bacterial growth is dependent on temperature (Apple *et al.*, 2006; Kirchman *et al.*, 2009; Nedwell, 1999). In most cases, there is a positive correlation between temperature and bacterial growth. However, also factors like substrate availability have an influence on bacterial growth. Especially the uptake of inorganic compounds is dependent on temperature. For instance, there is a strongly reduced uptake of nitrate at lower temperatures in algae and bacteria, resulting in a preference for ammonium, despite lower concentrations of ammonium compared to nitrate (Reay *et al.*, 1999).

1.1.2 Dissolved organic matter

Besides chemical and physical conditions of seawater, heterotrophic marine bacteria are mainly challenged by complex and changing nutrient conditions. Although sometimes high amounts of dissolved organic matter (DOM) are available, its utilisation is difficult because of chemical diversity, low concentration of individual compounds and seasonal fluctuations during bloom and collapse of algae populations. DOM represents a major pool of organic matter in the oceanic and global carbon cycle, which is summarised in figure 2. The amount of marine DOM of (at least) 700×10^{15} g carbon corresponds roughly to the amount of atmospheric CO_2, which is 750×10^{15} g carbon (Koch *et al.*, 2005). It comprises a broad variety of molecules, ranging from simple amino acids, lipids and sugars to larger polysaccharides, proteins and complex polymers. Due to the complexity of DOM, its

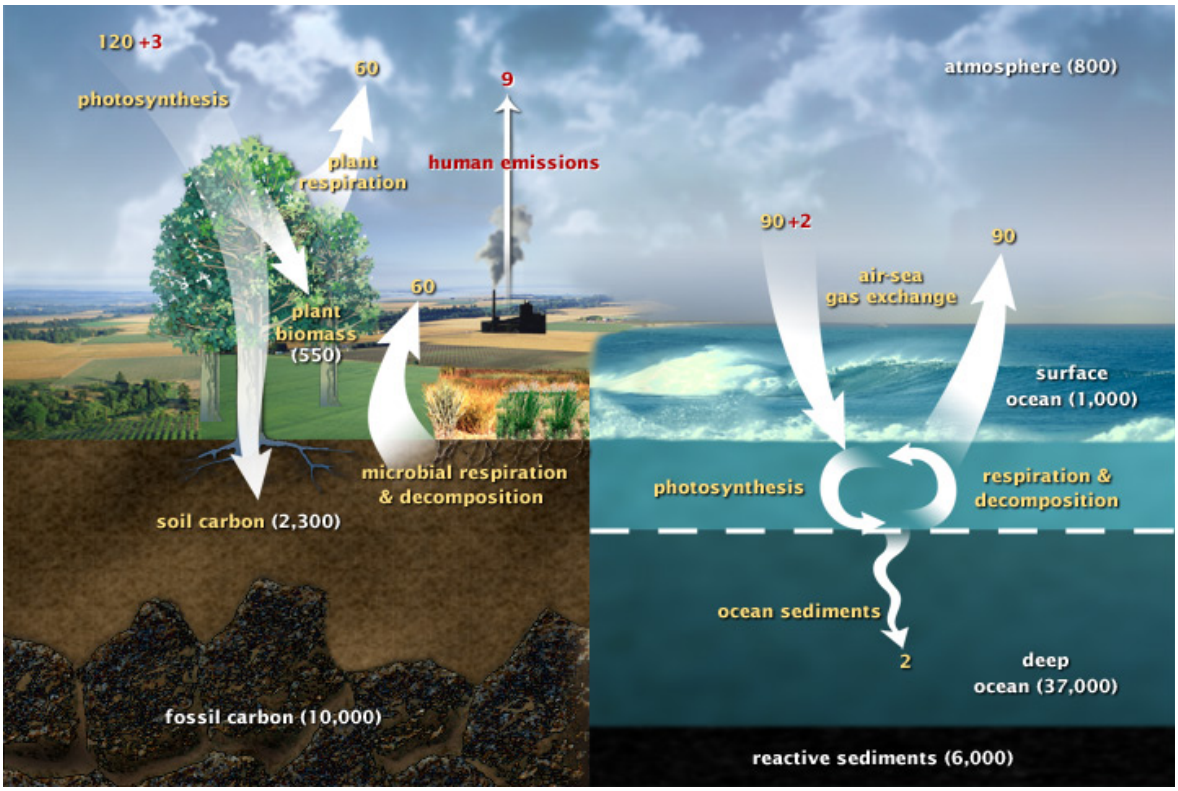

Figure 2: Overview of the global carbon cycle. Movement of carbon is represented by arrows; yellow numbers are natural fluxes, red are human impact and white numbers indicate stored carbon, readings in gigatons (= 10^9 t = 10^{15} g) per year. Source of this figure: National Aeronautics and Space Administration (NASA): http://earthobservatory.nasa.gov/Features/CarbonCycle/

molecular structure currently remains unclear, as established molecular approaches for characterisation only target operationally-defined subunits (Dittmar and Paeng, 2009). The molecular size comprises a broad range from 100 to 100 000 Da, mostly smaller than 2000 Da. This corresponds to a broad variability of chemical characteristics, already in respect to potential molecular elemental composition.

Although only a small fraction (< 5%) of marine DOM is considered to be terrestrial origin, which can be provided by rivers at estuaries, comparison of marine DOM with terrestrial DOM showed large similarity regarding molecular elemental composition (Koch *et al.*, 2005). Most of marine DOM is produced by photosynthetic plankton in the euphotic zone of the ocean and is either released actively or via natural decay after death, before it can serve as source for carbon, nitrogen and phosphor (Hansell *et al.*, 2009; Nebbioso and Piccolo, 2013). Within hours or days, released DOM can be converted by bacteria, whereas a small fraction remains non-degraded. It is unclear whether this refractory DOM is formed within months or whether it is comprised by released fossil compounds. Extreme conditions in the deep sea, such as geothermal heat and elevated pressure might catalyse

chemical reactions that result in the formation of polycyclic aromatic compounds resistant to biodegradation (Dittmar and Paeng, 2009).

1.1.3 Seasonal and regional variations of dissolved organic matter

Both oceanic streams and transportation of organic matter by organisms contribute to horizontal and vertical distribution of dissolved organic matter (DOM) within the ocean. Generally, warmer regions (e.g. the Mediterranean Sea or tropic regions) comprise higher concentrations of about 70 to 80 µM dissolved organic carbon, compared to polar regions with about 40 to 50 µM dissolved organic carbon (Hansell *et al.*, 2009). Quantitative data in publications of the last decade differ, depending on sampling time, sampling location, sampling method and analytical approaches (Pettine *et al.*, 2001).

Higher temperatures in summer favour growth of phytoplankton, resulting in seasonal algae blooms that can be observed in coastal and oceanic regions. Thus, DOM concentration fluctuates with the seasons, reaching higher concentrations in summer than in winter. Furthermore, the composition of DOM may also change, even during an algae bloom, as shown e.g. by Ittekkot (1982). The concentration of dissolved sugars remained relatively constant during bloom, about 320 to 410 µg/l, whereas concentration of dissolved amino acids decreased from 350 µg/l in the early stages of bloom, to less than 150 µg/l towards the end of bloom (Ittekkot, 1982). However; the higher amount of DOM in the summer is not only a result of algae bloom. Especially in coastal regions there is a higher input of organic compounds through rivers. Further, inability of bacteria to consume all of the produced compounds keeps the amount of DOM temporarily on those high levels (Pettine *et al.*, 1999, 2001).

The most abundant small compounds utilisable by bacteria are carbohydrates and amino acids, in which the concentrations of carbohydrates are 10 to 20-fold higher than those of amino acids. Most dominant during algae blooms are glucose, fructose, galactose, mannose and xylose, plus particular amino acids, like glutamate, serine, glycine, histidine, aspartate, threonine and lysine (Ittekkot, 1982; Pettine *et al.*, 1999). However, as Sarmento *et al.* (2013) have shown, the released amino acids differ strongly depending on algae species.

1.2 The Roseobacter clade and Phaeobacter inhibens

1.2.1 The Roseobacter clade

The marine ecosystem comprises many different bacterial clades, some which only inhabit very specific environments, others which are more globally distributed, like Cyanobacteria, Planctobacteria, marine Actinobacteria, Bacteroidetes and Proteobacteria (Giovannoni and Stingl, 2005). Amongst the latter, the Roseobacter clade, which comprises a high variability of physiologically diverse isolates (Brinkhoff *et al.*, 2008), is one of the most abundant and worldwide distributed heterotrophic bacterial groups. Its members are classified as *Alphaproteobacteria*, belonging to the family of *Rhodobacteraceae* and were first described by Shiba in 1991. The name Roseobacter refers to the pink photosynthesis carotenoids of the first isolates of this clade.

Members of the Roseobacter clade are physiologically versatile, inhabiting a broad range of marine environments. Besides coastal regions, members of the Roseobacter clade could be isolated from temperate and polar regions, sediments, macroalgae and invertebrates (Wagner-Döbler and Biebl, 2006; Brinkhoff *et al.*, 2008). This also correlates to the metabolic versatility of the Roseobacter clade, comprising denitrifying species, like *Roseobacter denitrificans*, or strains which can produce bacteriochlorophyl α, like *Dinoroseobacter shibae* and *Janaschia* spp. This bacteriochlorophyl capacitates to perform aerobic anoxygenic photosynthesis, which produces energy without synthesis of organic carbon, and thus can be useful in case of nutrient shortage. Others, e.g. *Oceanibulbus indolifex* or *Phaeobacter* spp. produce antibiotics (Wagner-Döbler *et al.*, 2004; Brinkhoff *et al.*, 2004). Other important compounds, produced by many members of the Roseobacter clade, are acylated homoserine lactones, which function as quorum sensing molecules and regulate many metabolic processes (Neumann *et al.*, 2013; Patzelt *et al.*, 2013; Zan *et al.*, 2014). Many of these metabolic features of the Roseobacter clade are encoded by genes located on extrachromosomal elements. Most members of the Roseobacter possess several plasmids, up to 12 different, as in case of *Marinovum algicola* DG 898 (Pradella *et al.*, 2010). As these plasmids contain ecologically relevant genes and can be transferred via horizontal gene-transfer, they might be a reason for the ecological and evolutionary success of the Roseobacter clade (Petersen *et al.*, 2013).

Despite their global distribution, members of the Roseobacter clade are not the only dominant and omnipresent bacterial groups in marine environments, but rather dominate distinct, but ecologically relevant niches. They are the most common primary surface-colonising bacterial group in temperate coastal waters. Potential surfaces range from stones or particles to algae, invertebrates or even animals. Surface colonisation can be beneficial, e.g. as a protection against adverse environments, or to enhance metabolic cooperation under nutrient-rich conditions, or to facilitate horizontal gene transfer (Dang *et al.*, 2007).

In regard to surface-colonisation, many members of the Roseobacter clade were isolated from algae, like *D. shibae* from *Prorocentrum lima* (Biebl *et al.*, 2005) or *P. inhibens* 2.10 from *Ulva australis* (Martens *et al.*, 2006). This indicates symbiotic lifestyle between members of the Roseobacter clade and phytoplankton, as described by Geng and Belas (2010a) and Seyedsayamdost *et al.* (2011). As a matter of fact, many microalgae cannot grow normally without bacterial symbionts; therefore bacterial colonisation might be beneficial, in which cases these symbiotic mechanism are not well understood. Antibiotics produced by members of the Roseobacter clade, e.g. tropodithietic acid, can suppress growth of potential parasites and produced auxins might enhance growth. In return, algae provide nutrients or vitamins (Rao *et al.*, 2007). Observations that the Roseobacter clade is the unique predominant subgroup in the decay-phytoplankton bloom period (Liu *et al.*, 2013) underlines this assumption. Furthermore, Alonso-Sáez and coworkers (2007) showed that the Roseobacter clade is not only one of the most abundant bacterial clade upon seasonal collapse of algae blooms, but also one of the most active (Alonso-Sáez *et al.*, 2007; Alonso-Sáez and Gasol, 2007). A possible explanation for these observations, could be the metabolic and nutritional versatility of the Roseobacter clade, which favours growth under nutrient-rich conditions, like seasonal bloom periods of phytoplankton. Thus, this clade also contributes strongly to conversion of organic matter and to the marine carbon cycle. Particular members of the Roseobacter clade, e.g. *Silicibacter pomeroyi* might also play an important role for sulfur cycling in the ocean by degrading the algal osmolyte 3-dimethylsulfoniopropanoate, yielding dimethylsulfide and other carbon and sulfur compounds (Wagner-Döbler and Biebl, 2006).

The number of isolates and sequenced genomes of the Roseobacter clade is continuously growing, due to simple cultivation in the laboratory and due to their

ecological relevance. Currently, the Roseobacter clade comprises at least 54 described genera and 135 species reflecting physiological and genetic diversity of this bacterial clade (Breider *et al.*, 2014).

1.2.2 The genus Phaeobacter and the strain P. inhibens DSM 17395

Presently, the genus *Phaeobacter* comprises six species, which were isolated from different marine environments (Table 1). The first *Phaeobacter* strain was isolated 1998 from larval of the scallop *Pecten maximus*, in Galicia, Spain, and was first named *Roseobacter gallaeciensis* (Ruiz-Ponte *et al.*, 1998), which was 2006 reclassified as *Phaeobacter gallaeciensis* BS107 (Martens *et al.*, 2006). The name *Phaeobacter* was given because of the brown pigmentation, which is true for all *Phaeobacter*, except for *P. caeruleus*, which is blue pigmented (Vandecandelaere *et al.*, 2009). However this clustering is ambiguous, as shown recently through the analysis of genome-scale data and phenotypic characteristics. For this reason it was suggested that only *P. inhibens* and *P. gallaeciensis* compose the *Phaeobacter* cluster, and the others should be regrouped (Breider *et al.*, 2014).

Table 1: Available *Phaeobacter* isolates (as listed by the DSMZ).

Species	Comments	References
P. arcticus DSM 23566	From marine sediment, Arctic ocean.	(Zhang *et al.*, 2008)
P. caeruleus DSM 24564	From marine biofilm on stainless steel electrode, Italy, Genoa harbour. Bacteria form blue pigmented colonies.	(Vandecandelaere *et al.*, 2009)
P. daeponensis DSM 23529	From tidal flat sediment, Korea, Daepo Beach.	(Vandecandelaere *et al.*, 2008; Yoon *et al.*, 2007)
P. gallaeciensis DSM 26640 (= CIP 105210)	From larval cultures of scallop *Pecten maximus*, Spain, Galicia. Deposited as *P. gallaeciensis* BS107.	(Martens *et al.*, 2006; Ruiz-Ponte *et al.*, 1998)
P. inhibens DSM 16374	From German Wadden Sea. Deposited as *P. inhibens* ^{T5}.	(Martens *et al.*, 2006)
P. inhibens DSM 17395	Alleged type strains, deposited as CIP 105210 and DSM 17395 are not identical.	(Martens *et al.*, 2006; Buddruhs *et al.*, 2013)
P. inhibens DSM 24588	From surface of green macroalga *Ulva australis*. Originally deposited as *P. gallaeciensis* 2.10.	(Martens *et al.*, 2006; Buddruhs *et al.*, 2013)
P. leonis DSM 25627	From marine sediment beneath the sea floor, France, Mediterranean Sea, Gulf of Lions.	(Gaboyer *et al.*, 2013)

Phaeobacter species are strictly aerobic and chemoheterotrophic bacteria that form ovoid rods and are motile by means of polar flagella. Generally, growth conditions of this genus comprise an NaCl concentration range from 0.01 to 1.5 M, a pH range from 6.0 to 9.5, and a temperature range from 4 to 37 °C. Although *Phaeobacter* is nitrate reductase, amylase, tweenase and gelatinase negative, it employs a broad range of substrates, ranging from amino acids, sugars and disaccharides to carboxylates (Martens *et al.*, 2006).

The strain used in this study, *P. inhibens* DSM 17395, was originally deposited as *P. gallaeciensis* DSM 17395, which should correspond to the *P. gallaeciensis* strain BS107 (= CIP 105210), as described by Ruiz-Ponte *et al.* (1998) and Martens *et al.* (2006). As recently shown, the alleged identical type strains are not identical in respect to genetic and phenotypic analyses. Whereas the type strain CIP 105210 corresponds most likely to the original *P. gallaeciensis* type strain BS107; strain DSM 17395 is closer related to *P. inhibens* DSM 16374 and was thus reallocated to the species *P. inhibens* (Buddruhs *et al.*, 2013).

The genome of *P. inhibens* DSM 17395 comprises a 3.8 million basepairs (bp) long chromosome and three plasmids of the size 65 kbp, 78 kbp and 262 kbp. The largest plasmid contains important genes required for biosynthesis of the antimicrobial compound tropodithietic acid. This antibiotic inhibits growth of competitors, especially the fish pathogen *Vibrio* spp. (D'Alvise *et al.*, 2012; 2013), but showed also strong antibacterial effect on human pathogens, e.g. *Staphylococcus aureus* (Porsby *et al.*, 2011). Biosynthesis of tropodithietic acid is regulated by quorum-sensing and co-occurs with formation of the brown pigment (Berger *et al.*, 2011).

First metabolomic and proteomic analyses of *P. inhibens* DSM 17395 were conducted 2009, using glucose-containing minimal medium and a time-course experiment setup (Zech *et al.*, 2009). These analyses revealed that abundance of enzymes and metabolites of the central metabolism remained relatively constant upon entry into the stationary growth phase, contrary to model organisms like *Escherichia coli* and *Bacillus subtilis*. The authors stated that this "stand-by" operation is more beneficial than energy-consuming adaptation of proteome accessory, as cells can utilise newly provided substrates faster without requiring a lag-phase.

Another characteristic of *P. inhibens* and other members of the Roseobacter clade is the absence of the phosphofructokinase. Thus, glucose is not degraded via Embden-Meyerhof-

Parnas pathway (also known as glycolysis), but via the phosphorylative Entner-Doudoroff pathway. This was verified for *P. inhibens* DSM 17395 and *D. shibae* DFL 12^T (= DSM 16493^T) by flux analysis using isotopic labelled [1-^{13}C] glucose (Fürch *et al.*, 2009).

1.3 Systems biology

Systems biology intends to study the whole structure, composition and dynamics of a biological system, in this case a bacterial cell. As cellular processes are strongly interconnected, several "omics-approaches", like genomics, transcriptomics, proteomics and metabolomics are combined to improve the understanding of the nature of a cell. In addition to quantitative experimentations, mathematical simulation and modelling in an iterative process are included. This allows to draw and test new hypotheses and improve the understanding of the investigated system (Kell, 2004).

An overview of the output obtained by the "omics-approaches" is shown in figure 3. Precise and reliable genome information that provide the potentials and limitations of an organisms to distinct treatment, are the basis of the systems biological approach and essential for data interpretation. Consecutive "omics-analyses" reveal the actual responses, such as transcription of particular genes, which can be detected within minutes or a few hours after treatment. An overview about the methods applied in transcriptomics, from RNA extraction to sequencing and consecutive data analysis is provided e.g. by Sorek and Cossart (2010). Both transcriptomic and subsequent proteomic analyses benefit from the uniform chemistry of their analytes, capacitates to cover almost the whole transcriptome and proteome.

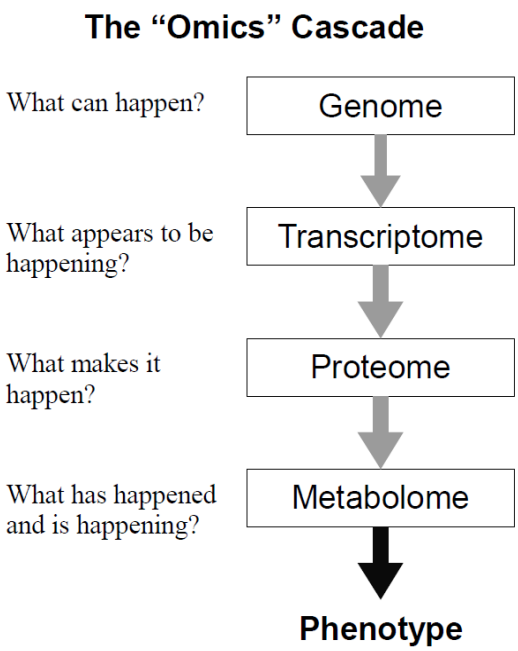

Figure 3: The "Omics" cascade of systems biological approaches. It comprises complex datasets that, if integrated, enables an entire description of a cell's response to the tested treatment. Amongst these, the metabolome is the most predictive. This figure was adapted from Dettmer *et al.* (2007).

Conducting proteomic analyses automatically takes into account the regulation at posttranscriptional and posttranslational level. The complexity of the proteome requires at least one preliminary separation step, which is often performed by one- or two-dimensional gel-electrophoresis. Proteins are typically digested, preferably by sequence-specific enzymes, yielding peptides, i.e. low molecular weight molecules that are easier to be separated and analysed by liquid chromatography – mass spectrometry (LC-MS) than an intact protein (Cox and Mann, 2011). Further methods, principal quantitative approaches and recent advances in mass spectrometry on the field of proteomics are provided e.g. by Bantscheff *et al.*, 2012; Righetti *et al.*, 2004.

The metabolome, the final level of the "Omics" cascade, amplifies changes in the proteome (Kell, 2006). It is not only closest to phenotype and therefore most predictive to phenotype, but also the most dynamic, which responds to a treatment within seconds, i.e. even before any gene-regulatory mechanisms are applied. Further, it comprises the highest versatility of analytes, in regard to chemical characteristics and concentration ranges (Dettmer *et al.*, 2007).

This study investigates the impact of nutrient compositions on the metabolism of *P. inhibens* DSM 17395 by applying mainly metabolomic analyses, which is described in detail in the following section.

1.4 Metabolomic analyses

1.4.1 Introduction to Metabolomics

The overall aim of metabolomic analyses is to obtain a qualitative and quantitative overview of the whole metabolome by analysing all metabolic intermediates in a given scenario, which is challenging due to the complexity and diversity of analytes. Metabolomic approaches were first conducted in plant research, as the plant kingdom provides a high variety of secondary metabolites, which is estimated to be around 200 000 different metabolite species (Hall, 2006; Weckwerth, 2003). So far, organisms studied via metabolomic analyses comprise microorganisms up to tissues of animals and humans. It must be noted that none of these studies really cover the whole metabolome. Instead, metabolic profiling is performed, which refers to the quantitative analysis of selected

metabolites, e.g. in the context of a distinct pathway or specific class of compounds. However, applying different methods allows to cover a broader range of metabolites and therefore fits better to the concept of an "omics-technique". Another possibility reducing complexity of the metabolome often used is metabolic fingerprinting, which intends not to identify each metabolite but rather to compare patterns (i.e. fingerprints) of metabolites that change in response to the treatment. In addition to that, the impact of the environment, i.e. imported or exported compounds in the medium, is often analysed, which is described by the term metabolic footprinting (Fiehn, 2002; Dettmer *et al.*, 2007). Without compound identification, though, any metabolically interesting pattern remains meaningless. Identification requires high-resolution mass spectrometry, software and supportive databases (Scalbert *et al.*, 2009).

1.4.2 Sample preparation techniques for bacterial metabolomics

Sample acquisition is primarily driven by the experimental design and the experimental type. When sampling biological samples, special care has to be taken to minimise the formation or degradation of metabolites after sampling due to remaining enzymatic activity or oxidation processes. Therefore, the metabolism has to be stopped immediately. In case of plants or cell tissues, a quenching method for this purpose is easily applied using liquid nitrogen, whereas it is more complicated to stop metabolism when handling aqueous cell suspensions.

As a matter of fact, cells have to be separated from the medium first, by centrifugation, (e.g. Börner *et al.*, 2007) or filtration (e.g. Bolten *et al.*, 2007), followed by washing of the obtained cell pellet. Alternatively it is also possible to mix the culture broth with a cold solvent, e.g. -40 °C methanol, to stop metabolism immediately without any prior separation step. (Bertini *et al.*, 2013). Such quenching methods often result in loss of membrane integrity, i.e. leakage of cells, loss of metabolites and less reliable quantification. Significant loss of metabolites can also occur when washing solution with insufficient ionic strength is applied, especially in case of gram negative bacteria (Bolten *et al.*, 2007). Once metabolism is stopped, an extraction procedure is conducted, which is mainly driven by the target metabolites. Most methods are based on liquid-liquid extraction or solid phase extraction and often include pre-concentration steps to improve detection of

low abundant metabolites. Matrixes like proteins or salts have to be removed, as these interfere with separation and ionisation (Dettmer *et al.*, 2007).

1.4.3 Gas chromatography – mass spectrometry

Gas chromatography coupled to mass spectrometry (GC-MS) along with liquid chromatography – mass spectrometry (LC-MS) is one of the most commonly used analysis method in metabolomics. Volatile compounds can be analysed directly via headspace with a GC instrument. Less volatile compounds have to be derivatised first, and are then vaporised in an injector and separated via the column containing silicone as stationary phase, the mobile phase, which is an inert gas (e.g. helium) and a temperature gradient.

To make compounds volatile, functional chemical groups are silylated, using common agents, like MSTFA (*N*-methyl-*N*-(trimethylsilyl)-trifluoro-acetamide) or BSTFA (*N,O*-bis(trimethylsilyl)-trifluoroacetamide). The derivatisation agents differ in regard to specificity and volatility of formed analytes. In case of MSTFA, which is applied in this study (Figure 4), modification targets are hydroxy-groups, carboxylates, amines, amides and thiols. Of these, carbohydrates have the highest specificity due to the high number of hydroxy-groups. Methoximation is usually applied prior to silylation (Figure 4A). This stabilises alpha-keto acids and keeps sugars in the open-ring conformation, slightly

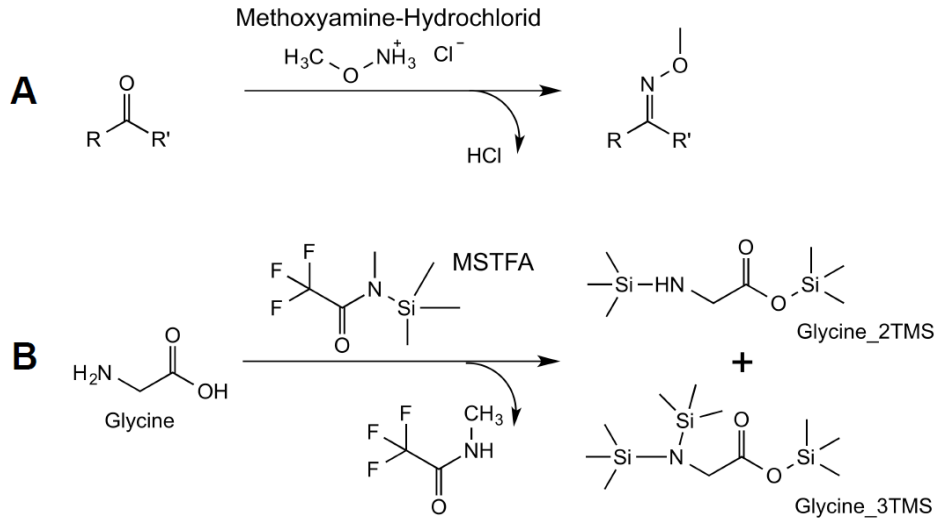

Figure 4: Conducted derivatisation reaction in this study. (A) First, aldehyde and keto-functions are methoximated. This also keeps sugars in the open ring structure, reducing the number of formed sugar analytes. (B) Next, compounds are silylated, using *N*-methyl-*N*-(trimethylsilyl)-trifluoro-acetamide (MSTFA). By silylation of target functions, compounds are thermally stabilised and become volatile. In most cases, silylation yields more than one analyte per metabolite.

reducing the number of obtained derivatives per sugar species.

Silylation is sensitive to moisture, thus samples and agents have to be completely free of water. Otherwise compounds can be degraded or derivatisation is less effective (Dettmer *et al.*, 2007). Special care has to be taken for data analysis and data correction, as derivatisation yields several derivatives per compound. Those distribution patterns can or might probably not correlate to each other (Kanani and Klapa, 2007). Moreover, conversions caused by derivatisation, e.g. arginine to ornithine, have to be taken into account (Halket *et al.*, 2005).

The key advantages of GC-MS are high inter-instrument reproducibility and the standardised electron ionisation with an electron energy of 70 eV. Several open and commercial mass spectrometry libraries are available that allow easy and confident identification. GC provides an excellent chromatographic separation for complex samples, which can even be improved by GC × GC (Górecki *et al.*, 2006) or alternatively by advanced TOF-MS spectrometer and improved data analysis to separate compounds computationally (Kell, 2004). Overall GC-MS provides high metabolite resolution, and quantification of metabolites, as well as reliable identification and can even be used for structural elucidation and annotation of unknown compounds (Strehmel *et al.*, 2013).

1.4.4 Liquid chromatography – mass spectrometry

Liquid chromatography (LC-MS) is another powerful analytical tool for separation and detection of metabolites. It is suitable for larger molecules, like the metabolic relevant coenzyme A intermediates, which cannot be analysed with GC-MS. By applying different columns, and elution buffers, a broad range of chemically different compounds can be analysed. These systems are often combined with electrospray ionisation (ESI), which vaporises the elute to fine drops that are then converted to gas. Small molecules (< 1000 Da) can be charged without degradation. Depending on the applied voltage either $[M+H]^+$ or $[M-H]^-$ can be analysed, which broadens the range of detectable compounds. A disadvantage of LC-MS is the lack of standardisation, which complicates comparison of retention time, ionisation and mass spectra between instruments and laboratories. Confident and well applicable and universal LC-MS databases for compound identification are still missing, despite recent efforts, e.g. NIST or MassBank (Dettmer *et al.*, 2007).

1.5 Objectives

Marine bacteria have been subject of many recent studies and reviews, which focused mainly on genomic analyses and phylogenetic classifications. Due to the abundance, metabolic activity and contribution to the carbon cycle, bacteria play a major role for marine ecosystems. Amongst marine bacteria, the Roseobacter clade represents one of the most active and metabolic versatile bacterial clade. This study focuses on the characterisation of the metabolism of *Phaeobacter inhibens* DSM 17395 as model organism of the Roseobacter clade and of heterotrophic marine bacteria. Of particular interest in this study were metabolic abilities and limitations in regard to different nutrient conditions.

First, substrate range for carbon and nitrogen sources were determined using phenotypic microarray analysis. Further, the standard repertoire of synthesised metabolites was defined using [U-^{13}C] glucose. These analyses, along with the published genome sequence (Thole *et al.*, 2012) formed the basis for consecutive detailed metabolomic and proteomic analyses. Combined "omics-experiments" were accomplished in close cooperation with the research group of Prof. Ralf Rabus (ICBM), who conducted cultivation and proteomic analyses, whereas I performed whole GC-MS-based metabolomic analyses, from sample preparation to data processing and detailed statistical analysis. Following six scenarios were studied: (1) Complex medium and glucose-containing minimal medium were used to mimic nutrient-rich conditions during an algae bloom, respectively nutrient poor conditions. (2) In a time-dynamic experiment, uptake and utilisation of casamino acids were investigated. (3) Influence of plasmids on growth and amino acid uptake were studied using selected plasmid-cured strains. (4) Single amino acids and (5) carbohydrates as single carbon sources were used to study and to refine complex catabolic networks, which remained unclear or incomplete in the original genome annotation. (6) Metabolic responses to limited ammonium content were studied over a whole growth curve.

Through theses experiments a general understanding of the metabolic properties of the bacterium was generated, which contributes to the understanding of its adaptation strategies and success of *P. inhibens* DSM 17395 in marine environments.

2 Material and methods

Particular experiments were conducted in close cooperation with the research group of Prof. Ralf Rabus (Institute for Chemistry and Biology of the Marine Environment (ICBM) of the Carl von Ossietzky Universität Oldenburg, Department General and Molecular Microbiology), who conducted proteomic analyses, as well as cultivation and sampling for the main experiments.

2.1 Equipment and instruments

All instrument used in this study are listed in table 2. Instruments present at the Institute for Chemistry and Biology of the Marine Environment are marked with ICBM.

Table 2: Equipment and instruments used in this study.

Equipment	Manufacturer
GC-MS systems	
(1) Leco	
MPS 2 XL autosampler	Gerstel (Mülheim a.d. Ruhr, Germany)
7890 Agilent GC	Agilent (Santa Clara, USA)
Leco Pegasus 4D mass spectrometer	Leco Instruments (Mönchengladbach, Germany)
(2) Jeol	
MPS 2 Twister autosampler	Gerstel (Mülheim a.d. Ruhr, Germany)
6890N Agilent GC	Agilent (Santa Clara, USA)
Accu TOF GC JMS-T100GC	JEOL (Germany) GmbH (Eching, Germany)
(3) DSQ II	
Autosampler 3000	Thermo Fisher Scientific (Dreieich, Germany)
Thermo GC Ultra	Thermo Fisher Scientific (Dreieich, Germany)
DSQII	Thermo Fisher Scientific (Dreieich, Germany)
LC-MS system	
Ultimate 3000	Dionex (München, Germany)
Bruker MicroQTOF II MS	Bruker Daltonik (Bremen, Germany)
Equipment for proteomic analyses (ICBM)	
Typhoon 9400 scanner	GE Healthcare (München, Germany)
Proteineer spII and dp systems	Bruker Daltonik (Bremen, Germany)
UltraflexIII MALDI-TOF/TOF MS	Bruker Daltonik (Bremen, Germany)
Ultimate 3000 nanoLC	Dionex (München, Germany)
AmaZon ETD	Bruker Daltonik (Bremen, Germany)
Incubator	
Certomat BS-1 (orbit:50 mm)	Sartorius (Göttingen, Germany)

Table 2: Equipment and instruments used in this study. (Continued)

Equipment	Manufacturer
Incubator BD 53	Binder (Tuttlingen, Germany)
CH-4103 (ICBM)	Infors AG (Bottmingen, Switzerland)
Bioreactor Labfors II (ICBM)	Infors AG (Bottmingen, Switzerland)
Photometer	
Genesys 6 spectrophotometer	Thermo Fisher Scientific (Dreieich, Germany)
UV-Vis spectrophotometer UV-1800 (ICBM)	Shimadzu (Duisburg, Germany)
UV 1240 mini (ICBM)	Shimadzu (Duisburg, Germany)
Centrifuges	
Centrifuge 5424	Eppendorf (Hamburg, Germany)
Centrifuge 5810R (rotors: F34-6-38, F45-30-11)	Eppendorf (Hamburg, Germany)
Avanti J-E (rotors: JLA-10.500, JA-14)	Beckman Coulter (Krefeld, Germany)
Vacuum Dryer	
Speed Vac Concentrator 5301	Eppendorf (Hamburg, Germany)
CentriVap Centrifugal	Labconco (Kansas City, USA)
Others	
Autoclave Varioklav 25T and 135S	H+P Labortechnik (Oberschleißheim, Germany)
Balance Discovery DV214C	OHAUS (Gießen, Germany)
Incubator (80 °C)	Melag Medizintechnik (Berlin, Germany)
Incubator ED400	Binder (Tuttlingen, Germany)
Microscope Axiostar (ICBM)	Zeiss AG (Göttingen, Germany)
Microscope Axiostar plus	Zeiss AG (Göttingen, Germany)
Microwave HMT 842C 1300W	Bosch (Gerlingen-Schillerhöhe, Germany)
Mix Mate	Eppendorf (Hamburg, Germany)
OmniLog-Incubator/Reader	Biolog (Hayward, CA, USA)
Precellys24 homogenizer	Peqlab (Erlangen, Germany)
Precision Balance Adventurer Pro AV2102C	OHAUS (Gießen, Germany)
Sanyo MDF-U53V -86 °C	Ewald Innovationstechnik (Nenndorf, Germany)
Sterile bench HERAsafe KS 12 and KS 18	Thermo Fisher Scientific (Dreieich, Germany)
Turbidimeter	Biolog (Hayward, CA, USA)
Ultra pure water system Arium	Sartorius (Göttingen, Germany)
Ultrasonic bath Sonorex Digitec DT 255 H	Bandelin electronic (Berlin, Germany)
Vacuum pump Laboport SCC840	KNF Neuberger (Freiburg, Germany)

2.2 Consumables

Table 3: Consumables used in this study.

Material	Manufacturer
GC-MS equipment	
CIS 4 glass liner (71 × 1 mm), filled with silanized glass wool	Gerstel (Mülheim a.d. Ruhr, Germany)
Crimp glass vials and crimp caps	Chromatographie Zubehör Trott (Kriftel, Germany)
DB-5MS (30 m × 0.25 mm × 0.25 μm)	Agilent (Santa Clara, USA)

Table 3: Consumables used in this study. (Continued)

Material	Manufacturer
Glass vials with cap	CS (Langerwehe, Germany)
Microinlets for glass vials	CS (Langerwehe, Germany)
Silicon septae	Chromacol (Welywyn Garden City, UK)
Syringes	CS (Langerwehe, Germany), Restek (Bad Homburg, Germany) or Thermo Fisher Scientific (Dreieich, Germany)
Trace 2000 Liner (2 mm × 2.75 mm × 120 mm)	Restek (Bad Homburg, Germany)
ZB-5MS + 5 m Guardian column (30 m × 0.25 mm inner diameter)	Phenomenex (Aschaffenburg, Germany)
Others	
Cuvettes, Polystyrol, 1.5 ml	Sarstedt (Nürnbrecht, Germany)
Erlenmeyer flasks with 3 or 4 baffles, 100, 300, 500 and 1000 ml	W. O. Schmidt Laboratoriumsbedarf, (Braunschweig, Germany)
Glass beads, 70-110 µm	Kuhmichel GmbH (Ratingen, Germany)
Phenotypic Microarrays: PM1, PM2A, PM3B	AES Chemunex (Bruchsal, Germany)
Pipette tips, 10, 200, 1000, 1200, 5000, 10000 µl	Eppendorf (Hamburg, Germany) or Sarstedt (Nürnbrecht, Germany)
Polypropylen reaction tubes, 1.5 ml and 2 ml	Eppendorf (Hamburg, Germany)
Polypropylen tubes, 15 ml, 50 ml	Greiner Bio-One GmbH (Frickenhausen, Germany)
Precellys tubes, 2 ml and caps	Peqlab (Erlangen, Germany)
Sterile filters, Filtropur 0.2 µm	Sarstedt (Nürnbrecht, Germany)

2.3 Chemicals

If not indicated otherwise, chemicals and reagents of highest quality marked with the term “purest” or “for analytical purpose” were utilised. The substances were purchased from the manufacturers Carl Roth (Karlsruhe, Germany), CS GmbH (Langerwehe, Germany), Euriso-Top GmbH (Saarbrücken, Germany), Fisher Scientific (Schwerte, Germany) and Sigma-Aldrich (Steinheim, Germany).

2.4 Organism

Table 4: Strains of *Phaeobacter inhibens* DSM 17395 used in this study. Strains were maintained in glycerol stocks at -80 °C.

Strain	Description	Reference
DSM 17395	Wild-type strain	(Buddruhs *et al.*, 2013), obtained from the DSMZ
Δ65kb	DSM 17395, cured from 65 kbp plasmid	J. Petersen (DSMZ)

Table 4: Strains of *Phaeobacter inhibens* DSM 17395 used in this study. (Continued)

Strain	Description	Reference
Δ262kb	DSM 17395, cured from 262 kbp plasmid	J. Petersen (DSMZ)
Δ65kbΔ262kb	DSM 17395, cured from 65 kbp and 262 kbp plasmid	J. Petersen (DSMZ)
"M3"	Natural isolate, which lacks the 262 kbp plasmid	(Petersen *et al.*, 2011), provided by T. Brinkhoff (ICBM)

2.5 Media and supplements

All water-based media and solutions were prepared with salt-free, particle filtered and sterile filtered ultra pure water from an ultra pure water system (Arium, Sartorius). Autoclavation for sterilisation of media was conducted for 20 min at 121 °C and 1 bar overpressure.

2.5.1 Salt water medium (minimal medium)

The media was essentially prepared as described previously (Zech *et al.*, 2009) with some minor modifications. It consist of four components: Basic A (salt solution), Basic B ($NaHCO_3$), 1 ml/l of a trace element stock solution (1000x) and a carbon source, which was provided as individual solution or was included to Basic A. The concentration of the corresponding stock solutions was adapted individually to meet the requirements of substrate solubility and final medium volume. Therefore only final concentrations of the respective compounds are provided here.

Basic A – final concentration in the medium:

Na_2SO_4	4.0 g/l
KH_2PO_4	0.2 g/l
NH_4Cl	0.25 g/l
NaCl	20.0 g/l
$MgCl_2 \times 6\ H_2O$	3.0 g/l
KCl	0.5 g/l
$CaCl_2 \times 2\ H_2O$	0.15 g/l

Filled up with ultra pure water and autoclaved for sterilisation. Due to the high salt content, maximum concentration was 7.5x, used for Biolog Phenotypic Microarray Analysis.

Basic B – final concentration in the medium:

$NaHCO_3$	0.19 g/l

Filled up with ultra pure water and autoclaved for sterilisation. Maximum concentration of this stock solution was 100x.

Trace element stock solution (1000x) – 1 ml/l medium

H_2O	25 ml
$Fe(II)SO_4 \times 7H_2O$	1.05 g
HCl, 25% (w/v)	6.5 ml
Tritiplex III (Na_2EDTA)	2.6 g

Dissolved and adjusted pH to 6.0 to 6.5 before adding the next components

H_3BO_3	15 mg
$MnCl_2 \times 4\ H_2O$	50 mg
$CoCl_2 \times 6\ H_2O$	95 mg
$NiCl_2 \times 6\ H_2O$	12 mg
$CuCl_2 \times 2H_2O$	1 mg
$ZnSO_4 \times 7H_2O$	72 mg
$Na_2MoO_4 \times 2H_2O$	18 mg

Filled up to 500 ml with ultra pure water and sterile filtrated

Carbon sources – final concentration in the medium:

Glucose	5 mM, respectively 11 mM in "adaptation to growth with complex medium" experiment (Section 2.13.1)
[U-^{13}C] glucose	5 mM
Casamino acids / Caseinhydrolysate (A157, Carl Roth)	10 g/l. This amino acid mixture was provided together with low concentrated Basic A (1.11x) and was autoclaved for sterilisation.
Succinate	20 mM
L-tryptophan	5 mM
L-phenylalanine	5 mM
L-methionine	20 mM
L-leucine	15 mM
L-isoleucine	15 mM
L-valine	15 mM
L-histidine	15 mM
L-lysine	15 mM
L-threonine	15 mM
N-acetyl-glucosamine	5 mM
Mannitol	5 mM
Sucrose	2.5 mM
Xylose	5 mM

If necessary, pH was adjusted to 7. If not mentioned otherwise, carbon sources were sterile filtrated.

2.5.2 Bacto Marine Broth (complex medium)

For complex medium, ready compositions were used: either 37.1 g/l DIFCO 2216 (DIFCO, Lawrence, KS, USA) or 40.1 g/l Marine Bouillon CP73.1 (Carl Roth, Karlsruhe, Germany). For solid medium, 15 g/l agar was added prior to autoclaving.

2.5.3 Biolog-inoculum solutions

Biolog-inoculum solution 1

IF-0a GN/GP (1.2x) (Biolog, Hayward, CA, USA)	5.0 ml
Basic A (7.5x)	0.6 ml
Basic B (100x)	0.05 ml
Ultra pure water (sterile)	0.35 ml

Biolog-inoculum solution 2

IF-0a GN/GP (1.2x) (Biolog, Hayward, CA, USA)	8.33 ml
Basic A (7.5x)	1.2 ml
Basic B (100x)	0.1 ml
Trace Element stock solution (1000x)	0.012 ml
Ultra pure water (sterile)	0.238 ml
Redox Dye Mix D (100x) (Biolog, Hayward, CA, USA)	0.12 ml

2.5.4 Solutions for GC-MS analysis

Ribitol stock solution

0.05 g ribitol were dissolved in 0.25 l ultra pure water. The solution was sterile filtered, aliquoted and stored at -20 °C.

Methoxyamine/pyridine solution

Methoxyamine hydrochloride was dissolved 20 mg/ml in pyridine prior to usage.

Alkane time standard (retention index calibration mix)

Decane, $C_{10}H_{22}$	12.5 mg, respectively 17.1 µl
Dodecane, $C_{12}H_{26}$	12.5 mg, respectively 16.7 µl
Pentadecane, $C_{15}H_{32}$	12.5 mg, respectively 16.2 µl
Nonadecane, $C_{19}H_{40}$	12.5 mg
Docosane, $C_{22}H_{46}$	12.5 mg
Octacosane, $C_{28}H_{58}$	12.5 mg

Dotriacontane, $C_{32}H_{66}$	12.5 mg
Hexatriacontane, $C_{36}H_{74}$	12.5 mg

The alkanes were dissolved in 25 ml cyclohexane and aliquoted, resulting in a concentration of 0.5 g/l for each alkane. For GC-MS measurement 6 µl of this stock solution were added to 48 µl cyclohexane.

2.6 Software

Table 5: Software used in this study.

Software	Description
ChemSketch (Freeware Version 12.01) (Advanced Chemistry Development, Inc.)	Program for sketching molecules
ChemBioDraw (Version 13.0.2.3020 for Mac OS X) (Cambridgesoft)	Program for sketching molecules
ChromaTOF (Version 4.24) (Leco Instruments)	Vendor software for GC-MS data acquisition and evaluation
DataAnalysis software (Version 4.0 SP5, Build 283) (Bruker Daltonic)	Vendor software for LC-MS data acquisition and analysis
EnzymeDetector (Quester and Schomburg, 2011) (http://edbs.tu-bs.de)	Program for comparative pathway prediction based on genome annotation from different sources
Hystar (Version 3.2, Build 44) (Bruker Daltonic)	Vendor software for controlling and synchronising all components of the LC-MS system
itool	Internal Python/MySQL-based script for GC-MS data. Sums analytes of metabolite and calculates mean values and errors for each sample group and metabolite.
Maestro (Versions 1.2.3.5 and 1.4.24.2) (Gerstel)	Vendor software for controlling and synchronising the Gerstel autosampler with GC-MS system
MassCenterMain (Version 2.3.0.1) (Jeol)	Vendor software for GC-MS data acquisition and evaluation
MetaboliteDetector (Hiller *et al.*, 2009), TU-BS branch (various developmental versions released 2012 to 2013) (http://md.tu-bs.de)	Program for GC-MS analysis
MultiExperiment Viewer (Saeed *et al.*, 2003) (Version 4.7.3)	Program for statistical analysis and visualisation of scientific data
OmniLog – OL PM FM and OL PM Par (both version 1.20.02) (Biolog)	Program for data evaluation and visualisation of kinetic respiration plots
OmniLog – PM DC (Version 1.30.01) (Biolog)	Administration software of the OmniLog Incubator/Reader

Table 5: Software used in this study. (Continued)

Software	Description
OriginPro (64-bit Academic Versions: 8.6.0 and 9.0.0G) (OriginLab)	Program for visualisation of scientific data
R (Version 3.1.1 for Windows7, and 3.1.0 for MacOS X) (R Foundation for Statistical Computing)	Program for statistical analysis and visualisation of scientific data
Xcalibur (Version 2.0.7) (Thermo Fisher Scientific)	Vendor software for GC-MS data acquisition and evaluation
XCMS (Smith *et al.*, 2006; Tautenhahn *et al.*, 2008; Benton *et al.*, 2010)	R package for LC-MS data analysis

2.7 Databases

Table 6: Databases used in this study.

Database	Description
BRENDA (Schomburg *et al.*, 2012) (http://www.brenda-enzymes.org)	Database for enzymes and ligands
Chemspider (http://www.chemspider.com)	Chemical database
Golm Metabolome Database (http://gmd.mpimp-golm.mpg.de)	Open source mass spectral library
KEGG (Kanehisa *et al.*, 2014) (http://www.genome.jp/kegg)	Database for pathways and compounds
MASCOT (http://www.matrixscience.com)	Database for identification and characterisation of proteins
MassBank (Horai *et al.*, 2010) (http://www.massbank.jp)	Open source mass spectral library
MetaCyc (Caspi *et al.*, 2014) (http://www.metacyc.org)	Database of experimentally elucidated metabolic pathways and compounds
MD Library, Version: 2014-03-31	In-house library of EI mass spectra and retention indices. Contains 1531 entries from 1031 chemical standards; and 1087 entries of unidentified compounds.
NCBI (http://www.ncbi.nlm.nih.gov/)	National Center for Biotechnology Information that provides amongst others biomedical and genomic information
NIST08 Mass Spectral Database (http://www.nist.gov/)	Commercial EI mass spectral library
UniProtKB/**Swiss-Prot** (http://www.uniprot.org/)	Manually curated protein database

2.8 Microbial techniques

2.8.1 Biolog phenotypic microarray analysis

Wild-type stock cultures were streaked onto MB agar plates and incubated for 48 h at 28 °C, transferred once to a fresh agar plate and incubated for another 24 h. Obtained colonies were picked with a sterile cotton stick and resuspended into a reaction tube containing 6 ml of Biolog-inoculum solution 1 until a turbidity of 42% was reached. Then, 2 ml of it were transferred to 10 ml Biolog-inoculum solution 2. For PM3B plate (test for nitrogen substrate range), Basic A contained no NH_4Cl; instead of sterile H_2O, 1 M succinate was used as carbon source in the Biolog-inoculum solution 2. The resulting mixture was used to inoculate the Biolog phenotypic microarrays with 100 µl per well. Each well contained one single dried substrate, which were either carbon sources (PM1 and PM2A) or nitrogen sources (PM3B).

The microarrays were incubated for 72 h at 28 °C in the OmniLog-Incubator/Reader; every 15 minutes pictures of the plates were taken automatically to record colouring of the wells. Data were analysed with the vendor software OmniLog-PM FM and OmniLog-PM Par. Each plate was analysed in duplicate.

2.8.2 Isotope labelling

Stock cultures were streaked onto MB agar plates and incubated for 48 h at 28 °C. A single colony was picked to inoculate 20 ml minimal medium (in a 100 ml Erlenmeyer flask with three baffles) containing 5 mM glucose as carbon source. The pre-culture was incubated at 28 °C in a shaker (150 rpm, BS-1, Sartorius) and then used to incubate fresh medium containing either glucose or [U-^{13}C] glucose to $OD_{600\ nm} = 0.01$. After another 48 h, main cultures (200 ml medium in 1 l Erlenmeyer flasks with three baffles) supplied with either glucose or [U-^{13}C] glucose were inoculated and incubated under same conditions as pre-cultures. Cells were harvested at ¾ OD_{max} by centrifugation (30100 × *g*, 5 min, 4 °C). Obtained cell pellets were resuspended in 3.7% (w/v) NaCl solution and distributed to 50 ml polypropylene tubes, centrifuged (10414 × *g*, 3 min, 4 °C), the obtained cell pellets were washed again and immediately prepared for GC-MS-based metabolomic analysis.

Metabolite extraction and derivatisation for GC-MS analysis was performed essentially as described in section 2.11. Cell pellets were resuspended in 1.5 ml ethanol containing 22.5 µl of a 0.2 mg/ml ribitol solution. After phase separation, 1 ml of the polar phase were transferred to a 2 ml reaction tube and dried in a vacuum concentrator overnight.

2.8.3 Study of coenzyme A derivatives linked with tryptophan degradation

To analyse tryptophan-degradation specific coenzyme A derivatives, cells were grown on 5 mM L-tryptophan, or 20 mM succinate (reference condition) in a Certomat BS-1 (150 rpm, Sartorius). Two adaptation cycles, transferring actively grown cells to fresh medium, were conducted before inoculating main cultures. Samples were harvested at ½ OD_{max} by centrifugation (10414 × *g*, 4 °C, 5 min). Supernatants were removed and the remaining cell pellets, approximately 20 mg dry mass each, were immediately frozen in liquid nitrogen and stored at -80 °C until further analysis with LC-MS.

2.8.4 Cultivation conditions for main experiments

Erlenmeyer flasks with three baffles, were filled 1/5 – 1/4 to their maximum volume capacity with medium. Then, flasks were inoculated with stock culture (or substrate-adapted cells stored at -80 °C in glycerol-containing medium) diluted 10^{-1} to 10^{-4}. For the consecutive adaptation steps and up-scaling, flasks were inoculated with 2% (v/v) to 5% (v/v) of actively growing culture at half-maximal optical density (½ OD_{max}). Incubation was done at 28 °C in a shaker (100 rpm, CH-4103, Infors).

Cells for GC-MS-based metabolomic and proteomic analyses were harvested at ½ OD_{max} by centrifugation (14300 × *g*, 20 min, 4 °C). The obtained cell pellets were washed in Tris/HCl buffer (100 mM + 5 mM $MgCl_2 \times 6H_2O$, pH 7.5), 0.9% or 3.7% (w/v) NaCl and centrifuged again. The washed cell pellets were resuspended in wash solution, distributed into 2 ml reaction tubes and centrifuged (16000 × *g*, 3 min, 4 °C). The wet mass of the resulting cell pellets were determined and then directly frozen in liquid N_2 and stored at -80 °C. For exometabolomic analysis 1.5 ml – 1.8 ml of the culture supernatant obtained by centrifugation and/or filtration (0.2 µm, Minisart, Sartorius, Göttingen) were immediately frozen at -80 °C.

2.9 Proteomic analyses

Proteomic analyses, comprising differentiation of extracellular proteins, as well as soluble and membrane-enriched fraction of intracellular proteins, were conducted by cooperation partners from the ICBM in Oldenburg (research group of Prof. Ralf Rabus). Proteins were analysed using 2D DIGE with cyano dyes for quantification, SDS-PAGE, MALDI-TOF-MS and shotgun nano LC-MS. Identification of peptide sequences was performed on a MASCOT server searching against the genome of *P. inhibens* DSM 17395 (Thole *et al.*, 2012). Only results, required for interpretation of metabolomic data are included in the corresponding chapters. Details of the methods and results are provided in the corresponding joint publications (Zech *et al.*, 2013a; Zech *et al.*, 2013b; Drüppel *et al.*, 2014; Wiegmann *et al.*, 2014).

2.10 Analysis of coenzyme A derivatives

2.10.1 Extraction of coenzyme A derivatives

Cells were resuspended in 1 ml methanol, containing 0.2 µg/ml biochanin A as internal standard, and transferred to cryo tubes with 600 mg glass beads (70 – 110 µm). Cell lysis was conducted using a Precellys24 homogenizer at -10 °C and 6800 rpm shaking speed for 3 × 30 seconds, with equivalent short breaks between the three shaking cycles. Cell lysates were transferred to 10 ml ice cold 25 mM ammonium acetate (pH 6) and centrifuged (5 min, 10000 × *g*, 4 °C).

Extraction of coenzyme A derivatives was performed on Strata XL-AW solid phase extraction columns (Phenomenex, Aschaffenburg, Germany). Before application of the supernatant, the solid phase extraction columns were pretreated sequentially with 1 ml methanol, 1 ml methanol: ultra pure water: formic acid (50:45:5) and 1 ml ultra pure water. After passing the ammonium acetate supernatant through the columns with a vacuum of 900-800 mbar for approximately 5 min, the column were rinsed with 1 ml ammonium acetate (pH 7.2) and 1 ml methanol, and were then dried at 700 mbar vacuum for 3 min. Analytes were eluted by 2 × 500 µl methanol containing 2% (v/v) ammonia solution (27% ammonia in water) and then dried in a centrifugal-vacuum concentrator at 14 °C. For

analysis samples were dissolved in 200 µl sample buffer (25 mM ammonium formate, pH 3.5, 2% v/v methanol).

2.10.2 Liquid chromatography – mass spectrometry analysis

Coenzyme A derivatives were analysed with a Dionex Ultimate 3000 system, coupled to a Bruker MicroTOF QII mass spectrometer with an electrospray ionisation interface. 50 µl of the samples were injected into the LC system and separated essentially as described previously by Peyraud *et al.* (2009). Separation was done with a C_{18} analytical column (Gemini 150 × 2.0 mm, particle size 3 µm, Phenomemex, Aschaffenburg, Germany) at a flow rate of 220 µl/min and 35 °C. Solvent A was 50 mM formic acid adjusted to pH 8.1 with NH_4OH and solvent B was methanol. The following gradient of B was applied: 0 min, 5%; 1 min, 5%; 19 min, 30%; 26 min, 95%, 30 min, 95%. The mass spectrometer was operated in ESI+ mode with a rate of 3 Hz for data acquisition and automated MS2 acquisition. Mass range was set to 90-1178 *m/z* with an end plate offset of -500 V, capillary voltage of 4500 V, 1.2 bar nebulizer pressure, 8 l/min dry gas and 200 °C dry temperature. A detailed list of the applied MS and MS2 settings is provided in Table 7.

Table 7: Mass spectrometry settings for analysis of coenzyme A derivatives. The MicroTOF QII mass spectrometer was operated in ESI+ mode, using the following settings for MS, MS2, and MS2 fragmentation.

MS settings	
Transfer Funnel 1 RF	200 Vpp (Volts peak to peak)
Transfer Funnel 2 RF	200 Vpp
Transfer ISCID Energy	0 eV
Transfer Hexapole RF	150 Vpp
Quadrupol Ion energy	5 eV
Quadrupol Low mass	100 *m/z*
Collision Cell Collision Energy	7 eV
Collision Cell Collision RF	150 Vpp
Collision Cell Transfer Time	80 µs
Collision Cell Pre Pulse Storage	5 µs
MS2 settings	
Threshold (cts)	2000
Smart Exclusion	2
Active Exclusion	on
Exclude after (spectra)	2
Release after (min)	0.2

Table 7: Mass spectrometry settings for analysis of coenzyme A derivatives. (Continued)

MS2 fragmentation			
Isolation mass	**Isolation width**	**Collision Energy**	**Charge state**
500	8	35	1
		25	2
		20	3
1000	10	50	1
		40	2
		35	3
2000	15	75	1
		50	2
		45	3

2.10.3 Data processing and peak identification

Internal mass calibration with sodium formate cluster and data export to MZXML format was realised with DataAnalysis software (Bruker Daltonic). Processing of the peak data was then conducted with the R package XCMS under R version 3.0.3, parameters are provided in table 8.

Table 8: Settings for LC-MS data processing, using the R package XCMS.

Parameter	**Value**
peakwidth	c(5,24)
snthresh	1
prefilter	c(1,200)
mzCenterFun	“wMeanApex3”
integrate	1
mzdiff	0.4
fitgauss	TRUE
scanrange	c(700, 5000)
noise	0
Peak alignment and retention time were performed with XCMS methods group and retcor in two iterations with these parameters:	
method	“nearest”
mzVsRTbalance	15
mzCheck	0.2
rtCheck	20
kNN	15 (for the first iteration); 10 (for the second grouping)
missing	3
extra	2
smooth	“loess”
span	0.2

Table 8: Settings for LC-MS data processing, using the R package XCMS. (Continued)

Parameter	Value
family	"symmetric"
plottype	"mdevden" with missing = 1
extra	1 (for the second iteration of retcor)

A final grouping step was conducted with the same group parameters as the second iteration. Missing values were calculated by the fillPeaks methods. Peak data were exported as csv-table.

Peak identification was carried out via the accurate masses of $[M+2H]^{2+}$ ions and retention times of synthetic standards. For substances with no chemical standards available, both the calculation of the molecular masses from $[M+2H]^{2+}$ and $[M+H]^{+}$ ions and the prediction of sum formulas from accurate masses and isotopic patterns using the DataAnalysis software, were applied for their identification. MS2 fragmentation was used to confirm the coenzyme A moiety when possible. Identification of isomers was partially possible in the biological context but not based on LC-MS2 data alone.

2.11 Sample preparation for GC-MS analysis

Samples were prepared according to the recently described method (Zech *et al.*, 2013a). This procedure involves the extraction of metabolites from the cell-pellets and removal from any water-based solvent and derivatisation of the samples. Details and modifications for the main experiments are provided in sections 2.13 and 2.14.

2.11.1 Extraction of intracellular metabolites

Cell pellets were resuspended in 1.5 ml ethanol, containing 30 or 60 µl of a 0.2 mg/ml ribitol solution. For cell lysis, cell suspensions were incubated in an ultrasonic bath for 15 min at 70 °C. Samples were cooled on ice, followed by addition of 1.5 ml water and mixing. Then, 1 ml chloroform was added and samples were shaken vigorously for chloroform extraction of hydrophobic compounds from the aqueous phase. After phase separation by centrifugation (3900 × *g*, 5 min, 4 °C), 500 µl or 1 ml of the polar phase were transferred to a 2 ml reaction tube or alternatively to a 1.3 ml crimp glass vial in case of automated derivatisation. Samples were dried in a vacuum concentrator overnight and stored at -20 °C until further processing.

2.11.2 Preparation of culture supernatants

An appropriate amount of the culture supernatants were spiked with a polar solvent and a 0.2 mg/ml ribitol solution and then dried in a vacuum concentrator overnight and stored at -20 °C until further processing. The used volume of the supernatants were adapted to their corresponding concentration, to detect low concentrated compounds without detector saturation by the high concentrated substrates.

2.11.3 Derivatisation reaction

The two-step derivatisation reaction (methoximation using a methoxyamine hydrochloride solution with a concentration of 20 mg/ml in pyridine followed by silylation applying MSTFA) was performed as follows: 40 µl methoxyamine/pyridine were added to the dried sample and incubated for 90 min at 30 °C with constant mixing. Then 60 µl MSTFA were added and samples were incubated for 30 min at 37 °C followed by 2 h at 25 °C with constant agitation. The samples were centrifuged at 14000 × *g* for 5 min and the supernatants were transferred into glass vials for GC-MS analysis. In case of automated derivatisation, a MPS 2 XL autosampler coupled to the Leco Pegasus 4d GC × GC TOF MS system was used. Here, the final incubation time was reduced from 2 h to 1 h.

2.12 Gas chromatography – mass spectrometry analysis

For metabolomic analyses three different GC-MS systems were available, whereas most samples were analysed with the Leco Pegasus 4d GC × GC TOF MS. The Jeol JMS-T100GC was used for the exometabolomic analysis of "carbohydrate degradation" (Section 2.13.5) and "ammonium limited growth condition" experiments (Section 2.13.6), using a splitless and split (1:15) injection method. Further, it was used for an additional intracellular metabolome analysis of "carbohydrate degradation" (Section 2.13.5) and "isotope labelling" experiments (Section 2.8.2), both using splitless injection. The DSQ II GC-MS was used for the analysis of the supernatants derived from the "dynamics of amino acid utilisation" experiment (Section 2.13.2). As time standard, every 20 measurements, an alkane mix (Section 2.5.4) was analysed to allow reproducibility of the measurements.

2.12.1 Leco Pegasus 4 d GC × GC TOF MS

Samples were analysed using a Leco Pegasus 4d GC × GC TOF MS, operated in GC-TOF mode, and equipped with a MPS 2 XL autosampler. Calibration of the mass spectrometer was conducted according to the manufacturer with perfluorotributylamine. Samples (1 µL) were injected in splitless mode into a programmed temperature vaporising (PTV) injector (Gerstel), which was equipped with a 71 × 1 mm CIS 4 glass liner, filled with silanized glass wool. After an initial time of 0.02 min at 70 °C the temperature was increased with 12 K/s to 330 °C, which was then held constant for 5 min. Gas chromatography was performed with a 7890 Agilent GC, equipped with a ZB-5MS column (Phenomenex) or with the identically constructed DB-5MS column (Agilent). The helium flow was set to constant at 1.2 ml/min, respectively 1.0 ml/min in case of the experiment "adaptation to growth with complex nutrients" (Section 2.13.1). After 1 min at 70 °C the GC oven temperature was increased by 10 K/min to 330 °C, which was then held constant for 3 to 8 min, depending on deterioration of the column. The transfer line was set to 275 °C, the ion source temperature was 250 °C and the detector voltage was adjusted according to the sample concentration and the daily performance of the instrument. Overall the detector voltage was set 200 V higher than the output of the automatic tuning. Solvent delay was adjusted according to the deterioration of the column; around 300 s. After solvent delay time, full mass spectra were collected from 45 to 600 *m*/*z* at 8 scans/s, or 20 scans/s, with the ChromaTOF software.

2.12.2 Jeol JMS-T100GC Accu TOF MS

Samples were analysed using the Accu TOF GC JMS-T100GC, equipped with a MPS 2 Twister autosampler. Tuning with Perflourorokerosene (MasCom, Bremen, Germany) was conducted according to the manufacturer's instructions. Samples (1 µl) were injected in splitless or in split mode (1:15) into a programmed temperature vaporising (PTV) injector (Gerstel), equipped with a 71 x 1 mm CIS 4 glass liner, filled with silanized glass wool. After an initial time of 0.02 min at 70 °C the temperature was increased with 12 K/s to 330 °C, followed by 330 °C for 5 min. Gas chromatography was performed with a 6890N Agilent GC, equipped with a ZB-5MS column. Helium flow was set to constant

1.2 ml/min. After 1 min at 70 °C the GC oven temperature was increased to 330 °C at 10 K/min, followed by an additional constant temperature period at 330 °C for 3 min. The transfer line temperature was set to 250 °C. Electron impact mode at 70 eV was used for ionisation; ion source temperature was set to 200 °C, the detector voltage was adjusted according to sample concentration and daily performance of mass spectrometer, which was a value of about 2400 V. The emission current was set to 300 µA. Solvent delay was adjusted according to deterioration of the column. After solvent delay time, full scan mass spectra were collected from 45 to 600 *m/z* at 5 scans/s with the MassCenter Main Software.

2.12.3 DSQ II GC-MS

Determination of the amino acid depletion profile was performed on a Thermo GC Ultra coupled to a DSQ II mass spectrometer equipped with an AS3000 autosampler. In summary, 1 µl of the derivatised sample was injected in split mode (1:25) into a PTV injector (Thermo Fisher Scientific). After an initial time of 0.2 min at 70 °C, temperature was increased to 330 °C at a rate of 14 K/min, followed by an additional constant temperature period at 330 °C for 5 min. GC was performed over 60 min on a ZB-5MS column. Helium flow was set to 1.2 ml/min. After 1 min at 70 °C, temperature was increased to 76 °C with 1 K/min and then to 325 °C with 6 K/min, followed by a constant temperature period at 325 °C for 10 min. The transfer line temperature was set to 275 °C. Ion source temperature was set to 220 °C. After 5.8 min (solvent delay time), full-scan mass spectra were collected from 40 to 460 *m/z* at 2.5 scans/s using the Xcalibur software.

2.13 Setup of main experiments

To exclude potential misleading results due to minor variations of cultivation procedures; all samples of the joint experiments combining proteomic and metabolomic analyses originate from the same biological replicates and were generated by the research group of Prof. Ralf Rabus (ICBM, Oldenburg, Germany). Cultivation and sampling were conducted in Oldenburg as described in section 2.8.4, details and modifications are provided in section 2.14. Washed cell-pellets (around 100 mg wet mass) and cell-free supernatants for GC-MS-based metabolomic analyses were delivered on dry ice.

2.13.1 Adaptation to growth with complex medium

To study the adaptation of *P. inhibens* DSM 17395 to seasonally fluctuating nutrient conditions, medium mimicking nutrient depleted or nutrient-rich conditions during algae bloom, were used for cultivation. Minimal medium contained 2 g/l (≈ 11 mM) glucose as carbon source (GM medium), complex medium (MB medium) contained 5 g/l peptone and 1 g/l yeast extract as carbon source. In addition to Erlenmeyer flask cultures, cells were cultivated in process-controlled fermenter, for which phosphate concentration in the minimal medium was reduced to 0.15 M, and one fermenter (1500 ml medium) was used as inoculum for four fermenter cultures operated in parallel. Details of the fermenter setup are provided in (Zech *et al.*, 2013a). Reference state were cultures grown in Erlenmeyer flasks with glucose. Contrary to this publication, here metabolomic data was only compared between samples derived from bioreactors, using cultures grown in glucose as reference state for statistical data analysis.

2.13.2 Dynamics of amino acid utilisation

In this time-dynamic experiment, uptake and utilisation of casamino acids were investigated. Minimal medium contained 10 g/l casamino acids (A157, Carl Roth, Karlsruhe, Germany). Sampling points were 10, 15, 20, 25, 30 and 35 h after inoculation. Reference state was the first sampling point, 10 h, respectively 0 h (uninoculated medium) in case of supernatants.

2.13.3 Casamino acid consumption by plasmid-cured strains

The impact of the smallest and the largest plasmid on growth and casamino acid utilisation was studied using the following plasmid-cured strains: Δ65kb, Δ262kb, Δ65kbΔ262kb, the natural isolate “M3” lacking the 262 kbp plasmid, plus the wild-type strain DSM 17395 as reference (see table 4 for details). Cells were cultivated in minimal medium containing 10 g/l casamino acids (A157, Carl Roth, Karlsruhe, Germany). Here, only samples for exometabolomic analyses were taken, in particular 18, 24 and 36 h after inoculation; reference state was t_0 (uninoculated medium).

2.13.4 Amino acid degradation

Single amino acids were used to study and to refine complex catabolic networks, which were unclear in regard to the original genome annotation. Minimal medium contained one of nine selected amino acids or succinate (20 mM) as reference condition. The selected amino acids were: *L*-tryptophan (5 mM), *L*-phenylalanine (5 mM), *L*-methionine (20 mM), *L*-leucine (15 mM), *L*-isoleucine (15 mM), *L*-valine (15 mM), *L*-histidine (15 mM), *L*-lysine (15 mM), and *L*-threonine (15 mM). Sampling was performed at ½ OD_{max}, plus t_0 for exometabolomic analysis.

2.13.5 Carbohydrate degradation

Single carbohydrates were used to study and to refine complex catabolic networks, which were unclear in regard to the original genome annotation. Minimal medium contained one of five selected carbohydrates or succinate (20 mM) as reference condition. The selected carbohydrates were: *N*-acetyl-glucosamine (5 mM), mannitol (5 mM), sucrose (2.5 mM), glucose (5 mM) and xylose (5 mM). Sampling was performed at ½ OD_{max}, plus t_0 for exometabolomic analysis.

2.13.6 Metabolic responses to ammonium limited growth condition

The metabolic responses of *P. inhibens* DSM 17395 to limited ammonium content were studied using minimal medium with only 1 mM NH_4Cl concentration (instead of 4.7 mM). 5 mM glucose were provided as carbon source. Sampling was performed 15, 20, 25, 30, 40, 50, 60, 75 and 90 h after inoculation, plus t_0 for exometabolomic analysis. Reference state was t_{30} (½ OD_{max}).

2.14 Details and modifications of main experiments

Harvesting, sample preparation and GC-MS analysis of conducted main experiments (Section 2.13) were essentially performed as described in sections 2.8.4, 2.11 and 2.12. Details and modifications are listed in table 9.

Table 9: Overview of sample preparation modifications for GC-MS analysis of main experiments, conducted in cooperation with the ICBM (see Section 2.13). (1) Adaptation to growth with complex nutrients; (2) Dynamics of amino acid utilisation; (3) Casamino acid consumption by plasmid-cured strains; (4) Amino acid degradation; (5) Carbohydrate degradation; (6) Metabolic responses to ammonium limited growth condition.* MSTFA was spiked 10% (v/v) with alkane mix; [a], sum of biological and technical replicates.

	(1)	(2)	(3)	(4)	(5)	(6)
Intracellular metabolomic analysis						
Number of replicates[a]	3 or 12	12		12	12	5-6
Washing solution for cell pellets	Tris/HCl buffer	Tris/HCl buffer		0.9% (w/v) NaCl	3.7% (w/v) NaCl	3.7% (w/v) NaCl
Ribitol content (µl) per 1.5 ml ethanol	60	60		60	30	30
Volume of polar phase dried for analysis (µl)	500	500		500	1000	1000
Derivatisation	manual	manual		automatic	manual	manual
Methoxyamine (µl)	40	40		20	40	40
MSTFA (µl)	70 *	60		35	60	60
GC-MS instruments	Leco	Leco		Leco	Leco Jeol	Leco
Injection method	splitless	splitless		splitless	splitless	splitless
Scans per second	20	8		8	8 (Leco) 5 (Jeol)	8
Exometabolomic analysis						
Number of replicates[a]	3-6	4	4	4	4	4
Harvesting procedure for supernatants	centri-fugation	centri-fugation & filtration	centri-fugation & filtration	filtration	filtration	filtration
Volume of supernatant used for analysis (µl)	90 (of MB medium) 25 (of minimal medium)	100	20	50	50	150
Added solvent	H_2O	ethanol	ethanol	H_2O	H_2O	H_2O
Volume of solvent added (µl)	110 (for MB medium) 175 (for minimal medium)	500	180	100	100	100
Volume of ribitol solution (µl)	8	20	14.4	8	8	40
Derivatisation	manual	manual	automatic	automatic	manual	manual
Methoxyamine (µl)	40	40	40	40	40	40
MSTFA (µl)	60 *	60	70	60	60	60
GC-MS instrument	Leco	DSQ	Leco	Leco	Jeol	Jeol
Injection methods	splitless	split 1:25	splitless	splitless	splitless, split 1:15	splitless, split 1:15
Scans per second	20	2.5	8	8	5	5

2.15 GC-MS data processing

Raw data obtained from the GC-MS instruments were exported as NetCDF (network common data format) files without data smoothing, except for data obtained from the Jeol JMS-T100GC Accu TOF MS, where noise was removed using a filter-treshold of 20%. Data was processed using the correspondent latest releases of TU-BS branch of the MetaboliteDetector software (Hiller *et al.*, 2009), which was under development from 2011 to 2013 by Christian Nieke (TU Braunschweig). This software automatically deconvolutes all mass spectra from a chromatogram and calculates the retention indices based on the formula 1 using a retention index (RI) marker, in this case an alkane mix (Section 2.5.4).

$$RI^{(T)} = 100 \cdot [(y - x) \cdot (\frac{\log(t_i) - \log(t_x)}{\log(t_y) - \log(t_x)}) + x] \qquad \text{(Formula 1)}$$

with $RI^{(T)}$ = retention index in a temperature gradient,
x = number of carbon atoms of the alkane eluting before the analyte,
y = number of carbon atoms of the alkane eluting after the analyte,
t_i = retention time of the analyte,
t_x = retention time of the alkane eluting before the analyte,
t_y = retention time of the alkane eluting after the analyte.

Additionally, the retention indices were aligned to the internal standard ribitol (RI = 1727.1), by moving the chromatograms in average about 2 RI units forward or backward. Compounds were automatically identified by comparison of mass spectra and retention indices with a defined spectra-library (MD-Library 2014-03-31) as described by Hiller *et al.* (2009), using a cut-off score of 70% similarity. For most metabolites, one appropriate fragment ion for quantification (in regard to specificity and intensity) was defined in the library. Otherwise, one unique fragment ion was selected by the software for each individual metabolite. If necessary, quantification ions were curated manually.

Reproducible compounds (detectable in at least 50% of all samples belonging to one sample group) that could not be identified were added to the library and regarded to be formed specifically under tested conditions. Unidentified compounds are termed “Unknown” and possess an identifier created by retention index, an acronym of the organism and experimentalist, and a consecutive number, e.g. “Unknown#1361.3-pin-mhe_010”. Unknowns, originating from the Golm Metabolome Database are mostly named with “NA” and a consecutive number.

To reduce the number of zero-values for compounds of low abundance, an extended

single ion chromatogram scan was performed. Here, chromatograms are searched in a user-defined retention range (maximal 5 RI units, respectively 2 in case of sugar compounds) for the selected quantification ion; the outcome of this scan was checked manually. Data were normalised by the internal standard ribitol and blank was deduced. Then, data were normalised to the exact cell wet mass and finally by a central normalisation to the reference state (Figure 5). Next, all methoximated and/or silylated derivatives originating from one single compound were summed, using itool.

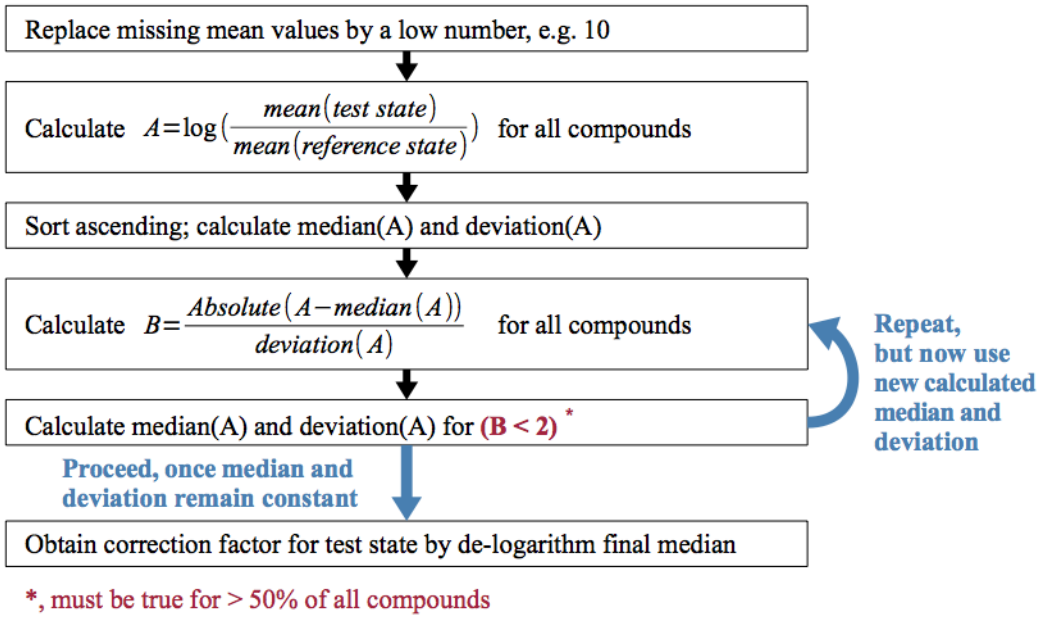

Figure 5: Procedure for central normalisation to deduce influence of sample concentrations.

2.16 Statistical data analysis

2.16.1 Significance tests

Due to the limited sample numbers in metabolomics and related "omics experiments", conducting proper statistical data analysis is challenging and requires correct assumptions and selection of appropriate tests to avoid false discoveries. The applied procedure here is based on recommendations of Broadhurst and Kell (2006) and was performed as follows.

For each sample-group, each metabolite was tested on normal distribution, using the Shapiro-Wilk test, which possesses high power and is still reliable for sample numbers, $n < 50$ (Shapiro and Wilk, 1965). Null hypothesis is that quantification via GC-MS result

in normal distributed data, which is not necessarily the case, especially for overloaded or weak signals. If the p-value was < 0.1, the null hypothesis was rejected, meaning that the corresponding metabolite was not normal distributed in that specific sample group. However, as higher p-values do not necessarily validate normal distribution, the null hypothesis was also rejected, if the variances were high, e.g. in case of individual outliers.

ANOVA (Analysis of Variance) with Holm-Bonferroni correction (Holm, 1979) and the non-parametric Kruskal-Wallis test (Kruskal and Wallis, 1952) with false discovery rate control (Benjamini and Hochberg, 1995) were used to recognise metabolites with altered abundances between sample groups; p-values < 10^{-4} were considered to be significant. For detailed elucidation of these differences, each test condition was tested against the reference condition, and in case of time-course experiments also two sequent sampling points were tested against each other. If both conditions to be compared, were normal distributed, a both sided t-test, assuming equal variances, with Holm-Bonferroni correction was used; otherwise the non-parametric Wilcoxon-Mann-Whitney test (Wilcoxon, 1945; Mann and Whitney, 1947) with false discovery rate control was used. If not indicated otherwise, for both tests p-values < 10^{-3} were regarded to be significant.

Further, fold changes of metabolite abundances (quotient of the mean values 'test state' and 'reference state') were included into the analysis; fold changes > 2, or < 0.5 were considered to be significant, depending on variances. Errors of fold changes were calculated using propagation of uncertainty (Formula 2).

$$error\ of\ fold\ change = \sqrt{\left(\left(\frac{(SE(t))}{(mean(t))}\right)^2 + \left(\frac{(SE(r))}{(mean(r))}\right)^2\right)} \cdot \left(\frac{mean(t)}{mean(r)}\right) \qquad \text{(Formula 2)}$$

with t = test state,
r = reference state,

$SE = standard\ error = \frac{standard\ deviation}{\sqrt{(n)}}$, n = number of replicates.

2.16.2 Visualisation of datasets

For intuitive understanding of the complex datasets, obtained by metabolomic analyses, visualisation was of special importance. Visualisation was conducted with the softwares OriginPro, R and MultiExperiment Viewer (Section 2.6) on basis of post-processed result tables obtained from MetaboliteDetector (Section 2.15).

Hierarchical clustering was applied to recognise correlation between sample groups and between metabolites. Metabolites and samples are clustered according to their similarity, which is represented by the euclidean distances of a dendrogram. Correlation analyses were mostly based on Spearman's rank correlation. Alternatively, Pearson coefficient or Kendall's (τ) coefficient were used. Heatmaps were applied to visualise metabolite abundances, or correlation, on basis of colouring, for this data had to be log2-transformed first. Scatterplots were used to directly compare the metabolite abundances between two states by plotting normalised peak areas on a double logarithmic scale. Further, for better visualisation of the differences, a bisecting line was inserted.

3 Results

3.1 Biolog phenotypic microarray analysis

For determination of substrate-uptake and utilisation capabilities of *Phaeobacter inhibens* DSM 17395, phenotypic microarray analysis was applied. 190 carbon sources (PM1 and PM2), and 95 nitrogen sources (PM3) were tested. The procedure of this analysis is described in detail in section 2.8.1.

In this assay, the respiratory activity of the bacterium was measured by monitoring colour changes of the tetrazolium dye. The dye is colourless and turns purple when reduced by electrons, here by reduction equivalents like NADH or NADPH (Bochner, 2009). The colour change was monitored over 72 h, resulting in kinetic plots for each substrate. To evaluate the bacterial response to specific substrates, area, height and slope of the obtained curves were taken into account. However, a positive response is actually only an indicator of transport capabilities and presence of required catabolic enzymes, but does not necessarily prove usability of the substrate for anabolic purposes, whereas negative spots clearly indicate missing transporter and/or catabolic enzymes.

Overall 81 carbon sources (Figure 6) and 72 nitrogen sources (Figure 7) were clearly positive in regard to respiratory activity.

3.1.1 Carbon sources

The strongest responses for carbon sources were observed for amino acids and monosaccharides (Figure 6). All tested *L*-amino acids were clearly positive, with the exception of *L*-valine (P4), which gave only a weak response and *L*-pyroglutamate (P3), which was negative. Also amino acid derivatives (O3, O8) and dipeptides (F1, G1, G6, H1) were clearly positive, whereas of tested *D*-amino acids (A9, B1, D2, F4) only *D*-alanine was positive. Similar strong responses as for amino acids were observed for carboxylates, like pyruvate (H8), *L*-lactate (B9), acetate (C8), butanoates derivatives (D7, E7, L10, L12, M8), and TCA cycle intermediates (A5, D6, F2, F5, G11).

Common natural sugars, like *N*-acetyl-glucosamine (A3), *D*-galactose (A6), *D*-fructose (C7), *D*-glucose (C9), *D*-xylose (D8) and *D*-mannitol (B11) were positive, whereas other

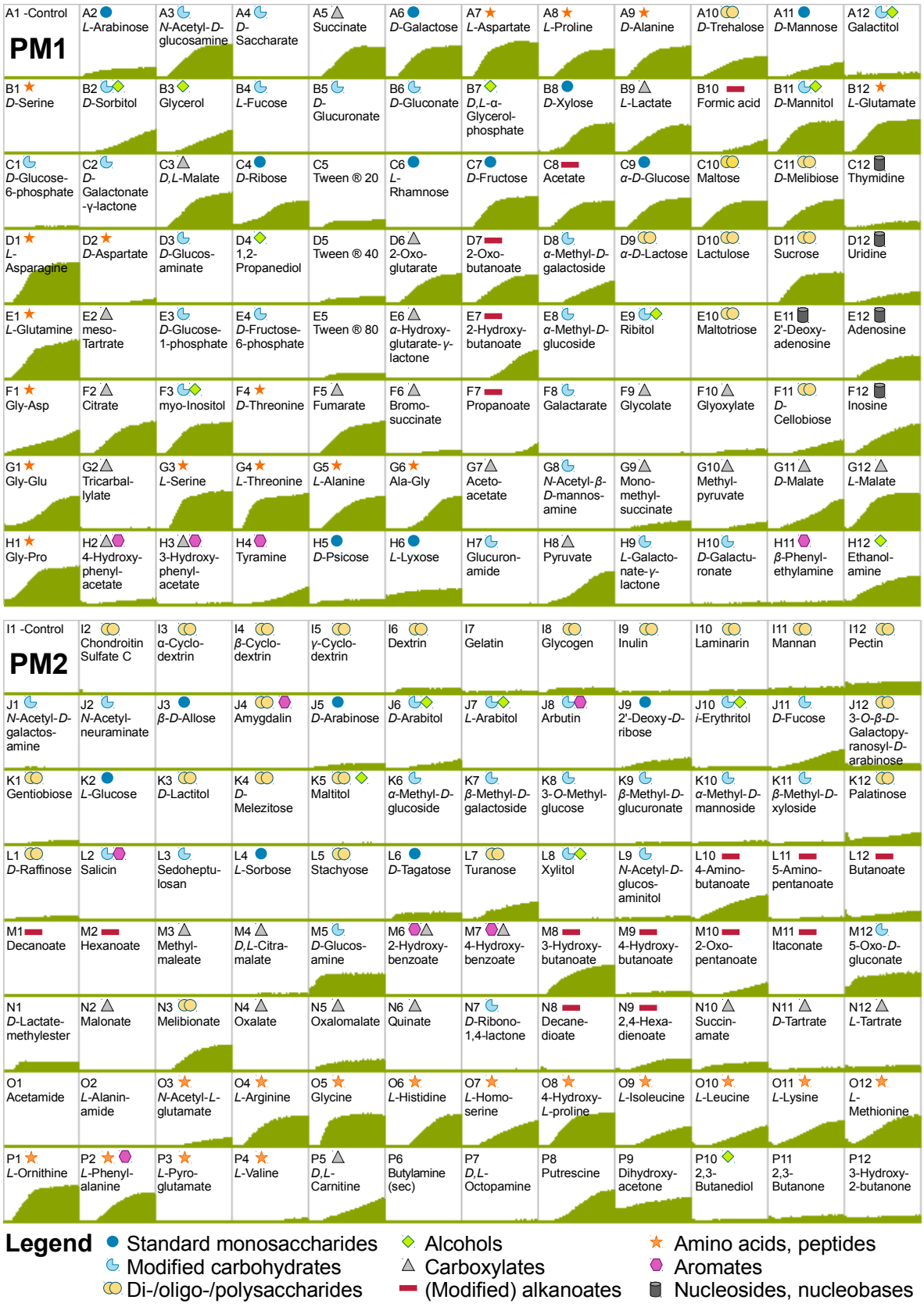

Figure 6: Phenotypic microarray analysis of carbon sources. The curves represent the amount of reduced tetrazolium dye as indicator for respiratory activity; which was monitored over 72 h in PM1 (lines A – H) and PM2A (lines I - P); the orthogonal scale was set to a maximum of 500.

monosaccharides and especially sugar-derivatives, like acidic monosaccharides (A4, B5, B6, F8, H10), phosphorylated sugars (C1, E3, E4), or methylated sugars (K6 – K11), were negative. Otherwise, some of the tested disaccharides showed strong responses (e.g. A10, C10, C11, D11, F11), whereas oligo- and polysaccharides were negative (Q2 – Q12), with the exception of dextrin (Q6) and glycogen (Q8), which might probably be positive.

The range of utilisable carbon sources also includes some nucleosides (C12, D12, E12, F12), some amines, like ethanolamine (H12), tyramine (H4) or putrescine (P8), plus modified short-chain fatty acids, like 2-oxopentanoate (M10) and propanoate (F7). Simple short-chain fatty acids were weakly positive, whereas longer chains, like decanoate (M1) or hexanoate (M2) gave no response at all, which was also true for aromatic compounds, e.g. hydroxyphenlyacetate (H2, H3), *β*-phenylethylamine (H11) and hydroxybenzoate (M6, M7).

3.1.2 Nitrogen sources

P. inhibens DSM 17395 utilises several substrates as nitrogen sources (Figure 7). Ammonia was the only one of tested inorganic nitrogen sources (Q2 – Q4) that gave a positive response. Urea (Q5) was negative, as well as the structurally similar compound biuret (Q6). Of the remaining tested N sources almost all were positive, with similar strong responses. All tested *L*- and *D*- amino acids were positive (Q7 – S12) with the exception of *D*-lysine (S7) and *L*-pyroglutamate (T3). Most of amines and amides, derived from sugars or simple carboxylates were positive (T4 – V1). Nucleosides, nucleobases and associated catabolic intermediates (V2 – W6), aminated short-chain fatty acids (W7 – W12) and all tested dipeptides (X1 – X12) can also serve as nitrogen source for *P. inhibens* DSM 17395.

3.1.3 Substrates tested as carbon and nitrogen sources

Some of the substrates were tested both as carbon and nitrogen source. Most were positive or negative in both tests. Four had specific single usability as carbon or nitrogen source. Tyramine (H4, U3) was only positive as carbon source, whereas 5-amino-pentanoate (L11, W11), *D*-aspartate (D2, S5) and *D*-serine (B1, S8) were only positive as nitrogen sources. Butylamine, *β*-phenylethylamine, *N*-acetyl-galactosamine and *N*-acetyl-

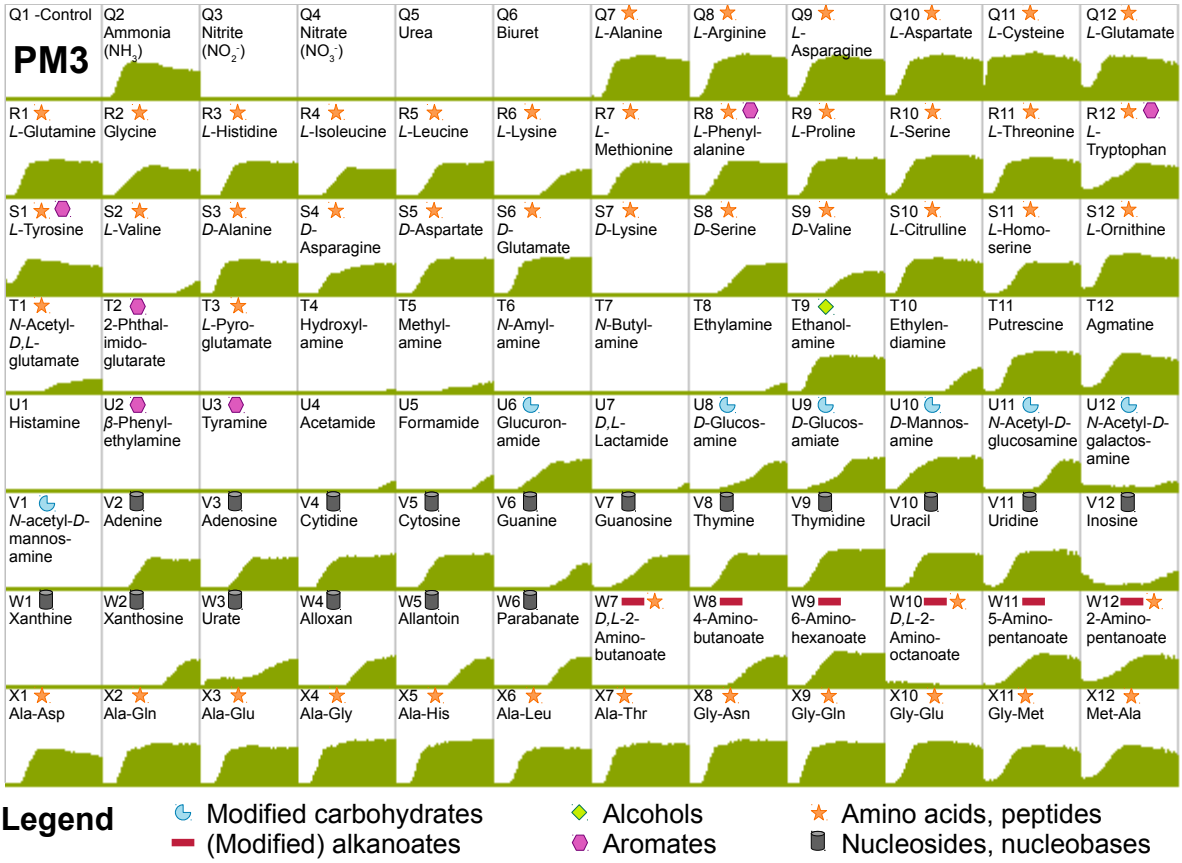

Figure 7: Phenotypic microarray analysis of nitrogen sources. The curves represent the amount of reduced tetrazolium dye as indicator for respiratory activity; which was monitored over 72 h in PM3B (lines Q - W); the orthogonal scale was set to a maximum of 500.

mannosamine could neither be used as carbon nor as nitrogen source. *L*-amino acids (except for pyroglutamate), the nucleosides thymidine, adenosine, uridine and inosine, the dipeptides Ala-Gly and Gly-Glu, as well as 4-aminobutanoate, ethanolamine, putrescine, *D*-glucosamine and *N*-acetyl-glucosamine were positive under both test conditions.

3.2 Isotope labelling

P. inhibens DSM 17395 was supplied with standard glucose or [U-^{13}C] glucose, cells were harvested at ¾ OD_{max}, intracellular metabolites extracted from cells were analysed via GC-MS. By comparison of spectra derived from cells cultivated with isotopic labelled or unlabelled glucose, *m/z* shifts could be observed as a result of integration of ^{13}C instead of ^{12}C atoms into biomolecules. This enabled determination of compounds of biological origin. Still, whether such compounds were indeed synthesised by *P. inhibens* DSM 17395 or were formed from labelled compounds during sampling procedure might be ambiguous.

Clear *m/z* shifts were observed for 61 metabolites, whereas low concentrated compounds could not be analysed due to limited spectra quality. Three compounds (benzoate, lactate and octanoate) showed minor *m/z* shifts and have to be regarded as partial contaminants. 20 compounds, amongst these solvents, like cyclohexane and pyridine, as well as carbon-free compounds, phosphate, hydroxylamine and borate, showed no isotope labelling. This was also true for some organic compounds, like hexadecanoate, octadecanoate and toluate.

This experiment also enabled detection of 20 new unknowns, showing clear *m/z* shift of mass fragments and were added to the internal mass spectral library. Due to labelling, structure-prediction of these compounds was partially possible (Table 10). A list of labelled and unlabelled compounds is provided in the supplementary material S1.

Table 10: Unidentified compounds detected in *P. inhibens* DSM 17395, that showed clear *m/z* shifts when the bacterium was supplied with [U-^{13}C] glucose. Compounds are sorted ascending by retention index; scenario numbers correspond to main experiments as defined in section 2.14.

Compound	Detected in scenarios	Structure prediction
Unknown#1004.0-pin-mhe_001	4,5,6	small molecule, about 3 carbons
Unknown#1361.3-pin-mhe_010	1,2,5	4 carbons, probably pyrimidine derivative
Unknown#1366.9-pin-mhe_011	2,4,5	5 carbons
Unknown#1456.4-pin-mhe_014	2	4 or 5 carbons, probably (di-)carboxylate
Unknown#1589.9-pin-mhe_029		minimum 5 carbons, N-containing, only 1 TMS.
Unknown#1635.2-pin-mhe_031	1,2,4,5	2 or more TMS groups
Unknown#1651.8-pin-mhe_032	5,6	6 carbons, probably sugar
Unknown#1671.7-pin-mhe_019		6 carbons, minimum 2 TMS groups, might contain amine and carboxylate.
Unknown#1684.4-pin-mhe_034		6 carbons, minimum 2 TMS groups, might contain amine and carboxylate.
Unknown#1830.2-pin-mhe_038	1,2,5	sugar compound of more than 6 carbons
Unknown#1856.7-pin-mhe_040	5	probably sugar
Unknown#1937.2-pin-mhe_021	5	hexose-acid
Unknown#1946.5-pin-mhe_024	2,5	hexose, might contain a carboxy group
Unknown#1955.0-pin-mhe_027	5	hexose-acid
Unknown#2018.7-pin-mhe_028	2,4,5	phosphorylated, might be pentose-phosphate
Unknown#2078.9-pin-mhe_042	4	modified sugar
Unknown#2135.2-pin-mhe_044		similar to hexose-phosphate
Unknown#2334.1-pin-mhe_051	2,5	similar to hexose
Unknown#2363.8-pin-mhe_052	1	similar to hexose-phosphate
Unknown#2678.8-pin-mhe_069		similar to disaccharide

3.3 Main experiments

3.3.1 Adaptation to growth with complex nutrients

3.3.1.1 Growth characteristics

P. inhibens DSM 17395 was cultivated in peptone and yeast-extract containing complex medium (MB medium) or in glucose-containing minimal medium (GM medium). This scenario simulates nutrient-rich conditions during collapse of phytoplanktonic bloom, respectively replenished nutrient conditions. Cells were cultivated in Erlenmeyer flasks and process-controlled bioreactors and were harvested for analysis at ½ OD_{max}. Samples from Erlenmeyer flasks, glucose medium served as reference condition.

Due to medium adapted cells, no noticeable lag-phase was observed for either media. MB medium yielded considerably shorter lag-phase, higher growth rate and higher maximum optical density, compared to minimal medium (Figure 8).

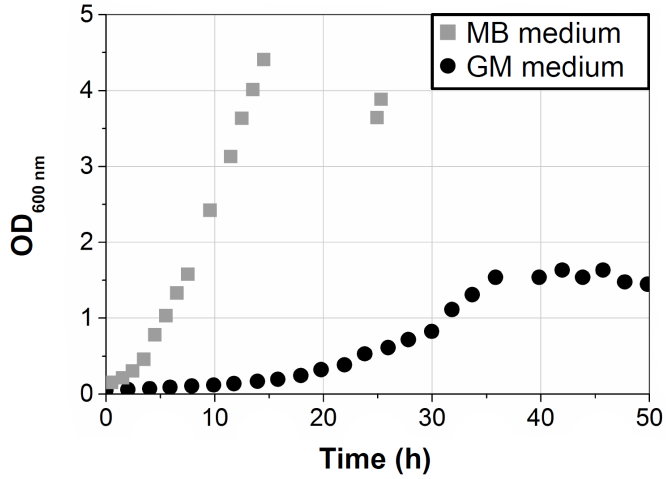

Figure 8: Growth of *P. inhibens* DSM 17395 in Marine Broth medium and glucose-containing minimal medium. Cultivation was conducted in process-controlled bioreactors. Abbreviations: MB medium, Marine Broth medium (complex medium); GM medium, glucose-containing minimal medium.

3.3.1.2 Extracellular metabolomic analysis

The actual composition of MB medium is unclear in regard to availability and concentration of individual organic molecules. GC-MS analysis of the medium allowed identification of 54 different compounds. Compared to t_0, 49 compounds were less

abundant at ½ OD_{max}, two were more abundant, which were urea (≈ 90-fold higher concentrated), and 2-hydroxyphenylacetate (only detected at ½ OD_{max}). Three compounds showed no abundance changes: cyano-alanine, glucose, and borate. For most of the identified substrates, complete consumption or depletion rates of more than 50% of the initially provided amount were observed. Only three substrates were less than 20% depleted (phenylalanine, threonine and 4-hydroxybutanoate). In contrast to this, amino acids (especially glutamate, glycine, alanine and aspartate), organic acids, (citrate and succinate) and specific disaccharides showed high depletion rates. Also some nucleosides and nucleobases were significantly depleted. A complete list of identified substrates and their depletion rate at ½ OD_{max} is provided in the supplementary material S2.

3.3.1.3 Intracellular metabolomic analysis

Both proteomic and metabolomic analyses revealed considerable intracellular differences between the two tested media. Samples derived from MB medium revealed a rich repertoire of proteins, comprising a high number of different transporters and catabolic enzymes for several substrates (Zech *et al.*, 2013a). The metabolomic dataset consists of 155 detected compounds, 134 of which could be identified; 99 of these identified had a fold change > 1.5, or < 0.67. Correlation analysis combined with hierarchical clustering revealed that medium was the main responsible factor for metabolic abundance changes. Cultivation vessels, i.e. Erlenmeyer flask or bioreactor had minor impact on sample clustering, which might be due to the vessel or biological variances (Figure 9).

Here, only samples derived from bioreactors were compared and statistically evaluated. Most metabolites were not normally distributed. Thus the significance of abundance changes was determined using the non-parametric Wilcoxon-Mann-Whitney test with false discovery rate control. Moderate significant p-values < 0.01 were observed for 56 of the identified metabolites, significant p-values < 0.001 were observed for 28 metabolites. For metabolites, absent in one of the tested groups, no p-value could be calculated (Supplementary material S3).

Abundance changes involve metabolites both more abundant and less abundant in cells derived from MB medium (Figure 10, Table 11, Supplementary material S3). Amongst the higher concentrated metabolites were imported substrates, especially amino acids, dipeptides and disaccharides (e.g. proline, tryptophan, tyrosine, glycyl-glycine, lactose,

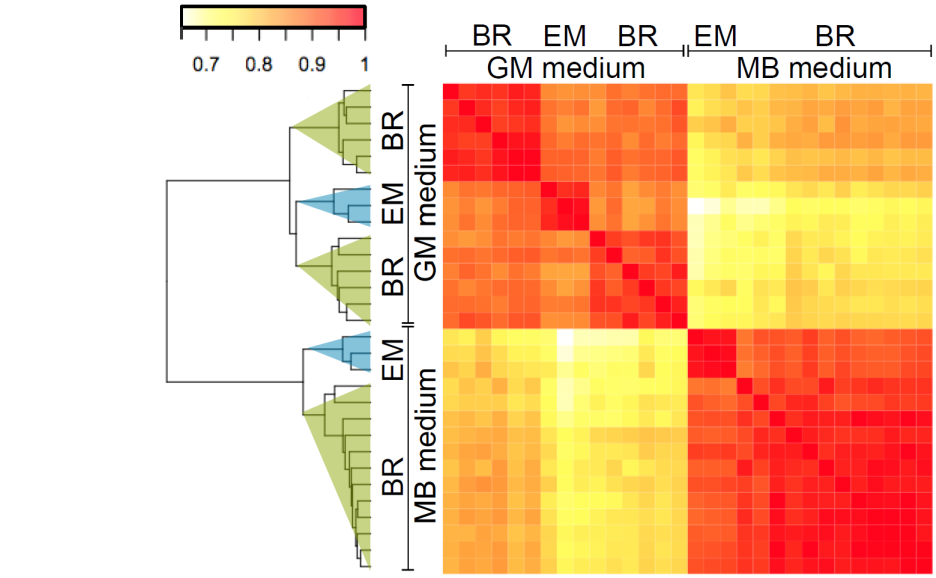

Figure 9: Correlation matrix of intracellular metabolomic data from the experiment "adaptation to growth with complex nutrients". Spearman method was used for calculation of correlation; which is visualised as heatmap, red colour represents high correlation. Dendrogram is based on euclidean distance. Abbreviations: GM medium, glucose minimal medium; MB medium, Marine Broth medium; BR, samples derived from bioreactor; EM, derived from Erlenmeyer flasks.

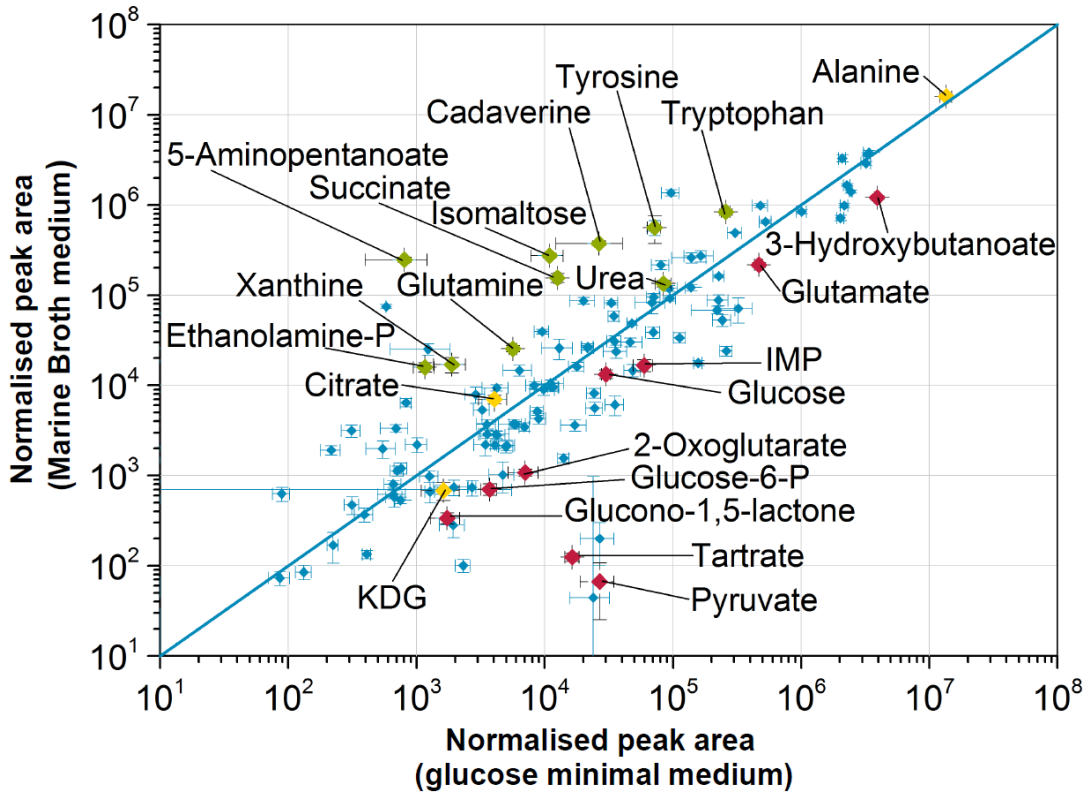

Figure 10: Scatter plot of intracellular metabolomic data from cultivation in bioreactor with complex or minimal medium. Normalised peak areas of identified metabolites were plotted in double logarithmic scaling. Colouring of metabolites: green: significant increased; red: significant decreased; yellow: not significant changed abundance in cells grown in complex medium. Abbreviations: IMP, inosine-5'-monophosphate; KDG, 2-keto-3-deoxy-gluconate.

isomaltose and maltotriitol). Accordingly, also intermediates involved in degradation of amino acids were very abundant (e.g. 5-aminopentanoate, cadaverine and 4-hydroxy-phenylacetate). In addition, some purines and pyrimidines were more abundant (e.g. uridine-5'-monophosphate, guanosine-5'-monophosphate, adenosine-5'-monophosphate, xanthine and hypoxanthine), whereas inosine-5'-monophosphate and adenine were significantly less abundant.

Further, elevated levels of $C_{18:1}$, glycerol-3-phosphate and ethanolamine-phosphate were observed. These or similar membrane associated compounds were not detected extracellularly, in contrast to detected nucleosides and nucleobases that were significantly depleted at ½ OD_{max} (Supplementary material S2). Accordingly, some of such compounds were more abundant, especially xanthine and hypoxanthine, which are associated with purine degradation, respectively with purine salvage pathway.

Several metabolites were less abundant compared to cells derived from minimal medium (e.g. 3-hydroxybutanoate and tartrate). Especially intermediates associated with Entner-Doudoroff pathway and Embden-Meyerhof-Parnas pathway, which are used for glucose degradation in *P. inhibens* DSM 17395 (Zech *et al.*, 2009) were less abundant, (e.g. glucose-6-phosphate, glucono-1,5-lactone, 2-keto-3-deoxy-gluconate and pyruvate).

Table 11: Fold changes of selected intracellular metabolites from the experiment "adaptation to growth with complex nutrients". Fold changes of abundance in cells grown in MB medium, as compared to cells grown in minimal medium. Significance of abundance changes was calculated with Wilcoxon-Mann-Whitney test and false discovery rate control: * p-value < 0.01; ** p-value < 0.001. See supplementary material S3 for complete list of metabolites.

Metabolites	Fold change	Metabolites	Fold change
Adenine	0.3 ± 0.1 **	Inosine-5'-monophosphate	0.3 ± 0.1 *
Adenosine-5'-monophosphate	4.3 ± 1.0 **	Isomaltose	25.2 ± 14.5 *
5-Aminopentanoate	≈300 ± 147 **	2-Keto-3-deoxy-gluconate	0.4 ± 0.2
Cadaverine	14.2 ± 7.7 **	Lactose	14.1 ± 3.7 *
Citrate	1.7 ± 0.5	Malate	1.9 ± 0.7
Ethanolaminephosphate	14 ± 3 **	Maltotriitol	≈100 ± 43
Fumarate	0.1 ± 0.0 **	Octadecenoate ($C_{18:1}$)	2.2 ± 0.6
Glucono-1,5-lactone	0.2 ± 0.0	2-Oxoglutarate	0.2 ± 0.0 *
Glucose-6-phosphate	0.2 ± 0.0 **	Proline	1.6 ± 0.2 *
Glutamate	0.5 ± 0.0 **	Pyruvate	<0.01 ± 0 *
Glutamine	4.5 ± 0.5 **	Succinate	12.4 ± 1.6 **
Glycerol-3-phosphate	2.5 ± 0.3 **	Tartrate	0.1 ± 0 **
Glycyl-glycine	4.8 ± 1.6 *	Tryptophan	3.2 ± 0.4 **
Guanosine-5'-monophosphate	4.1 ± 1.0 *	Tyrosine	7.9 ± 1.8 **
3-Hydroxybutanoate	0.3 ± 0.0 *	Uridine-5'-monophosphate	8.9 ± 11.4
4-Hydroxyphenylacetate	7.1 ± 3.3	Xanthine	9.0 ± 6.2 *
Hypoxanthine	2.8 ± 0.7		

The lower abundances of intermediates that are associated with carbohydrate catabolism is contradicted by the detected higher amounts of disaccharides.

Catabolic pathways feed into the TCA cycle, which was recently reconstructed for *P. inhibens* DSM 17395 (Zech *et al.*, 2009). Interestingly enough, enzymes of this cycle were only slightly elevated (Zech *et al.*, 2013a), whereupon abundances of metabolic intermediates were considerably and differentially changed. Citrate was slightly more abundant, 2-oxoglutarate and fumarate were significantly less abundant, whereas succinate and malate were more abundant. The low abundance of 2-oxoglutarate correlates with glutamate, but not with glutamine abundance.

3.3.2 Dynamics of amino acid utilisation

3.3.2.1 Growth characteristics and amino acid depletion profile

P. inhibens DSM 17395 was cultivated in minimal medium supplied with 1% (w/v) casamino acids as carbon source. Growth is characterised by a maximum growth rate of 0.17 h^{-1} and an OD_{max} of 4.8 after 35 h of incubation (Figure 11A).

To study the dynamics of amino acid utilisation, supernatants and cells were sampled across the growth curve, i.e. in the lag-phase (t_{10}), exponential growth phase (t_{15}, t_{20}) transition to stationary phase (t_{25}) and stationary phase (t_{30}, t_{35}); subscript numbers represent cultivation time in hours. Supernatants were analysed via GC-MS to determine the depletion pattern of the 15 detectable amino acids. Due to preparation of casamino acids by acidic hydrolysation of casein, glutamine and asparagine are converted to glutamate, and aspartate respectively. Histidine concentration is below limit of detection. Cysteine and tryptophan are not present. The depletion profile is visualised in figure 11B. Most abundant amino acids are glutamate, proline, leucine and serine. Although most amino acids were essentially utilised in parallel, depletion of individual amino acids after 20 h incubation time is quite different. Amino acids were categorised according to their depletion at t_{20}, (I): rapid, i.e. > 50% utilised (arginine, glycine, aspartate and glutamate), (II) moderate utilisation, i.e. about 28 – 48 % (lysine, alanine, leucine, methionine, tyrosine, proline); slow utilisation, i.e. less than 24% utilisation (serine, phenylalanine and threonine), and (IV) none, i.e. no significant utilisation observed (valine, isoleucine). Growth is neither C nor N limited, at the onset of stationary-phase, t_{25}, since sufficient amino acids are still

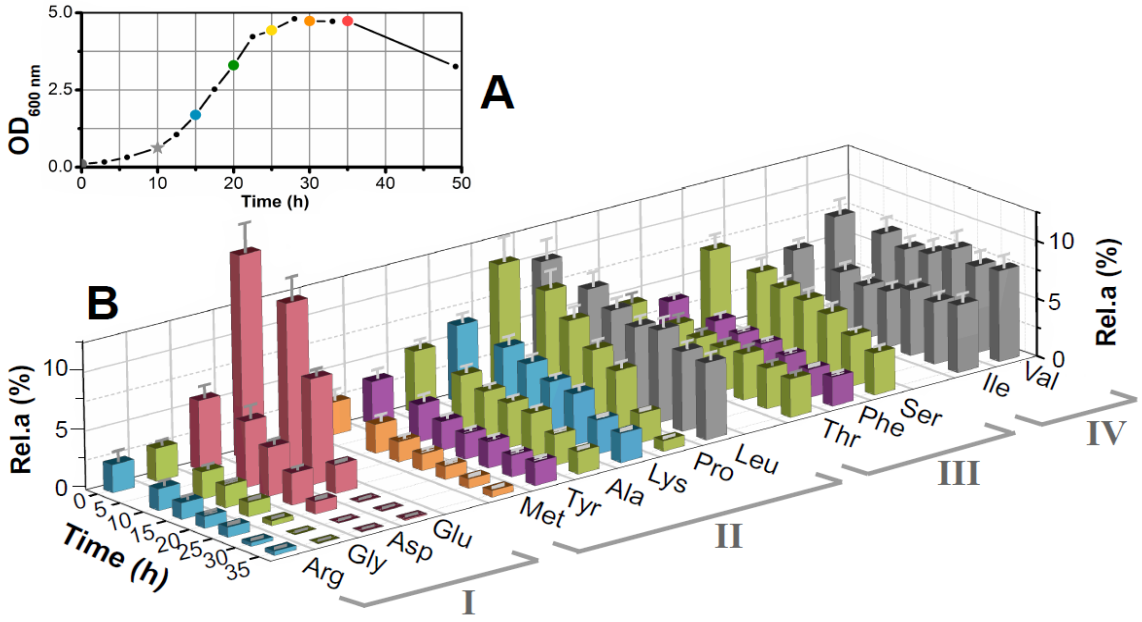

Figure 11: Growth curve of *P. inhibens* DSM 17395 in minimal medium with casamino acids and correspondent time-resolved depletion profiles of provided substrates. (A) Growth curve, as determined by measuring optical density, coloured dots mark sampling points. (B) Depletion profiles of 15 detected amino acids in cell-free culture supernatant. The relative abundance (Rel.a) is given in % of the theoretically pool of all amino acids available at t_0, as calculated on basis of peptide sequences of bovine casein. Categories I to IV according to their differing depletion grades at t_{20}.

available. Beyond t_{25}, after complete consumption of glutamate, amino acids of categories II and III showed higher depletion rates, especially alanine, lysine, proline and serine.

The supernatants were also screened for compounds exported by *P. inhibens* DSM 17395. Besides some metabolites derived from amino acid metabolism (2-hydroxy-phenylacetate and 2-isopropylmalate), a continuous massive accumulation of urea was observed across the time-course (Supplementary material S4).

3.3.2.2 Intracellular metabobolomic analysis

In addition to 1747 proteins as a result of the combination of the different proteomic approaches (Zech *et al.*, 2013b), 111 metabolites were detected, 94 of which could be identified (Supplementary material S5). Of the identified metabolites, 86 showed changed abundances of > 1.5 or < 0.67 in at least one of the test states compared to the reference state t_{10}. As the reference state comprised lowest intracellular metabolite abundances, abundance changes compared to reference were mostly also statistically significant. Accordingly, samples from t_{10} differed strongly from all other samples, as revealed by

Pearson correlation (Figure 12A). Sampling points clustered according to growth phases, although only minor differences of metabolite compositions over the following sampling points were observed. These differences became more apparent through the calculation of Kendall's (τ) coefficient (Figure 12B), and were elucidated by testing consecutive sampling points against each other, either with t-test or with Wilcoxon-Mann-Whitney test, depending on data distribution.

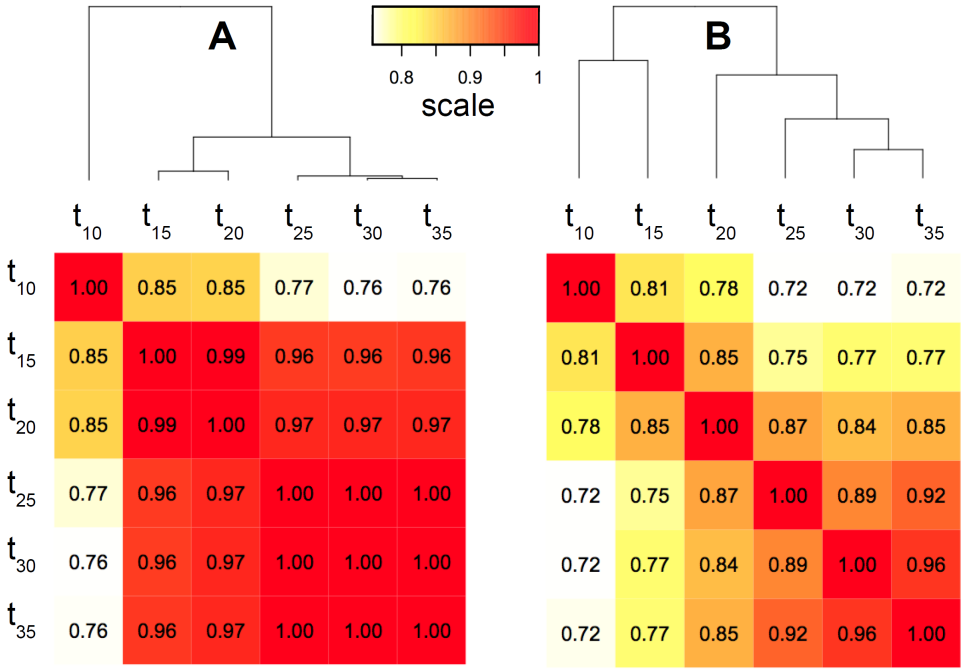

Figure 12: Correlation matrixes of intracellular metabolomic data from the experiment "dynamics of amino acid utilisation". Correlation was calculated with Pearson coefficient (A) or with Kendall's (τ) coefficient (B), and was visualised as heatmap. Red colour represents high correlation between sampling points. Dendrograms are based on euclidean distance. Subscript numbers represent the sampling points in hours. Lag-phase is represented by t_{10}, exponential growth-phase by t_{15} and t_{20}, transition phase from exponential growth to stationary phase by t_{25}, the stationary phase by t_{30} and t_{35}.

For each of the investigated growth-phases specific metabolic characteristics could be determined; the most remarkable results will be described here. The complete list of metabolites and their abundances during the time-course is provided in the supplementary material S5.

The lag-phase is represented by sampling point t_{10}, and is characterised by low metabolite abundances, i.e. most metabolites were more abundant in consecutive sampling points, except for homocysteine, pyroglutamate, putrescine and citrate, which were most abundant at t_{10}. Only few metabolites showed constant abundances over the whole time-course, e.g. adenine, guanine, malate and 2-oxoglutarate.

Accordingly, most metabolites increased significantly in abundance between lag-phase and exponential growth phase (t_{15}, t_{20}), including peptidoglycane associated compounds (alanyl-alanine and 2,6-diaminopimelate), some amino acids (e.g. proline) and intermediates of amino acid catabolism (e.g. cadaverine and pipecolate). Further, highest concentrations of 3-hydroxy- and 4-hydroxybutanoate were observed during exponential growth phase. Others, like the diamines spermidine and putrescine, decreased, as well as the membrane associated compounds glycerol-3-phosphate and glycerol-phospho-glycerol during this growth-phase.

The transition phase between exponential growth and stationary phase is represented by t_{25}. It coincides with the complete consumption of the preferred substrate glutamate. Accordingly, considerable intracellular metabolic abundance shifts could be observed in this growth phase (Figure 13A). Intracellularly, alternative substrates increased in abundance between t_{20} and t_{25}, e.g. alanine, serine, threonine and lysine. For the last one, corresponding catabolic intermediates could be detected (2-aminoadipate, 5-amino-pentanoate, cadaverine and pipecolate), all of which were significantly more abundant at t_{25} compared to t_{20}. Further, also increased abundances for compounds associated with gluconeogenesis or glucose degradation (e.g. dihydroxyacetone phosphate, 6-phospho-gluconate and 2-keto-3-deoxy-gluconate) could be observed. Some nucleotides and derivatives (e.g. adenosine, uridine and uridine-5'-monophosphate), and some fatty acids (e.g. dodecanoate and octadecenoate) were slightly more abundant.

Upon entry into stationary phase (Figure 13B), continued abundance-increase for most of these metabolites was observed (e.g. 6-phosphogluconate, serine and lysine), whereas only few decreased in abundance (e.g. *N*-acetyl-glutamate and glucose). Notably, some lysine degradation intermediates showed opposite abundance patterns: whereas abundance of 2-aminoadipate increased, abundance of 5-aminopentanoate decreased significantly. Between the two sampling points of stationary-phase, t_{30} and t_{35}, only minor differences could be observed. These were rather decline of abundances (e.g. glucose, *N*-acetyl-glutamate, threonine and proline) than rise of abundances (e.g. *β*-alanine, 2-aminoadipate and guanine). However, most metabolites did not show significant abundance changes between these two sampling-points.

In contrast to dynamic abundance-changes, which were observed for a broad range of different metabolites, intracellular concentration of the five detected TCA cycle

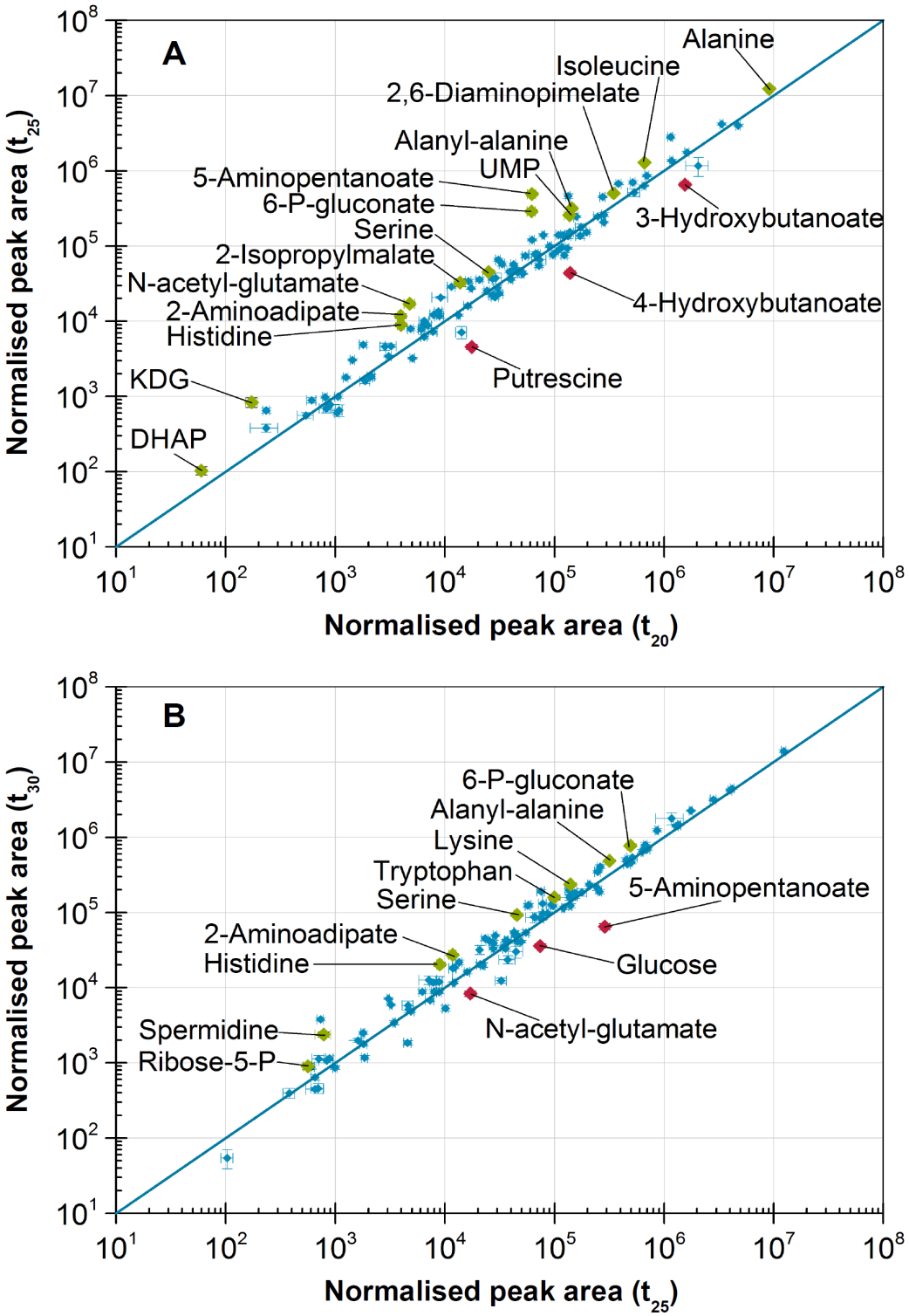

Figure 13: Intracellular metabolic changes in transition phase from exponential growth to stationary phase during cultivation on casamino acids. Normalised peak areas of all metabolites were plotted in double-logarithmic scale. Colouring: green: increased abundance, red: decreased abundance as compared to correspondent previous sampling point. (A) Metabolic shift from t_{20} (exponential growth) to t_{25}. (B) Metabolic shift from t_{25} to t_{30} (stationary phase). Abbreviations: DHAP, dihydroxyacetone phosphate; KDG, 2-keto-3-deoxy-gluconate; UMP, uridine-5'-monophosphate.

intermediates remained relatively constant over the whole time-course. Still, significant abundance changes could be observed for citrate and succinate, but these changes only concern the transition phase from lag-phase to exponential growth-phase. In contrast, fumarate abundances increased steadily during cultivation (Supplementary material S5).

Notably, all 20 proteinogenic amino acids could be detected intracellularly. This includes extracellularly low abundant histidine plus the missing amino acids cysteine, tryptophan, asparagine and glutamine. The intracellular distribution patterns of the last two mentioned amino acids correlate with aspartate, respectively glutamate, i.e. show relatively constant abundances over the whole time-course. However, cysteine and tryptophan are temporarily low abundant at t_{20}, with moderately rise of abundance after t_{20}, whereas abundance of histidine increased clearly after t_{20} (Supplementary material S5).

3.3.3 Casamino acid consumption by plasmid-cured strains

3.3.3.1 Growth characteristics

Most members of the Roseobacter clade possess several plasmids, that encode essential genes for metabolic features and thus are probably one key-element for the global distribution of the Roseobacter clade (Petersen *et al.*, 2013). *P. inhibens* DSM 17395 possesses three extrachromosomal elements, the largest, 262 kbp, is the most relevant plasmid for growth, as it encodes genes for tropodithietic acid biosynthesis. The other two plasmids contain metabolic relevant genes, like hexose-isomerases on the 65 kbp plasmid or the glycine cleavage system on the 78 kbp plasmid.

In this study, the impact of these extrachromosomal elements on growth and substrate utilisation were investigated. For this, the natural "M3" mutant strain, which lacks the 262 kbp plasmid, the three plasmid-cured strains (Δ65kb, Δ262kb, Δ65kbΔ262kb), which lack the 65 kbp, the 262 kbp or both plasmids, as well as the wild-type strain, which served as reference, were cultivated in minimal medium supplied with 1% (w/v) casamino acids. In addition to measurements of optical density, culture supernatants were analysed to study probable different amino acid depletion of these strains. Some minor differences of growth characteristics as compared to time-dynamic amino acid utilisation experiment (see Figure 11A, section 3.3.2.1) could be observed. Here, wild-type reached higher OD_{max} (about 7.0 instead of 5.0).

Growth of Δ262kb, Δ65kbΔ262kb and "M3" mutant strain differed considerably from wild-type, as they reached significant higher OD_{max}, ranging from about 10 in case of Δ262kb up to 15 in case of Δ65kb262kb. While maximum growth rate of Δ262kb was similar to wild-type (both $\mu_{max} \approx 0.18$), "M3" mutant strain and Δ65kb262kb grew considerably faster ($\mu_{max} \approx 0.23$). In contrast to this Δ65kb showed similar growth characteristics as the wild-type (Figure 14).

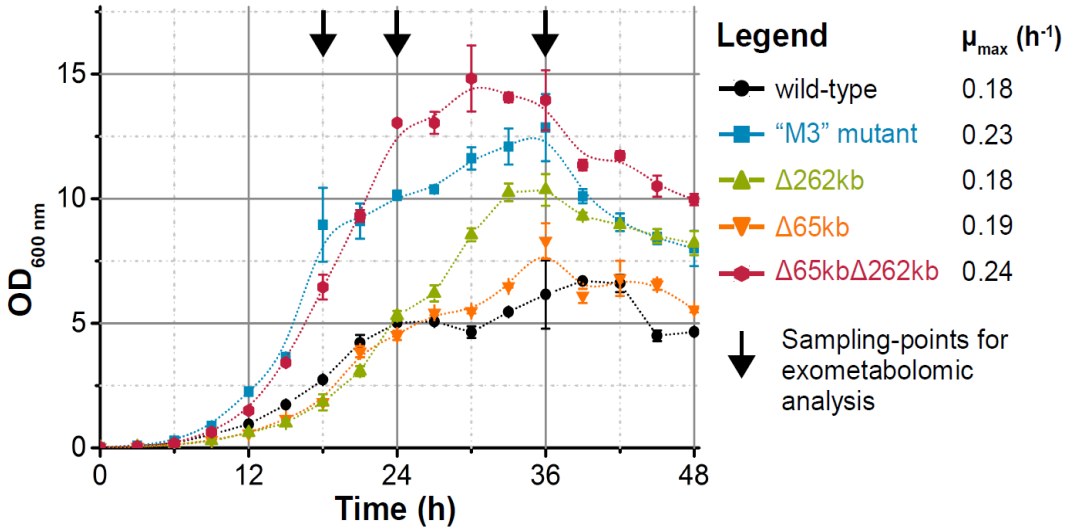

Figure 14: Growth of *P. inhibens* DSM 17395 plasmid-cured strains in casamino acid medium. Beside wild-type, the plasmid-cured strains Δ262kb, Δ65kb, Δ65kb262kb, plus the natural mutant strain "M3", which lacks the 262 kb plasmid, were cultivated in minimal medium, supplied with 1% (w/v) casamino acids. For better visualisation, dot-lines were included.

3.3.3.2 Depletion profile of casamino acids

Samples for exometabolomic analyses were taken during cultivation: after 18 h (exponential growth), 24 h and 36 h incubation. The conducted analyses revealed that depletion profiles of provided amino acids differed considerably between studied strains (Figure 15). While only moderate consumption of amino acids was observed for wild-type (as observed previously, see Figure 11, Section 3.3.2.1), strains lacking the 262 kbp plasmid consumed all provided amino acids. This also includes isoleucine and valine, which were not utilised significantly by the wild-type. However, the depletion profile of amino acids observed for wild-type and Δ65kb were similar.

According to depletion grades of amino acids in the exponential growth phase of the wild-type strain, amino acids were categorised into four groups (see Section 3.3.2.1), ranging from I (favoured amino acids) to IV (not significantly used) (Figure 15E). This

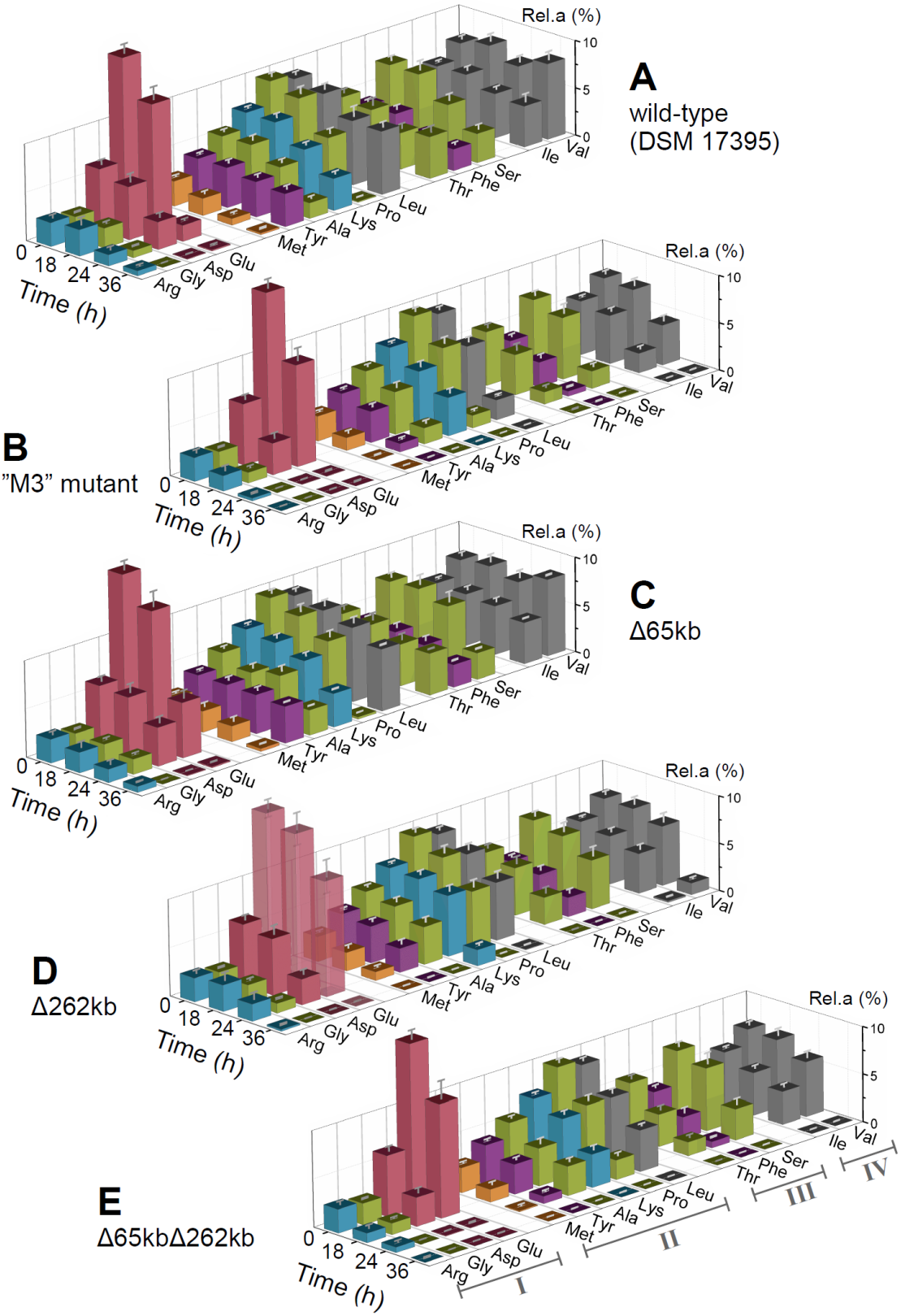

Figure 15: Depletion profiles of casamino acids by wild-type and plasmid-cured strains of *P. inhibens* DSM 17395. The relative abundance (Rel.a) is given in (%) of the theoretically whole pool of amino acids available at t_0. (A) wild-type, (B) "M3" mutant, (C) Δ65kb, (D) Δ262kb, (E) Δ65kbΔ262kb. Categories I to IV according to their differing depletion grades in the exponential growth phase by the wild-type strain as defined in section 3.3.2.1.

preference pattern did not differ between wild-type and the other strains, despite considerable higher consumption rates. All strains preferred the amino acids of category I (arginine, glycine, aspartate and glutamate) as primary nutrient source. Of amino acids of category II, methionine, and proline were slightly more preferred than lysine and leucine by the three strains lacking the 262 kbp plasmid. However, no clear preference by Δ262kb, Δ65kbΔ262kb or "M3" mutant strain for any amino acid of category III (threonine, phenylalanine or serine) was observed; instead similar depletion rates were observed. In contrast to this, in case of the two amino acids of category IV, isoleucine was slightly preferred to valine.

Interestingly, although Δ262kb and "M3" mutant strain should be genetically quite similar, considerable differences in growth and depletion profiles between these two strains were observed. While in case of "M3" mutant strain, most amino acids were already consumed after 24 h, only moderate consumption after 24 h was observed for Δ262kb. By comparison of Δ65kb with wild-type, loss of the smallest plasmid had only minor impact on growth and amino acid consumption. But, if comparing Δ65kb with Δ65kbΔ262kb considerably stronger effects could be observed, as Δ65kbΔ262kb grew significantly faster, reached higher OD_{max} and consumed amino acids faster than Δ262kb.

3.3.4 Amino acid degradation

To study and to refine complex catabolic networks, which remained unclear in regard to the original genome annotation, *P. inhibens* DSM 17395 was grown in minimal medium supplied with one of nine selected *L*-amino acids (tryptophan, phenylalanine, methionine, leucine, isoleucine, valine, histidine, lysine and threonine), or succinate as reference condition. The sampling point for metabolomic analyses was ½ OD_{max}. In addition to GC-MS-based metabolomic analysis, LC-MS analysis was applied to study coenzyme A dependent degradation of tryptophan (see Sections 2.8.3 and 2.10).

3.3.4.1 Growth characteristics

The used substrate concentrations were C-equivalent, with exception of tryptophan and phenylalanine, where only half the amount of carbon was provided. Though, growth characteristics differed considerably dependent on the provided amino acid. According to

reached OD_{max}, substrates were grouped into low OD_{max} (≈ 1.0 to 1.3), moderate OD_{max} (≈ 1.6) (Figure 16A) and high OD_{max} (≈ 2.4 to 3.0) (Figure 16B). Lowest OD_{max} was observed for methionine, associated with slowest growth and longest lag-phase. Amongst the substrates of the first group, highest growth and shortest lag-phases were observed for phenylalanine and histidine, whereas lysine and tryptophan resulted in moderate growth (Figure 16A). Cultures provided with threonine and succinate grew fastest (≈ 2.0 h^{-1}) and had shortest lag-phases. Although branched chain amino acids resulted in high OD_{max}, only a moderate growth rate was observed (1.0 h^{-1}), plus considerably prolonged lag-phases were observed, especially in case of isoleucine (Figure 16B).

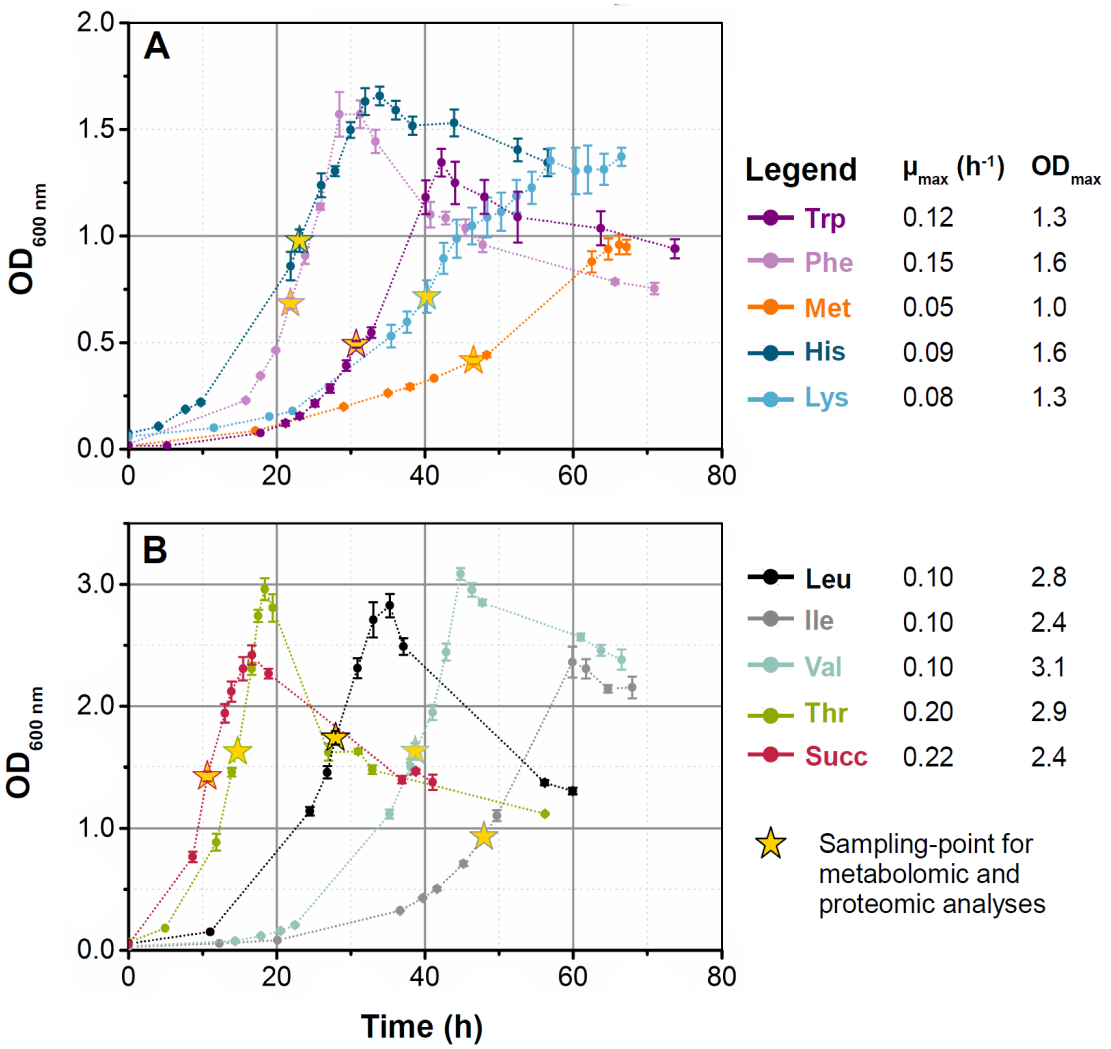

Figure 16: Growth of *P. inhibens* DSM 17395 on selected amino acids. (A) Substrates resulting in low OD_{max}, (B) substrates resulting in high OD_{max}. For better visualisation dot-lines were included. Abbreviations of substrates: Trp, trytophan; Phe, phenylalanine; Met, methionine; His, histidine; Lys, lysine; Leu, leucine; Ile, isoleucine; Val, valine; Thr, threonine; Succ, succinate (reference condition).

3.3.4.2 Extracellular metabolomic analysis

The cell-free supernatant was screened for exported metabolites. Overall, 11 different metabolites could be identified extracellularly. Some were only detected under single cultivation conditions, e.g. 2-aminobenzoate and kynurenine in case of tryptophan, others were detected under several conditions, like 2-isopropylmalate and urea (Table 12).

Table 12: Extracellularly detected metabolites during growth on selected amino acids. Metabolites detected in the corresponding culture supernatant at ½ OD_{max} are marked with "x". Abbreviations of substrates: Trp, tryptophan; Phe, phenylalanine; Met, methionine; Leu, leucine; Ile, isoleucine; Val, valine; His, histidine; Lys, lysine; Thr, threonine; Succ, succinate.

Metabolites	Trp	Phe	Met	Leu	Ile	Val	His	Lys	Thr	Succ
2-Aminobenzoate (anthranilate)	x									
Cadaverine		x						x		
Fumarate										x
2-Hydroxyphenylacetate		x								
2-Isopropylmalate		x				x	x	x	x	
Kynurenine	x									
2-Methylmalonate					x					
4-Methylthio-2-oxobutanoate			x							
Phenethylamine		x								
Phenylpyruvate		x								
Urea		x	x	x	x	x	x	x	x	

3.3.4.3 Refinement of amino acid degradation pathways

The dataset of intracellular metabolomic analysis consists of 132 compounds, 110 of which could be identified. Of identified compounds, 80 were significantly altered in abundance by means of corrected p-value ($< 10^{-6}$) obtained by one of the two conducted multivariate analyses (ANOVA and Kruskal-Wallis test).

In regard to predicted amino acid degradation pathways only a limited number of intermediates could be detected. Some of these were specifically formed under correspondent cultivation conditions or showed considerably higher abundance compared to the reference condition, cells grown with succinate (Table 13, Supplementary material S6 and S7). Since GC-MS-based metabolomic analysis alone could not cover the whole amino acid degradation pathways, proteomic analyses were included to allow unambiguous refinement of these catabolic networks. The resulting networks are discussed in sections 4.3.4.3 to 4.3.4.9.

Table 13: Fold changes of selected intracellular metabolites involved in amino acid degradation from the experiment "amino acid degradation in *P. inhibens* DSM 17395". Explanation of symbols: x, compound only detected in marked test-condition; *, p-value < 0.01; **, p-value < 0.001; ***, p-value < 0.0001. Abbreviations of substrates: Trp, tryptophan; Phe, phenylalanine; Met, methionine; Leu, leucine; Ile, isoleucine; Val, valine; His, histidine; Lys, lysine; Thr, threonine. Complete list of metabolites including their fold changes, errors and p-values of significance is provided in the supplementary material S6 and S7.

Metabolites	Fold change in abundance as compared to cells grown with succinate								
	Trp	Phe	Met	Leu	Ile	Val	His	Lys	Thr
Tryptophan degradation									
2-Aminobenzoate (anthranilate)	2.92 **								
Alanine	0.20 ***	0.16 ***	0.28 ***	1.95 *	0.77	0.94	1.19	0.91	3.96 **
Phenylalanine degradation									
Phenylalanine	0.33 ***	0.43 ***	0.25 ***	0.39 **	0.51 *	0.48 ***	0.42 ***	0.46 **	0.51 **
Phenylpyruvate		2.80 **							0.15
Methionine degradation									
Methionine	0.33 ***	0.74	5.28 **	0.45 **	0.51 **	0.60 *	0.67 *	0.62 *	0.50 **
2-Oxobutanoate			7.11 **						
Leucine degradation									
Leucine	0.58 *	0.58 **	0.36 **	1.19	1.60 *	1.75	0.49	0.69	0.60
Isoleucine degradation									
Isoleucine	0.64	0.40 ***	0.69	0.37 **	24.9	0.93	0.56 *	0.58 *	0.83
3-Methyl-2-oxopentanoate					x				
Valine degradation									
Valine	0.21 ***	0.09 ***	0.10 ***	0.27 **	0.63	5.60 **	0.25 ***	0.37 ***	0.43 **
2-Oxoisovalerate						x			
Histidine degradation									
Urocanate							1.52		
Glutamate	0.03 **	0.06 **	0.07 **	0.64	1.00	0.58 *	1.26	0.25 **	1.32
Lysine degradation									
Lysine	0.05 **	0.13 **	0.36 *	0.24 **	0.55	0.42	0.50 **	3.18	1.12
2-Aminoadipate						0.35 **		0.63	0.04
5-Aminopentanoate			x		x		x	x	
Cadaverine	0.87	2.07 **	14.9 **	1.53 ***	4.39 **	1.57	10.5	116 **	1.12
Glutarate	0.14	0.16	2.22	1.53	6.22 **	1.44	9.29	142	0.15 **
Threonine degradation									
Threonine	0.60 **	0.43 ***	0.62	0.43 **	1.23	0.92	0.85	0.51 **	4.62 **
Glycine	0.45 **	0.32 ***	0.76	0.48 **	0.70	0.94	0.53 *	0.47 ***	0.39 **
Serine	0.42 *	0.54	0.68	0.91	1.56	1.04	1.00	0.72	0.94
Pyruvate	1.72 **	2.69 ***	1.44	2.00 **	1.79	0.77	1.73 ***	1.54 *	1.73 *
Other compounds associated with amino acid metabolism									
Homogentisate		3.72 **							
Hydantoin-5-propionate							x		
4-Hydroxyphenylacetate		3.14 **	0.45		0.06	1.03			
Phenylacetate		1.72 **							
Shikimate-3-phosphate	1.02	2.31	2.68 **	2.66 **	4.64 **	3.48 **	2.10 **	2.38	2.44 **
TCA Cycle									
2-Oxoglutarate	1.31	1.50 *	0.71	1.02	1.00	0.93	1.19	1.10	0.93
Citrate	1.16	1.11	0.57	1.10	0.97	1.04	2.24 *	2.70 ***	1.57
Fumarate	0.64	0.60 **	0.62	1.20	0.86	1.25	0.95	0.66 *	1.00
Malate	0.50 **	0.54 **	0.40 **	1.37	0.67	0.77	1.11	0.66 *	0.89
Succinate	0.55 *	0.45 ***	0.55	1.49 *	1.38	1.32	0.95	0.66	1.34 *

Colour scale for fold changes:	<0.1	<0.2	<0.4	<0.67	0.67–1.5	>1.5	>2.5	>5.0	>10.0

3.3.4.4 Coenzyme A analysis

While the coenzyme A (CoA)-dependent degradation pathways of branched chain amino acids and phenylalanine could be covered completely by conducted proteomic and GC-MS-based metabolomic analysis, tryptophan degradation remained ambiguous. Thus, an additional LC-MS analysis was performed to refine this pathway in *P. inhibens* DSM 17395. Cells grown on succinate served as reference.

Results of this analysis are shown in figure 17. Overall, 40 different CoA derivatives could be detected. Due to limited number of available standards, identification may be ambiguous in some cases. Data could not be normalised to the internal standard biochanin A, as this compound proved to be too different from target analytes, thus being inappropriate for sample preparation and chromatography conditions used.

According to Spearman rank correlation, CoA derivatives clustered into two groups: (I) more abundant in cells grown with succinate; (II) more abundant in cells grown with tryptophan. Amongst the first group are CoA derivatives involved in primary metabolism, like succinyl-CoA and acetyl-CoA; decanoyl-CoA, representing fatty acid metabolism, as well as butanoyl-CoA and 3-hydroxybutanoyl-CoA, which are associated with butanoate metabolism. Amongst the second group are CoA derivatives that have a cyclohexane-structure, are involved in benzoate degradation and may be derived from degradation of tryptophan (e.g. cyclohex-1,5-diene-1-carbanoyl-CoA or 2-hydroxy-5-oxo-cyclohex-1-carbonyl-CoA). Notably, also CoA intermediates associated with the other studied amino acid degradation pathways could be detected in low concentrations in both test and reference conditions (e.g. phenylacetyl-CoA and isovaleryl-CoA). Additionally, almost all intermediates of the ethylmalonyl-CoA pathway (e.g. methylsuccinyl-CoA and methylmalonyl-CoA), were very abundant in cells derived from cultivation with succinate.

3.3.4.5 General observations of metabolomic changes

Although only few detected metabolites are directly involved in the degradation of one of the nine studied amino acid degradation pathways, many additional significant changes in the metabolome could be observed, which were directly or indirectly associated with the correspondent catabolic processes. The most significant changes are shown in figure 18.

Some amino acids provided under corresponding cultivation conditions are very

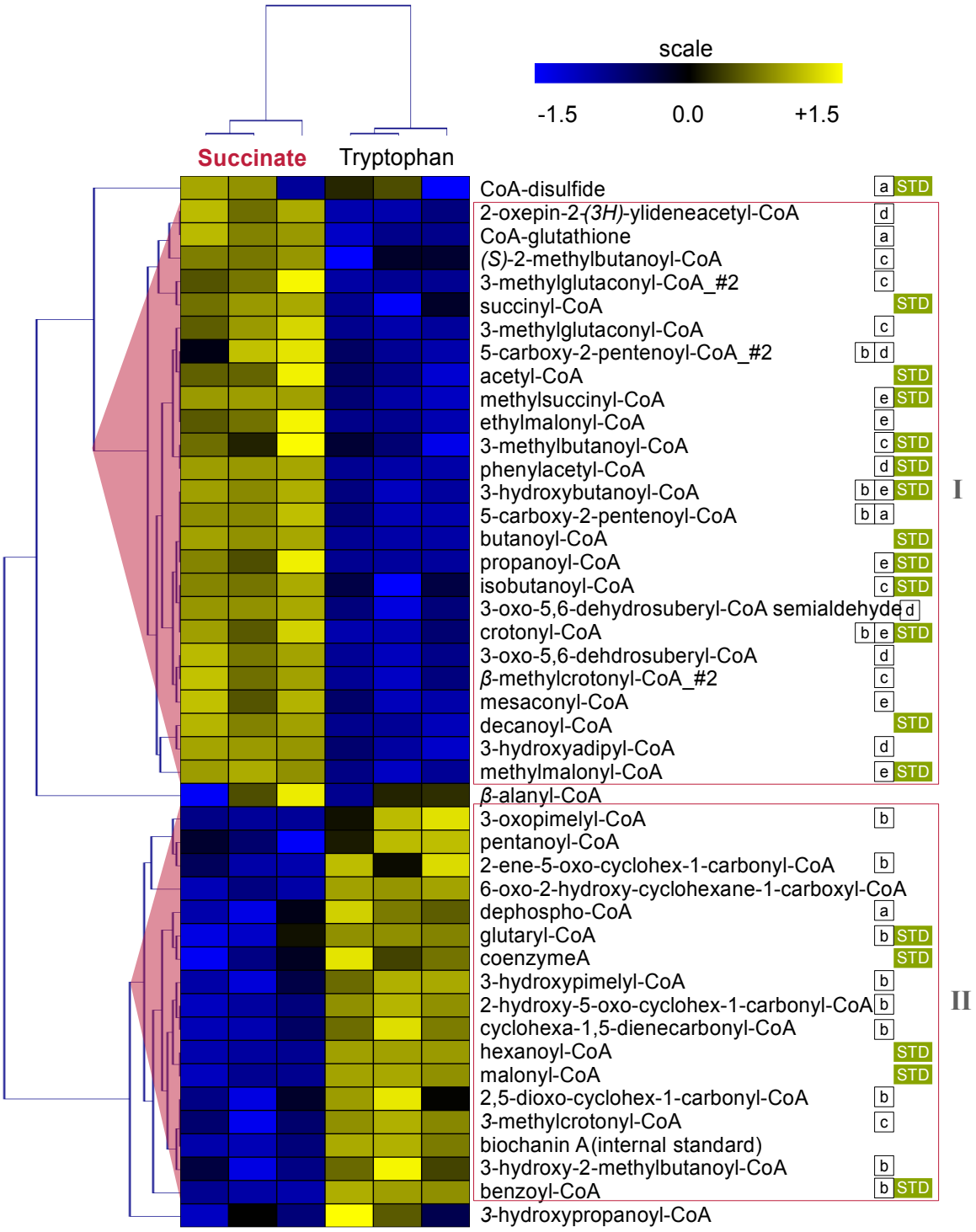

Figure 17: Detected coenzyme A derivatives in cells grown on tryptophan or succinate. Abundances of coenzyme A (CoA) derivatives are visualised as heatmap by blue-yellow colour scale (low to high abundance). For plotting, data were normalised internally in MultiExperiment Viewer. Dendrograms showing correlation of samples and analytes were calculated using Spearman method. Abbreviations: a, artefact, formed during sample-preparation; b, associated with benzoate degradation; c, associated with branched-chain amino acid degradation; d, intermediate of phenylalanine degradation; e, intermediate of ethlylmalonyl-CoA pathway; STD, identified by a chemical standard.

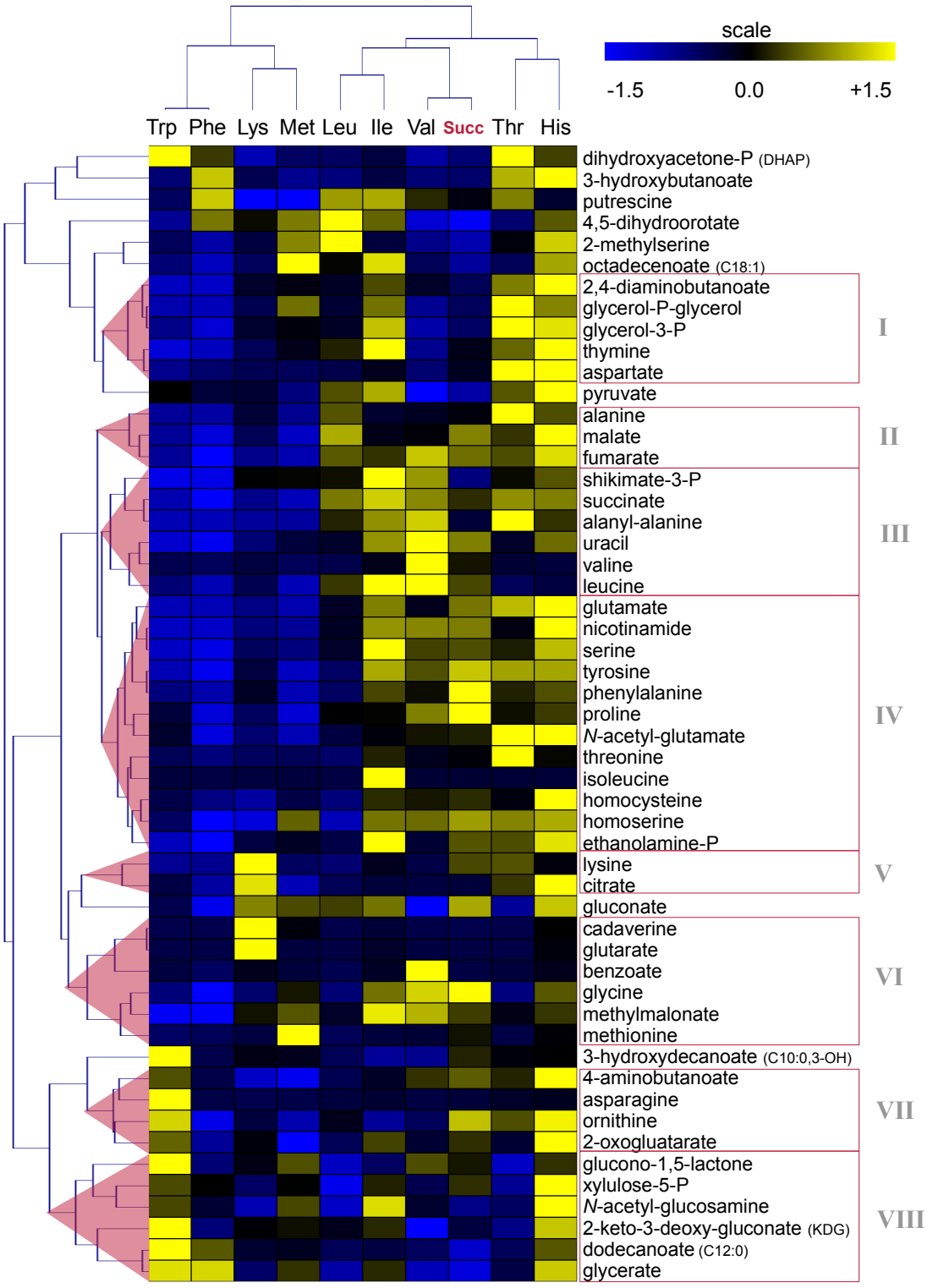

Figure 18: Heatmap of selected intracellular metabolites of the experiment "amino acid degradation". Abundances of metabolites are visualised by blue-yellow colour scale (low to high abundance). Clustering of growth conditions (one of 9 different amino acids or succinate (Succ) as single carbon source) and metabolites was calculated using Spearman method. For plotting, data were internally normalised in MultiExperiment Viewer. Marked clusters indicate metabolites that showed similar distribution pattern.

abundant intracellularly (methionine, isoleucine, valine, lysine and threonine). Otherwise, abundance of leucine is unchanged as compared to succinate-grown cells. Phenylalanine is even less abundant; tryptophan and histidine could not be detected.

Notably, overall intracellular amino acid concentration in cells grown with single amino acids (except for cells grown with either threonine or histidine) were considerably low, as compared to succinate-grown cells, especially in case of cells grown with either tryptophan, phenylalanine, methionine or lysine. This also includes glutamate, which is typically one of the most abundant amino acids in *P. inhibens* DSM 17395. Besides low amino acid concentrations, also nicotinamide and nicotinate were significantly less abundant in cells grown with tryptophan, phenylalanine, methionine or lysine (see clusters III and IV in Figure 18).

Another interesting finding is the high abundance of the lysine degradation intermediates cadaverine, 5-aminopentanoate and glutarate not only in cells grown with lysine, but also in cells grown with methionine, histidine and isoleucine. Side products of corresponding substrate amino acid degradation could be detected in some sample groups (e.g. hydantoin-5-propionate in histidine-grown cells or phenylactetate in phenylalanine-grown cells) (Table 13). Such compounds were also or alternatively detected in the medium (Table 12). Moreover, some methylated compounds were partially more abundant in cells grown with amino acids than compared to cells grown with succinate (e.g. 2-methylmalate and 2-methylserine). Notably, benzoate was very abundant in valine-grown cells. (Supplementary material S6 and S7).

3.3.5 Carbohydrate degradation

3.3.5.1 Growth characteristics and extracellular metabolomic analysis

To study and to refine complex catabolic networks, which were unclear in regard to the original genome annotation, *P. inhibens* DSM 17395 was cultivated in minimal medium supplied with one out of five selected carbohydrates (*N*-acetyl-glucosamine, mannitol, sucrose, glucose, xylose) or succinate as reference condition. Sampling point for metabolomic analyses was ½ OD_{max}.

Of used substrates, succinate was highest concentrated, therefore succinate resulted in highest OD_{max} (≈ 2.4), which was about twice as much as compared to the tested sugars.

Highest growth rate was observed for succinate and *N*-acetyl-glucosamine (about 0.2 h^{-1}), whereas glucose and xylose induced only half of that growth rate. Mannitol and sucrose resulted in significantly lower growth rates (0.02 h^{-1} to 0.04 h^{-1}) (Figure 19).

Depletion of the provided substrate at ½ OD_{max} correlates to the observed growth rate. In case of high growth rates (succinate and *N*-acetyl-glucosamine), more than 50% of the available substrate was consumed, whereas in case of slow growth rates (sucrose and mannitol), less than 25% of the substrate was consumed. Besides depletion of the substrate, extracellular metabolomic analysis revealed export of three compounds, all of which were detected in succinate medium. While fumarate was only detectable in succinate medium, 3-hydroxybutanoate could also be found in sucrose medium; pyruvate was also detected in sucrose and mannitol medium (Table 14).

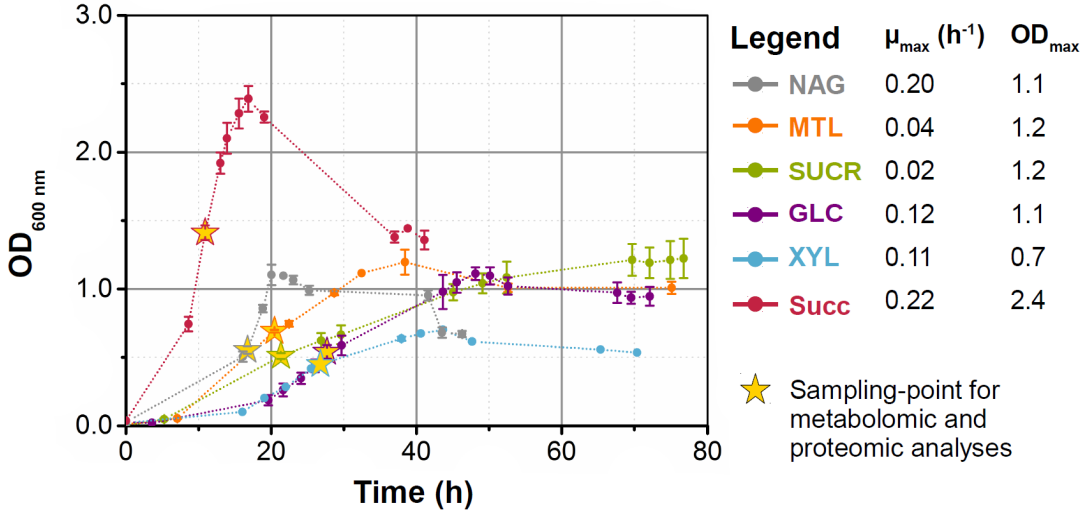

Figure 19: Growth of *P. inhibens* DSM 17395 on selected carbohydrates. For better visualisation, dot-lines were included. Abbreviations of substrates: NAG, *N*-acetyl-glucosamine; MTL, mannitol; SUCR, sucrose; GLC, glucose; XYL, xylose; Succ, succinate.

Table 14: Extracellularly detected metabolites during growth on selected carbohydrates. Abbreviations: x, compound detected in the corresponding culture supernatant at ½ OD_{max}.

Metabolites	Fold change in substrate abundance as compared to t_0					
	N-Acetyl-glucosamine	Mannitol	Sucrose	Gluose	Xylose	Succinate
N-Acetyl-glucosamine	0.46					
Mannitol		0.77				
Sucrose			0.81			
Glucose				0.61		
Xylose					0.57	
Succinate						0.45
Fumarate						x
3-Hydroxybutanoate			x			x
Pyruvate		x	x			x
Colour scale for fold changes:		<0.5	<0.75	<1.0		

3.3.5.2 Intracellular metabolomic analysis

The metabolomic dataset consists of 130 metabolites, 116 of which could be identified. Of all identified metabolites, 65 were significantly changed in abundance (corrected p-value of t-test or Wilcoxon-Mann-Whitney test < 0.001) in at least one of the tested substrate conditions (cells grown with single carbohydrates), compared to the reference (cells grown with succinate). This was underlined by conducted correlation analysis on basis of Pearson coefficient, which revealed low correlation between reference and test-conditions (ranging from 0.66 to 0.74). Cells grown with *N*-acetyl-glucosamine also differed strongly from the other studied growth conditions, but showed at least moderate correlation of about 0.82 to cells grown with mannitol or xylose. However, growth with mannitol, xylose, glucose or sucrose resulted in similar metabolomic composition, with correlation values ranging from 0.89 to 0.94. (Figure 20).

The catabolism of selected carbohydrates consists of (1) a peripheral degradation pathway, mostly specific for the correspondent carbohydrates, (2) central metabolism, involving Entner-Doudoroff pathway, lower branch of Embden-Meyerhof-Parnas pathway and pentose phosphate pathway. These pathways of central metabolism are shared for the degradation of different carbohydrates. Despite structural similarities of target analytes, that resulted in ambivalent identification of some compounds, degradation of all studied carbohydrates could be almost completely covered by conducted metabolomic analysis. Blind spots, especially in regard to transporters, were covered by proteomic analyses and thus allowed refinement of this catabolic network, which is explained and discussed in section 4.3.5.1. Detected metabolic intermediates involved in degradation of studied carbohydrates are listed in table 15. Most of these intermediates were considerably more abundant in cells grown with carbohydrates compared to cells grown with succinate. Amongst, these are provided substrates, like *N*-acetyl-glucosamine, mannitol and sucrose, as well as intermediates of Entner-Doudoroff pathway. In regard to this pathway, highest fold changes were observed for glucono-1,5-lactone, gluconate, 6-phosphogluconate and 2-keto-3-deoxy-gluconate. Some phosphorylated intermediates of Entner-Doudoroff pathway are unstable (Strohhäcker *et al.*, 1993). This is why here and in the other main experiments, in some cases the phosphorylated intermediates are represented by their dephosphorylated analogues. Abundance changes of intermediates involved in the lower branch of Embden-Meyerhof-Parnas pathway and pentose phosphate pathway were moderately more

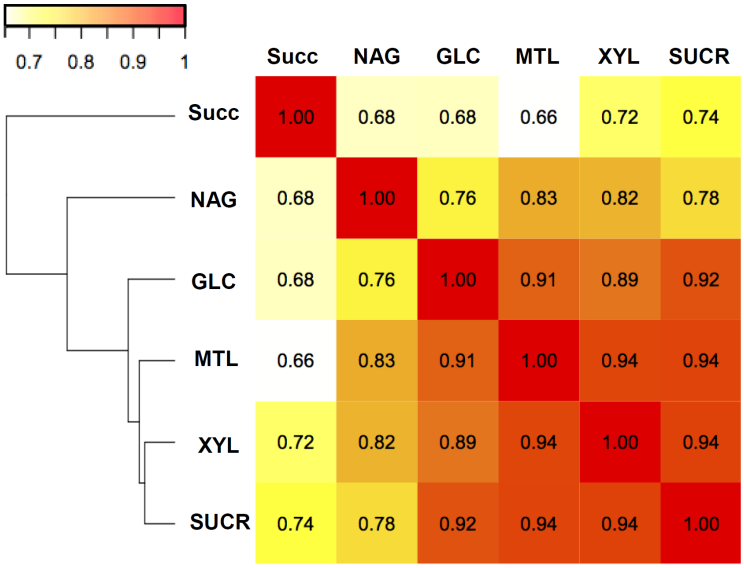

Figure 20: Correlation matrix of intracellular metabolomic data from the experiment "carbohydrate degradation". Pearson coefficient was used for calculation of correlation, which is visualised as heatmap, red colour represent high correlation. Dendrogram is based on euclidean distance. Abbreviations for substrates: Succ, succinate (reference condition); NAG, *N*-acetyl-glucosamine; GLC, glucose; MTL, mannitol; XYL, xylose; SUCR, sucrose.

abundant compared to cells grown with succinate.

Carbohydrate degradation ends in acetyl-CoA, which feeds into the TCA cycle by formation of citrate. Accordingly, citrate was significantly more abundant in cells grown with *N*-acetyl-glucosamine, glucose or xylose. While abundance of 2-oxoglutarate did not differ between cells grown with succinate and cells grown with single carbohydrates, the remaining detected intermediates of the TCA cycle (succinate, fumarate and malate) were considerably lower concentrated in cells grown with single carbohydrates. Sole exception were cells grown with *N*-acetyl-glucosamine; here 2-oxoglutarate, fumarate and malate were significantly more abundant as compared to cells grown with succinate.

In addition to these metabolic changes directly associated with carbohydrate degradation, further considerable changes were observed. For example, in cells grown with *N*-acetyl-glucosamine elevated concentrations of *N*-acetyl-glutamate, *O*-acetyl-serine and iminodiacetate were observed. Another interesting finding are the formation of particular C_4-carboxylates (erythronate, threonate and tartrate), which were high concentrated in cells grown on single carbohydrates (Table 15). Acidic sugars (e.g., glucosaminate and ribonate) were also formed under these conditions. Notably, there were also several metabolites that were less abundant in cells grown with carbohydrates, especially amino acids, butanoates and some lipid and phospholipid headgroup components (Supplementary material S8).

Table 15: Fold changes of selected intracellular metabolites involved in carbohydrate degradation from the experiment "carbohydrate degradation in *P. inhibens* DSM 17395". Abbreviations: [a], Fold change in metabolite abundance as compared to cells grown with succinate; x, compound only detected in test condition; n.d., not detected in test condition; XX, compound only detected in test condition, but intense peak observed here; *, compound probably dephosphorylated during extraction. Complete list of metabolites, including p-values for abundance changes, is provided in the supplementary material S8.

Metabolites	Fold change [a]				
	N-Acetyl-glucosamine	Mannitol	Sucrose	Glucose	Xylose
Carbohydrate metabolism					
N-Acetyl-glucosamine	12.0 ± 0.6	1.33 ± 0.16	1.69 ± 0.23	2.65 ± 0.29	1.36 ± 0.17
Glucose/Glucosamine/Sorbitol-6-P	0.03 ± 0.01	0.12 ± 0.08	0.66 ± 0.31	47.3 ± 25.7	0.33 ± 0.18
Glucosamine	0.49 ± 0.07		0.12 ± 0.02		0.12 ± 0.02
Mannitol	0.76 ± 0.14	19.9 ± 2.5	1.02 ± 0.09	0.47 ± 0.06	0.43 ± 0.03
Fructose	0.73 ± 0.05	8.27 ± 0.66	17.3 ± 1.7	2.21 ± 0.20	1.05 ± 0.12
Sucrose			x		
Glucose	1.59 ± 0.07	2.00 ± 0.10	0.78 ± 0.04	1.04 ± 0.07	0.86 ± 0.05
Xylose			x		XX
Xylulose	0.81 ± 0.08	0.76 ± 0.07	0.52 ± 0.06	0.87 ± 0.10	0.87 ± 0.13
Central metabolism					
Entner-Doudoroff pathway					
Fructose-6-phosphate	0.07 ± 0.06	0.02 ± 0.01	4.28 ± 2.15	4.30 ± 2.44	0.44 ± 0.36
Glucose/Galactose/Mannose-6-P	0.03 ± 0.01	0.04 ± 0.02	0.16 ± 0.06	0.30 ± 0.12	0.14 ± 0.06
Glucono-1,5-lactone *	4.70 ± 0.32	8.99 ± 0.57	9.83 ± 0.71	22.4 ± 2.3	4.99 ± 0.42
Galactonate / Gluconate *	11.4 ± 1.8	4.62 ± 0.74	8.06 ± 1.26	26.0 ± 3.7	6.58 ± 1.34
6-Phosphogluconate	0.24 ± 0.09	0.96 ± 0.37	5.05 ± 1.98	15.8 ± 6.0	0.17 ± 0.16
2-Keto-3-deoxy-gluconate (KDG) *	30.5 ± 4.3	4.66 ± 2.49	1.87 ± 0.10	3.18 ± 0.28	2.05 ± 0.13
Glyceraldehyde *	1.05 ± 0.13	0.75 ± 0.11	0.50 ± 0.07	0.64 ± 0.08	0.76 ± 0.09
Lower branch of Embden-Meyerhof-Parnas pathway					
Dihydroxyacetone phosphate	1.68 ± 0.33	0.31 ± 0.15	0.39 ± 0.09	0.63 ± 0.17	0.60 ± 0.18
1,3-Dihydroxyacetone *	0.77 ± 0.04	0.95 ± 0.05	1.00 ± 0.06	1.12 ± 0.08	0.98 ± 0.05
3-Phosphoglycerate	3.77 ± 0.44	1.58 ± 0.16	1.66 ± 0.23	8.75 ± 1.04	2.60 ± 0.31
2-Phosphoglycerate	1.64	0.42	0.80	2.70	
Phosphoenolpyruvate	1.95 ± 0.28	1.77 ± 0.24	1.27 ± 0.21	4.43 ± 0.66	1.84 ± 0.28
Pyruvate	7.71 ± 1.29	3.62 ± 0.60	3.11 ± 0.54	3.84 ± 0.57	5.35 ± 0.77
Pentose phosphate pathway					
Erythrose-4-P	3.74 ± 2.99	2.75 ± 2.68	5.45 ± 5.20	0.48 ± 0.35	0.99 ± 0.93
Ribose	1.02 ± 0.05	2.30 ± 0.08	0.81 ± 0.07	0.89 ± 0.07	2.45 ± 0.11
Xylulose-/ Ribulose-5-P	0.09 ± 0.06		0.05 ± 0.05	0.17 ± 0.11	1.00 ± 1.00
TCA Cycle					
Citrate	4.00 ± 0.58	1.28 ± 0.14	0.89 ± 0.15	5.06 ± 0.83	4.39 ± 0.72
2-Oxoglutarate	1.90 ± 0.12	0.73 ± 0.05	0.60 ± 0.04	1.10 ± 0.11	1.31 ± 0.10
Succinate	0.60 ± 0.06	0.30 ± 0.02	0.07 ± 0.01	0.13 ± 0.01	0.24 ± 0.02
Fumarate	2.11 ± 0.20	0.71 ± 0.06	0.35 ± 0.03	0.37 ± 0.05	0.52 ± 0.05
Malate	3.45 ± 0.35	0.48 ± 0.04	0.28 ± 0.03	0.34 ± 0.04	0.40 ± 0.04
Amino acid derivatives					
N-Acetyl-glutamate	6.77 ± 0.41	0.78 ± 0.06		0.87 ± 0.07	1.08 ± 0.12
O-Acetyl-serine	18.6 ± 4.4	11.8 ± 3.9	0.91 ± 0.38	3.08 ± 0.67	11.5 ± 3.9
Ornithine	1.46 ± 0.74	0.41 ± 0.11	0.22 ± 0.06	0.38 ± 0.11	1.04 ± 0.32
Organic acids					
Erythronate	8.23 ± 0.88	2.70 ± 0.28	1.61 ± 0.21	2.90 ± 0.35	1.91 ± 0.24
Iminodiacetate	31.1 ± 5.9	1.90 ± 0.36	0.77 ± 0.15	5.64 ± 1.17	2.13 ± 0.41
Tartrate	0.68 ± 0.15	1.59 ± 0.40	10.8 ± 2.2	169 ± 37	3.06 ± 0.68
Threonate	2.59 ± 0.72	4.20 ± 0.77	29.6 ± 5.5	13.1 ± 2.6	2.64 ± 0.54
Urea	0.98 ± 0.18	0.80 ± 0.34	0.26 ± 0.07	0.69 ± 0.18	0.27 ± 0.05

Colour scale for fold changes:	n.d.	<0.1	<0.2	<0.4	<0.67	0.67 – 1.5	>1.5	>2.5	>5.0	>10.0

3.3.6 Metabolic responses to ammonium limited growth condition

Nitrogen is one of the key elements that limits bacterial growth in marine environments. Most of inorganic nitrogen in the ocean is available as nitrate (NO_3^-), whereas ammonium (NH_4^+) content is considerably lower. Of these, only ammonium can be utilised by *P. inhibens* DSM 17395 as nitrogen source (see Biolog phenotypic microarray analysis, Figure 7). To study the metabolic response of *P. inhibens* DSM 17395 to growth under nitrogen limited conditions, cells were cultivated in minimal medium providing only 1 mM ammonium (instead of 4.7 mM) and were harvested for metabolomic analysis along the time-course.

3.3.6.1 Growth characteristics and extracellular metabolomic analysis

Growth is characterised by a lag-phase of about 15 to 20 h and an OD_{max} (600 nm) of about 1.2, which was reached after 40 h. Afterwards, the optical density remained relatively constant (Figure 21). Further, ammonium concentration and cellular N/C ratio were determined along the time-course (performed by Sebastian Koßmehl, ICBM Oldenburg). These analyses revealed that the whole amount of provided ammonium was imported within the first 20 h. Accordingly, the highest cellular N/C ratio was observed at the beginning of cultivation, decreasing from t_{15} to t_{30} until this ratio remained constant. GC-MS analysis of the culture supernatant enabled detection of low amounts of 3-hydroxybutanoate during stationary phase (Figure 21). This, besides the substrate glucose (which could not be quantified), was the only organic compound detected in the medium via GC-MS.

3.3.6.2 Intracellular metabolomic analysis

Samples for GC-MS-based metabolomic analysis were taken across the time-course from early growth stage (t_{15}) to late stationary phase (t_{90}); samples from ½ OD_{max} (t_{30}) served as reference. Cultivation and harvesting were conducted by Sebastian Koßmehl (ICBM, Oldenburg). Overall, 114 metabolites could be detected, 91 of which could be identified. Most metabolites were significantly changed in abundance as compared to the reference condition. Therefore, also abundance changes between consecutive sampling points were elucidated. For this purpose, depending on data distribution, either t-test or

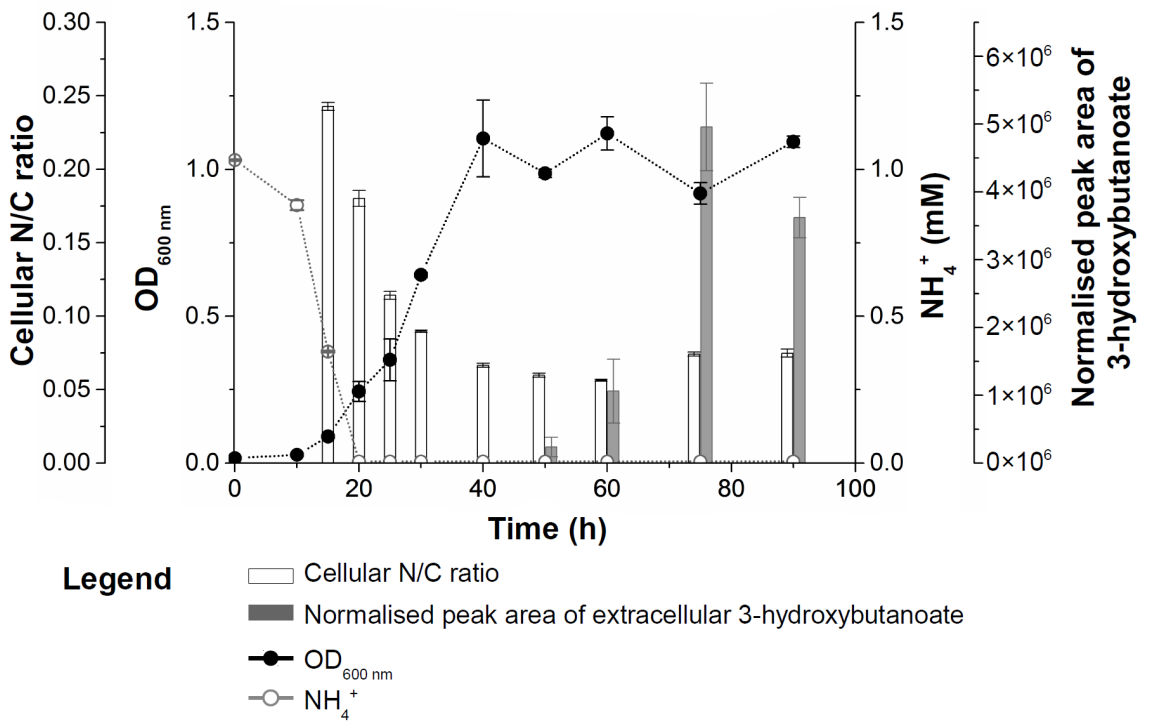

Figure 21: Growth of *P. inhibens* DSM 17395 under limited ammonium concentration. Growth was observed by measuring the optical density at 600 nm. Ammonium content in the medium was determined enzymatically, the cellular N/C ratio were determined with a Vario El cube (Elementar Analysensysteme, Hanau, Germany) as described previously by Zech *et al.* (2013a), each conducted by Sebastian Koßmehl (ICBM Oldenburg). The amount of 3-hydroxybutanoate in the medium was determined via GC-MS. For better visualisation, dot-lines were included.

Wilcoxon-Mann-Whitney test were applied. In both cases, p-values were corrected. Overall, 29 compounds showed significant p-values (< 0.01) for consecutive sampling points. This number may be underestimated, since considerable fold changes were mostly observed between consecutive sampling points. However, these abundance shifts were mostly not significant, because the applied tests were inappropriate for the limited number of replicates (in average 5 or 6).

As revealed by Spearman correlation, samples clustered according to growth-phases, resulting in four different groups (Figure 22). The first group, comprising t_{15} and t_{20}, was similar to the second group, comprising the consecutive samples from t_{25}, t_{30} and t_{40}. Metabolic composition at these five sampling-points differed considerably from metabolic composition of the other two groups in stationary phase (t_{50}, t_{60}) and (t_{75}, t_{90}). According to this hierarchical cluster analysis, considerable differences between early and late stationary phase were apparent.

Two characteristics are responsible for observed clustering: (1) number of detected metabolites at the corresponding sampling points, (2) the overall metabolite concentration.

Both were highest at early growth phases (around t_{15} to t_{25}). Exponential growth phase (t_{30}) marks the point, when both number of detected compounds and metabolite concentration considerably and continuously decreased, until only a few compounds remained. This striking metabolic shift of selected metabolites is visualised in a heatmap in figure 22. The complete list of metabolites is provided in the Supplementary material S9. Most

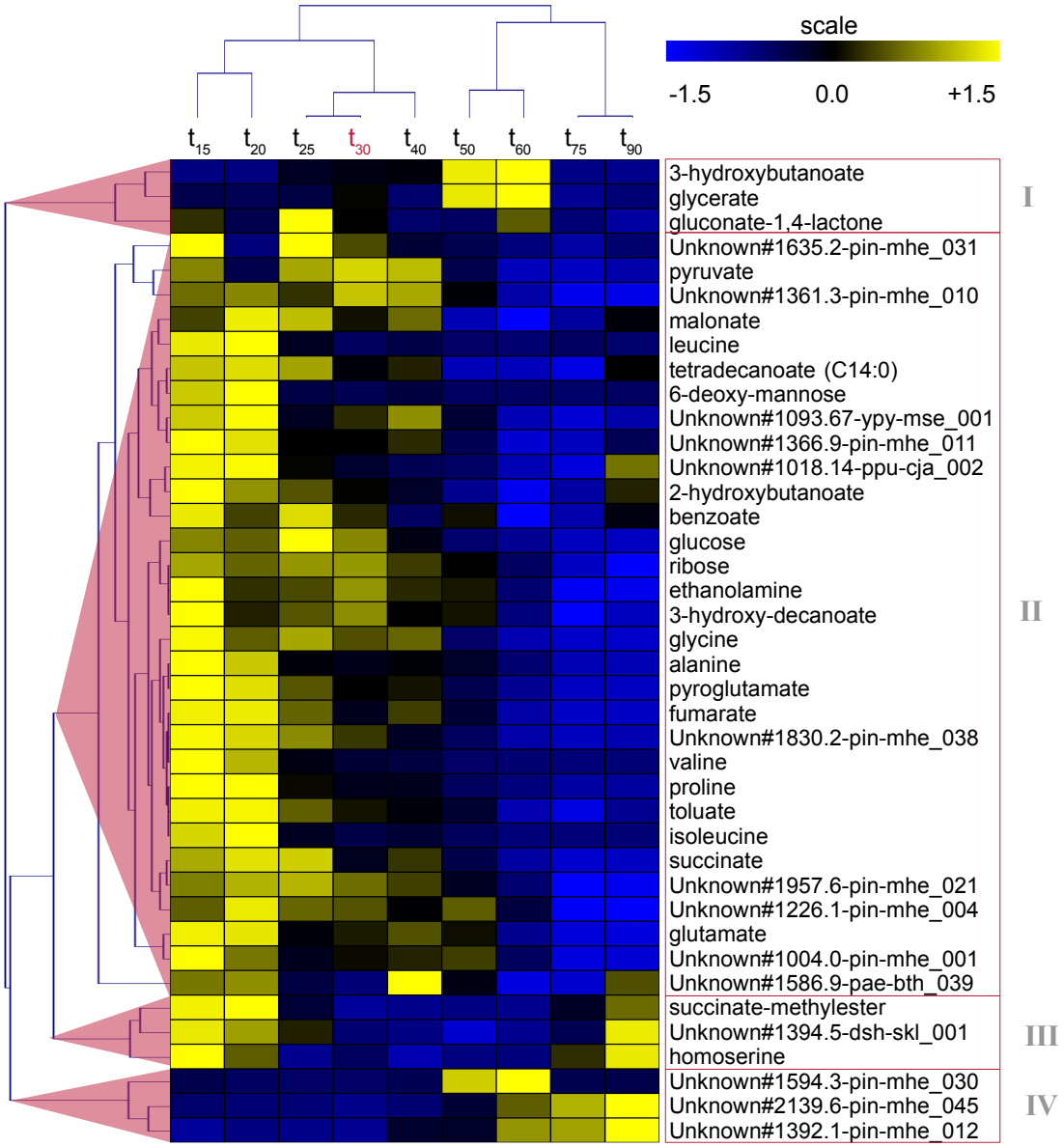

Figure 22: Heatmap of selected intracellular metabolites of experiment "metabolic response to ammonium limited growth condition". Abundances of metabolites across the time course are visualised by blue-yellow colour scale (low to high abundance). Subscript numbers on top of figure represent the sampling-time in hours. Correlation for clustering of sampling point and metabolites was calculated using spearman method. For plotting, metabolites were internally normalised in MultiExperiment Viewer. Marked clusters indicate metabolites that showed similar distribution pattern across the time course.

metabolites were more abundant at early sampling points (cluster II in figure 22). Only a few metabolites were more abundant in the stationary phase (clusters I and IV). Amongst the latter were some unidentified compounds, as well as 3-hydroxybutanoate, which was very abundant at t_{50} and t_{60}. This coincides with detection of 3-hydroxybutanoate in the medium from t_{50} and following sampling points.

Interestingly enough, many metabolites were not or only detected in low concentrations during stationary phase. This also includes compounds that are usually very abundant in *P. inhibens* DSM 17395 or even increase in abundance during stationary phase, when grown on 4.7 mM ammonium, like glutamate, tartrate or glucuronate (Zech *et al.*, 2009).

Amongst the metabolites most abundant in the early growth phase were some intermediates of central metabolism, e.g. succinate, fumarate, malate and 2-keto-3-deoxy-gluconate. Further, in accordance to higher cellular N/C ratio (Figure 21) at the beginning of cultivation, many nitrogen-containing compounds were most abundant at t_{15} and t_{20}. This comprises amino acids, diamines, aminobutanoates and nucleobases. Further, it should be noted that the overall number of detected nitrogen-containing compounds was considerably lower compared to all other conducted experiments in this study.

The most significant metabolic shifts from the early growth phase to exponential growth phase, as well as from exponential growth phase to stationary phase are summarised in figure 23. Further results are provided in the Supplementary material S9.

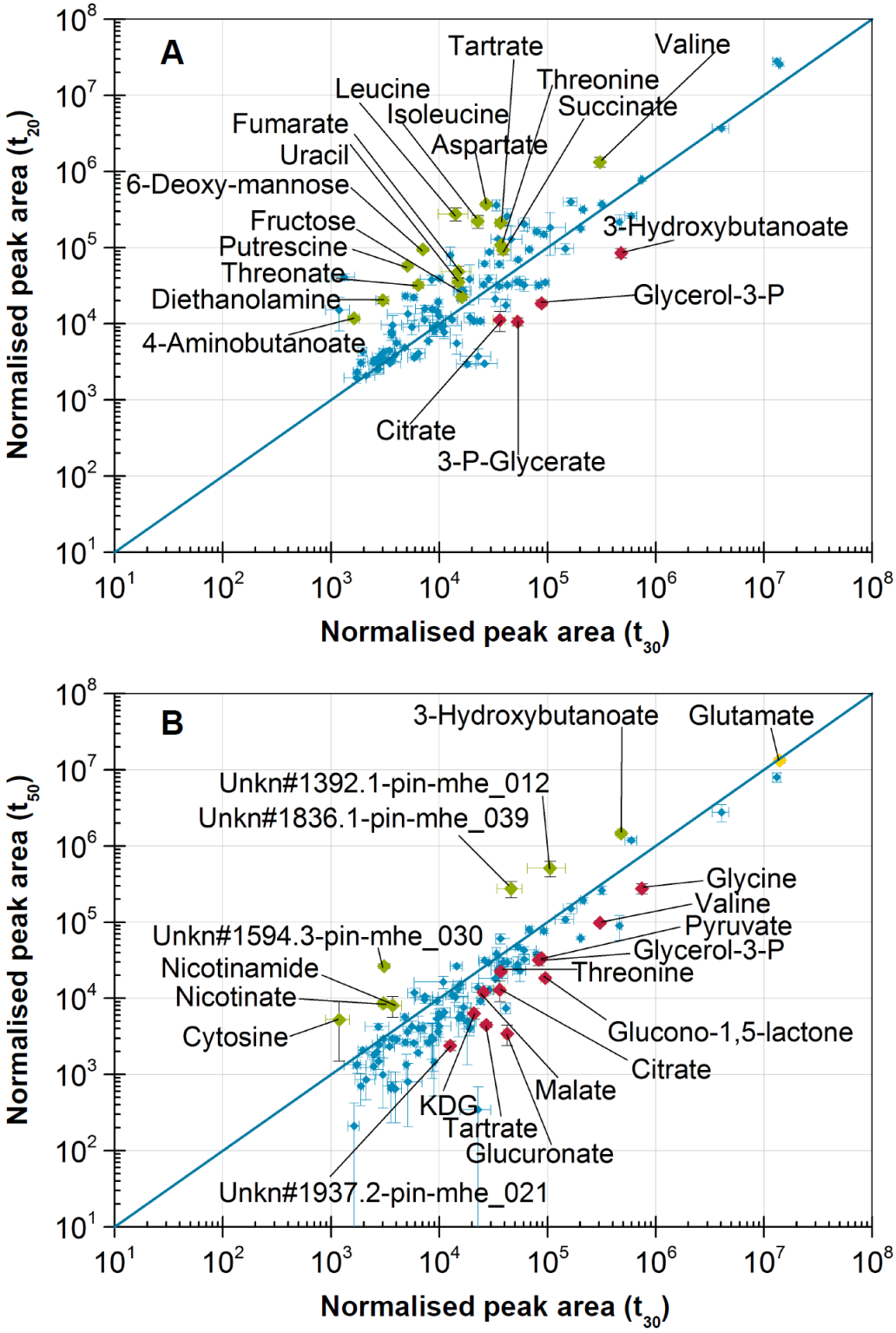

Figure 23: Intracellular metabolic changes during growth with limited ammonium concentration. Normalised peak areas of all metabolites were plotted in double-logarithmic scale. Colouring: green: increased abundance, red: decreased abundance as compared to the reference t_{30}. (exponential growth phase). (A) Comparison between t_{20} and t_{30}. (B) Comparison between stationary phase, t_{50} and t_{30}. Abbreviations: KDG, 2-keto-3-deoxy-gluconate.

4 Discussion

4.1 Biolog phenotypic microarray analysis

4.1.1 Carbon sources

The Biolog phenotypic microarray analysis was applied to define the substrate range of *Phaeobacter inhibens* DSM 17395 for carbon and nitrogen sources. Overall, 81 out of 190 carbon sources were tested positive (Figure 6), revealing a broad range utilisable substrates.

Since only respiratory activity was measured, positive responses did not necessarily prove usability for anabolic purposes. Some substrates tested positive, were negative tested on growth, which were citrate (Buddruhs *et al.*, 2013), *L*- and *D*-arabinose and *D*-fucose (Wiegmann *et al.*, 2014), as well as ethanolamine (determined by Felix Pritsch in the context of his bachelor of science thesis, 2012). However, all 20 proteinogenic amino acids and most monosaccharides can be used for growth (Drüppel *et al.*, 2014; Wiegmann *et al.*, 2014). These substrates showed fast kinetics and strongest colour changes (Figure 6) and were also preferred utilised when grown in Marine Broth medium (Section 3.3.1.2). Thus *P. inhibens* DSM 17395 is well adapted to its natural habitat, as these compounds, along with dipeptides and simple carboxylates belong to the most abundant low molecular substrates available in marine environments, especially during seasonal bloom periods of phytoplankton (Ittekkot, 1982; Pettine *et al.*, 1999). This could also be an explanation for observed high abundances and metabolic activity of members of the Roseobacter clade during seasonal bloom and collapse of phytoplankton populations (Alonso-Sáez *et al.*, 2007; Alonso-Sáez and Gasol, 2007). The broad substrate range revealed for *P. inhibens* DSM 17395 is also true for closely related strains *P. inhibens* DSM 16374 and *P. gallaeciensis* CIP 105210, as shown recently by Buddruhs *et al.* (2013). However, such a broad substrate range is not a general characteristic for the Roseobacter clade, as for example *Dinoroseobacter shibae* DFL 12^T can only utilises 19 of 190 tested carbon sources (Rex *et al.*, 2013). Interestingly, bromosuccinate can be used by *P. inhibens* DSM 17395 and *D. shibae* DFL 12^T. Halogenic compounds can be formed by ozon (Narukawa *et al.*, 2003), or be produced by algae as protectant against bacteria and fungi (Cabrita *et al.*,

2010). This could be a specific adaptation to life with algae and an explanation for observed association of the Roseobacter clade with algae (Brinkhoff *et al.*, 2008).

Substrates that were tested negative, were mostly uncommon compounds, e.g. synthetic *L*-glucose, lactulose, *D*-amino acids or the polysorbates Tween 20, 40 and 80. Otherwise, oligo- and polysaccharides, which were tested negative, are available in marine environments (e.g. Sakugawa *et al.*, 1990). This negative test results, however, were in accordance to previous findings, that *P. inhibens* DSM 17395 is tweenase, gelatinase and amylase negative (Ruiz-Ponte *et al.*, 1998; Martens *et al.*, 2006; Buddruhs *et al.*, 2013). Amongst negative tested substrates were also tartrate, 5-aminopentanaote, gluconate and glucuronate, which were very abundant in *P. inhibens* DSM 17395 in particular conducted experiments of this study. Since catabolic enzymes for these substrates are encoded on the genome, missing transporters are probably reason for this negative result, whereby for 5-aminopentanoate, definitely a transporter must be available, as it was used as nitrogen source. However, probably this transporter is only expressed under nitrogen limited conditions. Such regulation upon nitrogen limited condition was for example shown for 4-aminobutanoate import in *Escherichia coli* (Brechtel and King, 1998).

Interestingly *L*-valine gave a stronger response as nitrogen source than as carbon source, indicating its better usability as amino donor than as carbon source. After import of valine, only one transamination reaction is required to obtain the nitrogen for anabolic purposes, whereas further energy-demanding degradation reactions are required until usable as carbon source (the correspondent pathway is discussed in section 4.3.4.7, figure 27).

4.1.2 Nitrogen sources

72 of 95 tested nitrogen sources were positive, revealing a broad range of transporters. Most of tested substrates have an easy accessible nitrogen (e.g. an amino-group), that require few enzymatic reactions (like transamination or deamination) to provide the nitrogen for anabolic purposes. Also nucleobases, whose concentration in seawater can reach about 9 µg/l and are usually rapidly degraded by bacteria (Montani *et al.*, 1988), were utilised by *P. inhibens* DSM 17395 as nitrogen source. As shown by Felix Pritsch in the context of his bachelor of science thesis (2012), *P. inhibens* DSM 17395 can use single nucleobases, such as adenine or uracil (i.e. without bound ribose), merely as nitrogen

source. Not all nitrogen atoms of nucleobases are usable, as revealed by export of urea, which is in accordance with nucleobase degradation in bacteria (Vogels and Van der Drift, 1976) and observed formation of urea by marine bacteria when supplied with nucleobases (Berg and Jørgensen, 2006). All *L*-amino acids and dipeptides tested positive as carbon source, were also tested positive as nitrogen source, as correspondent nitrogen atoms are easy accessible and require not necessarily specific transaminases.

Amongst negative tested nitrogen sources were short-chain amines (i.e. compounds without a carboxylate group), as well as amides. Urea was negative, due to missing urease in *P. inhibens* DSM 17395. Accordingly, urea is rather used to dispose of excess nitrogen and thus was detected in culture supernatant of *P. inhibens* DSM 17395 when provided with nitrogen-rich substrates, like casamino acids (Section 3.3.2.1). Amongst inorganic nitrogen sources, only ammonia was tested positive, although nitrate and nitrite comprise much higher concentrations in marine environments. This non-utilisability of nitrate is compensated by the broad range of utilisable organic nitrogen sources.

4.1.3 General observations

Overall, for most tested substrates (C and N sources), respiratory activity was observed within the first 12 h of incubation, indicating the relative fast adaptation of *P. inhibens* DSM 17395 to changing nutrient conditions. This, along with the broad substrate range enables to utilise almost any available substrate, which is beneficial in marine environments, as provided substrates are extremely versatile and low concentrated. The broad substrate range of *P. inhibens* DSM 17395 is accomplished by transporters that have broader substrate range, e.g. branched-chain amino acid transporter (discussed in section 4.3.2.1), as well as catabolic pathways that are shared by several substrates, e.g. Entner-Douodroff pathway for carbohydrates (Section 4.3.5) or enzymes with broader substrate specificity, e.g. in case of branched-chain amino acid degradation (Section 4.3.4.7).

4.2 Isotope labelling

Isotope labelling was applied to distinguish between metabolites of biological origin and potential contaminants. Biological origin could be confirmed for 61 metabolites, which

comprised all common detectable metabolites of primary metabolism, like TCA cycle intermediates and typical compounds, such as amino acids and carbohydrates.

Notably, several saturated fatty acids were unlabelled. Most probably these compounds derived from plastic consumables; whereas significant abundance increases, e.g. as determined during growth on casamino acids (Section 3.3.2.2) cannot be explained by contaminants alone, but must be of biological origin. Also benzoate was mostly unlabelled, but is usually detected in *P. inhibens* DSM 17395 and was even significantly more abundant when grown on valine (Section 3.3.4.5). It probably derived from degradation of 4-aminobenzoate or maybe other aromatic compounds, like tryptophan. In contrast to this, toluate was completely unlabelled. Accordingly no significant abundance change was observed for this compound in any of conducted experiments, except for the final experiment "metabolic response to growth under limited ammonium" (Section 3.3.6.2), where it decreased along with most other metabolites over the course of time. The origin of this aromatic contamination currently remains unclear.

4.3 Main experiments

In this section, results from metabolomic analysis of conducted cooperation experiments were discussed by including correspondent proteomic data of joint publications. Detailed information about methods and results of proteomic analyses are provided in the correspondent publications (Table 16). A list of discussed enzymes, together with EC numbers and gene-loci tags are provided in the supplementary material S10.

Table 16: Source of discussed proteomic data.

	Name of experiment	**Reference**
(1)	Adaptation to growth with complex nutrients	(Zech *et al.*, 2013a)
(2)	Dynamics of amino acid utilisation	(Zech *et al.*, 2013b)
(3)	Casamino acid consumption by plasmid-cured strains	No proteomic analyses performed.
(4)	Amino acid degradation	(Drüppel *et al.*, 2014)
(5)	Carbohydrate degradation	(Wiegmann *et al.*, 2014)
(6)	Metabolic responses to ammonium limited growth condition	Proteomic analyses still in progress, thus not included.

4.3.1 Adaptation to growth with complex nutrients

4.3.1.1 Growth characteristics

Cultivation of *P. inhibens* DSM 17395 in complex medium (MB medium) and glucose minimal medium (GM medium) was applied to simulate nutrient-rich conditions during collapse of phytoplanktonic bloom, respectively replenished nutrient conditions. Observed shorter lag-phase, higher μ_{max} and OD_{max} upon growth with MB medium compared to GM medium, resulted from different amount of provided carbon: 229 mM in case of MB medium, 66 mM in case of GM medium. According to this, also considerable higher O_2 consumption rate and CO_2 production rate were observed in MB medium (Table 17). Interestingly enough, whereas provided carbon in GM medium was almost completely consumed, cells grown in MB medium entered stationary phase although more than 50% of initially provided carbon was still available. Thus, growth seems not to be C limited, which was also observed during cultivation on casamino acids (Section 3.3.3.1). However, whereas in case of casamino acids, remaining carbon sources were definitely utilisable by *P. inhibens* DSM 17395, remaining substrates in MB medium may not be utilisable. Probably, remaining carbon sources were polymers, like proteins or polysaccharides, which cannot be utilised by *P. inhibens* DSM 17395 as revealed by Biolog phenotypic microarray analysis (Section 3.1.1). Additionally, formation of tropodithietic acid and acyl-

Table 17: Physiological properties of *P. inhibens* DSM 17395 during growth in complex medium and minimal medium in process-controlled bioreactors. Abbreviations: MB medium, Marine Broth medium; GM medium, glucose-containing minimal medium. Shown data were taken from table 1 in (Zech *et al.*, 2013a).

Physiological properties during growth	MB medium	GM medium
Exponential growth phase		
Maximum specific growth rate, μ_{max} (h^{-1})	0.36 ± 0.0	0.10 ± 0.0
Biomass formation rate (mg l^{-1} h^{-1})	81.8 ± 2.6	26.4 ± 2.0
O_2 consumption rate (mmol l^{-1} h^{-1})	4.27 ± 1.1	0.60 ± 0.0
CO_2 production rate (mmol l^{-1} h^{-1})	3.44 ± 0.5	0.66 ± 0.0
Entry into stationary phase		
Optical density (measured at 600 nm)	4.23 ± 0.3	1.97 ± 0.1
Cellular dry weight (mg/l)	1186.5 ± 79.9	646.0 ± 5.0
Total carbon consumed (mmol/l)	96.60 ± 4.8	60.30 ± 1.6
Total O_2 consumption (mmol/l)	59.37 ± 12.3	22.61 ± 0.1
Total CO_2 production (mmol/l)	47.96 ± 4.3	24.90 ± 1.3
Cellular N/C ratio	0.208	0.085

homoserine-lactones as determined by Berger *et al.* (2012) upon growth on MB medium could contribute to limit further growth of *P. inhibens* DSM 17395. Other factors, such as insufficient O_2 supply or inappropriate pH are unlikely, as these parameters were controlled and kept constant in a process controlled bioreactor.

Due to the high amount of peptone and yeast extract, MB medium is nitrogen-rich. Accordingly, a considerable higher cellular N/C ratio was determined in cells derived from MB medium (Table 17). This is reflected by intracellular metabolomic analysis. Here, considerable higher abundances of several nitrogen-containing compounds, like amino acids, nucleosides and nucleobases, were observed. Further, the high intracellular amounts of glycyl-glycine, 5-aminopentanoate, cadaverine and spermidine could also be interpreted as temporary nitrogen-storage.

4.3.1.2 Extracellular metabolomic analysis

Substrate depletion. Analysis of MB medium revealed high depletion of several provided substrates. Amongst most depleted substrates were amino acids and particular carbohydrates that showed also strong responses as carbon sources in the Biolog phenotypic microarray analysis (Section 3.1.1). Interestingly, some substrates that showed strong response in phenotypic microarray analysis, were only moderately consumed in MB medium (e.g. arginine, threonine, lysine, serine). This indicates preferences of *P. inhibens* DSM 17395 for particular substrates, when providing complex substrate mixture. Several factors, such as efficiency or inhibition of uptake or catabolism can be responsible for this observation, which was also observed for many other bacteria before (e.g. Strobel, 1993; Görke and Stülke, 2008; Jojima *et al.*, 2010; Rabus *et al.*, 2014).

Exported compounds. The export of 2-hydroxyphenylacetate, which was also detected in medium with phenylalanine as single carbon source (Table 12) resulted probably from degradation of phenylalanine or similar compounds. This side product cannot be utilised, which is also true for the structural similar compounds 3- and 4-hydroxyphenylacetate (both negative in Biolog phenotypic microarray analysis, Figure 6). Export of urea is the main flow to dispose of excess nitrogen, which is obtained by degradation of N-rich compounds, like amino acids. All enzymes involved in the urea cycle were detected, except for argininosuccinate lyase (Figure 24). Urea also originated from purine catabolism, as each degraded purine molecule yields one molecule urea plus additional ammonium.

4.3.1.3 Intracellular metabolomic analysis

Statistical data analysis. To exclude any potential impact of the cultivation vessel on metabolic abundance changes (see Figure 9), metabolomic data were elucidated different to the published approach (Zech *et al.*, 2013a). Only data from bioreactors were used, because of following reasons: First, cultivation in bioreactors was process-controlled; thus impact of pH or oxygen supply on metabolism was minimised. Second, larger replicate numbers allowed an even more robust statistical analysis. Main cause for non-normally distributed metabolomic data were extreme concentration differences of intracellular metabolites between the two cultivation conditions. For interpretation of data, cells derived from minimal medium served as reference condition.

Substrate import. High abundance of several metabolites observed in cells derived from MB medium can partially result from insufficient applied washing procedure. However, as many of these compounds could not be detected extracellularly, uptake is in most cases more probable. Several transport systems could be detected by proteomic analyses. For substrate uptake, many substrate-specific ABC transporter were identified by proteomic analyses. Further, 13 different outer-membrane embedded porins were detected that allow the unspecific passage of solutes into the periplasm for molecules < 200 Da, which is the case for most provided substrates in the medium, except for long-chain fatty acids, derived from extracellular lipid degradation (Zech *et al.*, 2013a).

Membrane components. Import of extracellular fatty acids and associated compounds (e.g. $C_{18:1}$, $C_{12:0}$ and glycerol-3-phosphate) might be accomplished by flip-flop mechanisms across the outer membrane as described e.g. by Gurtovenko and Vattulainen (2007) and Schaffer (2002). Further, a putative glycerol-3-P-diester uptake system is encoded on the genome (not identified by proteomic analyses), which could be used for import of ethanolamine-based lipids (Zech *et al.*, 2013a). Since corresponding enzymes for degradation of ethanolamine-phosphate are not encoded on the genome, ethanolamine-phosphate accumulated intracellularly. In contrast to this, degradation of glycerol-3-phosphate and fatty acids could be covered by proteomic analysis. Correspondent enzymes were not changed in abundance, except for acyl-CoA dehydrogenase, which was more abundant in cells derived from MB medium (Figure 24). Thus, fatty acid degradation seems to be less relevant under these cultivation, despite the fact of exported enzymes for lipid degradation (Zech *et al.*, 2013a). Instead, the higher abundances of membrane

associated compounds could be a result of higher growth rate. However, intracellular concentration of alanyl-alanine and 2,6-diaminopimelate, both involved in peptidoglycan biosynthesis, did not change between the two tested growth conditions (Supplementary material S3).

Nucleotide metabolism. High growth-rate did not affect abundances of enzymes for nucleotide metabolism, with exception of adenylate kinase, CTP synthase and carbamoyl-phosphate synthase, that were slightly more abundant in cells grown in MB medium (Zech *et al.*, 2013a). However, nucleotide biosynthesis is regulated by allosteric feedback inhibition, which explains these unchanged enzyme concentrations. Biosynthesis of inosine-5'-monophosphate (IMP) is inhibited by guanosine-5'-monophosphate (GMP), and adenosine-5'-monophosphate (AMP) and thus IMP does not accumulate in cells (Ledesma-Amaro *et al.*, 2013). Since both AMP and GMP were more abundant in cells derived from MB medium, IMP was less abundant. Further, higher abundance of catabolic intermediates xanthine and hypoxanthine was observed. Therefore, in accordance with depletion of some representative nucleotides and nucleobases in the medium (Supplementary material S2) and slightly more abundant unspecific ABC nucleoside transporter (Zech *et al.*, 2013a), uptake of these compounds for catabolic purposes is very likely.

Diamine formation. High abundance of cadaverine in cells grown in MB medium, resulted most probably from degradation of imported lysine (see section 4.3.4.4 for discussion of lysine degradation), as cadaverine was not detectable in the medium. In contrast to this, spermidine could be imported from the medium, which might be accomplished by a spermidine/putrescine specific ABC transporter. 2 out of 4 subunits of this transporter could be identified by proteomic analysis. Besides uptake, degradation of arginine and ornithine could also contribute to high abundance of spermidine (Figure 24). These diamines can have several functions, e.g. as signalling molecules or as protection against oxygen toxicity (Kusano *et al.*, 2008). However, maybe these compounds just accumulated, as known polyamine antiporters (Kusano *et al.*, 2008; Tomitori *et al.*, 2012) are not encoded. Therefore, excess nitrogen had to be exported via urea.

Amino acid degradation. Several amino acids were available in MB medium and were utilised by *P. inhibens* DSM 17395. Alanine and glycine, both strongly depleted, might be imported by an alanine/glycine cation symporter (gene loci: PGA1_c07110 and PGA1_78p00280), which were identified by proteomic analyses. Both amino acids are

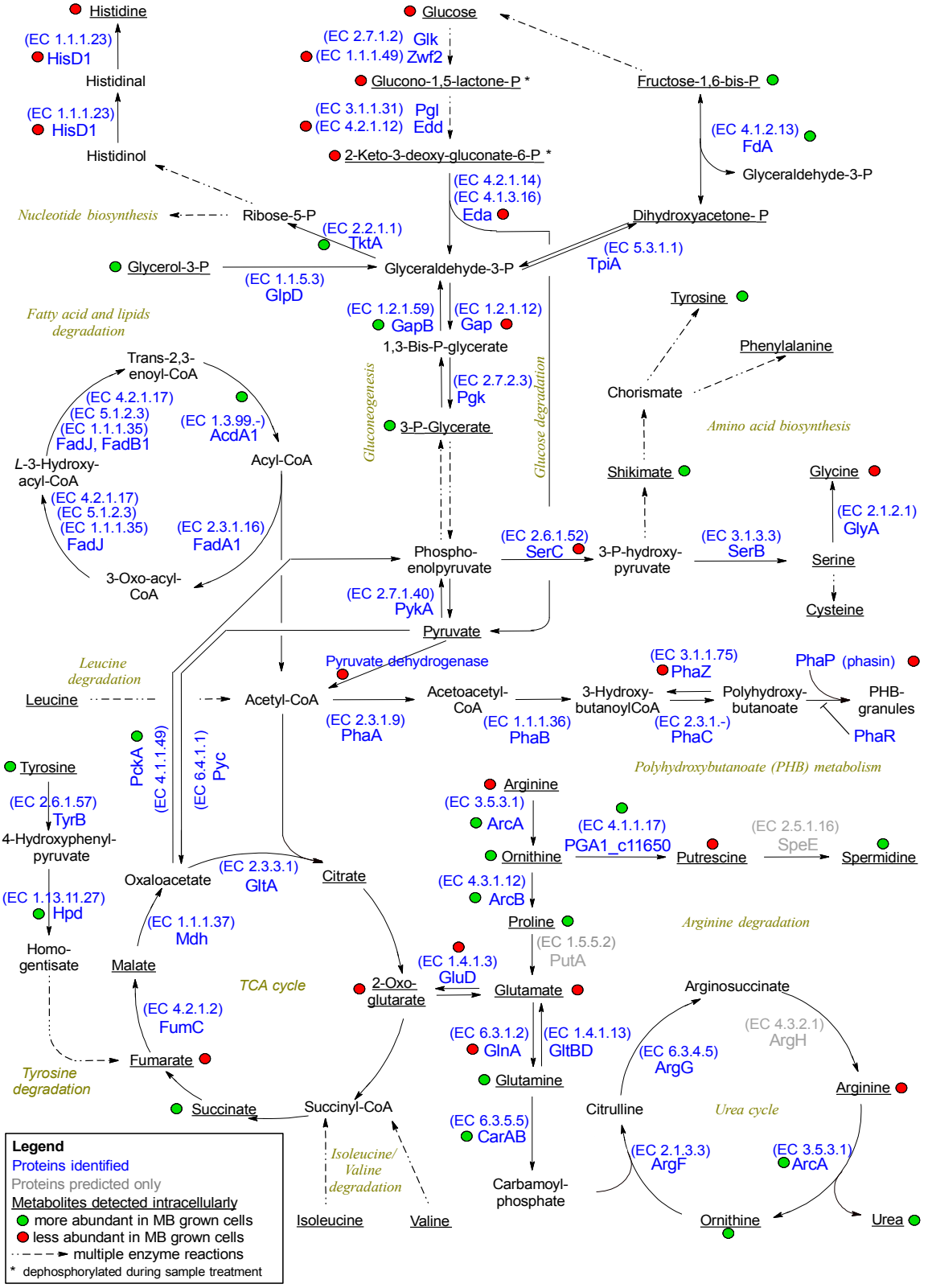

Figure 24: Overview of selected pathways that are active when grown in MB medium or glucose minimal medium. Metabolites were analysed by GC-MS, proteins by several proteomic approaches as described in joint publication (Zech *et al.*, 2013a). Further information to detected metabolites and enzymes are provided in the supplementary material S3 and S10.

degraded via pyruvate to acetyl-CoA. In case of alanine, degradation is accomplished by alanine dehydrogenase. Glycine degradation involves two catalytic steps: First, glycine is methylated via glycine hydroxymethyl-transferase; then resulting serine is deaminated via serine deaminase to obtain pyruvate. All required enzymes were detected by proteomic analysis. Shortness of these pathways might be a reason for preferred utilisation. High depletion rate was also observed for proline and glutamate. Degradation of these two amino acids feed into the TCA cycle via 2-oxoglutarate. Accordingly, complete consumption at ½ OD_{max} is probably main responsible for significant lower abundance of glutamate and 2-oxoglutarate (Figure 24) in cells grown in MB medium as compared to cells grown in minimal medium. Alternatively, considering the putative role of glutamate as compatible solute, its concentration might be reduced, due to the enormous import of substrates.

Polyhydroxybutanoate (PHB) metabolism. 3-hydroxybutanoate, which was abundant in cells grown on glucose and could be detected in all other conducted main experiments, is associated with PHB metabolism. Biosynthesis of this polymer requires plenty acetyl-CoA and reducing equivalents, in this case NADPH (Senior and Dawes, 1971; Madison and Huisman, 1999). Since acetyl-CoA is end-product of glucose degradation, biosynthesis of PHB might be directly induced under this condition (Figure 24). This could also be a specific adaptation to nutrient limiting conditions, since PHB can function as temporary energy and carbon storage that can easily be hydrolysed, yielding 3-hydroxybutanoate monomers. Thus, PHB guarantees efficient growth, as shown by De Eugenio *et al.* (2010) for *Pseudomonas putida*. Furthermore, synthesis of PHB might be used to replenish $NADP^+$, as suggested recently for *D. shibae* $DFL12^T$ (Laass *et al.*, 2014). Since $NADP^+$ is important for some oxidation reactions, such as conversion of glucose-6-phosphate by glucose-6-phosphate-dehydrogenase, *P. inhibens* DSM 17395 could tune its metabolism to sole carbon source (i.e. glucose) utilisation.

TCA cycle. Degradation of branched-chain amino acids that were moderately consumed, resulted in formation of succinyl-CoA and thus to elevated concentration of succinate. Moreover, imported succinate from the medium may contribute to this high intracellular succinate amount. Increased abundance of malate might be explained by degradation of aspartate to oxaloacetate. Latter compound can be converted to malate by reversible malate dehydrogenase reaction (e.g. Ohshima and Sakuraba, 1986). Lower

abundance of fumarate reflects minor relevance of tyrosine degradation, which yields fumarate as end-product. Interestingly, concentration of citrate was not significantly changed. This indicates similar actively condensation of oxaloacetate and acetyl-CoA to citrate, under both growth conditions, although in case of cells grown in MB medium, more pathways yielded acetyl-CoA, compared to cells grown in minimal medium, where only one catabolic pathway was active (Figure 24). Thus it appears that on the one hand, simultaneous utilisation of complex nutrients is inefficient, and that on the other hand, *P. inhibens* DSM 17395 is capable to tune its metabolism to efficient utilisation of only one single substrate, maybe by polyhydroxybutanoate metabolism, as discussed above.

Carbohydrate degradation. Although several carbohydrates, especially disaccharides, were available in MB medium and were imported, degradation of these substrates was not very active; in contrast to gluconeogenesis. Key-enzymes of the Entner-Doudoroff pathway (6-phosphogluconate dehydratase and 2-dehydro-3-deoxy-6-phosphogluconate aldolase) and catabolic intermediates were considerably less abundant in cells grown in MB medium (Figure 24) as compared to cells grown in glucose-containing minimal medium. Due to instability of particular phosphorylated intermediates of Entner-Doudoroff-pathway, such as 2-keto-3-deoxy-6-phosphogluconate (Strohhäcker *et al.*, 1993), only correspondent dephosphorylated compounds were detected and will refer in this and all other experiments to the correspondent phosphorylated intermediates. The observed down-regulation of Entner-Doudoroff pathway in cells grown in MB medium is contradicted by high intracellular abundances of disaccharides. Either, these disaccharides were stored temporarily or appropriate catabolic enzymes were missing. In case of lactose and maltotriose, missing enzymes are very probable, as Biolog phenotypic microarray analysis was negative (Section 3.1.1). Moreover, the pyruvate dehydrogenase multienzyme complex was less abundant in cells grown in MB medium. This indicates minor relevance of this enzyme complex under this condition compared to growth in minimal medium. Since many catabolic pathways that are active during growth in MB medium directly yield acetyl-CoA, this enzyme complex can easily by be circumvented.

4.3.2 Dynamics of amino acid utilization

4.3.2.1 Growth characteristics and extracellular metabolomic analysis

Growth. Cultivation of *P. inhibens* DSM 17395 with casamino acids in a time-dynamic experiment was applied to study time-resolved amino acid utilisation. The provided amino acids, each at different concentrations, reflect naturally occurring amino acid mixtures, similar to hydrolysates of microalgae (Brown, 1991). Remarkably, cells entered stationary phase, although sufficient amino acids were still available and amino acids were still imported. Stop of growth was also observed during growth in MB medium, and was in both cases, probably a result of quorum-sensing, due to formation of acyl-homoserine-lactones under these conditions as shown by Berger *et al.* (2012).

Amino acid depletion. Amino acids were utilised simultaneously, but with different depletion rates. Rapid utilisation of glutamate, aspartate, arginine and glycine was independent of provided concentrations or complexity of catabolic pathways. One may speculate whether glutamate preference results from time-delayed release of amino acids: glutamate in the early stage of phytoplanktonic bloom, compared to high abundances of aspartate, glycine, alanine and lysine after collapse of phytoplankton populations (Ittekkot, 1982). Overall, observed preference pattern for amino acids are similar to that in MB medium. In contrast to growth in MB medium, where no significant uptake differentiation of the three branched-chain amino acids was observed, clear preference for leucine was observed during growth on casamino acids. This preference can be caused by different factors, such as specificity of the shared transport system, e.g. shown for *Campylobacter jejuni* (Ribardo and Hendrixson, 2011), or inhibition of transportation by other amino acids, including branched-chain amino acids, as observed in *Corynebacterium glutamicum* (Ebbighausen *et al.*, 1989). Transport of branched-chain amino acids can also be affected by pH (Driessen *et al.*, 1987). Further, as shown by Yu *et al.* (2014) the branched-chain amino acid transaminase can have clear specificity for either leucine, isoleucine or valine derived 2-oxoacids..

Exported metabolites. To dispose of excess nitrogen from degradation of amino acids, urea was exported, as observed before during growth in MB medium (Section 3.3.1.2). Two intermediates of urea cycle were detected intracellularly (ornithine and arginine), whose concentration remained relatively constant, whereas urea itself was only detected

extracellularly and increased considerably with cultivation time. Partially, urea could also originate from carbodiimide (Khorana, 1953). Carbodiimide may be formed from arginine at high temperatures (e.g. autoclavation) (Lewis and Wolfenden, 2014). The extracellular increase of 2-isopropylmalate is surprising. It indicates overflow metabolism under nutrient excess. Adverse effects from imbalanced cellular metabolism is then compensated by export of overflow metabolites (Carneiro *et al.*, 2011). However, formation of 2-isopropylmalate as intermediate of leucine biosynthesis is directly inhibited by leucine. Due to high intracellular abundance of leucine, accumulation of 2-isopropylmalate should not occur, unless this feedback inhibition is defective in *P. inhibens* DSM 17395.

4.3.2.2 Intracellular metabolomic analysis

In this section, time-dynamic intracellular metabolic changes will be discussed in the context of their correspondent pathways. An overview about these pathways is provided in figure 25.

Amino acid degradation. Degradation of imported amino acids could be confirmed by proteomic analysis identifying all relevant key enzymes (e.g. glutamate dehydrogenase, aspartate aminotransferase and the glycine cleavage system). Glutamate was the preferred substrate, therefore complete consumption of glutamate at t_{25}, resulted in significantly metabolic changes. Substrate utilisation was shifted, e.g. to alanine. Accordingly, abundance and activity of alanine dehydrogenase increased after t_{25} (Zech *et al.*, 2013b). Other strongly depleted amino acids in this phase were proline, serine and lysine. As proline degradation proceeded via glutamate to 2-oxoglutarate, glutamate concentration was kept constant. In case of lysine degradation, several catabolic intermediates could be detected. 5-aminopentanoate and 2-aminoadipate represent two different branches of lysine degradation that are both used in *P. inhibens* DSM 17395. Different time-dependent distribution of these two compounds is remarkable and indicates different purposes of these two branches (see section 4.3.4.4 for discussion). Import and degradation of other amino acids is reflected by extracellular amino acid depletion, by intracellular accumulation of correspondent amino acids and high abundances of several catabolic enzymes.

Amino acid biosynthesis. Glutamine and asparagine could be easily synthesised by amination of imported glutamate and aspartate. Since cysteine was not provided in the

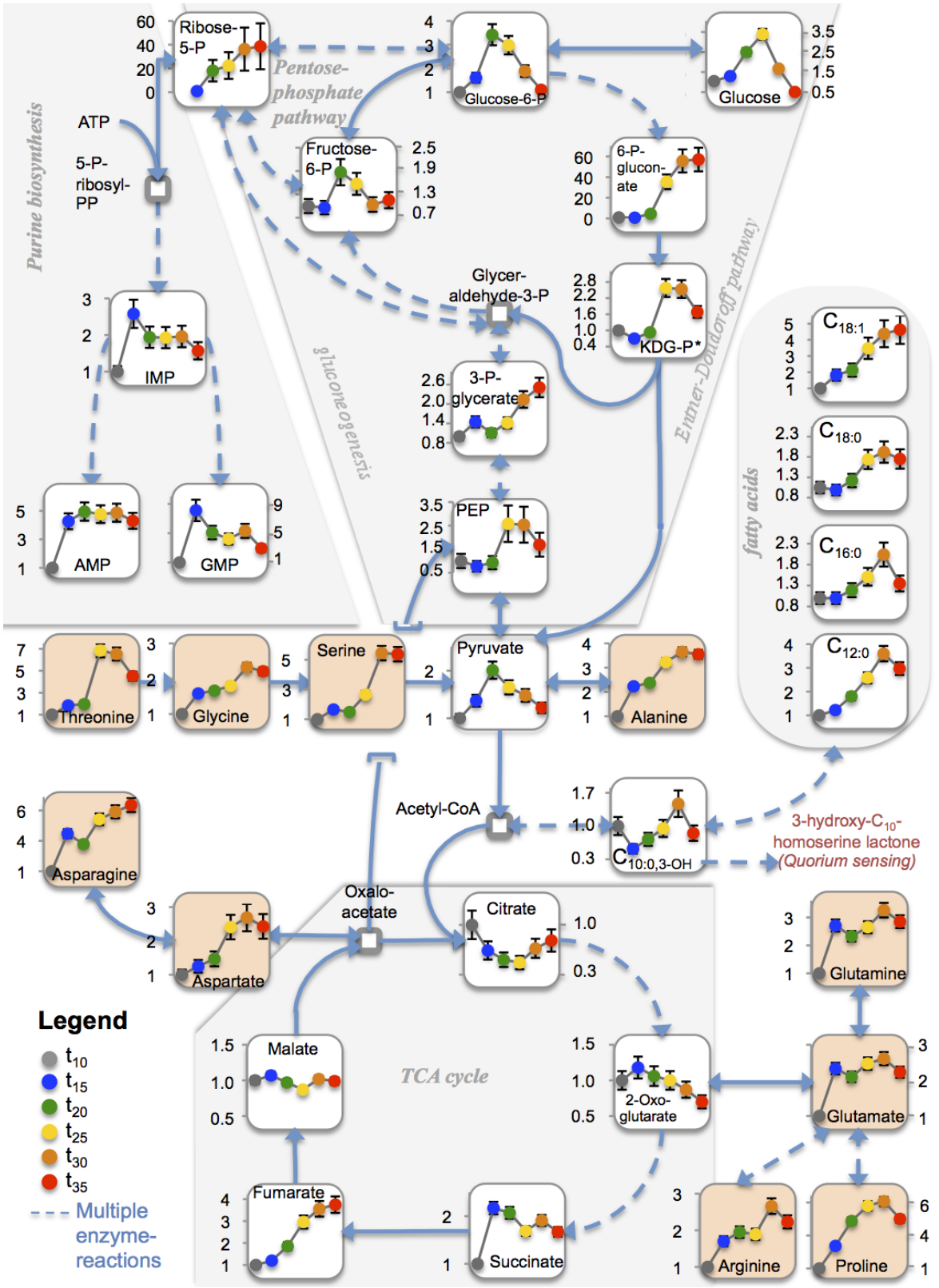

Figure 25: Overview of time-dynamic metabolic changes during growth on casamino acids. Relative abundances are shown as fold changes to reference state (t_{10}), orange squares mark amino acids. Abbreviations: *, compound dephosphorylated during sample treatment; AMP, adenosine-5'-monophosphate; ATP, adenosine-5'-triphosphate; GMP, guanosine-5'-monophosphate; IMP, inosine-5'-monophosphate; KDG, 2-keto-3-deoxy-gluconate; PEP, phosphoenolpyruvate.

medium, it had to be synthesised. Intracellular cysteine concentration increased significantly between t_{20} and t_{30}, coinciding with high abundance of correspondent biosynthetic enzymes until t_{30} (Zech *et al.*, 2013b). Further, also tryptophan had to be synthesised, as casamino acids did not contain any tryptophan. Biosynthesis was indicated by slightly increased abundance of tryptophan upon entry into the stationary phase. However, enzymes of tryptophan biosynthesis were not identified in this experiment. Whether increased abundance of histidine in the stationary phase resulted from biosynthesis or uptake from the medium is unclear, since neither specific enzymes of histidine biosynthesis, nor of histidine degradation could be detected in this experiment.

Fatty acids and acyl homoserine lactone formation. Increase of fatty acids during exponential growth phase, can be explained by higher needs of these precursors for cell membranes (Schujman and Mendoza, 2005). Concentration of dodecanoate and octadecenoate even slightly raised during transition to stationary phase, although abundance of fatty acid biosynthetic enzymes (enoyl-[acyl-carrier-protein] reductase (NADH) and 3-Oxoacyl-[acyl-carrier-protein] reductase) decreased in stationary phase. Though, formation of fatty acids continued in stationary phase, maybe as result of generated acetyl-CoA from degradation of some amino acids (e.g. serine, glycine and leucine).

Another explanation for increase of fatty acids over time, could be related to 3-hydroxy-C_{10}-homoserine lactone, the characteristic quorum sensing molecule of *P. inhibens* DSM 17395. Its formation under growth with casamino acids was confirmed by Berger *et al.* (2012). The precursor 3-hydroxydecanoate can either reactivated to generate longer alkyl-chains, or be condensed with S-adenosyl-methionine to mentioned quorum sensing molecule. Formation of acylhomoserine lactones yields 5-methylthioadenosine (Dickschat, 2010), which explains elevated amounts of latter compound. Notably, as Seyedsayamdost *et al.* (2011) have shown, *P. gallaeciensis* BS107 reacts to *p*-coumarate, probably by formation of *p*-coumaryl-homoserine lactone. This might explain increased abundance of structural similar compound 2-hydroxycoumarate, which is derived from phenylalanine metabolism.

Peptidoglycan and phospholipid headgroup components. The growth curve is reflected by similar abundance curves of alanyl-alanine and 2,6-diaminopimelate, probably because of their role in peptidoglycan formation and remodelling (Typas *et al.*, 2012). This

was contradicted by the time-dependent abundance distribution of phospholipid headgroup components, which were highest concentrated at t_{15}.

Nucleotide associated compounds. Efficient growth requires high amounts of nucleotides for gene replication. Accordingly, most compounds involved in purine and pyrimidine metabolism were considerably high abundant from t_{15} until stationary phase. As regulation is feedback inhibited (Ledesma-Amaro *et al.*, 2013; Reaves *et al.*, 2013), abundance changes for correspondent enzymes were not observed. Further, constant abundance levels for most of these compounds, especially for nucleobases also indicates active role of purine and pyrimidine salvage pathway.

Gluconeogenesis and Entner-Doudoroff pathway. In contrast to growth with complex nutrients, carbohydrates were absent in casamino acid medium. Therefore, higher gluconeogenic activity was required to maintain relevant metabolic functions (e.g. cell wall formation or pentose phosphate pathway). Accordingly, abundances of fructose-1,6-bisphosphate, fructose-6-phosphate, glucose and glucose-6-phosphate significantly increased in the early stage of growth, reaching highest amounts around t_{20}. Interestingly, disaccharides were not detected, indicating their minor role as storage compound or compatible solute in *P. inhibens* DSM 17395. Upon formation of glucose, also intermediates involved in glucose degradation via Entner-Doudoroff pathway were detected. An explanation could be the postulated constitutive expression of the glucokinase (Wiegmann *et al.*, 2014). Abundances of these intermediates increased significantly during transition phase to stationary phase and reached along with the key enzyme 6-phospho-gluconolactonase highest concentration in stationary phase. Carbohydrate degradation in *P. inhibens* DSM 17395 is discussed in more detail in section 4.3.5.1.

TCA cycle. While concentration of citrate, 2-oxoglutarate, succinate and malate remained relative constant after t_{15}, concentration of fumarate steadily increased, especially from t_{15} to t_{25}. The increase of fumarate could result from degradation of tyrosine, despite the minor role of tyrosine as substrate. Furthermore, the overall constant concentration of TCA cycle intermediates indicate rapidly reuse of these compounds for anabolism. Or amino acid degradation was slower than expected, as indicated by high abundances of intracellular amino acids and thus resulted only into low feed into the TCA cycle. Enzymes of TCA cycle displayed constant abundances, except for isocitrate dehydrogenase, which slightly increased in stationary phase.

4.3.3 Casamino acid consumption by plasmid-cured strains

P. inhibens DSM 17395 strains, lacking one or two plasmids, were cultivated on casamino acids to study the impact of plasmids on growth and substrate utilisation. Since strains lacking the 262 kbp plasmid reached considerable higher OD_{max} compared to the wild-type, essential genes that inhibit growth have to be located on this plasmid. Usually, quorum sensing is applied to trigger entry into the stationary phase. For this, members of the Roseobacter clade possess *luxI*, which encodes homoserine lactone synthase and a *luxR* gene, which is a response regulator (Schaefer *et al.*, 2008). As shown for *D. shibae* DFL12^T, Δ*luxI* resulted in considerable higher growth rate, higher cell density and reduced diversity of cell morphology (Patzelt *et al.*, 2013). In contrast to this, Δ*luxI* mutants of *P. inhibens* DSM 17395 showed delayed biosynthesis of tropodithietic acids, as biosynthesis of this antibiotic is apparently upregulated by homoserine lactones (Berger *et al.*, 2012). However, in *P. inhibens* DSM 17395 *luxI* and *luxR* are located on the chromosome, as well as genes for peripheral synthesis pathways for the quorum sensing signalling molecules. Maybe a histidine kinase located on the 262 kbp plasmid (PGA1_262p02120) is involved in quorum sensing as described for *Vibrio harveyi* (Waters and Bassler, 2005). Another explanation for higher OD_{max} could be the loss of essential genes for tropodithietic acid, which are encoded on the 262 kbp plasmid. Tropodithietic acid can also function as signal molecule, as it induces its own biosynthesis, thus it was suggested that it is used as quorum-sensing molecule (Geng and Belas, 2010b; Zan *et al.*, 2014). Therefore, the considerable higher OD_{max} reached by strains lacking the 262 kbp strongly implicates the dominant role of tropodithietic acid for growth regulation in *P. inhibens* DSM 17395.

Based on the genome sequence data, utilisation of amino acids is not affected directly by genes located the 65 kbp and/or 262 kbp plasmid. Most genes involved in amino acid degradation are located on the chromosome, with exception of 3-oxo-5,6-dehydrosuberyl-CoA semialdehyde dehydrogenase, involved in phenylalanine degradation (Supplementary material S10). Therefore, apart from higher consumption rate, amino acid utilisation preferences did not differ between tested strains. However, higher impact on amino acid utilisation could be expected by loss of the 78 kbp plasmid, as the relevant glycine cleavage system is encoded on this plasmid (Supplementary material S10).

4.3.4 Amino acid degradation

Cultivation of *P. inhibens* DSM 17395 on one of nine amino acids (phenylalanine, lysine, histidine, methionine, leucine, isoleucine, valine, threonine and tryptophan) as single carbon source was applied to study and to refine these catabolic networks. Cells grown on succinate served as reference condition. Based on the original annotated genome (Thole *et al.*, 2012), degradation of these nine amino acids remained unclear, e.g. due to missing enzymes or alternative pathways were possible. By combination of metabolomic, proteomic, enzymatic and bioinformatic approaches, unclear pathways could be resolved. In addition to published data of this cooperation experiment (Drüppel *et al.*, 2014), LC-MS data from coenzyme A analysis of cells grown on succinate were included here. The refined pathways are discussed in the subsections 4.3.4.3 to 4.3.4.9. Further, some additional metabolic features were observed in *P. inhibens* DSM 17395 during growth on individual amino acids, which is discussed in subsection 4.3.4.10.

4.3.4.1 Growth characteristics

Only half of carbon was provided in case of tryptophan and phenylalanine as compared to the other substrates, therefore growth on these two amino acids only resulted in moderate OD_{max}. In case of lysine and histidine relative low OD_{max} indicate inefficient substrate utilisation, whereas in case of methionine production of toxic sulfur-containing compounds and acids, like methanethiol, are probably main responsible for slow growth and low OD_{max}. As response to toxic compounds, scanning electron microscopy revealed that growth on methionine resulted in formation of prolonged cells (Drüppel *et al.*, 2014). Of the three branched-chain amino acids, shortest lag-phase was observed for leucine, indicating more effective utilisation as compared to isoleucine and valine, which was also noticed when *P. inhibens* DSM 17395 was provided with casamino acid mixture (Section 3.3.2). Specificity of branched chain amino acid uptake and degradation for one of these three amino acids was also observed in other bacteria (Ebbighausen et al, 1989; Ribardo and Hendrixson, 2011; Yu *et al.*, 2014).

4.3.4.2 Exometabolomic analysis

Extracellularly detected compounds were either intermediates involved in catabolism of correspondent substrates or side products of studied catabolic pathways. Export might compensate overflow metabolism, as observed e.g. for *E. coli* (Carneiro *et al.*, 2011). Such overflow metabolites were 2-aminobenzoate and kynurenine, intermediates of tryptophan degradation (see Section 4.3.4.9), as well as cadaverine, an intermediate of lysine degradation, which was detected in the supernatant of lysine and phenylalanine medium. Alternatively, exported compounds could be dead-end products from side reactions of catabolism, such as phenethylamine, which derived from phenylalanine by aromatic-*L*-amino-acid decarboxylase, or 2-hydroxyphenylanine, which derived from phenylpyruvate by 4-hydroxyphenyl pyruvate dioxygenase (Figure 26).

Another example for a dead-end product is 2-methylmalonate, which was found in medium supplied with isoleucine. It was most probably produced by an aldehyde dehydrogenase (NAD^+ or $NADP^+$) from methylmalonate semialdehyde, which is an intermediate of valine and isoleucine degradation. 2-methylmalonate could not be degraded further, as orthologues of (*S*)-methylmalonyl-CoA hydrolase (EC 3.1.2.17) are not encoded on the genome, which explains export of this intermediate.

Export of urea under all substrate conditions, except for tryptophan and succinate, again confirms the dominant role of urea cycle to dispose of excess nitrogen.

4.3.4.3 Refinement of phenylalanine degradation

Most bacteria, including *P. inhibens* DSM 17395, do not possess orthologues of phenylalanine 4-monoxygenase (EC 1.14.16.1) (Fitzpatrick, 2003). Accordingly, degradation of phenylalanine via initial hydroxylation to tyrosine and subsequent tyrosine degradation is rather uncommon for bacteria. Despite elevated concentrations of homogentisate, one representative of tyrosine degradation, major role of this pathway for phenylalanine degradation could be excluded. The only possibility to direct phenylalanine to homogentisate has to be accomplished via 4-hydroxyphenylacetate, which was significant more abundant in cells grown on phenylalanine. However, formation of 4-hydroxyphenylactate, as well as consecutive hydroxylation has to proceed via side reactions, since specific enzymes, which could catalyse correspondent reactions were not

identified by proteomic analyses, and orthologues were not found on the genome.

Therefore, degradation of phenylalanine proceeds via phenylacetate pathway as described by Teufel *et al.* (2010), which is visualised in figure 26. To direct phenylalanine to phenylacetyl-CoA several routes were found in databases, like KEGG (Kanehisa *et al.*, 2014), or MetaCyc (Caspi *et al.*, 2014). In *P. inhibens* DSM 17395, transamination of phenylalanine by aromatic amino acid aminotransferase produces phenylpyuvate, which is then directly converted to phenylacetyl-CoA by indolepyruvate ferredoxin oxidoreductase. Both enzymes were identified by proteomic analysis. Alternative routes to produce phenylacetyl-CoA are incomplete, but may be active through unspecific side reactions of identified enzymes, as indicated by detection of intermediates, such as phenylacetate. Followed degradation of phenylacetyl-CoA to succinyl-CoA could be completely covered by proteomic analysis. These findings could be underlined by detection of three out of six coenzyme A derivatives in succinate grown cells, in which amino acid degradation was partially active.

4.3.4.4 Refinement of lysine degradation

Of the 20 proteinogenic amino acids, highest number of possible degradation pathways have been described for lysine, listing 10 different in MetaCyc (Caspi *et al.*, 2014). The genome annotation of *P. inhibens* DSM 17395 suggested enzyme candidates for several lysine degradation pathways. Based on conducted analyses, two main branches were found to be active (Figure 26).

The first branch is accomplished by initial decarboxylation of lysine by lysine/ornithine decarboxylase (identified by proteomic analyses) to cadaverine. Then, one of two class III aminotransferases, which were identified by proteomic analyses, produces 1-piperideine or 5-aminopentanal. No enzyme candidate for conversion of 1-piperideine to 5-aminopentanal could be predicted by genome analysis. In case of 5-aminopentanal, an aldehyde dehydrogenase could be identified by proteomic analyses. The resulting 5-aminopentanoate is transaminated to glutarate semialdehyde. This reaction is catalysed by one of the two mentioned aminotransferases. Oxidation by mentioned aldehyde dehydrogenase yields glutarate. The final activation of glutarate to glutaryl-CoA is accomplished by a succinyl-CoA/formyl-CoA transferase or a putative glutaryl-CoA ligase (PGA1_c27870), which were identified by proteomic analyses.

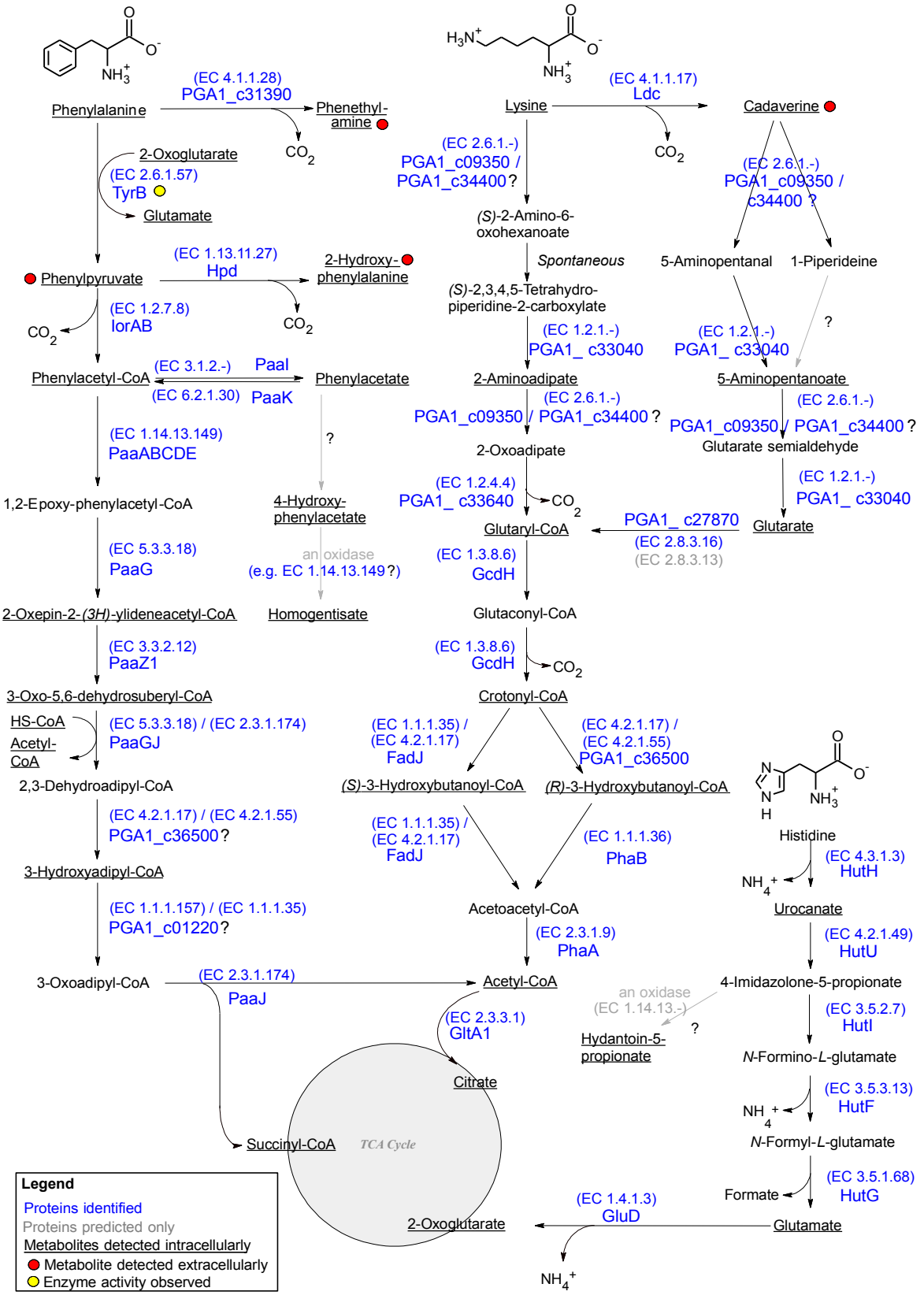

Figure 26: Refined degradation pathways for phenylalanine, lysine and histidine in *P. inhibens* DSM 17395. CoA derivatives were detected via LC-MS in cells grown on succinate. Other data from GC-MS and proteomic analyses as described in the joint publication (Drüppel *et al.*, 2014).

Proteomic data suggests, that the second branch via 2-aminoadipate is accomplished by the same enzymes as for the first branch, with exception of the final step from 2-oxoadipate to glutaryl-CoA, which is catalysed by a specific 2-oxoisovalerate dehydrogenase, which was identified by proteomic analyses. Initial transamination of lysine yields (*S*)-2-amino-6-oxohexanoate, which is converted spontaneously to (*S*)-2,3,4,5-tetrahydropiperidine-2-carboxylate or maybe to structure isomer pipecolate, which could be detected during growth on casaminoacids. Then, an aldehyde dehydrogenase produces 2-aminoadipate, which is transaminated to 2-oxoglutarate and finally activated to glutaryl-CoA.

The two branches merge at glutaryl-CoA, whose degradation is accomplished by conversion to crotonyl-CoA and followed decarboxylation to crotonyl-CoA. Both steps are catalysed by glutaryl-CoA dehydrogenase, as described for *Pseudomonas* sp. (Härtel *et al.*, 1993). The consecutive conversion to acetoacetyl-CoA may either proceed via *R*- or *S*-enantiomer of 3-hydroxybutanoyl-CoA. Coenzyme A analysis allowed identification of 3-hydroxybutanoyl-CoA, but without a discrimination between its enantiomers. According to proteomic data, probably both options are active. Acetoacetyl-CoA could not be detected, as it is instable at pH > 6 (King and Reiss, 1985) and thus not compatible with pH conditions used for sample preparation and LC-MS analysis. The final cleavage of acetoacetyl-CoA to two molecules acetyl-CoA is accomplished by acetyl-CoA acetyltransferase. All enzymes involved in degradation of glutaryl-CoA pathway were identified by proteomic analyses.

Currently it is unclear, whether both branches of lysine degradation to glutaryl-CoA are used in equal measure. The low abundance of 2-aminoadipate, indicates a minor role compared to degradation via cadaverine, or effective and fast catalytic processes. Further, diverse intracellular abundances of correspondent key-metabolites, when grown on complex medium, with casamino acid, or lysine alone, suggests different purposes of these two degradation branches. Since 5-aminopentanoate was only positive as nitrogen source in the Biolog phenotypic microarray analysis (Section 3.1.3), the branch via 5-aminopentanoate might serve primarily as nitrogen salvage.

Notably, although all enzymes for the widespread saccharopine pathway for lysine degradation are encoded on the genome, none of them were lysine-specifically produced (Drüppel *et al.*, 2014).

4.3.4.5 Refinement of histidine degradation

Two intermediates of histidine degradation were identified via GC-MS, which were urocanate and glutamate. Both were not significantly changed in abundance as compared to succinate-grown cells. However, all enzymes involved in histidine degradation could be identified by proteomic analysis. Correspondent genes are organised in one single gene cluster (Drüppel *et al.*, 2014). This agrees with findings, that histidine degradation is highly conserved and widespread in bacteria (Bender, 2012). According to metabolomic and proteomic data, histidine is degraded via 5-steps to glutamate, as described for *Pseudomonas* species (Bender, 2012) (Figure 26). The detected intermediate hydantoin-5-propionate belongs to alternative degradation pathway, which is not active due to missing orthologues of required enzymes.

4.3.4.6 Refinement of methionine degradation

According to genomic data, methionine degradation via 2-oxobutanoate could be conducted either by a 5-step conversion via 5-methyl-thioadenosine and homocysteine, or directly by methionine-γ-lyase (Kreis and Hession, 1973). The first option was only theoretical, since for bacteria it is only described for anabolic purposes (Cooper, 1983). Accordingly, methionine degradation in *P. inhibens* DSM 17395 proceeds via the direct step, which was revealed by conducted metabolomic and proteomic analyses. Methionine-γ-lyase and corresponding enzyme activity were detected. Further, the resulting product 2-oxobutanoate was more abundant in cells grown on methionine as compared to cells grown on succinate. Interestingly enough, protein c16590, which is encoded next to methionine-γ-lyase was detected by proteomic analyses. This protein shares functional domains of the E1 complex of the pyruvate dehydrogenase complex. Since c16590 was very abundant in methionine grown cells, it could enable to catalyse conversion of 2-oxobutanoate to propanoyl-CoA by modification of the pyruvate dehydrogenase (Drüppel *et al.*, 2014). The subsequent degradation of propanoyl-CoA to succinyl-CoA could completely be covered by proteomic analyses. Further, involved CoA intermediates were detected in cells grown on succinate. The refined methionine degradation is visualised in figure 27.

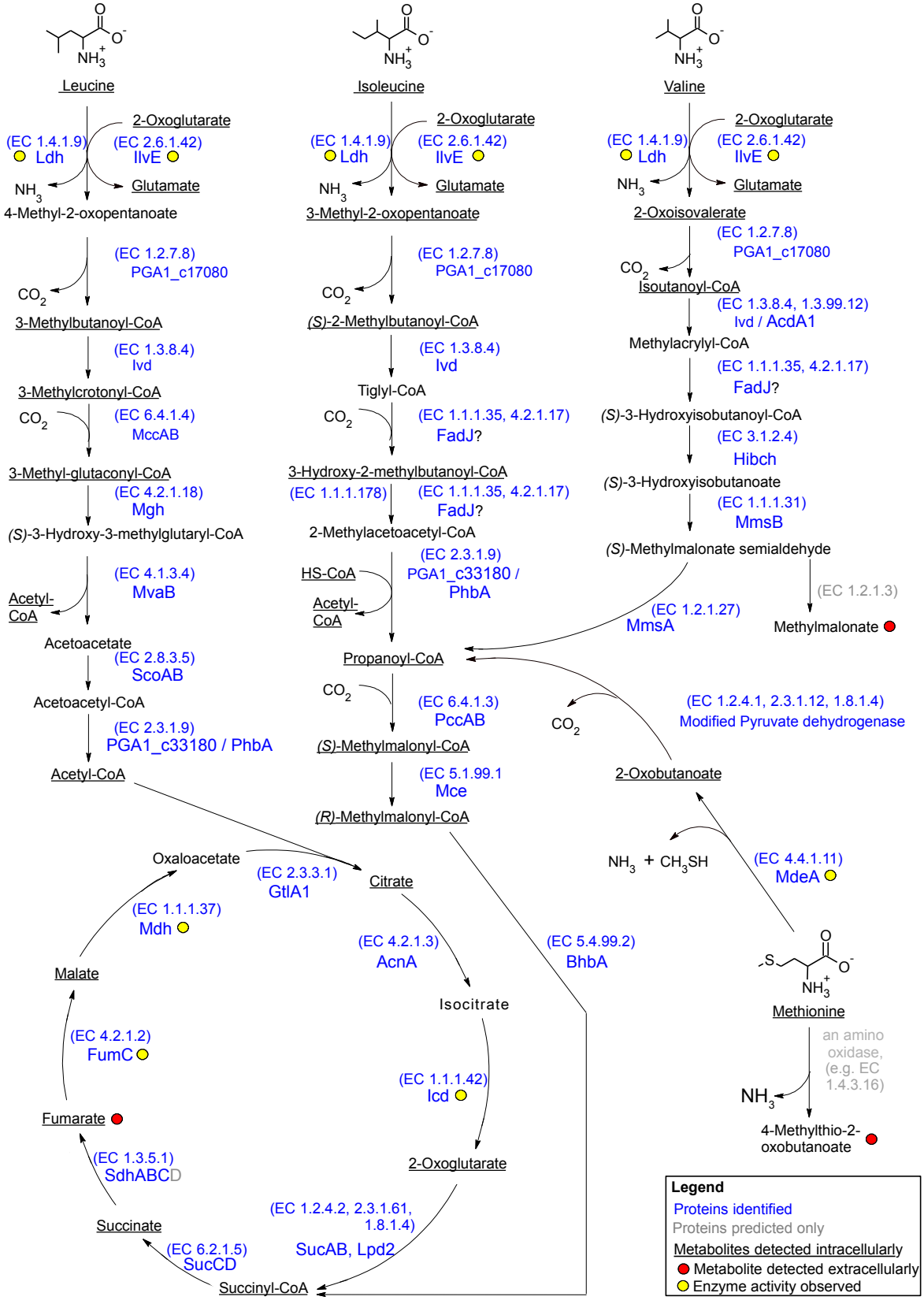

Figure 27: Refined degradation pathways for methionine, leucine, isoleucine and valine in *P. inhibens* DSM 17395. CoA derivatives were detected via LC-MS in cells grown on succinate. Other data from GC-MS and proteomic analyses as described in the joint publication (Drüppel *et al.*, 2014).

4.3.4.7 Refinement of branched-chain amino acid degradation

Degradation of branched chain amino acids is well described and is accomplished by initially deamination, followed by the conversion to a coenzyme A thioester. Consecutive degradation proceeds via several coenzyme A intermediates (Massey *et al.*, 1976). Since these compounds were not compatible with GC-MS, these pathways could not be covered by GC-MS-based metabolomic analysis. Some of involved coenzyme A derivatives could be detected in cells grown on succinate by LC-MS analysis. Remaining blind spots could be completely covered by proteomic analysis, which allowed complete reconstruction of leucine, isoleucine and valine degradation, which is visualised in figure 27. Notably, the first three reactions are identical for these three branched chain amino acids and were conducted by the same set of enzymes (Figure 27). For initial deamination of the amino acid, two enzymes were detected by proteomic analyses: branched-chain amino acid transferase and leucine dehydrogenase. Notably, leucine degradation finally yields acetyl-CoA, whereas both isoleucine and valine are directed via propanoyl-CoA to succinyl-CoA as described for methionine degradation.

4.3.4.8 Refinement of threonine degradation

Based on genome data, three different enzymes were possible for initial threonine degradation (threonine ammonia lyase, threonine aldolase and threonine-3-dehydrogenase). Since only presence and corresponding activity of the latter enzyme was detected, only one pathway is active, which is visualised in figure 28. Threonine degradation is initialised by oxidation to 2-amino-3-oxobutanoate. After cleavage to acetyl-CoA and glycine, resulting glycine is degraded via identified glycine cleavage system to ammonia, CO_2 and a methylene group with tetrahydrofolate as acceptor molecule. Alternatively, glycine is converted to serine by methylene-tetrahydrofolate-dependent serine hydroxymethyltransferase, which was identified by proteomic analyses. Interestingly, glycine is significant lower abundant in cells grown on threonine, indicating high consumption rate of glycine by these two enzymes. Deamination of serine to pyruvate might be accomplished by serine dehydratase, which could not be detected here by proteomic analyses, but was detected during growth in MB medium (Zech *et al.*, 2013a). The elevated concentration of the product pyruvate indicates that this reaction is active either through

that specific enzyme or through a similar unspecific enzyme. The final step, conversion of pyruvate to acetyl-CoA is accomplished by pyruvate dehydrogenase, all subunits could be detected by proteomic analysis.

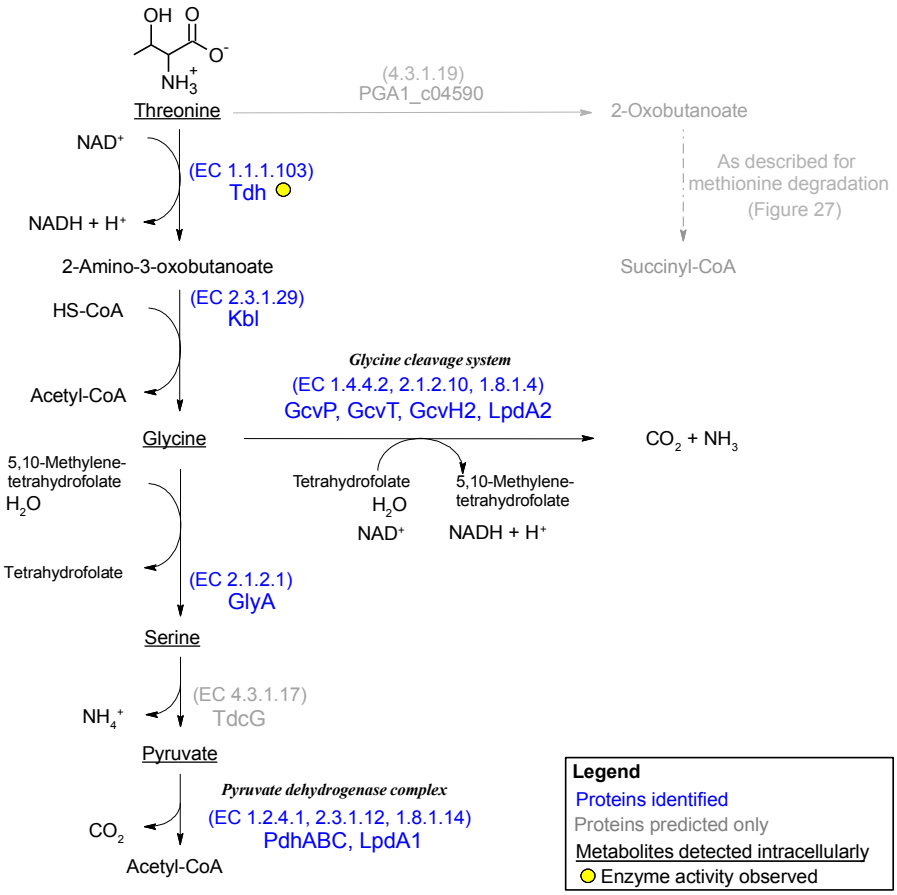

Figure 28: Refined threonine degradation in *P. inhibens* DSM 17395. Metabolites were analysed via GC-MS, proteins as described in the joint publication (Drüppel *et al.*, 2014).

4.3.4.9 Refinement of tryptophan degradation

According to conducted analyses, tryptophan degradation is initialised by conversion to *N*-formyl-*L*-kynurenine. The corresponding enzyme could be detected by proteomic analysis. For the consecutive conversion to *L*-kynurenine, no enzyme homologue of arylformidase could be predicted from the genome. Although, this enzyme could not be detected by proteomic analysis, corresponding enzyme activity was observed. Furthermore, the product kynurenine was detected in the culture supernatant via GC-MS. Protein-Blast of arylformidase of *Rhodobacter capsulatus* SB 1003 against the genome of *P. inhibens* DSM 17395 predicted a gene candidate for arylformidase, which could be confirmed by transcript analysis. Cleavage of kynurenine by kynureninase (identified by proteomic

analyses) yields 2-aminobenzoate and alanine. The latter compound is degraded via pyruvate to acetyl-CoA (Figure 29). Degradation of 2-aminobenzoate remained unclear. Based on proteomic data it was suggested, that identified 2-aminobenzoate-CoA ligase activates 2-aminobenzoate, which is then reduced to 2-amino-5-oxocyclohex-1-ene-carboxyl-CoA as described for *Azoarcus evansii* (Schühle *et al.*, 2001), (Figure 29).

But consecutive *β*-oxidation to acetyl-CoA has not been described so far (Fuchs, 2008) and neither could be based on proteomic data. Coenzyme A analysis allowed identification of hexanoyl-CoA and pentanoyl-CoA, both are more abundant in cells grown on tryptophan compared to cells grown on succinate (Figure 17). These two compounds might be derived from *β*-oxidation. Though, correspondent precursors, including 2-amino-benzoyl-CoA could not be identified. Instead, elevated concentrations of benzoyl-CoA and other CoA intermediates with a cyclohexane-ring structure were observed. This indicates some kind of benzoyl-CoA degradation as described for bacteria under anaerobic conditions (e.g. Heider *et al.*, 1998; Fuchs *et al.*, 2011), respectively some kind of aerobic hybrid pathway (Díaz *et al.*, 2013). Benzoyl-CoA could be produced through deamination of 2-aminobenzoyl-CoA. As Altenschmidt *et al.* (1991) have shown, the identified aminobenzoyl-CoA ligase can also activate benzoate. Thus, alternative to proposed published tryptophan degradation in *P. inhibens* DSM 17395 (Drüppel *et al.*, 2014), 2-aminobenzoate might be deaminated first, and then activated to benzoyl-CoA (Figure 29). Benzoyl-CoA degradation is most likely conducted by an alternative degradation, operable under aerobic condition, which has so far not yet been described before. The proposed sequential degradation of benzyol-CoA, based on detected coenzyme A intermediates is visualised in figure 29. The final degradation steps from 3-hydroxypimelyl-CoA to malonyl-CoA, plus further degradation of malonyl-CoA can be accomplished by different enzymes encoded on the genome.

4.3.4.10 General observations

The substrate amino acids were under correspondent cultivation conditions intracellularly significant more abundant as compared to cells grown on succinate, especially in case of cells grown on methionine, isoleucine, valine, lysine or threonine. This was either caused by insufficient washing efficiency, or resulted from faster uptake than followed degradation process. In contrast to this, decreased abundance of

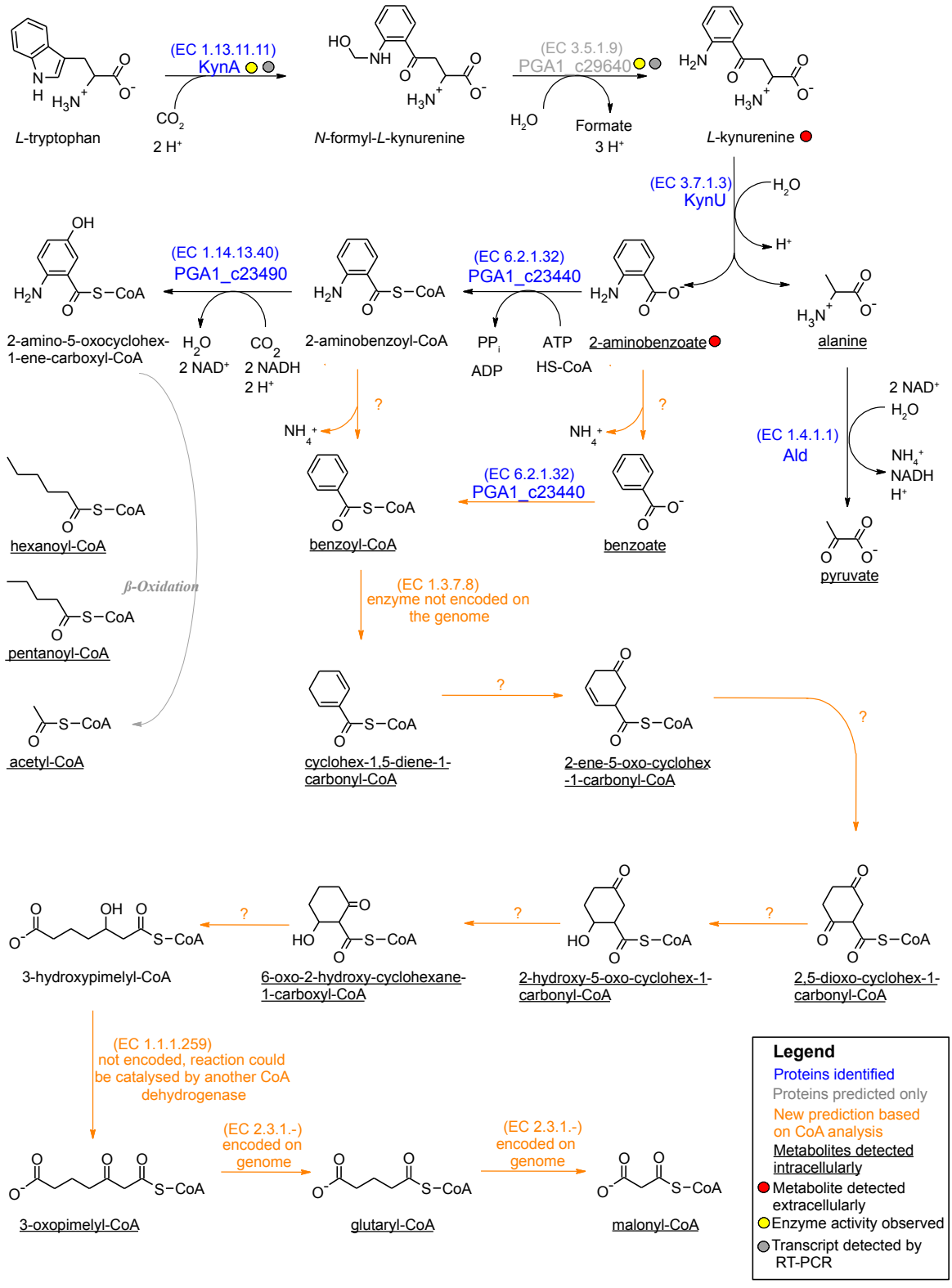

Figure 29: Refined tryptophan degradation in *P. inhibens* DSM 17395. CoA derivatives were specifically formed when grown on tryptophan and were detected via LC-MS. Other data included in this figure, such as GC-MS and proteomic data were obtained as described in joint publication (Drüppel *et al.*, 2014).

phenylalanine and constant concentration of leucine under correspondent cultivation conditions, indicate higher efficiency of initial substrate degradation (Table 13).

Another striking result was the overall low abundances of intracellular amino acids in most of the cells grown on single amino acids, especially in case of cells grown on tryptophan, phenylalanine, methionine or lysine (see figure18, supplementary material S6 and S7) as compared to cells grown on succinate. This is even more surprising, since additional nitrogen was provided (amino-group of the amino acid) compared to cells grown on succinate. The overall amino acid content correlates to the glutamate content, as glutamate is the most important nitrogen donor for amino acid biosynthesis (Merrick and Edwards, 1995). Accordingly, amino acid content of cells grown on histidine was similar to cells grown on succinate, because glutamate was obtained as the end product of histidine degradation and two out of three nitrogen atoms of histidine are released as utilisable ammonium (see figure 26). The amino acid content is further indirectly influenced by the TCA cycle. Any anabolic process drains intermediates of the TCA cycle, which have to be replenished.

The glyoxylate-shunt, described e.g. for *E. coli* as short-cut of the TCA cycle (Cortay *et al.*, 1989), is not operable in *P. inhibens* DSM 17395, as the key enzyme isocitrate lyase or orthologues genes are not encoded on the genome. Instead, anaplerotic reactions have to be used. However, of described enzymatic reactions, pyruvate carboxylase phosphoenol-pyruvate carboxykinase and malic enzyme were less abundant in cells grown on single amino acids compared to cells grown on succinate. Sole exception were cells grown on methionine; here malic enzyme was considerably more abundant compared to cells grown on succinate (Drüppel *et al.*, 2014). Thus, the ethylmalonyl-CoA pathway (Figure 30), which could be almost completely reconstructed for *P. inhibens* DSM 17395 based on proteomic data and LC-MS-based coenzyme A analysis, is used for replenishment of the TCA cycle.

The ethylmalonyl-CoA pathway was first described by Alber *et al.* (2006). But two reactions are still uncharacterised: (1) (*S*)-ethylmalonyl-CoA to methylsuccinyl-CoA, (2) methylsuccinyl-CoA to mesaconyl-CoA. The correspondent products of these two reactions could be detected in *P. inhibens* DSM 17395. However, it remains unclear, which enzymes catalyse these two reactions, as correspondent enzymes were not identified by proteomic analyses. A mutase has to catalyse the first reaction, the second reaction could

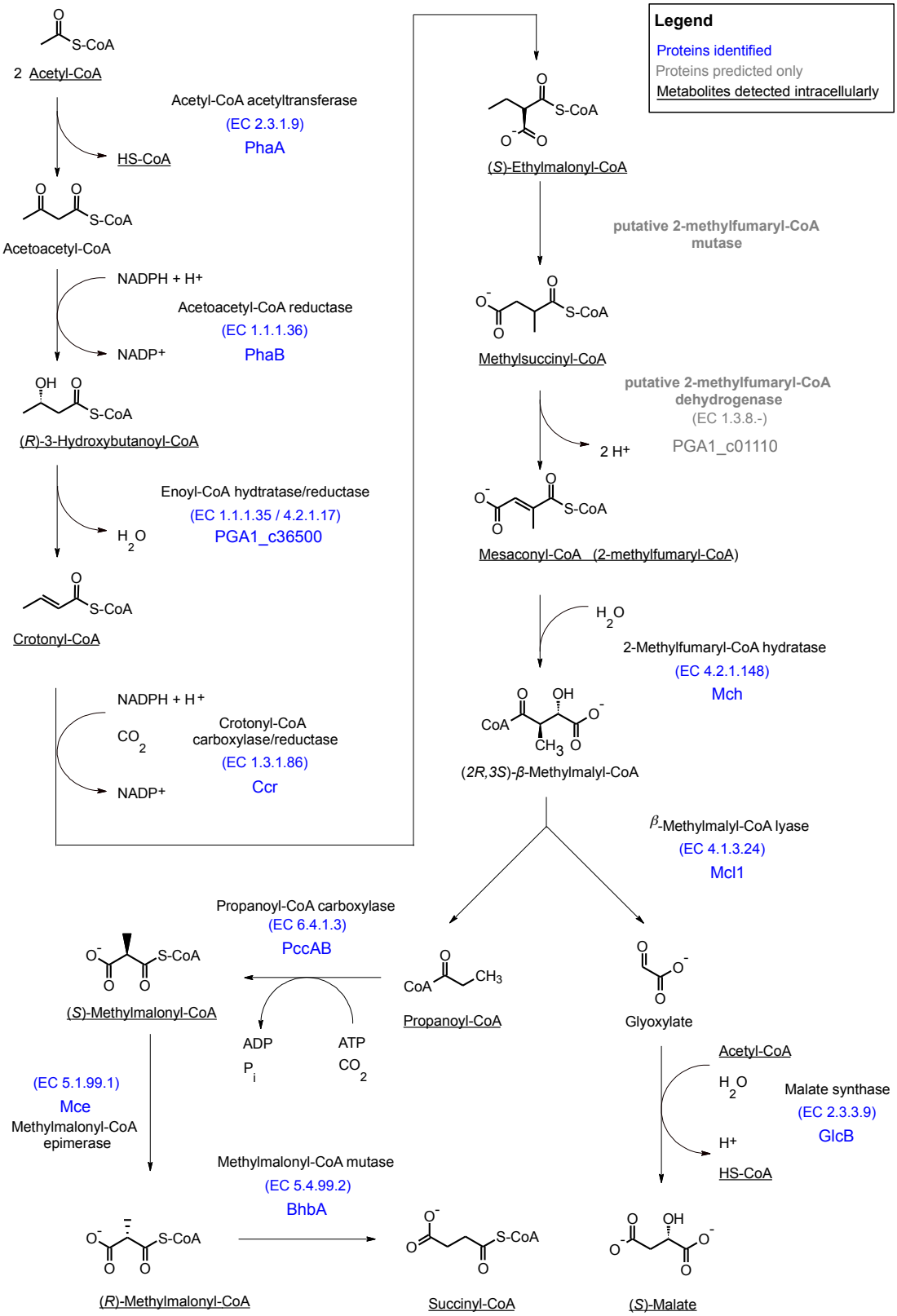

Figure 30: Ethylmalonyl-CoA pathway in *P. inhibens* DSM 17395. CoA derivatives were detected via LC-MS in cells grown on succinate. Included protomic data was taken from published joint experiment (Drüppel *et al.*, 2014).

be catalysed by a putative 2-methylfumaryl-CoA-dehydrogenase as described for *Rhodobaccter sphaeroides* (Erb *et al.*, 2009). An orthologue of second enzyme was found on the genome of *P. inhibens* DSM 17395 (PGA1_c01110).

Interestingly, key-enzymes of the ethylmalonyl-CoA pathway (crotonyl-CoA carboxylase and crotonyl-CoA reductase) were most abundant in cells grown on leucine and lysine (Drüppel *et al.*, 2014). In case of leucine this could be explained by formation of acetoacetyl-CoA and acetyl-CoA upon degradation of leucine that could directly injected into the ethylmalonyl-CoA pathway. In case of lysine, crotonyl-CoA is formed upon degradation of lysine. Overall, enzymes of ethylmalonyl-CoA pathway were more abundant in cells grown on single amino acids, except for cells grown on histidine, where replenishment of the TCA cycle might be less relevant, due to higher glutamate content.

Higher amounts of cadaverine, detected in cells grown on lysine, methionine, isoleucine or histidine, indicate purpose of cadaverine as nitrogen salvage. Polyamine formation could be a response of *P. inhibens* DSM 17395 to growth with amino acid rich medium, since polyamines were also detected in higher abundances during growth with complex nutrients and casamino acids (Sections 3.3.1 and 3.3.2). Presence of cadaverine resulted also in higher abundances of degradation products, such as 5-aminopentanoate and glutarate.

4.3.5 Carbohydrate degradation

P. inhibens DSM 17395 was cultivated on one out of five selected carbohydrates or succinate to study their utilisation and degradation. The studied carbohydrates represent the most relevant carbohydrate classes available in marine environments, such as *N*-acetyl-glucosamine, which is component of chitin, the second most abundant polymer in the environment. Chitin is component of fungal cell wall, exosceletons of worms, molluscs, insects and part of peptidoglykane of gram negative bacteria (Rinaudo, 2006). Sucrose is the most abundant disaccharide, which is formed by higher plants during photosynthesis (Reid and Abratt, 2005). Mannitol represents sugar alcohols, it is used as compatible solute by algae (Iwamoto and Shiraiwa, 2005). Glucose represents the most abundant neutral hexose, xylose represents a neutral pentose. As Poretsky *et al.* (2010) have shown, members of the Roseobacter clade have the highest number of transporter associated genes

amongst heterotrophic marine bacteria. This also explains observation that the Roseobacter clade dominates glucose uptake in marine environments (Alonso and Pernthaler, 2006). Thus, studying carbohydrate degradation is of major relevance to understand ecological success of the Roseobacter clade.

4.3.5.1 Refinement of carbohydrate degradation

The major route for glucose degradation was recently reconstructed for *P. inhibens* DSM 17395 by metabolomic, fluxomic and proteomic analyses (Zech *et al.*, 2009; Fürch *et al.*, 2009; Zech *et al.*, 2013a). Based on genome data, the peripheral degradation pathways for alternative sugars remained unclear. By combining metabolomic, proteomic, enzymatic and bioinformatic analysis the complete pathways could be refined, which is visualised in figure 31 and was published recently (Wiegmann *et al.*, 2014).

Transport. Carbohydrates can pass the outer membrane via porins. The transport across the cytoplasmic membrane is accomplished by ABC transporters as revealed by proteomic analyses. Such ABC transporter have a high specificity and high efficiency for low substrate concentrations up 10^{-6}-fold concentration differences, but are less energy efficient than phosphotransferase systems (Davidson and Maloney, 2007). Though, due to the generally low substrate concentrations in marine environments, employing ABC transporters represents an adaptation strategy of *P. inhibens* DSM 17395 to its environment. Notably, under each cultivation condition different transporter complexes were produced, indicating specificity for the correspondent carbohydrate class. However, the transporter produced during growth on glucose, is also capable importing sucrose and xylose and thus indicates low specificity of glucose import (Figure 31). Succinate import is accomplished via a TRAP transporter (Mulligan *et al.*, 2011; Walmsley *et al.*, 1992). Since this transportation is ATP-independent, uptake of succinate is less energy demanding than other substrates that are imported by ABC transporters, like carbohydrates and amino acids.

***N*-acetyl-glucosamine degradation.** The initial phosphorylation of *N*-acetyl-glucosamine was unclear, but could be resolved to be catalysed by identified *N*-acetyl-glucosamine kinase. The resulting product was then cleaved to acetate and glucosamine-6-phosphate. Activation of acetate by identified acetate-CoA ligase allows a short-cut of *N*-acetyl-glucosamine degradation, which is a beneficial feature allowing faster utilisation of the substrate for anabolic purposes, explaining the higher growth rates (Figure 19).

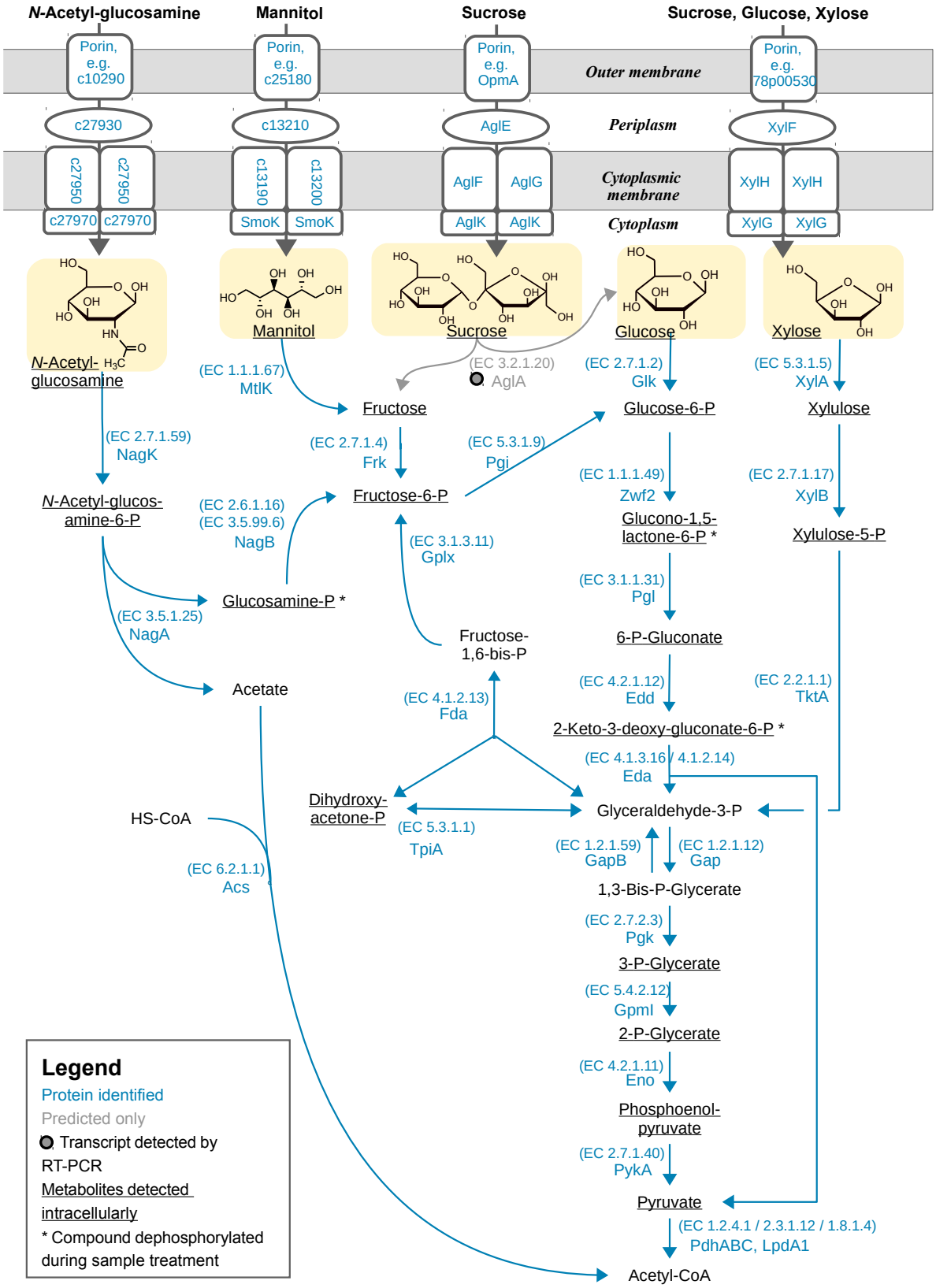

Figure 31: Refined carbohydrate degradation pathways in *P. inhibens* DSM 17395. Metabolites were analysed via GC-MS, proteins were analysed as described in joint publication (Wiegmann *et al.*, 2014).

Isomerisation of glucosamine-6-phosphate to fructose-6-phosphate is catalysed by specifically produced NagB in cells grown with *N*-acetyl-glucosamine. This protein functions most probably as glutamine-fructose-6-phosphate transaminase or alternatively as glucosamine-6-phosphate deaminase. In contrast to this, GlmS, another glutamine-fructose-6-phosphate transaminase was less abundant in cells grown on *N*-acetyl-glucosamine and more abundant under the other substrate conditions. Thus, NagB is used for catabolism, GlmS for anabolism. Finally, a conversion to glucose-6-phosphate allows degradation by the Entner-Doudoroff pathway (Figure 31).

Peripheral degradation of the other carbohydrates. Mannitol degradation proceeds probably by mannitol 2-dehydrogenase, which was produced specifically upon growth on mannitol or sucrose. Phosphorylation by fructokinase, which was identified by proteomic analyses, then yields fructose-6-phosphate, which is degraded analogue to *N*-acetyl-glucosamine. Sucrose degradation proceeds by initially cleavage into glucose and fructose. The responsible enzyme *α*-glucosidase was not detected by proteomic analysis, but was detected by transcript analysis. Fructose is degraded as described for mannitol degradation. Glucose degradation is initialised by phosphorylation of the substrate. Since *P. inhibens* DSM 17395 does not possess a phosphotransferase uptake system, which phosphorylates glucose upon import, phosphorylation is conducted by phosphoglukokinase. The resulting glucose-6-phoshphate is then degraded by the Entner-Doudoroff pathway. Data indicated that glucokinase is expressed constitutive, as it is solitary localised on the genome (Wiegmann *et al.*, 2014). Xylose degradation proceeds by initial isomerisation to xylulose, followed by phosphorylation to xylulose-5-phosphate. Further degradation is linked with pentose phosphate pathway. Besides glyceraldehyde-3-phosphate, which is directly inserted into the Embden-Meyerhof-Parnas pathway, pentose phosphate pathway also yields fructose-6-phosphate, which is degraded via Entner-Doudoroff pathway.

Entner-Doudoroff pathway, Embden-Meyerhof-Parnas pathway and TCA cycle. Since all carbohydrates, including xylose are degraded via the Entner-Doudoroff pathway followed by degradation via the Embden-Meyerhof-Parnas pathway, most intermediates were considerably more abundant in cells grown on single carbohydrates compared to cells grown on succinate. This was underlined by high abundance of correspondent enzymes. In contrast to this, enzymes specifically involved in gluconeogenesis, such as pyruvate carboxylase and glyceraldehyde-3-phosphate dehydrogenase were more abundant in cells

grown on succinate. This also explains presence and higher abundance of some intermediates of Embden-Meyerhof-Parnas pathway in cells grown on succinate. Notably, proteomic analysis revealed that proteins involved in pentose phosphate pathway, pyruvate dehydrogenase complex and the TCA cycle showed mainly no abundance changes between the six studied substrate conditions. This was contradicted by lower abundances of all intermediates of the TCA cycle, except for citrate, in cells grown on single carbohydrates compared to cells grown on succinate. Sole exceptions were cells grown on *N*-acetyl-glucosamine, where citrate, 2-oxoglutarate, fumarate and malate were considerably more abundant as compared to cells grown on succinate. The reason for abundance changes of TCA cycle intermediates are different entry points into the TCA cycle (i.e. citrate in case of carbohydrate degradation or simply import of succinate in case of reference condition) and draining of intermediates for anabolic purposes.

4.3.5.2 General observations

Formation of acetylated compounds. In cells grown on *N*-acetyl-glucosamine, considerable higher amounts of acetylated metabolites were detected. Biosynthesis of detected *O*-acetyl-serine involves acetyltransferase and cysteine synthase, both enzymes were detected, but showed no abundance changes. This was also true for arginine biosynthesis bifunctional protein (Wiegmann *et al.*, 2014), which catalyses formation of *N*-acetyl-glutamate, which was abundant under this condition. Thus, higher biosynthesis rates in these cases were accomplished by higher abundance of the precursor acetyl-CoA.

Formation of C_4-carboxylates. The biosynthesis and purpose of the very abundant C_4-carboxylates (tartrate, erythronate and threonate) in cells grown on single carbohydrates is not clear. Database survey, e.g. BRENDA (Schomburg *et al.*, 2012) revealed only few known enzyme reactions, producing or consuming these compounds. As Flint (1994) has shown, fumarase in *E. coli* uses tartrate as substrate and can perform reverse reaction. Thus, some C_4-intermediates of the TCA cycle could be used as precursor, e.g. by hydratisation of succinate as shown for meso-tartrate dehydrogenase (Kohn and Jakoby, 1966), but it seems not to be encoded on the genome of *P. inhibens* DSM 17395.

The abundance of C_4-carboxylates correlates with growth on individual carbohydrates. Therefore, involvement of intermediates and enzymes of Entner-Doudoroff pathway and Embden-Meyerhof-Parnas pathway are very likely. Maybe, tartrate was produced from

glycerate, glyceraldehyde or glycerate-3-phosphate by reverse reaction of tartrate decarboxylase. Another explanation may be the oxidation of erythrose-4-phosphate, an intermediate of the pentose phosphate pathway, to erythronate-4-phosphate. In *E. coli* K-12 this reaction is catalysed by an erythrose-4-phosphate dehydrogenase like enzyme (Zhao *et al.*, 1995). Notably, glyceraldehyde-3-phosphate dehydrogenase from *P. inhibens* DSM 17395 shows high similarity to this enzyme. Due to high abundant glyceraldehyde-3-phosphate dehydrogenase in cells grown on single carbohydrates (Wiegmann *et al.*, 2014), side-reaction could produce erythronate and the isomer threonate. Oxidation of threonate or erythronate would yield tartrate, as observed in plants (Helsper and Loewus, 1982).

So far, about the biological functions of C_4-carboxylates in *P. inhibens* DSM 17395 can only be speculated. Tartrate is known to inhibit enzymes, such as malate dehydrogenase (Voegele *et al.*, 1999) or fumarase (Genda *et al.*, 2006) and to chelate metal-ions (Violante *et al.*, 2010). C_4-carboxylates might be used as compatible solute or temporary carbon storage. As Mustakhimov *et al.* (2010) have shown for halophilic bacteria, concentration of tartrate and other C_4-dicarboxylates concentration increased as response to osmotic stress. This indicates a potential role of tartrate as compatible solute in *P. inhibens* DSM 17395.

4.3.6 Metabolic responses to ammonium limited growth condition

Cultivation under ammonium limited medium conditions (1 mM NH_4Cl) was applied to study the metabolic responses of *P. inhibens* DSM 17395 to such starvation conditions, in a time-course experiment.

Growth characteristics. Growth characteristics were similar to those with 4.7 mM NH_4Cl in the “carbohydrate degradation” experiment (see section 3.3.5.1). The determined cellular N/C ratio at the beginning of cultivation (≈0.24) was similar to cells grown in MB medium upon entry into the stationary phase (≈0.21) (Table 17) and to cellular N/C ratio in natural planctonic bacteria in lakes (≈0.2) (Nagata, 1986). Apparently, due to nitrogen starvation, the cellular N/C ratio decreased considerably over the following cultivation time, finally being lower than during growth with sufficient ammonium (Table 17). This was reflected by decline of nitrogen-containing metabolites (e.g. amino acids) over time (Figure 22), which could also be observed in a similar study with the fission yeast *Schizosaccharomyces pombe* (Sajiki *et al.*, 2013).

Ammonium assimilation and nitrogen control. In almost all cells, glutamate and glutamine are the key nitrogen donors for anabolic processes. Therefore, incorporation of nitrogen is facilitated by assimilation of ammonium with 2-oxoglutarate, which yields glutamate (Merrick and Edwards, 1995). In *P. inhibens* DSM 17395 this is accomplished by glutamate synthase or glutamate dehydrogenase and consecutive glutamate-ammonia ligase, which produces glutamine. Accordingly, complete consumption of ammonium at t_{20} resulted in time-delayed intracellular increase of 2-oxoglutarate, as also observed for *S. pombe* (Sajiki *et al.*, 2013) and simultaneous decrease of glutamate at t_{25}. Upon this nitrogen starvation, most probably gene expression of glutamate synthase and transporters for ammonium and organic nitrogen sources is upregulated as shown for *P. putida* under nitrogen limiting conditions (Poblete-Castro *et al.*, 2012). Since nitrogen assimilation reactions are energy-demanding, it is, along with biosynthesis of nitrogen-containing compounds, strongly regulated in bacteria (Merrick and Edwards, 1995; Leigh and Dodsworth, 2007). This may be the explanation for the apparent biosynthesis stop of nitrogen-containing compounds, respectively for the slow decline over time, such as nucleobases and aminobutanoates.

Metabolic changes upon nitrogen starvation. Due to the early nitrogen starvation, around t_{20} to t_{25}, abundance of metabolites already decreased between t_{25} and t_{30}, i.e. before ½ OD_{max} was reached. This decrease also included nitrogen-free compounds, such as carbohydrates and intermediates of the TCA cycle. Upon entry into stationary phase, some amino acids became temporarily more abundant. Since biosynthesis of nitrogen-containing compounds is assumed to be slowed down, these compounds have to derive from degradation of proteins. Elevated levels of 5-aminopentanoate at t_{40}, an intermediate of lysine degradation, underlines this hypothesis.

In contrast to this, elevated concentrations of nicotinate and nicotinamide in the stationary phase, might either be result of degradation of NAD, or might be involved in nitrogen control, as it was shown for the NAD synthetase in *Rhodobacter* sp. (Merrick and Edwards, 1995).

The increase of intracellular and extracellular 3-hydroxybutanoate upon entry into the stationary phase indicated formation of polyhydroxybutanoate, which was also shown recently for *P. putida* under nitrogen-limiting conditions (Poblete-Castro *et al.*, 2012). This formation could be a direct response to starvation conditions and could also contribute to

the low cellular N/C ratio.

Although most metabolites decreased in abundance during stationary phase, some unknown compounds increased markedly in that phase. Some of those unknown compounds were specific for this experiment. In stationary phase, bacteria show general stress responses, as investigated and reviewed several times (e.g. Kolter *et al.*, 1993; Tani *et al.*, 2002; Nyström, 2004). Thus one may speculate, whether these unknown compounds were formed as stress response.

5 Conclusion

Heterotrophic marine bacteria are mainly challenged by nutrient conditions, which comprise a high complexity, diversity and seasonal fluctuation. To unravel how marine bacteria can overcome such conditions, the metabolism of *P. inhibens* DSM 17395 was studied in detail by combining metabolomic and proteomic approaches.

In this thesis, several key characteristics were determined explaining the special adaptation of this bacterium to its native environment. The broad substrate range for carbon and nitrogen sources, as revealed by Biolog phenotypic microarray analysis, facilitate the bacterium to utilise any available substrate. High number of different transporters, encoded on the genome, as well as multiple functionality of particular catabolic enzymes contribute to this skill. *P. inhibens* DSM 17395 uses mostly ABC transporters that are very efficient at typical low substrate concentrations in seawater.

MB medium represents complex nutrient conditions that are typical (seasonal) in the natural environments of *P. inhibens* DSM 17395. In most bacteria metabolite repression is active, resulting in utilisation of only one or few different compounds (Görke and Stülke, 2008). In contrast to this, *P. inhibens* DSM 17395 is capable to tune its metabolism to simultaneous utilisation of several substrates. In accordance with observed high intracellular concentrations of imported substrates, first priority is to import substrates to safe them against potential competitors. Alternatively, metabolism was efficiently adapted to one specific substrate, if only one was provided. Formation of disaccharides is rather exclusively induced upon active utilisation of carbohydrates. As alternative for energy and carbon storage, *P. inhibens* DSM 17395 builds poly-3-(*R*)-hydroxybutanoate. Biosynthesis of this polymer could also be used to replenish $NADP^+$, allowing to tune particular catabolic pathways.

Cultivation on casamino acids in a time-dynamic experiment showed that *P. inhibens* DSM 17395 used most of supplied substrates simultaneously. Upon complete consumption of preferred substrates, the metabolism switched quickly to utilisation of alternative substrates. Cells entered stationary phase although sufficient utilisable amino acids were still available. The most probable reason for this was acyl-homoserine-lactone induced quorum sensing. However, the antibiotic tropodithietic acid, which is produced by *P. inhibens* DSM 17395, seems to have a higher impact on growth stop, as revealed by

cultivation of plasmid-cured strains. These strains lost the ability to produce this antibiotic and reached considerable higher cell densities.

Growth on individual substrates revealed some constraints of metabolism. Side reactions produced some unexpected dead-end products. These were exported, along with overflow intermediates and the waste product urea. Such exported compounds may have an impact on the carbon and nitrogen cycle in the marine habitat. Replenishment of TCA cycle for anabolic processes is inefficient, since the complex ethylmalonyl-CoA pathway is used in *P. inhibens* DSM 17395. The requirement of this pathway is diminished, if several substrates are utilised simultaneously that feed the TCA cycle at different entry-points. Furthermore particular catabolic pathways, such as lysine degradation generate precursors of the ethylmalonyl-CoA pathway. Therefore, *P. inhibens* DSM 17395 is rather adapted to growth on substrate mixtures.

Degradation of structural similar carbohydrates in *P. inhibens* DSM 17395 is performed efficiently. Only few enzymes are required for peripheral degradation, until all carbohydrates are degraded by the Entner-Doudoroff pathway. This pathway compensates absent phosphofruktokinase and non operable oxidative pentose phosphate pathway. The Entner-Doudoroff pathway generates per mol substrate 1 mol ATP and NADH less than glycolysis, but one mol NADPH more. The latter is important for anabolic purposes, e.g. amino acids and fatty acid biosynthesis.

Homologous enzymes of central metabolism and studied degradation pathways are widespread distributed across the Roseobacter clade (Drüppel *et al.*, 2014; Wiegmann *et al.*, 2014). Therefore, many of the observed metabolic features of *P. inhibens* DSM 17395 may be assigned to other members of the Roseobacter clade. The formation of structural unknown compounds and uncommon metabolites, e.g. tartrate, have so far not yet been assigned to perform biological functions. These detected uncommon compounds could be a specific adaptation to the marine environment, or even be a general characteristic of the Roseobacter clade.

References

Alber, B.E., Spanheimer, R., Ebenau-Jehle, C., Fuchs, G., 2006. Study of an alternate glyoxylate cycle for acetate assimilation by *Rhodobacter sphaeroides*. *Mol. Microbiol*. 61, 297–309.

Alonso, C., Pernthaler, J., 2006. *Roseobacter* and SAR11 dominate microbial glucose uptake in coastal North Sea waters. *Environ. Microbiol.* 8, 2022–2030.

Alonso-Sáez, L., Balagué, V., Sà, E.L., Sánchez, O., González, J.M., Pinhassi, J., Massana, R., Pernthaler, J., Pedrós-Alió, C., Gasol, J.M., 2007. Seasonality in bacterial diversity in north-west Mediterranean coastal waters: assessment through clone libraries, fingerprinting and FISH. *FEMS Microbiol. Ecol.* 60, 98–112.

Alonso-Sáez, L., Gasol, J.M., 2007. Seasonal Variations in the Contributions of Different Bacterial Groups to the Uptake of Low-Molecular-Weight Compounds in Northwestern Mediterranean Coastal Waters. *Appl. Environ. Microbiol.* 73, 3528–3535.

Altenschmidt, U., Oswald, B., Fuchs, G., 1991. Purification and characterization of benzoate-coenzyme A ligase and 2-aminobenzoate-coenzyme A ligases from a denitrifying *Pseudomonas sp. J. Bacteriol.* 173, 5494–5501.

Appeltans, W., Ahyong, S.T., Anderson, G., Angel, M.V., Artois, T., Bailly, N., Bamber, R., Barber, A., Bartsch, I., Berta, A., Błażewicz-Paszkowycz, M., Bock, P., Boxshall, G., Boyko, C.B., Brandão, S.N., Bray, R.A., Bruce, N.L., Cairns, S.D., Chan, T.-Y., Cheng, L., Collins, A.G., Cribb, T., Curini-Galletti, M., Dahdouh-Guebas, F., Davie, P.J.F., Dawson, M.N., De Clerck, O., Decock, W., De Grave, S., de Voogd, N.J., Domning, D.P., Emig, C.C., Erséus, C., Eschmeyer, W., Fauchald, K., Fautin, D.G., Feist, S.W., Fransen, C.H.J.M., Furuya, H., Garcia-Alvarez, O., Gerken, S., Gibson, D., Gittenberger, A., Gofas, S., Gómez-Daglio, L., Gordon, D.P., Guiry, M.D., Hernandez, F., Hoeksema, B.W., Hopcroft, R.R., Jaume, D., Kirk, P., Koedam, N., Koenemann, S., Kolb, J.B., Kristensen, R.M., Kroh, A., Lambert, G., Lazarus, D.B., Lemaitre, R., Longshaw, M., Lowry, J., Macpherson, E., Madin, L.P., Mah, C., Mapstone, G., McLaughlin, P.A., Mees, J., Meland, K., Messing, C.G., Mills, C.E., Molodtsova, T.N., Mooi, R., Neuhaus, B., Ng, P.K.L., Nielsen, C., Norenburg, J., Opresko, D.M., Osawa, M., Paulay, G., Perrin, W., Pilger, J.F., Poore, G.C.B., Pugh, P., Read, G.B., Reimer, J.D., Rius, M., Rocha, R.M., Saiz-Salinas, J.I., Scarabino, V., Schierwater, B., Schmidt-Rhaesa, A., Schnabel, K.E., Schotte, M., Schuchert, P., Schwabe, E., Segers, H., Self-Sullivan, C., Shenkar, N., Siegel, V., Sterrer, W., Stöhr, S., Swalla, B., Tasker, M.L., Thuesen, E.V., Timm, T., Todaro, M.A., Turon, X., Tyler, S., Uetz, P., van der Land, J., Vanhoorne, B., van Ofwegen, L.P., van Soest, R.W.M., Vanaverbeke, J., Walker-Smith, G., Walter, T.C., Warren, A., Williams, G.C., Wilson, S.P., Costello, M.J., 2012. The Magnitude of Global Marine Species Diversity. *Curr. Biol.* 22, 2189–2202.

Apple, J.K., Del Giorgio, P.A., Kemp, W.M., 2006. Temperature regulation of bacterial production, respiration, and growth efficiency in a temperate salt-marsh estuary. *Aquat. Microb. Ecol.* 43, 243–254.

Bantscheff, M., Lemeer, S., Savitski, M.M., Kuster, B., 2012. Quantitative mass spectrometry in proteomics: critical review update from 2007 to the present. *Anal. Bioanal. Chem.* 404, 939–965.

Bender, R.A., 2012. Regulation of the Histidine Utilization (Hut) System in Bacteria. *Microbiol. Mol. Biol. Rev.* 76, 565–584.

Benjamini, Y., Hochberg, Y., 1995. Controlling the false discovery rate: a practical and powerful approach to multiple testing. J. R. *Stat. Soc. Ser. B Methodol.* 289–300.

Benton, H.P., Want, E.J., Ebbels, T.M.D., 2010. Correction of mass calibration gaps in liquid chromatography–mass spectrometry metabolomics data. *Bioinformatics* 26, 2488–2489.

Berger, M., Neumann, A., Schulz, S., Simon, M., Brinkhoff, T., 2011. Tropodithietic Acid Production in

Phaeobacter gallaeciensis Is Regulated by N-Acyl Homoserine Lactone-Mediated Quorum Sensing. *J. Bacteriol.* 193, 6576–6585.

Berger, M., Brock, N.L., Liesegang, H., Dogs, M., Preuth, I., Simon, M., Dickschat, J.S., Brinkhoff, T., 2012. Genetic Analysis of the Upper Phenylacetate Catabolic Pathway in the Production of Tropodithietic Acid by *Phaeobacter gallaeciensis*. *Appl. Environ. Microbiol.* 78, 3539–3551.

Berg, G.M., Jørgensen, N.O.G., 2006. Purine and pyrimidine metabolism by estuarine bacteria. *Aquat. Microb. Ecol.* 42, 215–226.

Bertini, I., Hu, X., Luchinat, C., 2013. Global metabolomics characterization of bacteria: pre-analytical treatments and profiling. *Metabolomics.* 1–9.

Biebl, H., Allgaier, M., Tindall, B.J., Koblizek, M., Lünsdorf, H., Pukall, R., Wagner-Döbler, I., 2005. *Dinoroseobacter shibae* gen. nov., sp. nov., a new aerobic phototrophic bacterium isolated from dinoflagellates. *Int. J. Syst. Evol. Microbiol.* 55, 1089–1096.

Bochner, B.R., 2009. Global phenotypic characterization of bacteria. *FEMS Microbiol. Rev.* 33, 191–205.

Bolten, C.J., Kiefer, P., Letisse, F., Portais, J.-C., Wittmann, C., 2007. Sampling for Metabolome Analysis of Microorganisms. *Anal. Chem.* 79, 3843–3849.

Börner, J., Buchinger, S., Schomburg, D., 2007. A high-throughput method for microbial metabolome analysis using gas chromatography/mass spectrometry. *Anal. Biochem.* 367, 143–151.

Brechtel, C.E., King, S.C., 1998. 4-Aminobutyrate (GABA) transporters from the amine-polyamine-choline superfamily: substrate specificity and ligand recognition profile of the 4-aminobutyrate permease from *Bacillus subtilis. Biochem J* 333, 565–571.

Breider, S., Scheuner, C., Schumann, P., Fiebig, A., Petersen, J., Pradella, S., Klenk, H.-P., Brinkhoff, T., Göker, M., 2014. Genome-scale data suggest reclassifications in the *Leisingera-Phaeobacter* cluster including proposals for *Sedimentitalea* gen. nov. and *Pseudophaeobacter* gen. nov. *Front. Microbiol.* 5.

Brinkhoff, T., Bach, G., Heidorn, T., Liang, L., Schlingloff, A., Simon, M., 2004. Antibiotic Production by a *Roseobacter* Clade-Affiliated Species from the German Wadden Sea and Its Antagonistic Effects on Indigenous Isolates. *Appl. Environ. Microbiol.* 70, 2560–2565.

Brinkhoff, T., Giebel, H.-A., Simon, M., 2008. Diversity, ecology, and genomics of the *Roseobacter* clade: a short overview. *Arch. Microbiol.* 189, 531–539.

Broadhurst, D.I., Kell, D.B., 2006. Statistical strategies for avoiding false discoveries in metabolomics and related experiments. *Metabolomics* 2, 171–196.

Brown, M.R., 1991. The amino-acid and sugar composition of 16 species of microalgae used in mariculture. *J. Exp. Mar. Biol. Ecol.* 145, 79–99.

Buddruhs, N., Pradella, S., Göker, M., Päuker, O., Pukall, R., Spröer, C., Schumann, P., Petersen, J., Brinkhoff, T., 2013. Molecular and phenotypic analyses reveal the non-identity of the *Phaeobacter gallaeciensis* type strain deposits CIP 105210T and DSM 17395. *Int. J. Syst. Evol. Microbiol.* 63, 4340–4349.

Cabrita, M.T., Vale, C., Rauter, A.P., 2010. Halogenated Compounds from Marine Algae. *Mar. Drugs* 8, 2301–2317.

Carneiro, S., Villas-Bôas, S.G., Ferreira, E.C., Rocha, I., 2011. Metabolic footprint analysis of recombinant Escherichia coli strains during fed-batch fermentations. *Mol. BioSyst.* 7, 899-910

Caspi, R., Altman, T., Billington, R., Dreher, K., Foerster, H., Fulcher, C.A., Holland, T.A., Keseler, I.M., Kothari, A., Kubo, A., Krummenacker, M., Latendresse, M., Mueller, L.A., Ong, Q., Paley, S., Subhraveti, P., Weaver, D.S., Weerasinghe, D., Zhang, P., Karp, P.D., 2014. The MetaCyc database of metabolic pathways and enzymes and the BioCyc collection of Pathway/Genome Databases.

Nucleic Acids Res. 42, D459–D471.

Cooper, A.J.L., 1983. Biochemistry of Sulfur-Containing Amino Acids. *Annu. Rev. Biochem.* 52, 187–222.

Cortay, J.C., Bleicher, F., Duclos, B., Cenatiempo, Y., Gautier, C., Prato, J.L., Cozzone, A.J., 1989. Utilization of acetate in *Escherichia coli*: structural organization and differential expression of the ace operon. *Biochimie* 71, 1043–1049.

Costa, M.S. da, Santos, H., Galinski, E.A., 1998. An overview of the role and diversity of compatible solutes in Bacteria and Archaea, in: Antranikian, G. (Ed.), Biotechnology of Extremophiles, Advances in Biochemical Engineering/Biotechnology. Springer Berlin Heidelberg, pp. 117–153.

Cox, J., Mann, M., 2011. Quantitative, High-Resolution Proteomics for Data-Driven Systems Biology. *Annu. Rev. Biochem.* 80, 273–299.

D'Alvise, P.W., Lillebø, S., Prol-Garcia, M.J., Wergeland, H.I., Nielsen, K.F., Bergh, Ø., Gram, L., 2012. *Phaeobacter gallaeciensis* Reduces *Vibrio anguillarum* in Cultures of Microalgae and Rotifers, and Prevents Vibriosis in Cod Larvae. *PLoS ONE* 7, e43996.

D'Alvise, P.W., Lillebø, S., Wergeland, H.I., Gram, L., Bergh, Ø., 2013. Protection of cod larvae from vibriosis by *Phaeobacter* spp.: A comparison of strains and introduction times. *Aquaculture* 384–387, 82–86.

Dang, H., Li, T., Chen, M., Huang, G., 2007. Cross-Ocean Distribution of *Rhodobacterales* Bacteria as Primary Surface Colonizers in Temperate Coastal Marine Waters. *Appl. Environ. Microbiol.* 74, 52–60.

Dash, H.R., Mangwani, N., Chakraborty, J., Kumari, S., Das, S., 2013. Marine bacteria: potential candidates for enhanced bioremediation. *Appl. Microbiol. Biotechnol.* 97, 561–571.

Davidson, A.L., Maloney, P.C., 2007. ABC transporters: how small machines do a big job. *Trends Microbiol.* 15, 448–455.

De Eugenio, L.I., Escapa, I.F., Morales, V., Dinjaski, N., Galán, B., García, J.L., Prieto, M.A., 2010. The turnover of medium-chain-length polyhydroxyalkanoates in *Pseudomonas putida* KT2442 and the fundamental role of PhaZ depolymerase for the metabolic balance. *Environ. Microbiol.* 12, 207–221.

Dettmer, K., Aronov, P.A., Hammock, B.D., 2007. Mass spectrometry-based metabolomics. *Mass Spectrom. Rev.* 26, 51–78.

Dewapriya, P., Kim, S., 2014. Marine microorganisms: An emerging avenue in modern nutraceuticals and functional foods. *Food Res. Int.* 56, 115–125.

Díaz, E., Jiménez, J.I., Nogales, J., 2013. Aerobic degradation of aromatic compounds. *Curr. Opin. Biotechnol.* 24, 431–442.

Dickschat, J.S., 2010. Quorum sensing and bacterial biofilms. *Nat. Prod. Rep.* 27, 343.

Dittmar, T., Paeng, J., 2009. A heat-induced molecular signature in marine dissolved organic matter. *Nat. Geosci.* 2, 175–179.

Driessen, A.J., Jong, S. de, Konings, W.N., 1987. Transport of branched-chain amino acids in membrane vesicles of *Streptococcus cremoris*. *J. Bacteriol.* 169, 5193–5200.

Drüppel, K., Hensler, M., Trautwein, K., Koßmehl, S., Wöhlbrand, L., Schmidt-Hohagen, K., Ulbrich, M., Bergen, N., Meier-Kolthoff, J.P., Göker, M., Klenk, H.-P., Schomburg, D., Rabus, R., 2014. Pathways and substrate-specific regulation of amino acid degradation in *Phaeobacter inhibens* DSM 17395 (archetype of the marine *Roseobacter* clade). *Environ. Microbiol.* 16, 218–238.

Duarte, C.M., Hendriks, I.E., Moore, T.S., Olsen, Y.S., Steckbauer, A., Ramajo, L., Carstensen, J., Trotter, J.A., McCulloch, M., 2013. Is Ocean Acidification an Open-Ocean Syndrome? Understanding Anthropogenic Impacts on Seawater pH. *Estuaries Coasts* 36, 221–236.

Ebbighausen, H., Weil, B., Krämer, R., 1989. Transport of branched-chain amino acids in *Corynebacterium glutamicum*. *Arch. Microbiol.* 151, 238–244.

Eom, S.-H., Kim, Y.-M., Kim, S.-K., 2013. Marine bacteria: potential sources for compounds to overcome antibiotic resistance. *Appl. Microbiol. Biotechnol.* 97, 4763–4773.

Erb, T.J., Fuchs, G., Alber, B.E., 2009. (2*S*)-Methylsuccinyl-CoA dehydrogenase closes the ethylmalonyl-CoA pathway for acetyl-CoA assimilation. *Mol. Microbiol.* 73, 992–1008.

Fiehn, O., 2002. Metabolomics - the link between genotypes and phenotypes. *Plant Mol. Biol.* 48, 155–171.

Fitzpatrick, P.F., 2003. Mechanism of Aromatic Amino Acid Hydroxylation. *Biochemistry (Mosc.)* 42, 14083–14091.

Flint, D.H., 1994. Initial Kinetic and Mechanistic Characterization of *Escherichia coli* Fumarase A. *Arch. Biochem. Biophys.* 311, 509 – 516.

Fuchs, G., 2008. Anaerobic Metabolism of Aromatic Compounds. *Ann. N. Y. Acad. Sci.* 1125, 82–99.

Fuchs, G., Boll, M., Heider, J., 2011. Microbial degradation of aromatic compounds — from one strategy to four. *Nat. Rev. Microbiol.* 9, 803–816.

Fürch, T., Preusse, M., Tomasch, J., Zech, H., Wagner-Döbler, I., Rabus, R., Wittmann, C., 2009. Metabolic fluxes in the central carbon metabolism of *Dinoroseobacter shibae* and *Phaeobacter gallaeciensis*, two members of the marine *Roseobacter* clade. *BMC Microbiol.* 9, 209.

Gaboyer, F., Tindall, B.J., Ciobanu, M.-C., Duthoit, F., Le Romancer, M., Alain, K., 2013. *Phaeobacter leonis* sp. nov., an alphaproteobacterium from Mediterranean Sea sediments. *Int. J. Syst. Evol. Microbiol.* 63, 3301–3306.

Genda, T., Watabe, S., Ozaki, H., 2006. Purification and characterization of fumarase from *Corynebacterium glutamicum*. *Biosci. Biotechnol. Biochem.* 70, 1102–1109.

Geng, H., Belas, R., 2010a. Molecular mechanisms underlying roseobacter–phytoplankton symbioses. *Curr. Opin. Biotechnol.* 21, 332–338.

Geng, H., Belas, R., 2010b. Expression of Tropodithietic Acid Biosynthesis Is Controlled by a Novel Autoinducer. *J. Bacteriol.* 192, 4377–4387.

Giovannoni, S.J., Stingl, U., 2005. Molecular diversity and ecology of microbial plankton. *Nature* 437, 343–348.

Górecki, T., Panić, O., Oldridge, N., 2006. Recent Advances in Comprehensive Two−Dimensional Gas Chromatography (GC×GC). *J. Liq. Chromatogr. Amp Relat. Technol.* 29, 1077–1104.

Görke, B., Stülke, J., 2008. Carbon catabolite repression in bacteria: many ways to make the most out of nutrients. *Nat. Rev. Microbiol.* 6, 613–624.

Gruber, N., Galloway, J.N., 2008. An Earth-system perspective of the global nitrogen cycle. *Nature* 451, 293–296.

Gurtovenko, A.A., Vattulainen, I., 2007. Molecular Mechanism for Lipid Flip-Flops. *J. Phys. Chem. B* 111, 13554–13559.

Halket, J.M., Waterman, D., Przyborowska, A.M., Patel, R.K.P., Fraser, P.D., Bramley, P.M., 2005. Chemical derivatization and mass spectral libraries in metabolic profiling by GC/MS and LC/MS/MS. *J. Exp. Bot.* 56, 219–243.

Hall, R.D., 2006. Plant metabolomics: from holistic hope, to hype, to hot topic. *New Phytol.* 169, 453–468.

Hansell, D., Carlson, C., Repeta, D., Schlitzer, R., 2009. Dissolved Organic Matter in the Ocean: A Controversy Stimulates New Insights. *Oceanography* 22, 202–211.

Härtel, U., Eckel, E., Koch, J., Fuchs, G., Linder, D., Buckel, W., 1993. Purification of glutaryl-CoA dehydrogenase from *Pseudomonas* sp., an enzyme involved in the anaerobic degradation of benzoate. *Arch. Microbiol.* 159, 174–181.

Heider, J., Boll, M., Breese, K., Breinig, S., Ebenau-Jehle, C., Feil, U., Gad'on, N., Laempe, D., Leuthner, B., Mohamed, M.E.-S., Schneider, S., Burchhardt, G., Fuchs, G., 1998. Differential induction of enzymes involved in anaerobic metabolism of aromatic compounds in the denitrifying bacterium *Thauera aromatica. Arch. Microbiol.* 170, 120–131.

Helsper, J.P., Loewus, F.A., 1982. Metabolism of l-Threonic Acid in *Rumex x acutus* L. and *Pelargonium crispum* (L.) L'Hér. *Plant Physiol.* 69, 1365–1368.

Hiller, K., Hangebrauk, J., Jäger, C., Spura, J., Schreiber, K., Schomburg, D., 2009. MetaboliteDetector: Comprehensive Analysis Tool for Targeted and Nontargeted GC/MS Based Metabolome Analysis. *Anal. Chem.* 81, 3429–3439.

Holm, S., 1979. A simple sequentially rejective multiple test procedure. *Scand J Stat* 6, 65–70.

Horai, H., Arita, M., Kanaya, S., Nihei, Y., Ikeda, T., Suwa, K., Ojima, Y., Tanaka, K., Tanaka, S., Aoshima, K., Oda, Y., Kakazu, Y., Kusano, M., Tohge, T., Matsuda, F., Sawada, Y., Hirai, M.Y., Nakanishi, H., Ikeda, K., Akimoto, N., Maoka, T., Takahashi, H., Ara, T., Sakurai, N., Suzuki, H., Shibata, D., Neumann, S., Iida, T., Tanaka, K., Funatsu, K., Matsuura, F., Soga, T., Taguchi, R., Saito, K., Nishioka, T., 2010. MassBank: a public repository for sharing mass spectral data for life sciences. *J. Mass Spectrom.* JMS 45, 703–714.

Imhoff, J.F., Labes, A., Wiese, J., 2011. Bio-mining the microbial treasures of the ocean: New natural products. *Biotechnol. Adv.*, Marine Biotechnology in Europe European Science Foundation-COST Conference: "Marine Biotechnology: Future Challenges" 29, 468–482.

Ittekkot, V., 1982. Variations of dissolved organic matter during a plankton bloom: qualitative aspects, based on sugar and amino acid analyses. *Mar. Chem.* 11, 143–158.

Iwamoto, K., Shiraiwa, Y., 2005. Salt-Regulated Mannitol Metabolism in Algae. *Mar. Biotechnol.* 7, 407–415.

Jojima, T., Omumasaba, C.A., Inui, M., Yukawa, H., 2010. Sugar transporters in efficient utilization of mixed sugar substrates: current knowledge and outlook. *Appl. Microbiol. Biotechnol.* 85, 471–480.

Kanani, H.H., Klapa, M.I., 2007. Data correction strategy for metabolomics analysis using gas chromatography–mass spectrometry. *Metab. Eng.* 9, 39–51.

Kanehisa, M., Goto, S., Sato, Y., Kawashima, M., Furumichi, M., Tanabe, M., 2014. Data, information, knowledge and principle: back to metabolism in KEGG. *Nucleic Acids Res.* 42, D199–D205.

Karl, D., Letelier, R., Tupas, L., Dore, J., Christian, J., Hebel, D., 1997. The role of nitrogen fixation in biogeochemical cycling in the subtropical North Pacific Ocean. *Nature* 388, 533–538.

Kell, D.B., 2004. Metabolomics and systems biology: making sense of the soup. *Curr. Opin. Microbiol.* 7, 296–307.

Kell, D.B., 2006. Systems biology, metabolic modelling and metabolomics in drug discovery and development. *Drug Discov. Today* 11, 1085–1092.

Khorana, H.G., 1953. The Chemistry of Carbodiimides. *Chem. Rev.* 53, 145–166.

King, M.T., Reiss, P.D., 1985. Separation and measurement of short-chain coenzyme-A compounds in rat liver by reversed-phase high-performance liquid chromatography. *Anal. Biochem.* 146, 173–179.

Kirchman, D.L., Morán, X.A.G., Ducklow, H., 2009. Microbial growth in the polar oceans — role of temperature and potential impact of climate change. *Nat. Rev. Microbiol.* 7, 451–459.

Koch, B.P., Witt, M., Engbrodt, R., Dittmar, T., Kattner, G., 2005. Molecular formulae of marine and

terrigenous dissolved organic matter detected by electrospray ionization Fourier transform ion cyclotron resonance mass spectrometry. *Geochim. Cosmochim. Acta* 69, 3299–3308.

Kohn, L.D., Jakoby, W.B., 1966. [48] l- and mesotartaric acid dehydrogenase (crystalline), in: Willis A. Wood (Ed.), Methods in Enzymology, Carbohydrate Metabolism. Academic Press, pp. 236–240.

Kolter, R., Siegele, D.A., Tormo, A., 1993. The Stationary Phase of The Bacterial Life Cycle. *Annu. Rev. Microbiol.* 47, 855–874.

Kreis, W., Hession, C., 1973. Isolation and purification of L-methionine-alpha-deamino-gamma-mercaptomethane-lyase (L-methioninase) from *Clostridium sporogenes*. *Cancer Res.* 33, 1862–1865.

Kruskal, W.H., Wallis, W.A., 1952. Use of Ranks in One-Criterion Variance Analysis. *J. Am. Stat. Assoc.* 47, 583.

Kusano, T., Berberich, T., Tateda, C., Takahashi, Y., 2008. Polyamines: essential factors for growth and survival. *Planta* 228, 367–381.

Laass, S., Kleist, S., Bill, N., Drüppel, K., Kossmehl, S., Wöhlbrand, L., Rabus, R., Klein, J., Rohde, M., Bartsch, A., Wittmann, C., Schmidt-Hohagen, K., Tielen, P., Jahn, D., Schomburg, D., 2014. Gene Regulatory and Metabolic Adaptation Processes of *Dinoroseobacter shibae* DFL12T during Oxygen Depletion. *J. Biol. Chem.* 289, 13219–13231.

Ladau, J., Sharpton, T.J., Finucane, M.M., Jospin, G., Kembel, S.W., O'Dwyer, J., Koeppel, A.F., Green, J.L., Pollard, K.S., 2013. Global marine bacterial diversity peaks at high latitudes in winter. *ISME J.* 7, 1669–1677.

Ledesma-Amaro, R., Jiménez, A., Santos, M.A., Revuelta, J.L., 2013. Biotechnological production of feed nucleotides by microbial strain improvement. *Process Biochem.* 48, 1263–1270.

Leigh, J.A., Dodsworth, J.A., 2007. Nitrogen Regulation in Bacteria and Archaea. *Annu. Rev. Microbiol.* 61, 349–377.

Lewis, C.A., Wolfenden, R., 2014. The Nonenzymatic Decomposition of Guanidines and Amidines. *J. Am. Chem. Soc.* 136, 130–136.

Liu, M., Xiao, T., Sun, J., Wei, H., Wu, Y., Zhao, Y., Zhang, W., 2013. Bacterial community structures associated with a natural spring phytoplankton bloom in the Yellow Sea, China. *Deep Sea Res. Part II Top. Stud. Oceanogr.* 97, 85–92.

Madison, L.L., Huisman, G.W., 1999. Metabolic Engineering of Poly(3-Hydroxyalkanoates): From DNA to Plastic. *Microbiol. Mol. Biol. Rev.* 63, 21–53.

Maes, C., O'Kane, T.J., 2014. Seasonal variations of the upper ocean salinity stratification in the Tropics. *J. Geophys. Res. Oceans* 119, 1706–1722.

Mann, H.B., Whitney, D.R., 1947. On a Test of Whether one of Two Random Variables is Stochastically Larger than the Other. *Ann. Math. Stat.* 18, 50–60.

Martens, T., Heidorn, T., Pukall, R., Simon, M., Tindall, B.J., Brinkhoff, T., 2006. Reclassification of *Roseobacter gallaeciensis* Ruiz-Ponte *et al.* 1998 as *Phaeobacter gallaeciensis* gen. nov., comb. nov., description of *Phaeobacter inhibens* sp. nov., reclassification of *Ruegeria algicola* (Lafay *et al.* 1995) Uchino *et al.* 1999 as *Marinovum algicola* gen. nov., comb. nov., and emended descriptions of the genera *Roseobacter*, *Ruegeria* and *Leisingera*. *Int. J. Syst. Evol. Microbiol.* 56, 1293–1304.

Massey, L.K., Sokatch, J.R., Conrad, R.S., 1976. Branched-chain amino acid catabolism in bacteria. *Bacteriol. Rev.* 40, 42–54.

Merrick, M.J., Edwards, R.A., 1995. Nitrogen control in bacteria. *Microbiol. Rev.* 59, 604–622.

Mills, M.M., Ridame, C., Davey, M., La Roche, J., Geider, R.J., 2004. Iron and phosphorus co-limit nitrogen fixation in the eastern tropical North Atlantic. *Nature* 429, 292–294.

Montani, S., Tada, K., Okaichi, T., 1988. Purine and pyrimidine bases in marine particles in the Seto Inland Sea, Japan. *Mar. Chem.* 25, 359–371.

Mulligan, C., Fischer, M., Thomas, G.H., 2011. Tripartite ATP-independent periplasmic (TRAP) transporters in bacteria and archaea. *FEMS Microbiol. Rev.* 35, 68–86.

Mustakhimov, I.I., Reshetnikov, A.S., Khmelenina, V.N., Trotsenko, Y.A., 2010. Regulatory aspects of ectoine biosynthesis in halophilic bacteria. *Microbiology* 79, 583–592.

Nagata, T., 1986. Carbon and Nitrogen Content of Natural Planktonic Bacteria. *Appl. Environ. Microbiol.* 52, 28–32.

Narukawa, M., Kawamura, K., Hatsushika, H., Yamazaki, K., Li, S.-M., Bottenheim, J.W., Anlauf, K.G., 2003. Measurement of Halogenated Dicarboxylic Acids in the Arctic Aerosols at Polar Sunrise. *J. Atmospheric Chem.* 44, 323–335.

Nebbioso, A., Piccolo, A., 2013. Molecular characterization of dissolved organic matter (DOM): a critical review. *Anal. Bioanal. Chem.* 405, 109–124.

Nedwell, D.., 1999. Effect of low temperature on microbial growth: lowered affinity for substrates limits growth at low temperature. *FEMS Microbiol. Ecol.* 30, 101–111.

Neumann, A., Patzelt, D., Wagner-Döbler, I., Schulz, S., 2013. Identification of New *N*-Acylhomoserine Lactone Signalling Compounds of *Dinoroseobacter shibae* DFL-12T by Overexpression of *luxI* Genes. *ChemBioChem* 14, 2355–2361.

Nyström, T., 2004. Stationary-Phase Physiology. *Annu. Rev. Microbiol.* 58, 161–181.

Ohshima, T., Sakuraba, H., 1986. Purification and characterization of malate dehydrogenase from the phototrophic bacterium, *Rhodopseudomonas capsulata*. *Biochim. Biophys. Acta BBA - Protein Struct. Mol. Enzymol.* 869, 171–177.

Patzelt, D., Wang, H., Buchholz, I., Rohde, M., Gröbe, L., Pradella, S., Neumann, A., Schulz, S., Heyber, S., Münch, K., Münch, R., Jahn, D., Wagner-Döbler, I., Tomasch, J., 2013. You are what you talk: quorum sensing induces individual morphologies and cell division modes in *Dinoroseobacter shibae*. *ISME J* 7, 2274–2286.

Petersen, J., Brinkmann, H., Berger, M., Brinkhoff, T., Päuker, O., Pradella, S., 2011. Origin and Evolution of a Novel DnaA-Like Plasmid Replication Type in *Rhodobacterales*. *Mol. Biol. Evol.* 28, 1229–1240.

Petersen, J., Frank, O., Göker, M., Pradella, S., 2013. Extrachromosomal, extraordinary and essential—the plasmids of the *Roseobacter* clade. *Appl. Microbiol. Biotechnol.* 97, 2805–2815.

Pettine, M., Patrolecco, L., Manganelli, M., Capri, S., Farrace, M.G., 1999. Seasonal variations of dissolved organic matter in the northern Adriatic Sea. *Mar. Chem.* 64, 153–169.

Pettine, M., Capri, S., Manganelli, M., Patrolecco, L., Puddu, A., Zoppini, A., 2001. The Dynamics of DOM in the Northern Adriatic Sea. *Estuar. Coast. Shelf Sci.* 52, 471–489.

Peyraud, R., Kiefer, P., Christen, P., Massou, S., Portais, J.-C., Vorholt, J.A., 2009. Demonstration of the ethylmalonyl-CoA pathway by using ^{13}C metabolomics. *Proc. Natl. Acad. Sci.* 106, 4846–4851.

Poblete-Castro, I., Escapa, I.F., Jäger, C., Puchalka, J., Lam, C.M.C., Schomburg, D., Prieto, M.A., Santos, V.A.M. dos, 2012. The metabolic response of *P. putida* KT2442 producing high levels of polyhydroxyalkanoate under single- and multiple-nutrient-limited growth: Highlights from a multi-level omics approach. *Microb. Cell Factories* 11, 34.

Poretsky, R.S., Sun, S., Mou, X., Moran, M.A., 2010. Transporter genes expressed by coastal bacterioplankton in response to dissolved organic carbon. *Environ. Microbiol.* 12, 616–627.

Porsby, C.H., Webber, M.A., Nielsen, K.F., Piddock, L.J.V., Gram, L., 2011. Resistance and Tolerance to Tropodithietic Acid, an Antimicrobial in Aquaculture, Is Hard To Select. *Antimicrob. Agents Chemother.* 55, 1332–1337.

Pradella, S., Päuker, O., Petersen, J., 2010. Genome organisation of the marine *Roseobacter* clade member *Marinovum algicola*. *Arch. Microbiol.* 192, 115–126.

Pritsch, F., 2012. Metabolomanalyse von *Phaeobacter inhibens* DSM 17395 unter Verwendung von heterogenen Kohlenstoffquellen (Bachelor of science thesis). TU Braunschweig, Braunschweig.

Quester, S., Schomburg, D., 2011. EnzymeDetector: an integrated enzyme function prediction tool and database. *BMC Bioinformatics* 12, 376.

Rabus, R., Trautwein, K., Wöhlbrand, L., 2014. Towards habitat-oriented systems biology of "*Aromatoleum aromaticum*" EbN1. *Appl. Microbiol. Biotechnol.* 98, 3371–3388.

Rao, D., Webb, J.S., Holmström, C., Case, R., Low, A., Steinberg, P., Kjelleberg, S., 2007. Low Densities of Epiphytic Bacteria from the Marine Alga *Ulva australis* Inhibit Settlement of Fouling Organisms. *Appl. Environ. Microbiol.* 73, 7844–7852.

Reaves, M.L., Young, B.D., Hosios, A.M., Xu, Y.-F., Rabinowitz, J.D., 2013. Pyrimidine homeostasis is accomplished by directed overflow metabolism. *Nature* 500, 237–241.

Reay, D.S., Nedwell, D.B., Priddle, J., Ellis-Evans, J.C., 1999. Temperature Dependence of Inorganic Nitrogen Uptake: Reduced Affinity for Nitrate at Suboptimal Temperatures in Both Algae and Bacteria. *Appl. Environ. Microbiol.* 65, 2577–2584.

Reid, S.J., Abratt, V.R., 2005. Sucrose utilisation in bacteria: genetic organisation and regulation. *Appl. Microbiol. Biotechnol.* 67, 312–321.

Reul, N., Fournier, S., Boutin, J., Hernandez, O., Maes, C., Chapron, B., Alory, G., Quilfen, Y., Tenerelli, J., Morisset, S., Kerr, Y., Mecklenburg, S., Delwart, S., 2014. Sea Surface Salinity Observations from Space with the SMOS Satellite: A New Means to Monitor the Marine Branch of the Water Cycle. *Surv. Geophys.* 35, 681–722.

Rex, R., Bill, N., Schmidt-Hohagen, K., Schomburg, D., 2013. Swimming in Light: A Large-Scale Computational Analysis of the Metabolism of *Dinoroseobacter shibae*. *PLoS Comput Biol* 9, e1003224.

Ribardo, D.A., Hendrixson, D.R., 2011. Analysis of the LIV System of *Campylobacter jejuni* Reveals Alternative Roles for LivJ and LivK in Commensalism beyond Branched-Chain Amino Acid Transport. *J. Bacteriol.* 193, 6233–6243.

Righetti, P., Campostrini, N., Pascali, J., Hamdan, M., Astner, H., 2004. Quantitative proteomics: a review of different methodologies. *Eur. J. Mass Spectrom.* 10, 335.

Rinaudo, M., 2006. Chitin and chitosan: Properties and applications. *Prog. Polym. Sci.* 31, 603–632.

Ruiz-Ponte, C., Cilia, V., Lambert, C., Nicolas, J.L., 1998. Roseobacter gallaeciensis sp. nov., a new marine bacterium isolated from rearings and collectors of the scallop *Pecten maximus*. *Int. J. Syst. Bacteriol.* 48 Pt 2, 537–542.

Saeed, A.I., Sharov, V., White, J., Li, J., Liang, W., Bhagabati, N., Braisted, J., Klapa, M., Currier, T., Thiagarajan, M., Sturn, A., Snuffin, M., Rezantsev, A., Popov, D., Ryltsov, A., Kostukovich, E., Borisovsky, I., Liu, Z., Vinsavich, A., Trush, V., Quackenbush, J., 2003. TM4: a free, open-source system for microarray data management and analysis. *BioTechniques* 34, 374–378.

Sajiki, K., Pluskal, T., Shimanuki, M., Yanagida, M., 2013. Metabolomic Analysis of Fission Yeast at the Onset of Nitrogen Starvation. Metabolites 3, 1118–1129.

Sakugawa, H., Handa, N., Yagi, K., 1990. Distribution of glycosylglycerols and oligosaccharides in the marine environment and their ecological significance in the deep sea. *Mar. Biol.* 106, 309–313.

Sarmento, H., Romera-Castillo, C., Lindh, M., Pinhassi, J., Sala, M.M., Gasol, J.M., Marrasé, C., Taylor, G.T., 2013. Phytoplankton species-specific release of dissolved free amino acids and their selective consumption by bacteria. *Limnol. Oceanogr*. 58, 1123–1135.

Scalbert, A., Brennan, L., Fiehn, O., Hankemeier, T., Kristal, B.S., van Ommen, B., Pujos-Guillot, E., Verheij, E., Wishart, D., Wopereis, S., 2009. Mass-spectrometry-based metabolomics: limitations and recommendations for future progress with particular focus on nutrition research. *Metabolomics* 5, 435–458.

Schaefer, A.L., Greenberg, E.P., Oliver, C.M., Oda, Y., Huang, J.J., Bittan-Banin, G., Peres, C.M., Schmidt, S., Juhaszova, K., Sufrin, J.R., Harwood, C.S., 2008. A new class of homoserine lactone quorum-sensing signals. *Nature* 454, 595–599.

Schaffer, J.E., 2002. Fatty acid transport: the roads taken. *Am. J. Physiol. - Endocrinol. Metab.* 282, E239–E246.

Schomburg, I., Chang, A., Placzek, S., Söhngen, C., Rother, M., Lang, M., Munaretto, C., Ulas, S., Stelzer, M., Grote, A., Scheer, M., Schomburg, D., 2012. BRENDA in 2013: integrated reactions, kinetic data, enzyme function data, improved disease classification: new options and contents in BRENDA. *Nucleic Acids Res.* 41, D764–D772.

Schühle, K., Jahn, M., Ghisla, S., Fuchs, G., 2001. Two Similar Gene Clusters Coding for Enzymes of a New Type of Aerobic 2-Aminobenzoate (Anthranilate) Metabolism in the Bacterium *Azoarcus evansii*. *J. Bacteriol.* 183, 5268–5278.

Schujman, G.E., Mendoza, D. de, 2005. Transcriptional control of membrane lipid synthesis in bacteria. *Curr. Opin. Microbiol*. 8, 149–153.

Senior, P.J., Dawes, E.A., 1971. Poly-β-hydroxybutyrate biosynthesis and the regulation of glucose metabolism in *Azotobacter beijerinckii*. *Biochem J* 125, 55–66.

Seyedsayamdost, M.R., Case, R.J., Kolter, R., Clardy, J., 2011. The Jekyll-and-Hyde chemistry of *Phaeobacter gallaeciensis*. *Nat. Chem.* 3, 331–335.

Shapiro, S.S., Wilk, M.B., 1965. An Analysis of Variance Test for Normality (Complete Samples). *Biometrika* 52, 591.

Shiba, T., 1991. *Roseobacter litoralis* gen. nov., sp. nov., and *Roseobacter denitrificans* sp. nov., Aerobic Pink-Pigmented Bacteria which Contain Bacteriochlorophyll a. Syst. Appl. Microbiol. 14, 140–145.

Sintes, E., Witte, H., Stodderegger, K., Steiner, P., Herndl, G.J., 2013. Temporal dynamics in the free-living bacterial community composition in the coastal North Sea. *FEMS Microbiol. Ecol.* 83, 413–424.

Smith, C.A., Want, E.J., O'Maille, G., Abagyan, R., Siuzdak, G., 2006. XCMS: Processing Mass Spectrometry Data for Metabolite Profiling Using Nonlinear Peak Alignment, Matching, and Identification. *Anal. Chem.* 78, 779–787.

Sogin, M.L., Morrison, H.G., Huber, J.A., Welch, D.M., Huse, S.M., Neal, P.R., Arrieta, J.M., Herndl, G.J., 2006. Microbial diversity in the deep sea and the underexplored "rare biosphere." *Proc. Natl. Acad. Sci.* 103, 12115–12120.

Sorek, R., Cossart, P., 2010. Prokaryotic transcriptomics: a new view on regulation, physiology and pathogenicity. *Nat. Rev. Genet.* 11, 9–16.

Strehmel, N., Kopka, J., Scheel, D., Böttcher, C., 2013. Annotating unknown components from GC/EI-MS-based metabolite profiling experiments using GC/APCI(+)-QTOFMS. *Metabolomics* 1–13.

Strobel, H.J., 1993. Evidence for catabolite inhibition in regulation of pentose utilization and transport in the ruminal bacterium *Selenomonas ruminantium*. *Appl. Environ. Microbiol.* 59, 40–46.

Strohhäcker, J., Graaf, A.A. de, Schoberth, S.M., Wittig, R.M., Sahm, H., 1993. ^{31}P Nuclear magnetic resonance studies of ethanol inhibition in *Zymomonas mobilis*. *Arch. Microbiol.* 159, 484–490.

Subrahmanyam, B., Grunseich, G., Nyadjro, E.S., 2013. Preliminary SMOS Salinity Measurements and Validation in the Indian Ocean. *IEEE Trans. Geosci. Remote Sens.* 51, 19–27.

Sunda, W.G., Huntsman, S.A., 1997. Interrelated influence of iron, light and cell size on marine phytoplankton growth. *Nature* 390, 389–392.

Tani, T.H., Khodursky, A., Blumenthal, R.M., Brown, P.O., Matthews, R.G., 2002. Adaptation to famine: A family of stationary-phase genes revealed by microarray analysis. *Proc. Natl. Acad. Sci.* 99, 13471–13476.

Tautenhahn, R., Böttcher, C., Neumann, S., 2008. Highly sensitive feature detection for high resolution LC/MS. *BMC Bioinformatics* 9, 504.

Teufel, R., Mascaraque, V., Ismail, W., Voss, M., Perera, J., Eisenreich, W., Haehnel, W., Fuchs, G., 2010. Bacterial phenylalanine and phenylacetate catabolic pathway revealed. *Proc. Natl. Acad. Sci.* 107, 14390–14395.

Thole, S., Kalhoefer, D., Voget, S., Berger, M., Engelhardt, T., Liesegang, H., Wollherr, A., Kjelleberg, S., Daniel, R., Simon, M., Thomas, T., Brinkhoff, T., 2012. *Phaeobacter gallaeciensis* genomes from globally opposite locations reveal high similarity of adaptation to surface life. *ISME J.* 6, 2229–2244.

Tomitori, H., Kashiwagi, K., Igarashi, K., 2012. Structure and function of polyamine-amino acid antiporters CadB and PotE in *Escherichia coli*. *Amino Acids* 42, 733–740.

Typas, A., Banzhaf, M., Gross, C.A., Vollmer, W., 2012. From the regulation of peptidoglycan synthesis to bacterial growth and morphology. *Nat. Rev. Microbiol.* 10, 123–136.

Tyrrell, T., 1999. The relative influences of nitrogen and phosphorus on oceanic primary production. Nature 400, 525–531.

Vandecandelaere, I., Segaert, E., Mollica, A., Faimali, M., Vandamme, P., 2008. *Leisingera aquimarina* sp. nov., isolated from a marine electroactive biofilm, and emended descriptions of *Leisingera methylohalidivorans* Schaefer *et al.* 2002, *Phaeobacter daeponensis* Yoon *et al.* 2007 and *Phaeobacter inhibens* Martens *et al.* 2006. *Int. J. Syst. Evol. Microbiol.* 58, 2788–2793.

Vandecandelaere, I., Segaert, E., Mollica, A., Faimali, M., Vandamme, P., 2009. *Phaeobacter caeruleus* sp. nov., a blue-coloured, colony-forming bacterium isolated from a marine electroactive biofilm. *Int. J. Syst. Evol. Microbiol.* 59, 1209–1214.

Vauclare, Madern, D., Girard, E., Gabel, F., Zaccai, G., Franzetti, B., 2014. New insights into microbial adaptation to extreme saline environments. *BIO Web Conf.* 2, 10.

Violante, A., Cozzolino, V., Perelomov, L., Caporale, A.G., Pigna, M., 2010. Mobility and bioavailability of heavy metals and metalloids in soil environments. *J. Soil Sci. Plant Nutr.* 10, 268–292.

Voegele, R.T., Mitsch, M.J., Finan, T.M., 1999. Characterization of two members of a novel malic enzyme class. *Biochim. Biophys. Acta* 1432, 275–285.

Vogels, G.D., Van der Drift, C., 1976. Degradation of purines and pyrimidines by microorganisms. *Bacteriol. Rev.* 40, 403–468.

Wagner-Döbler, I., Biebl, H., 2006. Environmental biology of the marine Roseobacter lineage. *Annu. Rev. Microbiol.* 60, 255–280.

Wagner-Döbler, I., Rheims, H., Felske, A., El-Ghezal, A., Flade-Schröder, D., Laatsch, H., Lang, S., Pukall, R., Tindall, B.J., 2004. *Oceanibulbus indolifex* gen. nov., sp. nov., a North Sea alphaproteobacterium that produces bioactive metabolites. *Int. J. Syst. Evol. Microbiol.* 54, 1177–1184.

Walmsley, A.R., Shaw, J.G., Kelly, D.J., 1992. The mechanism of ligand binding to the periplasmic C4-dicarboxylate binding protein (DctP) from *Rhodobacter capsulatus*. *J. Biol. Chem.* 267, 8064–8072.

Waters, C.M., Bassler, B.L., 2005. QUORUM SENSING: Cell-to-Cell Communication in Bacteria. *Annu. Rev. Cell Dev. Biol.* 21, 319–346.

Weckwerth, W., 2003. Metabolomics in Systems Biology. *Annu. Rev. Plant Biol.* 54, 669–689.

Whitman, W.B., Coleman, D.C., Wiebe, W.J., 1998. Prokaryotes: The unseen majority. *Proc. Natl. Acad. Sci.* 95, 6578–6583.

Wiegmann, K., Hensler, M., Wöhlbrand, L., Ulbrich, M., Schomburg, D., Rabus, R., 2014. Carbohydrate Catabolism in *Phaeobacter inhibens* DSM 17395, a Member of the Marine *Roseobacter* Clade. *Appl. Environ. Microbiol.* 80, 4725–4737.

Wilcoxon, F., 1945. Individual Comparisons by Ranking Methods. *Biom. Bull.* 1, 80.

Yoon, J.-H., Kang, S.-J., Lee, S.-Y., Oh, T.-K., 2007. *Phaeobacter daeponensis* sp. nov., isolated from a tidal flat of the Yellow Sea in Korea. *Int. J. Syst. Evol. Microbiol.* 57, 856–861.

Yu, X., Wang, X., Engel, P.C., 2014. The specificity and kinetic mechanism of branched-chain amino acid aminotransferase from *Escherichia coli* studied with a new improved coupled assay procedure and the enzyme's potential for biocatalysis. *FEBS J.* 281, 391–400.

Zan, J., Liu, Y., Fuqua, C., Hill, R.T., 2014. Acyl-Homoserine Lactone Quorum Sensing in the *Roseobacter* Clade. *Int. J. Mol. Sci.* 15, 654–669.

Zech, H., Thole, S., Schreiber, K., Kalhöfer, D., Voget, S., Brinkhoff, T., Simon, M., Schomburg, D., Rabus, R., 2009. Growth phase-dependent global protein and metabolite profiles of *Phaeobacter gallaeciensis* strain DSM 17395, a member of the marine *Roseobacter*-clade. *PROTEOMICS* 9, 3677–3697.

Zech, H., Hensler, M., Koßmehl, S., Drüppel, K., Wöhlbrand, L., Trautwein, K., Hulsch, R., Maschmann, U., Colby, T., Schmidt, J., Reinhardt, R., Schmidt-Hohagen, K., Schomburg, D., Rabus, R., 2013a. Adaptation of *Phaeobacter inhibens* DSM 17395 to growth with complex nutrients. *PROTEOMICS* 13, 2851–2868.

Zech, H., Hensler, M., Koßmehl, S., Drüppel, K., Wöhlbrand, L., Trautwein, K., Colby, T., Schmidt, J., Reinhardt, R., Schmidt-Hohagen, K., Schomburg, D., Rabus, R., 2013b. Dynamics of amino acid utilization in *Phaeobacter inhibens* DSM 17395. *PROTEOMICS* 13, 2869–2885.

Zhang, D.-C., Li, H.-R., Xin, Y.-H., Liu, H.-C., Chi, Z.-M., Zhou, P.-J., Yu, Y., 2008. *Phaeobacter arcticus* sp. nov., a psychrophilic bacterium isolated from the Arctic. *Int. J. Syst. Evol. Microbiol.* 58, 1384–1387.

Zhao, G., Pease, A.J., Bharani, N., Winkler, M.E., 1995. Biochemical characterization of gapB-encoded erythrose 4-phosphate dehydrogenase of *Escherichia coli* K-12 and its possible role in pyridoxal 5'-phosphate biosynthesis. *J. Bacteriol.* 177, 2804–2812.

Supplementary material

S1: Complete list of ^{13}C labelled and unlabelled compounds in *P. inhibens* DSM 17395 after growth on [U-^{13}C] glucose.

Samples were prepared as described in section2.8.2 and analysed via GC-MS (sections 2.12.1 and 2.12.2).

Metabolites with clear isotope shift

1,6-Anhydro-glucose	Ethanolaminephosphate	2-Keto-3-deoxy-gluconate	Putrescine
3-Hydroxybutanoate	Fructose	Leucine	Pyroglutamate
3-Hydroxyecanoate	Fructose-6-phosphate	Lysine	Pyruvate
2-Methylmalate	Fumarate	Malate	Ribose
2-Oxoglutarate	Glucoheptonate-1,4-lactone	Maleate	Serine
2-Phosphoglycerate	Gluconate	Melibiose	Succinate
3-Phosphoglyerate	Gluconate-1,5-lactone	*N*-Acetyl-glutamate	Tartrate
Alanine	Glucose	*N*-Acetyl-glucosamine	Threonate
Aspartate	Glucose-6-phosphate	*N,N*-dimethyl-glycine/ or Glyoxylate	Threonine
β-Alanine	Glucuronate	Nicotinamide	Thymine
Carbodiimide	Glutamate	*O*-Acetylserine	Tyrosine
Citrate	Glycerate	Octadecenoate ($C_{18:1}$)	Uracil
Di-saccharides (RI 2740, 2754,	Glycerol-3-phosphate	Ornithine	Urea
2762, 2812, e.g. Trehalose, Maltose)	Glycerophosphoglycerol	Pentose-5-phosphate	Valine
Diethanolamine	Glycine	Phenylalanine	
Dihydroxyacetone phosphate	Isoleucine	Phosphoenolpyruvate	

Metabolites with weak isotope shift

Benzoate	Lactate	Octanoate ($C_{8:0}$)	

Unidentified compounds with clear isotope shift

Unknown#1004.0-pin-mhe_001	Unknown#1651.8-pin-mhe_032	Unknown#1946.5-pin-mhe_024	Unknown#2269.25-ypy-mse_027
Unknown#1361.3-pin-mhe_010	Unknown#1671.7-pin-mhe_019	Unknown#1955.0-pin-mhe_027	Unknown#2334.1-pin-mhe_051
Unknown#1366.9-pin-mhe_011	Unknown#1684.4-pin-mhe_034	Unknown#2018.7-pin-mhe_028	Unknown#2363.8-pin-mhe_052
Unknown#1456.4-pin-mhe_014	Unknown#1830.2-pin-mhe_038	Unknown#2078.9-pin-mhe_042	Unknown#2678.8-pin-mhe_069
Unknown#1589.9-pin-mhe_029	Unknown#1856.7-pin-mhe_040	Unknown#2090.48-ypy-mse_021	
Unknown#1635.2-pin-mhe_031	Unknown#1937.2-pin-mhe_021	Unknown#2135.2-pin-mhe_044	

Detected compounds, without isotope-shift

Borate	Hydroxylamine	Unknown#1169.8-pae-bth_013	NA109003_(classified_
Cyclohexane	Lumichrome	Unknown#1201.75-ppu-cja_004	unknown)_1104.97
Diphosphate	Octadecanoate ($C_{18:0}$)	Unknown#1248.7-cgl-sst_008	NA114002_(classified_
Dodecanol	Phosphate	Unknown#1277.1-ppu-cja_005	unknown)_1144.3
Glycerol	Pyridine	Unknown#1385.3-pae-bth_024	
Hexadecanoate ($C_{16:0}$)	Toluate	NA344 (RI 2070)	

S2: Identified extracellular metabolites in Marine Broth medium.
Abbreviations: [a], Fold change in abundance at ½ OD_{max}, as compared to sterile medium prior to inoculation; x, compound was not detected in reference condition; n.d. compound was not detected at ½ OD_{max}, indicating complete consumption of that substrate.

Metabolites	Fold change [a]	Metabolites	Fold change [a]
Amino acids, dipeptides and derivatives		**Carboxylates**	
Alanine	0.05 ± 0.02	4-Aminobutanoate	n.d.
Arginine	0.65 ± 0.13	Citrate	0.07 ± 0.02
Asparagine	0.47 ± 0.09	Erythronate	0.17 ± 0.13
Aspartate	0.29 ± 0.06	Glycerate	0.41 ± 0.09
β-Alanine	0.48 ± 0.12	Glycolate	0.26 ± 0.07
3-Cyano-alanine	1.03 ± 0.25	4-Hydroxybutanoate	0.89 ± 0.07
Glutamate	<0.01 ± 0	2-Hydroxyphenylacetate	x
Glycine	0.09 ± 0.03	Lactate	0.02 ± 0.02
Glycyl-glycine	0.05 ± 0.01	Maleamate	0.43 ± 0.03
Isoleucine	0.64 ± 0.06	Succinate	n.d.
Leucine	0.57 ± 0.11	Threonate	0.63 ± 0.10
Lysine	0.74 ± 0.09		
Methionine	0.25 ± 0.07	**Saccharides and derivatives**	
N,N-Dimethylglycine	n.d.		
Ornithine	0.4 ± 0.05	Arabinonate	0.42 ± 0.10
Phenylalanine	0.83 ± 0.04	Arabinose	0.11 ± 0.08
Proline	0.08 ± 0.01	Cellobiose / Maltose	n.d.
Pyroglutamate	0.91 ± 0.06	Glucose	1.17 ± 0.19
Serine	0.62 ± 0.09	Glycerol	0.17 ± 0.04
Threonine	0.94 ± 0.09	Lactose	<0.01 ± 0
Tryptophan	0.56 ± 0.07	Melibiose	n.d.
Tyrosine	0.64 ± 0.05	Myo-inositol	0.23 ± 0.10
Valine	0.6 ± 0.07	Sucrose	<0.01 ± 0
		Trehalose	n.d.
Others			
		Purines and Pyrimidines and derivatives	
Borate (inorganic)	0.98 ± 0.08		
Glycerol-3-phosphate	n.d.	Adenine	0.36 ± 0.09
Nicotinate	0.36 ± 0.08	Adenosine	0.01 ± 0.01
Phosphate (inorganic)	1.6 ± 0.75	Cytosine	0.33 ± 0.04
Spermidine	n.d.	Uracil	0.01 ± 0.01
Urea	94.2 ± 91.3		

Colour scale for fold changes:	<0.1	<0.25	<0.5	<0.75	0.75 – 1.25	>1.25	>10

S3: Fold changes of all intracellularly detected metabolites in the experiment "adaptation to growth with complex nutrients."

Significance of fold-changes were calculated with Wilcoxon-Mann-Whitney test and false discovery rate control. Abbreviations: GM, glucose minimal; MB, Marine Broth, BR, bioreactor; x, metabolite not detected in reference conditions but in test condition; n.d. metabolite not detected in respective cultivation condition.

Metabolites	Fold change in abundance as compared to GM EM			Comparison between bioreactors MB BR vs GM BR	
	Erlenmeyer flask	Bioreactor			
	MB medium	MB medium	GM medium	Fold change	p-Value
Amino acids, dipeptides and derivatives					
Alanine	0.49 ± 0.07	0.94 ± 0.10	0.80 ± 0.12	1.18 ± 0.13	0.17801
Alanyl-alanine	0.61 ± 0.15	1.11 ± 0.26	0.67 ± 0.21	1.65 ± 0.49	0.07038
Arginine	1.09 ± 0.05	0.31 ± 0.05	1.35 ± 0.21	0.23 ± 0.05	0.00190
Asparagine	1.86 ± 0.22	1.47 ± 0.18	1.50 ± 0.22	0.98 ± 0.13	0.88028
Aspartate	0.18 ± 0.05	0.38 ± 0.04	1.08 ± 0.12	0.36 ± 0.03	0.00028
β-Alanine	0.95 ± 0.42	2.10 ± 1.01	1.73 ± 0.85	1.21 ± 0.44	0.32434
β-Alanyl-lysine	x	x	x	1.05 ± 0.37	0.88028
Cysteine	0.37 ± 0.07	0.35 ± 0.06	0.40 ± 0.06	0.88 ± 0.17	0.41224
Cystine	0.08 ± 0.01	0.05 ± 0.01	0.29 ± 0.06	0.17 ± 0.05	0.00052
γ-Glutamyl-leucine	x	n.d.	n.d.		
Glutamate	0.20 ± 0.04	0.35 ± 0.06	0.76 ± 0.13	0.47 ± 0.04	0.00076
Glutamine	6.22 ± 0.56	4.13 ± 0.39	0.91 ± 0.08	4.51 ± 0.47	0.00028
Glycine	0.41 ± 0.02	0.62 ± 0.03	1.06 ± 0.04	0.58 ± 0.03	0.00028
Glycyl-phenylalanine	1.29 ± 0.07	0.30 ± 0.07	0.35 ± 0.05	0.86 ± 0.24	0.50571
Glycyl-glycine	18.8 ± 6.1	6.81 ± 2.14	1.41 ± 0.54	4.84 ± 1.64	0.00264
5-Hydroxy-lysine	x	x	n.d.	x	
Histidine	0.90 ± 0.17	0.27 ± 0.05	2.40 ± 0.47	0.11 ± 0.02	0.00028
Homocysteine	2.80 ± 1.43	1.03 ± 0.51	1.09 ± 0.59	0.94 ± 0.25	0.25089
Isoleucine	1.22 ± 0.17	1.85 ± 0.26	1.63 ± 0.26	1.14 ± 0.13	0.41224
Leucine	0.49 ± 0.10	1.28 ± 0.06	1.74 ± 0.12	0.73 ± 0.05	0.00125
Lysine	0.70 ± 0.06	1.08 ± 0.10	1.29 ± 0.16	0.84 ± 0.09	0.25089
Methionine	0.16 ± 0.06	0.37 ± 0.12	0.95 ± 0.33	0.39 ± 0.09	0.00255
N-Acetyl-glutamate	0.32 ± 0.09	0.46 ± 0.15	0.18 ± 0.09	1.59 ± 0.45	0.16188
Ornithine	1.92 ± 0.24	2.65 ± 0.34	1.29 ± 0.24	2.05 ± 0.30	0.00076
Phenylalanine	1.11 ± 0.18	1.76 ± 0.19	1.42 ± 0.21	1.24 ± 0.15	0.17801
Proline	1.55 ± 0.27	2.00 ± 0.36	1.27 ± 0.21	1.58 ± 0.18	0.00510
Serine	1.13 ± 0.15	1.22 ± 0.15	0.91 ± 0.13	1.33 ± 0.22	0.11054
Threonine	0.94 ± 0.17	1.88 ± 0.27	1.17 ± 0.22	1.61 ± 0.21	0.00190
Tryptophan	8.25 ± 2.57	11.8 ± 3.7	3.65 ± 1.15	3.25 ± 0.36	0.00028
Tyrosine	5.92 ± 1.86	6.37 ± 2.32	0.81 ± 0.27	7.85 ± 1.78	0.00028
Valine	0.55 ± 0.13	1.19 ± 0.16	1.32 ± 0.20	0.90 ± 0.09	0.64214
TCA cycle intermediates					
Citrate	4.85 ± 1.24	5.47 ± 1.35	3.16 ± 1.05	1.73 ± 0.468	0.07038
2-Oxoglutarate	0.03 ± 0.01	0.03 ± 0	0.17 ± 0.05	0.15 ± 0.04	0.00359
Succinate	12.5 ± 2.5	14.5 ± 1.8	1.17 ± 0.09	12.4 ± 1.6	0.00028
Fumarate	0.08 ± 0.03	0.05 ± 0.01	0.56 ± 0.10	0.09 ± 0.02	0.00028
Malate	1.79 ± 0.83	4.14 ± 1.45	2.21 ± 0.98	1.87 ± 0.66	0.09916
Organic acids					
2-Aminobutanoate	1.02 ± 0.26	1.29 ± 0.19	0.48 ± 0.09	2.69 ± 0.52	0.00105
5-Aminopentanoate	1300 ± 1300	3600 ± 3600	11.7 ± 13.05	309 ± 157	0.00028
Benzoate	0.83 ± 0.68	4.29 ± 3.52	3.76 ± 3.87	0.95 ± 0.31	0.44515
2-Coumarate	1.21	0.84	1.02	0.83 ± 0.09	0.06991
2,4-Diaminobutanoate	0.58 ± 0.10	0.39 ± 0.07	0.60 ± 0.17	0.65 ± 0.17	0.27525
2,6-Diaminopimelate	0.57 ± 0.04	0.59 ± 0.06	0.46 ± 0.08	1.27 ± 0.22	0.29720
Glutarate	x	x	n.d.	x	
Glycerate	1.33 ± 0.54	1.08 ± 0.22	4.96 ± 1.01	0.22 ± 0.05	0.00170
Glycolate	0.15 ± 0.04	0.26 ± 0.07	0.95 ± 0.20	0.27 ± 0.06	0.00033
3-Hydroxybutanoate	0.16 ± 0.02	0.29 ± 0.03	0.93 ± 0.10	0.31 ± 0.02	0.00970
4-Hydroxybutanoate	5.92 ± 1.49	8.49 ± 2.18	1.06 ± 0.27	8.02 ± 0.86	0.00028
4-Hydroxyphenylacetate	23.7 ± 6.3	8.45 ± 1.91	0.60 ± 0.25	7.07 ± 3.31	0.01187
2-Hydroxyglutarate	1.74 ± 0.73	1.35 ± 0.58	2.06 ± 0.99	0.65 ± 0.18	0.91309

S3: Fold changes of all intracellularly detected metabolites in the experiment "adaptation to growth with complex nutrients." (Continued)

Metabolites	Fold change in abundance as compared to GM EM			Comparison between bioreactors MB BR vs GM BR	
	Erlenmeyer flask	Bioreactor			
	MB medium	MB medium	GM medium	Fold change	p-Value
Indole-3-acetate	0.25 ± 0.03	0.45 ± 0.05	0.85 ± 0.08	0.53 ± 0.06	0.00125
Lactate	0.11 ± 0.03	0.19 ± 0.03	0.56 ± 0.09	0.34 ± 0.06	0.00190
2-Methyl-citrate	7.10 ± 5.84	0.58 ± 0.13	0.90 ± 0.17	0.64 ± 0.20	0.11281
3-Oxalomalate	0.41 ± 0.14	0.27 ± 0.04	0.43 ± 0.08	0.62 ± 0.08	0.00970
Pantothenate	1.13 ± 0.11	1.00 ± 0.11	0.45 ± 0.11	2.23 ± 0.54	0.00608
3-Phosphoglycerate	18.3 ± 9.6	11.6 ± 6.6	6.29 ± 3.59	1.84 ± 0.71	0.29720
Pyruvate	<0.01 ± 0	<0.01 ± 0	0.29 ± 0.10	<0.01 ± 0	0.00925
Shikimate	4.08 ± 1.34	5.72 ± 1.60	2.46 ± 0.86	2.33 ± 0.66	0.01310
Tartrate	<0.01 ± 0	<0.01 ± 0	0.85 ± 0.14	<0.01 ± 0	0.00028
Toluate	0.83 ± 0.20	1.42 ± 0.29	1.56 ± 0.35	0.91 ± 0.16	0.60349
Saccharides and derivatives					
Arabinose	0.43 ± 0.05	0.19 ± 0.03	0.30 ± 0.07	0.42 ± 0.12	0.00356
Arabitol	x	x	x	1.21 ± 1.20	0.25086
6-Deoxy-Mannose	0.69 ± 0.25	1.00 ± 0.17	1.13 ± 0.20	0.88 ± 0.11	0.20962
Fructose	0.26 ± 0.07	0.16 ± 0.06	1.11 ± 0.34	0.15 ± 0.05	0.00088
Fructose-1,6-bisphosphate	x	x	n.d.	x	
Fructose-1-phosphate	2.43 ± 1.11	1.92 ± 0.44	1.27 ± 0.18	1.51 ± 0.71	0.59558
Fructose-6-phosphate	0.32 ± 0.20	0.24 ± 0.15	0.34 ± 0.21	0.71 ± 0.09	0.02473
Glucoheptonate-1,4-lactone	0.32 ± 0.10	0.64 ± 0.13	2.11 ± 0.40	0.30 ± 0.06	0.00222
Gluconate-1,4-lactone	0.03 ± 0.02	0.02 ± 0.01	0.02 ± 0.02	0.94 ± 0.23	0.88028
Gluconate	0.06 ± 0.01	0.04 ± 0.01	0.19 ± 0.05	0.21 ± 0.06	0.01477
Glucono-1,5-lactone	0.06 ± 0.01	0.03 ± 0.01	0.18 ± 0.05	0.20 ± 0.06	0.01896
Glucuronate	n.d.	n.d.	n.d.	x	
Glucosamine-6-phosphate	<0.01 ± 0	0.02 ± 0	0.39 ± 0.07	0.03 ± 0.01	0.00163
Glucose	0.34 ± 0.03	0.39 ± 0.05	0.89 ± 0.10	0.44 ± 0.06	0.00035
Glucose-6-phosphate	0.09 ± 0.01	0.05 ± 0.01	0.27 ± 0.04	0.19 ± 0.04	0.00028
Glycerol	0.14 ± 0.09	0.14 ± 0.09	0.78 ± 0.40	0.18 ± 0.08	0.01310
Isomaltose (or similar)	46.2 ± 11.1	24.6 ± 6.0	0.98 ± 0.36	25.2 ± 14.5	0.00239
2-Keto-3-deoxy-gluconate (KDG)	0.24 ± 0.10	0.15 ± 0.05	0.44 ± 0.16	0.42 ± 0.15	0.16604
Lactose (or similar)	24.2 ± 3.50	28.6 ± 4.5	2.03 ± 0.42	14.1 ± 3.7	0.00105
Maltose	2.87	2.35	n.d.	x	
Maltotriitol (or similar)	x	x	x	129 ± 42.8	0.04752
Maltotriose (or similar)	x	x	n.d.	x	
Mannitol	1.50 ± 0.19	1.67 ± 0.22	1.38 ± 0.23	1.21 ± 0.15	0.20962
Melibiose	0.15 ± 0.02	0.10 ± 0.02	n.d.	x	
Myo-inositol	x	x	n.d.	x	
N-Acetyl-glucosamine	0.22 ± 0.09	0.18 ± 0.07	0.05 ± 0.02	3.65 ± 1.24	0.00222
Sorbose	x	x	n.d.	x	
Sucrose	2.09	1.23	2.74	0.45	0.16048
Trehalose	0.47 ± 0.11	0.41 ± 0.11	0.78 ± 0.09	0.52 ± 0.14	0.00028
Trehalose-6-phosphate	x	x	x	0.69 ± 0.78	0.19498
Ribose	2.00 ± 0.37	0.72 ± 0.25	0.44 ± 0.10	1.65 ± 0.55	0.72600
Xylose	0.66 ± 0.08	0.42 ± 0.07	0.76 ± 0.11	0.55 ± 0.11	0.01714
Xylulose	0.04 ± 0.02	0.02 ± 0.01	0.08 ± 0.02	0.22 ± 0.13	0.02473
Xylulose-5-phosphate	0.67 ± 0.23	0.41 ± 0.14	1.35 ± 0.41	0.33 ± 0.04	0.00088
Diamines					
Cadaverine	10.4 ± 6.1	16.6 ± 9.7	1.16 ± 0.92	14.2 ± 7.7	0.00028
Propane-1,3-diamine	0.33 ± 0.10	0.94 ± 0.22	2.20 ± 0.55	0.43 ± 0.09	0.01148
Putrescine	0.18 ± 0.03	0.14 ± 0.01	1.25 ± 0.14	0.11 ± 0.01	0.00028
Spermidine	10.1 ± 2.6	10.8 ± 2.5	1.39 ± 0.31	7.77 ± 1.11	0.00028
Membrane components					
Ethanolaminephosphate	110 ± 110	105 ± 105	7.63 ± 7.76	13.7 ± 3.0	0.00035
Glycerol-3-phosphate	0.91 ± 0.28	1.49 ± 0.16	0.60 ± 0.09	2.49 ± 0.34	0.00035
Glycerophosphoglycerol	0.35 ± 0.08	0.29 ± 0.07	0.44 ± 0.11	0.66 ± 0.18	0.44238
Tetradecanol	x	x	n.d.	x	
3-Hydroxydecanoate ($C_{10:0,\ 3\text{-}OH}$)	0.74 ± 0.13	1.11 ± 0.23	2.31 ± 0.50	0.48 ± 0.09	0.01477
Dodecanoate ($C_{12:0}$)	2.16 ± 0.33	0.89 ± 0.14	1.15 ± 0.20	0.78 ± 0.21	0.51965
Tetradecanoate ($C_{14:0}$)	0.14 ± 0.08	0.21 ± 0.12	0.32 ± 0.19	0.64 ± 0.20	0.02982
Hexadecanoate ($C_{16:0}$)	0.24 ± 0.06	0.42 ± 0.10	0.70 ± 0.17	0.59 ± 0.09	0.00171

S3: Fold changes of all intracellularly detected metabolites in the experiment "adaptation to growth with complex nutrients." (Continued)

Metabolites	Fold change in abundance as compared to GM EM			Comparison between bioreactors MB BR vs GM BR	
	Erlenmeyer flask	Bioreactor			
	MB medium	MB medium	GM medium	Fold change	p-Value
Octadecanoate ($C_{18:0}$)	0.26 ± 0.02	0.43 ± 0.06	0.86 ± 0.10	0.54 ± 0.08	0.00171
9-Octadecenoate ($C_{18:1}$)	4.76 ± 1.32	3.75 ± 0.94	1.71 ± 0.44	2.19 ± 0.58	0.02473
Purines, pyrimidines and derivatives					
Adenine	0.16 ± 0.02	0.19 ± 0.03	0.62 ± 0.07	0.30 ± 0.05	0.00064
Adenosine	1.02 ± 0.10	0.82 ± 0.09	1.01 ± 0.13	0.81 ± 0.12	0.20962
Adenosine-5'-monophosphate (AMP)	5.66 ± 0.54	3.36 ± 0.30	0.78 ± 0.18	4.32 ± 1.02	0.00028
Cytosine	<0.01 ± 0	0.29 ± 0.06	0.32 ± 0.08	0.92 ± 0.24	0.80836
4,5-Dihydroorotate	1.15 ± 0.19	1.60 ± 0.27	1.30 ± 0.23	1.24 ± 0.16	0.13807
Guanine	0.29 ± 0.08	0.39 ± 0.10	0.59 ± 0.16	0.66 ± 0.13	0.07926
Guanosine-5'-monophosphate (GMP)	3.63	4.03	1.29	4.14 ± 1.02	0.00163
Hypoxanthine	2.83 ± 0.35	3.56 ± 0.86	1.29 ± 0.27	2.76 ± 0.74	0.01477
Inosine-5'-monophosphate (IMP)	0.23 ± 0.03	0.14 ± 0.02	0.49 ± 0.09	0.28 ± 0.06	0.00432
Thymine	0.78 ± 0.14	1.11 ± 0.17	1.30 ± 0.24	0.86 ± 0.16	0.60349
Uracil	0.35 ± 0.07	0.95 ± 0.13	1.33 ± 0.21	0.71 ± 0.08	0.01896
Urate	0.50 ± 0.11	1.39 ± 0.22	1.25 ± 0.20	1.11 ± 0.08	0.16412
Uridine	1.81 ± 0.54	1.14 ± 0.28	0.93 ± 0.26	1.23 ± 0.22	0.13807
Uridine 5'-monophosphate (UMP)	14.6	8.86	1.00	8.86 ± 11.4	0.04752
Xanthine	4.54 ± 3.72	5.45 ± 4.06	0.60 ± 0.47	9.03 ± 6.19	0.00317
Others					
3-Amino-propane-1,2-diol	x	x	x	20.5 ± 20.5	0.00925
1,3-Dihydroxyacetone	0.02 ± 0.01	<0.01	5.12 ± 2.09	<0.01	0.16188
Dihydroxyacetone phosphate	0.35 ± 0.16	0.51 ± 0.27	0.67 ± 0.27	0.76 ± 0.14	0.00170
Diphosphate	x	x	n.d.	x	
Nicotinate	1.48 ± 0.20	2.54 ± 0.38	1.50 ± 0.19	1.70 ± 0.27	0.03697
Nicotinamide	0.66 ± 0.07	0.66 ± 0.04	0.65 ± 0.06	1.01 ± 0.10	0.85006
Phosphate	0.19 ± 0.02	0.49 ± 0.04	1.07 ± 0.09	0.45 ± 0.04	0.00035
Phosphate monomethyl ester	0.76 ± 0.20	1.39 ± 0.40	0.72 ± 0.24	1.93 ± 0.34	0.04369
Saccharopine	4.19 ± 2.59	1.04 ± 0.62	1.23 ± 0.73	0.85 ± 0.22	0.14452
Tryptamine	x	x	n.d.	x	
Urea	1.07 ± 0.19	4.80 ± 0.89	3.00 ± 0.66	1.60 ± 0.26	0.00853
Urocanate	1.83 ± 0.68	1.26 ± 0.48	4.06 ± 2.12	0.31 ± 0.12	0.16412
Unidentified compounds					
NA374 (RI_2172.3)	6.02 ± 1.57	3.27 ± 1.27	2.44 ± 0.97	4.01 ± 1.95	1.00000
NA411 (RI_2231.6)	x	x	n.d.	x	
NA438 (RI_2324.9)	61.1	71.8	4.93	29.2 ± 9.7	0.00239
Unknown#1475.5-pin-mhe_016	36.3 ± 17.3	102 ± 35.3	10.5 ± 4.3	23.2 ± 6.5	0.00608
Unknown#1570.6-pin-mhe_018	1.37 ± 0.68	1.23 ± 0.23	0.85 ± 0.10	1.44 ± 0.27	0.47064
Unknown#1586.9-pae-bth_039	0.84 ± 0.23	1.09 ± 0.18	1.49 ± 0.29	0.73 ± 0.11	0.09916
Unknown#1679.6-pin-mhe_020	0.64 ± 0.07	0.93 ± 0.07	1.24 ± 0.17	0.75 ± 0.10	0.16412
Unknown#1830.2-pin-mhe_038	0.77 ± 0.06	0.72 ± 0.05	0.94 ± 0.10	0.76 ± 0.09	0.08903
Unknown#2018.7-pin-mhe_028	1.22 ± 0.22	1.35 ± 0.19	0.61 ± 0.08	2.21 ± 0.33	0.00222
Unknown#2139.8-pin-mhe_046	1.55 ± 0.18	0.41 ± 0.08	0.08 ± 0.02	9.82 ± 2.23	0.00933
Unknown#2148.0-pin-mhe_047	0.12 ± 0.02	0.14 ± 0.02	0.14 ± 0.02	1.01 ± 0.13	0.80836
Unknown#2197.0-pin-mhe_048	8.01 ± 1.65	3.22 ± 0.80	2.29 ± 0.27	1.40 ± 0.36	0.91309
Unknown#2236.82-ypy-mse_026	1.23 ± 0.24	0.78 ± 0.12	0.34 ± 0.08	2.50 ± 0.68	0.02299
Unknown#2263.9-pin-mhe_049	2.32 ± 0.66	0.87 ± 0.31	0.53 ± 0.28	1.79 ± 0.90	0.07876
Unknown#2269.25-ypy-mse_027	0.96 ± 0.11	0.96 ± 0.11	0.33 ± 0.04	2.87 ± 0.36	0.00028
Unknown#2334.1-pin-mhe_051	2.51 ± 0.20	1.70 ± 0.12	1.73 ± 0.16	0.98 ± 0.38	0.88028
Unknown#2414.8-pin-mhe_057	x	x	x	125 ± 14.3	0.04752
Unknown#2423.9-pin-mhe_058	0.25 ± 0.02	0.46 ± 0.04	0.83 ± 0.07	0.56 ± 0.04	0.00033
Unknown#2548.1-pin-mhe_066	2.10 ± 0.49	1.99 ± 0.38	1.02 ± 0.25	2.34 ± 0.50	0.02392
Unknown#3363.5-pin-mhe_074	1.03 ± 0.43	0.68 ± 0.28	0.49 ± 0.22	2.76 ± 0.62	0.17801
Unknown#3423.2-pin-mhe_075	3.98 ± 1.19	0.40 ± 0.12	0.84 ± 0.28	0.60 ± 0.10	0.02657

Colour scale for fold changes:	<0.1	<0.2	<0.4	<0.67	0.67-1.5	>1.5	>2.5	>5.0	>10.0

p-value (Wilcoxon-Mann-Whitney Test, with false discovery rate control)	<0.001	<0.01	<0.05

S4: Fold changes of identified extracellular amino acids and metabolites in the experiment "dynamics of amino acid utilisation".

*, Compound not detected at t_0, therefore later sample point was taken as reference condition, marked by value "1.00".

Metabolites	Fold change in abundance as compared to t_0					
	t_{10}	t_{15}	t_{20}	t_{25}	t_{30}	t_{35}
Amino acids						
Alanine	0.88 ± 0.06	0.76 ± 0.03	0.72 ± 0.03	0.69 ± 0.04	0.49 ± 0.03	0.35 ± 0.02
Arginine	0.82 ± 0.08	0.62 ± 0.09	0.44 ± 0.06	0.38 ± 0.04	0.14 ± 0.03	0.16 ± 0.03
Aspartate	0.95 ± 0.10	0.70 ± 0.04	0.46 ± 0.05	0.18 ± 0.03	<0.01 ± 0	<0.01 ± 0
Glutamate	0.85 ± 0.07	0.52 ± 0.03	0.14 ± 0.01	<0.01 ± 0	<0.01 ± 0	<0.01 ± 0
Glycine	0.82 ± 0.07	0.67 ± 0.03	0.44 ± 0.02	0.14 ± 0.02	<0.01 ± 0	<0.01 ± 0.01
Isoleucine	0.92 ± 0.05	0.83 ± 0.06	0.88 ± 0.04	1.03 ± 0.04	0.97 ± 0.05	1.06 ± 0.06
Leucine	0.91 ± 0.06	0.80 ± 0.04	0.73 ± 0.04	0.78 ± 0.05	0.67 ± 0.04	0.65 ± 0.04
Lysine	0.93 ± 0.06	0.83 ± 0.04	0.71 ± 0.03	0.67 ± 0.05	0.44 ± 0.02	0.38 ± 0.02
Methionine	0.88 ± 0.10	0.62 ± 0.06	0.51 ± 0.05	0.4 ± 0.06	0.29 ± 0.04	0.2 ± 0.03
Phenylalanine	0.94 ± 0.05	0.84 ± 0.03	0.81 ± 0.02	0.73 ± 0.04	0.62 ± 0.02	0.64 ± 0.03
Proline	0.93 ± 0.07	0.76 ± 0.05	0.59 ± 0.04	0.49 ± 0.04	0.23 ± 0.02	0.08 ± 0.01
Serine	0.93 ± 0.07	0.86 ± 0.05	0.81 ± 0.06	0.75 ± 0.06	0.59 ± 0.03	0.49 ± 0.05
Threonine	0.94 ± 0.07	0.86 ± 0.05	0.84 ± 0.05	0.87 ± 0.06	0.77 ± 0.04	0.73 ± 0.04
Tyrosine	0.86 ± 0.09	0.67 ± 0.06	0.59 ± 0.04	0.61 ± 0.05	0.50 ± 0.04	0.54 ± 0.04
Valine	0.99 ± 0.07	0.91 ± 0.05	0.96 ± 0.06	1.10 ± 0.07	1.00 ± 0.06	1.05 ± 0.06
Others						
2-Aminobutanoate	0.91 ± 0.08	0.78 ± 0.05	0.74 ± 0.04	0.76 ± 0.05	0.57 ± 0.04	0.5 ± 0.04
Glycerol	0.24 ± 0.02	0.2 ± 0.02	0.19 ± 0.01	0.17 ± 0.02	0.18 ± 0.01	0.18 ± 0.02
3-Hydroxybutanoate	1.89 ± 0.39	2.65 ± 0.57	2.75 ± 0.71	4.16 ± 0.90	5.25 ± 1.58	2.22 ± 0.48
2-Hydroxyphenylacetate	1.20 ± 0.45	1.51 ± 0.62	2.51 ± 1.00	4.07 ± 1.59	4.19 ± 1.64	4.72 ± 1.85
2-Isopropylmalate *	1.00 ± 0.51	6.39 ± 3.06	8.96 ± 4.28	12.6 ± 6.0	13.7 ± 6.5	15.9 ± 7.6
N-Acetyl-serine *		1.00 ± 0.35	0.85 ± 0.22	0.43 ± 0.18		
Pyroglutamate	0.97 ± 0.08	0.79 ± 0.06	0.68 ± 0.06	0.64 ± 0.06	0.60 ± 0.04	0.60 ± 0.05
Urea	25.0 ± 18.4	94.0 ± 69.0	189.7 ± 139	354.9 ± 261	428.9 ± 315	488.8 ± 359

Colour scale for fold changes:	<0.1	<0.25	<0.5	<0.67	0.67 – 1.5	>1.5	>2.5	>5	>10

S5: Fold changes of all intracellularly detected metabolites in the experiment "dynamics of amino acid utilisation".

Symbols between sampling points represent significance of abundance changes, legend is provided at the bottom of this table. *, Compound not detected in reference condition (t_{10}), therefore a later sampling point was used as reference condition, marked by value "1.00".

Metabolites	Fold change in abundance as compared to reference condition (t_{10})				
	t_{15}	t_{20}	t_{25}	t_{30}	t_{35}
Amino acids and derivatives					
Alanine	2.23 ± 0.11	2.37 ± 0.16	3.23 ± 0.21	3.65 ± 0.23	3.55 ± 0.19
Arginine	1.70 ± 0.16	1.95 ± 0.16	1.89 ± 0.17	2.66 ± 0.23	2.23 ± 0.19
Asparagine	4.09 ± 0.37	3.23 ± 0.32	5.27 ± 0.50	5.89 ± 0.59	6.45 ± 0.63
Aspartate	1.25 ± 0.20	1.47 ± 0.22	2.41 ± 0.35	2.69 ± 0.41	2.43 ± 0.37
β-Alanine	1.68 ± 0.16	2.34 ± 0.26	2.46 ± 0.28	4.06 ± 0.41	5.35 ± 0.56
Cysteine	2.75 ± 0.16	1.34 ± 0.07	1.82 ± 0.10	3.93 ± 0.23	3.42 ± 0.28
Glutamate	2.33 ± 0.17	2.10 ± 0.16	2.47 ± 0.19	2.61 ± 0.19	2.23 ± 0.17
Glutamine	2.71 ± 0.24	2.33 ± 0.16	2.65 ± 0.16	3.26 ± 0.27	2.85 ± 0.23
Glycine	1.58 ± 0.08	1.66 ± 0.10	1.80 ± 0.10	2.33 ± 0.11	2.21 ± 0.11
Histidine	3.52 ± 0.32	3.64 ± 0.40	8.22 ± 0.84	18.6 ± 1.9	19.2 ± 1.9
Homocysteine	0.37 ± 0.06	0.38 ± 0.06	0.56 ± 0.09	0.73 ± 0.11	0.48 ± 0.08
Homoserine	1.43 ± 0.22	1.57 ± 0.23	1.25 ± 0.18	1.36 ± 0.20	1.48 ± 0.21
Isoleucine	1.45 ± 0.09	1.49 ± 0.08	2.90 ± 0.18	3.20 ± 0.19	2.94 ± 0.20
Leucine	1.92 ± 0.39	2.85 ± 0.51	2.75 ± 0.47	2.88 ± 0.41	2.55 ± 0.37
Lysine	1.99 ± 0.11	1.93 ± 0.11	3.43 ± 0.23	5.78 ± 0.42	6.19 ± 0.45
Methionine	0.81 ± 0.15	0.85 ± 0.15	0.86 ± 0.15	0.90 ± 0.16	0.82 ± 0.15
N-Acetyl-glutamate	0.76 ± 0.16	2.68 ± 0.39	9.59 ± 1.05	4.68 ± 0.60	2.63 ± 0.32
Ornithine	1.40 ± 0.18	1.18 ± 0.15	1.38 ± 0.19	1.65 ± 0.22	1.91 ± 0.26

S5: Fold changes of all intracellularly detected metabolites in the experiment "dynamics of amino acid utilisation". (Continued)

Metabolites	Fold change in abundance as compared to reference condition (t_{10})				
	t_{15}	t_{20}	t_{25}	t_{30}	t_{35}
Phenylalanine	2.35 ± 0.18	2.00 ± 0.19	2.06 ± 0.22	2.98 ± 0.27	2.93 ± 0.26
Proline	2.71 ± 0.16	4.60 ± 0.28	5.75 ± 0.35	6.10 ± 0.33	4.76 ± 0.30
Pyroglutamate	0.51 ± 0.08	0.53 ± 0.13	0.30 ± 0.09	0.46 ± 0.09	0.13 ± 0.03
Serine	1.65 ± 0.16	1.48 ± 0.13	2.66 ± 0.28	5.45 ± 0.52	5.37 ± 0.49
Threonine	1.84 ± 0.18	1.97 ± 0.16	6.84 ± 0.67	6.53 ± 0.58	4.52 ± 0.40
Tryptophan	2.23 ± 0.12	1.70 ± 0.11	1.88 ± 0.12	3.00 ± 0.26	3.09 ± 0.24
Tyrosine	1.91 ± 0.19	1.74 ± 0.18	3.06 ± 0.29	3.60 ± 0.41	2.99 ± 0.34
Valine	1.36 ± 0.14	1.88 ± 0.16	4.63 ± 0.43	5.23 ± 0.42	4.19 ± 0.36
Amino acid metabolism					
2-Aminoadipate	46.3 ± 31.2	69.3 ± 46.2	206 ± 138	480 ± 319	718 ± 478
5-Aminopentanoate	1.74 ± 0.60	0.87 ± 0.29	4.08 ± 1.35	0.92 ± 0.31	0.62 ± 0.21
2-Coumarate	4.45 ± 0.37	4.97 ± 0.46	7.69 ± 0.55	11.7 ± 0.82	11.3 ± 1.0
2,4-Diaminobutanoate	1.68 ± 0.09	3.21 ± 0.23	4.15 ± 0.25	3.64 ± 0.29	1.75 ± 0.18
2-Isopropylmalate	0.76 ± 0.07	9.22 ± 1.26	21.9 ± 2.9	8.30 ± 0.86	11.3 ± 0.9
Pipecolate	2.41 ± 0.17	4.46 ± 0.32	7.76 ± 0.61	16.9 ± 1.1	22.2 ± 1.5
Diamines					
Cadaverine	3.13 ± 0.33	6.37 ± 0.68	8.67 ± 0.93	8.55 ± 0.87	5.65 ± 0.56
Putrescine	1.03 ± 0.15	0.45 ± 0.05	0.12 ± 0.01	0.05 ± 0.01	0.03 ± 0
Spermidine	3.06 ± 0.42	1.06 ± 0.16	0.92 ± 0.19	2.81 ± 0.41	2.58 ± 0.36
Purines, pyrimidines and derivatives					
Adenine	1.05 ± 0.12	1.17 ± 0.14	0.94 ± 0.11	1.08 ± 0.12	0.97 ± 0.11
Adenosine	4.83 ± 0.67	11.5 ± 1.2	18.0 ± 1.8	15.4 ± 1.8	13.9 ± 1.9
Adenosine-5'-monophosphate (AMP)	4.27 ± 0.57	4.95 ± 0.68	4.77 ± 0.63	4.87 ± 0.69	4.30 ± 0.59
Cytosine	1.38 ± 0.08	1.09 ± 0.09	0.80 ± 0.06	0.78 ± 0.05	0.57 ± 0.06
4,5-Dihydroorotate	1.81 ± 0.15	2.56 ± 0.21	1.95 ± 0.16	1.93 ± 0.19	1.28 ± 0.11
Guanine	1.25 ± 0.08	1.10 ± 0.11	1.03 ± 0.10	0.97 ± 0.07	0.78 ± 0.06
Guanosine	1.14 ± 0.18	1.22 ± 0.27	2.77 ± 0.43	4.26 ± 0.88	6.40 ± 1.09
Guanosine-5'-monophosphate (GMP)	8.12 ± 1.47	5.09 ± 0.91	4.21 ± 0.75	5.32 ± 0.97	2.95 ± 0.53
Hypoxanthine	1.83 ± 0.14	1.82 ± 0.12	1.65 ± 0.10	1.58 ± 0.11	0.95 ± 0.08
Inosine-5'-monophosphate (IMP)	2.58 ± 0.39	1.94 ± 0.29	1.93 ± 0.27	1.96 ± 0.28	1.57 ± 0.23
Thymine	1.36 ± 0.10	2.32 ± 0.15	2.62 ± 0.15	2.15 ± 0.14	1.75 ± 0.11
Uracil	1.23 ± 0.09	1.14 ± 0.09	0.89 ± 0.07	1.06 ± 0.08	1.10 ± 0.08
Uridine	2.12 ± 0.16	2.86 ± 0.25	5.53 ± 0.43	5.27 ± 0.49	4.08 ± 0.35
Uridine 5'-monophosphate (UMP)	10.7 ± 5.4	19.3 ± 9.5	36.3 ± 17.6	26.5 ± 12.9	17.3 ± 8.5
Urate	1.28 ± 0.07	1.22 ± 0.08	1.51 ± 0.10	2.17 ± 0.15	2.50 ± 0.17
Xanthine	1.85 ± 0.14	1.92 ± 0.10	1.55 ± 0.08	1.40 ± 0.09	0.96 ± 0.06
Butanoates					
2-Aminobutanoate	3.01 ± 0.35	4.70 ± 0.52	4.70 ± 0.46	6.61 ± 0.58	8.28 ± 0.70
3-Hydroxybutanoate	10.6 ± 2.0	8.50 ± 1.66	3.60 ± 0.66	3.83 ± 0.67	2.12 ± 0.38
4-Hydroxybutanoate	24.3 ± 8.2	12.4 ± 4.1	3.91 ± 1.31	4.41 ± 1.46	2.49 ± 0.82
Fatty acids					
3-Hydroxydecanoate ($C_{10:0,\ 3\text{-}OH}$)	0.52 ± 0.09	0.72 ± 0.14	0.95 ± 0.17	1.47 ± 0.58	0.85 ± 0.17
Dodecanoate ($C_{12:0}$)	1.22 ± 0.10	1.80 ± 0.16	2.58 ± 0.22	3.60 ± 0.36	2.97 ± 0.28
Hexadecanoate ($C_{16:0}$)	1.00 ± 0.14	1.19 ± 0.17	1.51 ± 0.20	2.04 ± 0.42	1.35 ± 0.17
Octadecanoate ($C_{18:0}$)	0.94 ± 0.14	1.17 ± 0.20	1.69 ± 0.23	1.87 ± 0.31	1.70 ± 0.25
6-Octadecenoate ($C_{18:1}$)	1.82 ± 0.32	2.13 ± 0.39	3.48 ± 0.66	4.38 ± 0.91	4.63 ± 1.11
Peptidoglycan components					
Alanyl-alanine	5.48 ± 1.56	11.3 ± 3.3	24.9 ± 7.1	38.0 ± 10.9	45.3 ± 13.1
2,6-Diaminopimelate	3.59 ± 0.23	16.9 ± 0.9	24.7 ± 1.0	22.7 ± 1.3	17.6 ± 1.0
Phospholipid headgroup components					
1,3-Dihydroxyacetone	1.96 ± 0.30	2.98 ± 0.39	2.57 ± 0.30	3.16 ± 0.33	2.68 ± 0.35
Glycerophosphoglycerol	11.5 ± 4.2	0.24 ± 0.09	0.40 ± 0.11	0.41 ± 0.12	0.34 ± 0.13
Ethanolamine	7.64 ± 0.83	3.03 ± 0.35	1.85 ± 0.23	4.69 ± 0.50	2.79 ± 0.28
Glycerol	3.75 ± 1.33	1.59 ± 0.54	0.80 ± 0.30	1.42 ± 0.50	0.86 ± 0.29
Glycerol-3-phosphate	2.25 ± 0.15	1.20 ± 0.09	0.85 ± 0.06	1.16 ± 0.10	0.38 ± 0.04

S5: Fold changes of all intracellularly detected metabolites in the experiment "dynamics of amino acid utilisation". (Continued)

Metabolites	Fold change in abundance as compared to reference condition (t_{10})				
	t_{15}	t_{20}	t_{25}	t_{30}	t_{35}
TCA Cycle					
Citrate	0.64 ± 0.14	0.51 ± 0.11	0.47 ± 0.10	0.67 ± 0.14	0.78 ± 0.17
Fumarate	1.20 ± 0.12	1.86 ± 0.19	2.96 ± 0.30	3.56 ± 0.37	3.75 ± 0.39
Malate	1.07 ± 0.05	0.97 ± 0.06	0.87 ± 0.04	1.02 ± 0.06	0.99 ± 0.05
2-Oxoglutarate	1.18 ± 0.17	1.06 ± 0.16	1.00 ± 0.14	0.87 ± 0.12	0.70 ± 0.10
Succinate	2.17 ± 0.15	2.07 ± 0.14	1.69 ± 0.11	1.91 ± 0.13	1.67 ± 0.11
Pentose-Phosphate-Pathway					
Ribose-5-phosphate *	1.00 ± 1.41	18.1 ± 18.5	22.5 ± 22.5	36.3 ± 36.5	38.7 ± 38.8
Xylose	1.82 ± 0.21	1.27 ± 0.14	1.06 ± 0.16	1.70 ± 0.23	1.56 ± 0.17
Xylulose-5-phosphate	2.56 ± 1.39	5.97 ± 3.21	7.24 ± 3.88	6.51 ± 3.50	6.26 ± 3.37
Gluconeogenesis and Entner-Doudoroff pathway					
Phosphoenolpyruvate	0.77 ± 0.26	0.93 ± 0.31	2.58 ± 0.87	2.54 ± 0.86	1.69 ± 0.57
Dihydroxyacetone phosphate *		1.00 ± 1.41	20.7 ± 20.7	1.81 ± 2.22	1.85 ± 2.62
Fructose-1,6-bisphosphate *	1.00 ± 0.46	3.31 ± 1.11	1.83 ± 0.71	0.23 ± 0.17	0.78 ± 0.34
Fructose-6-phosphate	0.96 ± 0.13	1.87 ± 0.35	1.57 ± 0.29	1.04 ± 0.20	1.15 ± 0.23
Glucose	1.25 ± 0.08	2.45 ± 0.21	3.34 ± 0.28	1.62 ± 0.14	0.46 ± 0.07
Glucose-6-phosphate	1.61 ± 0.22	3.42 ± 0.44	2.98 ± 0.37	1.89 ± 0.23	1.10 ± 0.15
2-Keto-3-deoxy-gluconate (KDG)	0.70 ± 0.09	0.52 ± 0.08	2.50 ± 0.45	3.22 ± 0.39	2.10 ± 0.27
6-Phosphogluconate	0.80 ± 0.17	4.49 ± 0.97	35.5 ± 7.4	55.7 ± 11.3	57.0 ± 11.8
3-Phosphoglycerate	1.45 ± 0.17	1.11 ± 0.13	1.42 ± 0.16	2.14 ± 0.27	2.51 ± 0.30
Pyruvate	1.37 ± 0.15	2.01 ± 0.19	1.65 ± 0.14	1.48 ± 0.15	1.22 ± 0.11
Sugars					
1,6-Anhydro-glucose	0.84 ± 0.12	1.80 ± 0.25	2.81 ± 0.32	1.48 ± 0.20	0.55 ± 0.11
Gluconate / galactonate	1.17 ± 0.10	1.78 ± 0.20	4.85 ± 0.56	4.82 ± 0.45	3.35 ± 0.32
2-Amino-2-deoxy-gluconate	0.50 ± 0.04	0.41 ± 0.04	0.31 ± 0.02	0.59 ± 0.05	1.35 ± 0.10
N-Acetyl-glucosamine	2.77 ± 0.23	2.96 ± 0.27	1.73 ± 0.17	2.53 ± 0.26	2.40 ± 0.25
Others					
Glycerate	2.01 ± 0.17	1.67 ± 0.12	1.06 ± 0.07	1.96 ± 0.13	1.93 ± 0.13
5-Methylthio-adenosine	2.16 ± 0.15	5.54 ± 0.46	9.58 ± 0.74	8.92 ± 0.58	9.54 ± 0.71
Nicotinamide	1.31 ± 0.14	1.98 ± 0.20	2.21 ± 0.16	2.34 ± 0.18	1.93 ± 0.18
Nicotinate	2.29 ± 0.32	3.73 ± 0.54	4.82 ± 0.86	3.03 ± 0.41	2.96 ± 0.34
Phosphate	1.14 ± 0.07	1.32 ± 0.08	1.12 ± 0.06	1.18 ± 0.07	1.14 ± 0.07
Toluate	0.98 ± 0.06	1.15 ± 0.08	1.03 ± 0.06	1.14 ± 0.09	1.14 ± 0.07
Unidentified compounds					
Unknown#1195.3-pin-mhe_003	2.33 ± 0.55	3.29 ± 0.71	4.58 ± 0.99	4.51 ± 0.87	4.75 ± 0.97
Unknown#1345.9-pin-mhe_008	1.11 ± 0.14	2.02 ± 0.27	1.74 ± 0.25	1.72 ± 0.24	1.71 ± 0.22
Unknown#1361.3-pin-mhe_010	1.73 ± 0.14	2.01 ± 0.16	1.86 ± 0.17	2.89 ± 0.25	2.56 ± 0.22
Unknown#1440.7-pin-mhe_013	0.79 ± 0.03	0.80 ± 0.04	0.59 ± 0.02	0.67 ± 0.04	0.72 ± 0.03
Unknown#1679.6-pin-mhe_020	1.79 ± 0.32	1.97 ± 0.36	1.78 ± 0.36	2.31 ± 0.46	2.37 ± 0.42
Unknown#1771.2-pin-mhe_036	1.44 ± 0.34	2.09 ± 0.43	2.02 ± 0.46	1.36 ± 0.34	1.28 ± 0.32
Unknown#1953.9-pin-mhe_025	1.49 ± 0.09	1.69 ± 0.12	1.99 ± 0.13	1.78 ± 0.14	1.43 ± 0.13
Unknown#2088.0-pin-mhe_043	0.57 ± 0.10	0.77 ± 0.15	0.91 ± 0.27	1.52 ± 0.29	0.93 ± 0.44
Unknown#2334.1-pin-mhe_051	1.64 ± 0.14	3.21 ± 0.30	3.59 ± 0.29	3.58 ± 0.37	2.64 ± 0.26
Unknown#2370.5-pin-mhe_053	1.62 ± 0.23	3.76 ± 0.36	7.85 ± 0.70	8.07 ± 0.67	10.1 ± 1.1
Unknown#2394.5-pin-mhe_056	0.82 ± 0.07	1.49 ± 0.07	3.17 ± 0.09	7.41 ± 0.23	10.3 ± 0.4
Unknown#2442.5-pin-mhe_059 *		1.00 ± 0.16	2.51 ± 0.30	4.32 ± 0.50	4.17 ± 0.51
Unknown#2498.6-pin-mhe_062 *			1.00 ± 0.14	5.19 ± 0.58	7.02 ± 0.82
Unknown#2510.0-pin-mhe_063	1.01 ± 0.04	0.99 ± 0.05	0.82 ± 0.03	1.06 ± 0.05	1.03 ± 0.05
Unknown#2557.6-pin-mhe_067 *				1.00 ± 0.08	1.64 ± 0.14
Unknown#2602.0-pin-mhe_068 *		1.00 ± 0.34	1.55 ± 0.47	2.50 ± 0.57	2.53 ± 0.51
Unknown#3158.4-pin-mhe_073	2.30 ± 0.34	3.41 ± 0.52	4.62 ± 0.64	5.34 ± 0.75	4.39 ± 0.66

Colour scale for fold changes:	< 0.1	< 0.2	< 0.4	< 0.67	0.67 – 1.5	> 1.5	> 2.5	> 5.0	> 10.0

Significance of abundance changes between sampling points; corrected p-Values from t-test (●) or Wilcoxon-Mann-Whitney test (◆)

<0.0001 <0.001 <0.01 <0.05

S6: Fold changes of all intracellular metabolites of *P. inhibens* DSM 17395 detected in the experiment "amino acid degradation".
Abbreviation: x, compound not detected in reference condition, but in respective test condition. Substrates: Trp, tryptophan; Phe, phenylalanine; Met, methionine; Leu, leucine; Ile, isoleucine; Val, valine; His, histidine; Lys, lysine; Thr, threonine.

Metabolites	Fold change in abundance as compared to succinate grown cells								
	Trp	Phe	Met	Leu	Ile	Val	His	Lys	Thr
Amino acids and derivatives									
Alanine	0.20 ± 0.03	0.16 ± 0.02	0.28 ± 0.05	1.95 ± 0.26	0.77 ± 0.12	0.94 ± 0.12	1.19 ± 0.28	0.91 ± 0.12	3.96 ± 0.56
Asparagine	22.7 ± 3.4	1.27 ± 0.17	0.70 ± 0.07	1.05 ± 0.09	1.18 ± 0.12	0.78 ± 0.09	1.42 ± 0.18	0.44 ± 0.19	1.66 ± 0.16
Aspartate	0.18 ± 0.03	0.84 ± 0.18	0.70 ± 0.10	0.84 ± 0.11	1.00 ± 0.11	0.40 ± 0.04	3.35 ± 0.49	0.73 ± 0.15	3.63 ± 0.41
β-Alanine	0.67 ± 0.15	0.55 ± 0.10	0.52 ± 0.10	0.45 ± 0.08	0.57 ± 0.11	0.77 ± 0.14	0.82 ± 0.15	0.53 ± 0.10	0.73 ± 0.15
Cysteine			6.01 ± 0.55						0.50 ± 0.51
Glutamate	0.03 ± 0.02	0.06 ± 0.04	0.07 ± 0.02	0.64 ± 0.09	1.00 ± 0.11	0.58 ± 0.07	1.26 ± 0.18	0.25 ± 0.10	1.32 ± 0.12
Glycine	0.45 ± 0.06	0.32 ± 0.03	0.76 ± 0.15	0.48 ± 0.05	0.70 ± 0.09	0.94 ± 0.12	0.53 ± 0.07	0.47 ± 0.05	0.39 ± 0.04
Homocysteine	0.78 ± 0.08	0.96 ± 0.10	0.85 ± 0.15	0.60 ± 0.05	0.97 ± 0.11	1.00 ± 0.09	1.83 ± 0.24	0.41 ± 0.14	0.88 ± 0.07
Homoserine	0.72 ± 0.09	0.65 ± 0.06	1.17 ± 0.15	0.56 ± 0.07	0.90 ± 0.14	0.98 ± 0.11	0.80 ± 0.10	0.45 ± 0.07	1.02 ± 0.13
Isoleucine	0.64 ± 0.08	0.40 ± 0.04	0.69 ± 0.10	0.37 ± 0.05	24.9 ± 6.6	0.93 ± 0.14	0.56 ± 0.19	0.58 ± 0.07	0.83 ± 0.08
Leucine	0.58 ± 0.07	0.58 ± 0.07	0.36 ± 0.05	1.19 ± 0.15	1.60 ± 0.18	1.75 ± 0.30	0.49 ± 0.05	0.69 ± 0.09	0.60 ± 0.12
Lysine	0.05 ± 0.02	0.13 ± 0.05	0.36 ± 0.08	0.24 ± 0.05	0.55 ± 0.09	0.42 ± 0.08	0.50 ± 0.08	3.18 ± 1.05	1.12 ± 0.17
Methionine	0.33 ± 0.04	0.74 ± 0.32	5.28 ± 0.99	0.45 ± 0.04	0.51 ± 0.06	0.60 ± 0.08	0.67 ± 0.08	0.62 ± 0.18	0.50 ± 0.06
N-Acetyl-glutamate	0.99 ± 0.10	0.71 ± 0.09	0.59 ± 0.05	0.96 ± 0.08	0.88 ± 0.09	1.04 ± 0.11	1.30 ± 0.18	0.76 ± 0.08	1.82 ± 0.21
Ornithine	1.27 ± 0.40	0.12 ± 0.03	0.26 ± 0.04	0.65 ± 0.09	0.24 ± 0.04	0.42 ± 0.05	0.87 ± 0.11	0.54 ± 0.10	0.79 ± 0.09
Phenylalanine	0.33 ± 0.04	0.43 ± 0.05	0.25 ± 0.02	0.39 ± 0.04	0.51 ± 0.08	0.48 ± 0.04	0.42 ± 0.05	0.46 ± 0.05	0.51 ± 0.06
Proline	0.44 ± 0.06	0.25 ± 0.03	0.16 ± 0.02	0.54 ± 0.06	0.43 ± 0.07	0.66 ± 0.07	0.40 ± 0.05	0.37 ± 0.05	0.49 ± 0.06
Pyroglutamate	0.70 ± 0.14	1.26 ± 0.26	0.77 ± 0.07	0.92 ± 0.09	0.88 ± 0.09	0.78 ± 0.06	1.45 ± 0.15	1.10 ± 0.20	1.30 ± 0.13
Serine	0.42 ± 0.11	0.54 ± 0.08	0.68 ± 0.16	0.91 ± 0.14	1.56 ± 0.23	1.04 ± 0.10	1.00 ± 0.16	0.72 ± 0.13	0.94 ± 0.13
Threonine	0.60 ± 0.06	0.43 ± 0.04	0.62 ± 0.08	0.43 ± 0.04	1.23 ± 0.19	0.92 ± 0.13	0.85 ± 0.11	0.51 ± 0.06	4.62 ± 0.37
Tyrosine	0.24 ± 0.06	0.13 ± 0.04	0.22 ± 0.05	0.47 ± 0.07	0.90 ± 0.16	0.79 ± 0.12	0.72 ± 0.10	0.54 ± 0.09	0.98 ± 0.12
Valine	0.21 ± 0.03	0.09 ± 0.01	0.10 ± 0.01	0.27 ± 0.03	0.63 ± 0.14	5.60 ± 1.07	0.25 ± 0.03	0.37 ± 0.05	0.43 ± 0.05
Tryptophan degradation									
2-Aminobenzoate (anthranilate)	2.92 ± 0.25								
Phenylalanine degradation									
Phenylpyruvate		2.80 ± 0.48							0.15 ± 0.11
Methionine degradation									
2-Oxobutanoate			7.11 ± 0.04						
Isoleucine degradation									
3-Methyl-2-Oxopentanoate					x				

S6: Fold changes of all intracellular metabolites of *P. inhibens* DSM 17395 detected in the experiment "amino acid degradation". (Continued)

Metabolites	Fold change in abundance as compared to succinate grown cells								
	Trp	Phe	Met	Leu	Ile	Val	His	Lys	Thr
Valine degradation									
2-Oxoisovalerate						x			
Histidine degradation									
Urocanate							1.52 ± 0.55		
Lysine degradation									
2-Aminoadipate						0.35 ± 0.06		0.63 ± 0.14	0.04 ± 0.04
5-Aminopentanoate			x		x		x	x	
Cadaverine	0.87 ± 0.09	2.07 ± 0.30	14.9 ± 8.1	1.53 ± 0.09	4.39 ± 0.48	1.57 ± 0.11	10.5 ± 9.5	116 ± 16	1.12 ± 0.09
Glutarate	0.14 ± 0.10	0.16 ± 0.11	2.22 ± 0.46	1.53 ± 0.32	6.22 ± 1.29	1.44 ± 0.26	9.29 ± 8.35	142 ± 38	0.15 ± 0.05
Other compounds associated with amino acid metabolism									
Homogentisate		3.72 ± 0.41							
Hydantoin-5-propionate							x		
4-Hydroxyphenylacetate		3.14 ± 0.38	0.45 ± 0.17		0.06 ± 0.06	1.03 ± 0.12			
Phenylacetate		1.72 ± 0.19							
Shikimate-3-phosphate	1.02 ± 0.09	2.31 ± 0.20	2.68 ± 0.54	2.66 ± 0.55	4.64 ± 0.98	3.48 ± 0.74	2.10 ± 0.44	2.38 ± 0.61	2.44 ± 0.50
TCA Cycle									
2-Oxoglutarate	1.31 ± 0.12	1.50 ± 0.13	0.71 ± 0.06	1.02 ± 0.09	1.00 ± 0.12	0.93 ± 0.09	1.19 ± 0.14	1.10 ± 0.10	0.93 ± 0.09
Citrate	1.16 ± 0.20	1.11 ± 0.24	0.57 ± 0.07	1.10 ± 0.15	0.97 ± 0.18	1.04 ± 0.14	2.24 ± 0.44	2.70 ± 0.35	1.57 ± 0.24
Fumarate	0.64 ± 0.08	0.60 ± 0.05	0.62 ± 0.08	1.20 ± 0.14	0.86 ± 0.11	1.25 ± 0.13	0.95 ± 0.12	0.66 ± 0.06	1.00 ± 0.08
Malate	0.50 ± 0.07	0.54 ± 0.07	0.40 ± 0.07	1.37 ± 0.18	0.67 ± 0.11	0.77 ± 0.10	1.11 ± 0.17	0.66 ± 0.08	0.89 ± 0.11
Succinate	0.55 ± 0.07	0.45 ± 0.04	0.55 ± 0.10	1.49 ± 0.11	1.38 ± 0.14	1.32 ± 0.10	0.95 ± 0.09	0.66 ± 0.07	1.34 ± 0.10
Gluconeogenesis									
Dihydroxyacetone phosphate	1.83 ± 0.15	2.57 ± 0.33	1.33 ± 0.12	1.28 ± 0.33	1.04 ± 0.11	1.00 ± 0.10	0.96 ± 0.08	1.09 ± 0.09	1.66 ± 0.15
Fructose	1.70 ± 0.18	2.19 ± 0.25	1.20 ± 0.13	1.46 ± 0.56	0.96 ± 0.10	0.86 ± 0.10	0.64 ± 0.13	1.22 ± 0.19	0.96 ± 0.11
Fructose-1-phosphate	0.28 ± 0.15	0.11 ± 0.11	0.68 ± 0.11	0.65 ± 0.10	0.59 ± 0.10	0.64 ± 0.09	0.72 ± 0.12	1.05 ± 0.18	0.65 ± 0.11
Fructose-6-phosphate		0.59 ± 0.31	3.05 ± 1.72	1.15 ± 0.11	1.41 ± 0.15	2.06 ± 0.87	0.88 ± 0.15	1.54 ± 0.22	1.29 ± 0.11
Glucose	0.87 ± 0.11	1.23 ± 0.15	2.10 ± 0.74	1.22 ± 0.14	1.38 ± 0.25	1.20 ± 0.13	0.88 ± 0.12	1.09 ± 0.13	0.87 ± 0.14
Glucose-6-phosphate	0.10 ± 0.05	0.12 ± 0.06	0.39 ± 0.07	0.66 ± 0.14	0.44 ± 0.09	0.72 ± 0.14	0.55 ± 0.12	0.46 ± 0.09	0.64 ± 0.12
3-Phosphoglycerate	1.18 ± 0.14	1.14 ± 0.16	1.13 ± 0.15	0.98 ± 0.11	0.98 ± 0.13	1.11 ± 0.14	1.07 ± 0.13	1.05 ± 0.13	0.93 ± 0.10
Phosphoenolpyruvate	1.51 ± 0.17	1.78 ± 0.24	1.37 ± 0.12	1.03 ± 0.10	1.04 ± 0.13	1.05 ± 0.10	1.07 ± 0.10	1.13 ± 0.10	0.97 ± 0.09
Pyruvate	1.72 ± 0.14	2.69 ± 0.23	1.44 ± 0.17	2.00 ± 0.18	1.79 ± 0.36	0.77 ± 0.07	1.73 ± 0.13	1.54 ± 0.12	1.73 ± 0.17

S6: Fold changes of all intracellular metabolites of *P. inhibens* DSM 17395 detected in the experiment "amino acid degradation". (Continued)

Metabolites	Fold change in abundance as compared to succinate grown cells								
	Trp	Phe	Met	Leu	Ile	Val	His	Lys	Thr
Entner-Doudoroff pathway									
Gluconate / galactonate	0.83 ± 0.08	0.97 ± 0.10	1.14 ± 0.13	1.07 ± 0.07	0.90 ± 0.09	0.44 ± 0.02	0.81 ± 0.06	1.13 ± 0.10	0.62 ± 0.05
Gluconate-1,4-lactone	1.69 ± 0.13	1.02 ± 0.16	0.49 ± 0.03	0.54 ± 0.06	0.48 ± 0.04	1.33 ± 0.07	0.17 ± 0.07	0.50 ± 0.05	0.58 ± 0.05
Glucono-1,5-lactone	1.96 ± 0.20	1.66 ± 0.26	1.42 ± 0.17	0.81 ± 0.09	0.79 ± 0.11	1.16 ± 0.14	0.81 ± 0.10	1.12 ± 0.13	0.69 ± 0.07
Glyceraldehyde	1.07 ± 0.20	1.04 ± 0.20	1.06 ± 0.28	0.57 ± 0.21	1.44 ± 0.47	1.38 ± 0.23	1.70 ± 0.33	1.53 ± 0.30	0.86 ± 0.28
2-Keto-3-deoxy-gluconate (KDG)	1.90 ± 0.16	1.95 ± 0.24	1.43 ± 0.12	1.31 ± 0.13	1.10 ± 0.14	0.76 ± 0.07	1.06 ± 0.12	1.28 ± 0.12	0.97 ± 0.10
6-Phospho-gluconate	1.39 ± 0.43	0.12 ± 0.12	1.55 ± 0.31	1.80 ± 0.29	1.26 ± 0.19	1.11 ± 0.19	0.27 ± 0.15	1.00 ± 0.14	0.65 ± 0.21
Pentose phosphate pathway									
2-Deoxyribose		10.4 ± 4.8	6.23 ± 2.82	4.39 ± 2.03	4.58 ± 2.12		4.24 ± 1.96	4.79 ± 2.18	4.13 ± 1.89
Ribose-5-phosphate	0.97 ± 0.23	1.68 ± 0.28	1.18 ± 0.20	1.22 ± 0.20	0.82 ± 0.13	0.78 ± 0.10	0.91 ± 0.13	1.08 ± 0.17	1.02 ± 0.15
Xylose-1-phosphate	0.29 ± 0.21	0.75 ± 0.29	1.00 ± 0.15	1.00 ± 0.06	1.57 ± 0.26	0.64 ± 0.11	1.03 ± 0.09	1.28 ± 0.12	0.90 ± 0.08
Xylulose-5-phosphate	1.25 ± 0.13	2.01 ± 0.26	1.24 ± 0.09	0.85 ± 0.06	0.95 ± 0.09	0.93 ± 0.06	1.10 ± 0.08	1.01 ± 0.10	0.84 ± 0.07
Other sugars and derivatives									
1,6-Anhydro-glucose	3.68 ± 0.28	5.81 ± 0.43	5.53 ± 0.33	3.55 ± 0.24	11.0 ± 0.8	4.20 ± 0.20	3.08 ± 0.32	5.68 ± 0.44	2.10 ± 0.16
1-*O*-Methyl-*β*-galactopyranoside	1.57 ± 0.18	0.63 ± 0.07	0.63 ± 0.08	0.88 ± 0.11	1.61 ± 0.24	0.89 ± 0.11	0.16 ± 0.07	0.42 ± 0.04	0.36 ± 0.06
Hexose	0.82 ± 0.04	0.80 ± 0.06	0.85 ± 0.04	0.65 ± 0.03	0.73 ± 0.06	0.88 ± 0.03	0.61 ± 0.04	0.59 ± 0.03	0.59 ± 0.04
Arabinose	1.75 ± 0.17	2.63 ± 0.28	1.29 ± 0.12	1.07 ± 0.12	1.15 ± 0.13	1.30 ± 0.11	1.03 ± 0.13	1.20 ± 0.12	1.03 ± 0.10
Galactose	1.36 ± 0.20	0.64 ± 0.09	0.52 ± 0.08	0.44 ± 0.07	0.55 ± 0.07	0.89 ± 0.14	0.12 ± 0.07	0.45 ± 0.09	0.48 ± 0.08
Lipid and phospholipid headgroup components									
Ethanolamine	1.18 ± 0.19	1.82 ± 0.38	1.44 ± 0.27	1.23 ± 0.21	1.91 ± 0.28	1.18 ± 0.18	1.37 ± 0.20	1.57 ± 0.32	1.74 ± 0.23
Ethanolaminephosphate	0.57 ± 0.06	0.64 ± 0.07	1.01 ± 0.10	0.89 ± 0.08	1.36 ± 0.17	0.80 ± 0.08	1.01 ± 0.13	0.86 ± 0.09	1.06 ± 0.11
Glycerol-3-phosphate	1.00 ± 0.12	0.92 ± 0.11	1.83 ± 0.28	1.61 ± 0.18	2.30 ± 0.28	0.70 ± 0.08	1.98 ± 0.19	1.48 ± 0.18	2.94 ± 0.26
Glycerophosphoglycerol	0.37 ± 0.12	0.43 ± 0.13	3.46 ± 0.96	1.69 ± 0.50	2.59 ± 0.69	0.58 ± 0.16	2.21 ± 0.53	1.31 ± 0.44	5.10 ± 1.23
Octanoate ($C_{8:0}$)	1.07 ± 0.16	0.79 ± 0.10	0.63 ± 0.12	0.86 ± 0.13	0.80 ± 0.11	0.91 ± 0.13	0.63 ± 0.07	0.74 ± 0.11	0.95 ± 0.13
3-Hydroxydecanoate ($C_{10:0,\ 3\text{-}OH}$)	2.27 ± 0.26	1.67 ± 0.21	1.15 ± 0.20	0.97 ± 0.13	0.62 ± 0.08	0.70 ± 0.08	0.73 ± 0.08	1.08 ± 0.13	0.98 ± 0.11
Dodecanoate ($C_{12:0}$)	2.53 ± 0.27	3.14 ± 0.41	1.69 ± 0.22	1.51 ± 0.21	1.20 ± 0.17	1.28 ± 0.16	1.16 ± 0.14	1.52 ± 0.18	1.29 ± 0.15
Hexadecanoate ($_{C16:0}$)	0.87 ± 0.19	0.85 ± 0.19	1.54 ± 0.32	1.35 ± 0.23	1.78 ± 0.34	1.20 ± 0.22	1.23 ± 0.21	1.49 ± 0.27	0.79 ± 0.14
1-Hexadecanol	0.47 ± 0.11	0.42 ± 0.09	0.72 ± 0.18	0.95 ± 0.27	0.81 ± 0.19	1.34 ± 0.30	0.59 ± 0.14	0.66 ± 0.17	0.61 ± 0.14
Octadecanoate ($C_{18:0}$)	1.07 ± 0.23	1.25 ± 0.29	1.73 ± 0.32	1.43 ± 0.24	1.82 ± 0.34	1.22 ± 0.23	1.45 ± 0.30	1.50 ± 0.31	0.85 ± 0.16
9-Octadecenoate ($C_{18:1}$)	1.43 ± 0.12	1.77 ± 0.18	3.93 ± 0.31	2.11 ± 0.19	2.56 ± 0.24	1.40 ± 0.12	1.86 ± 0.18	1.53 ± 0.20	1.40 ± 0.15
Peptidoglycan components									
Alanyl-alanine	0.20 ± 0.12	0.29 ± 0.15	0.42 ± 0.18	1.94 ± 0.78	2.21 ± 0.77	2.91 ± 0.95	1.29 ± 0.56	0.41 ± 0.19	3.51 ± 1.34
Glucosamine-6-phosphate		0.48 ± 0.27	0.06 ± 0.06	0.90 ± 0.09	0.69 ± 0.06	0.85 ± 0.07	0.90 ± 0.11	0.30 ± 0.13	0.91 ± 0.06

S6: Fold changes of all intracellular metabolites of *P. inhibens* DSM 17395 detected in the experiment "amino acid degradation". (Continued)

Metabolites	Fold change in abundance as compared to succinate grown cells								
	Trp	Phe	Met	Leu	Ile	Val	His	Lys	Thr
N-Acetyl-glucosamine	1.62 ± 0.13	2.41 ± 0.35	1.73 ± 0.16	1.11 ± 0.14	1.54 ± 0.20	1.23 ± 0.12	1.38 ± 0.14	1.10 ± 0.15	1.14 ± 0.13
Butanoates									
2-Aminobutanoate	0.44 ± 0.12	0.49 ± 0.14	0.89 ± 0.27	0.59 ± 0.09	0.83 ± 0.15	0.87 ± 0.16	1.64 ± 0.26	0.91 ± 0.16	0.77 ± 0.19
4-Aminobutanoate	1.17 ± 0.07	1.24 ± 0.12	0.17 ± 0.07	0.71 ± 0.05	0.65 ± 0.08	0.95 ± 0.07	1.36 ± 0.61	0.29 ± 0.06	0.91 ± 0.04
3-Aminoisobutanoate	0.81 ± 0.23	0.71 ± 0.17	1.09 ± 0.22	0.97 ± 0.18	1.17 ± 0.20	1.03 ± 0.20	1.45 ± 0.27	1.16 ± 0.25	1.31 ± 0.28
2,4-Diaminobutanoate	0.80 ± 0.09	1.34 ± 0.14	1.58 ± 0.15	1.44 ± 0.19	1.44 ± 0.21	1.22 ± 0.14	1.97 ± 0.22	1.36 ± 0.16	1.77 ± 0.18
2-Hydroxybutanoate	1.86 ± 0.63	1.79 ± 0.42	0.84 ± 0.17	1.17 ± 0.25	1.22 ± 0.27	0.94 ± 0.23	1.11 ± 0.29	1.50 ± 0.33	1.63 ± 0.38
3-Hydroxybutanoate	1.07 ± 0.21	11.6 ± 2.5	0.62 ± 0.12	0.97 ± 0.19	1.55 ± 0.31	0.93 ± 0.18	5.98 ± 1.30	1.70 ± 0.32	5.56 ± 1.24
4-Hydroxybutanoate	0.40 ± 0.12	0.21 ± 0.05	0.85 ± 0.25	0.61 ± 0.15	1.09 ± 0.21	1.21 ± 0.25	0.81 ± 0.20	0.69 ± 0.16	0.80 ± 0.24
Nicotinamide metabolism									
Nicotinamide	0.31 ± 0.05	0.50 ± 0.09	0.47 ± 0.07	0.80 ± 0.07	1.03 ± 0.12	1.10 ± 0.10	1.13 ± 0.14	0.51 ± 0.11	0.73 ± 0.11
Nicotinate	0.38 ± 0.08	0.46 ± 0.10	0.55 ± 0.13	0.98 ± 0.25	0.66 ± 0.15	1.00 ± 0.31	0.61 ± 0.16	0.49 ± 0.11	0.95 ± 0.44
Purines, pyrimidines and derivatives									
Adenine				0.59 ± 0.57	1.77 ± 1.53		8.80 ± 6.45	0.72 ± 0.70	4.36 ± 3.09
Adenosine	0.56 ± 0.26	0.16 ± 0.16	0.24 ± 0.13	1.24 ± 0.22	1.00 ± 0.17	1.56 ± 0.26	0.79 ± 0.22	0.09 ± 0.09	0.95 ± 0.20
Cytosine	0.18 ± 0.07	0.17 ± 0.07	0.23 ± 0.04	0.70 ± 0.10	0.64 ± 0.09	0.71 ± 0.08	0.69 ± 0.10	0.26 ± 0.04	0.90 ± 0.10
4,5-Dihydroorotate	6.58 ± 3.92	33.4 ± 19.9	20.8 ± 12.4	28.4 ± 25.2	14.6 ± 8.7	2.81 ± 1.68	11.4 ± 6.8	13.8 ± 8.22	7.38 ± 4.40
Orotate	0.32 ± 0.17		2.65 ± 0.27	0.20 ± 0.11	0.51 ± 0.21	0.69 ± 0.06	2.09 ± 0.29	0.20 ± 0.14	18.4 ± 1.9
Thymine	0.22 ± 0.05	0.61 ± 0.11	1.29 ± 0.19	1.52 ± 0.17	2.12 ± 0.31	0.54 ± 0.05	1.76 ± 0.20	0.89 ± 0.12	1.61 ± 0.16
Uracil	0.32 ± 0.14	0.37 ± 0.12	0.78 ± 0.16	0.80 ± 0.15	1.01 ± 0.21	1.53 ± 0.23	0.75 ± 0.15	0.56 ± 0.09	0.69 ± 0.14
Uridine	0.71 ± 0.16	0.30 ± 0.17	0.76 ± 0.08	0.92 ± 0.09	0.95 ± 0.10	1.52 ± 0.12	0.81 ± 0.10	0.19 ± 0.10	2.69 ± 1.40
Others									
Benzoate	1.28 ± 0.22	1.05 ± 0.21	1.51 ± 0.21	0.98 ± 0.20	1.41 ± 0.25	10.8 ± 1.5	1.26 ± 0.23	1.93 ± 0.33	1.20 ± 0.19
Carbodiimide	0.96 ± 0.11	0.82 ± 0.09	1.12 ± 0.13	0.96 ± 0.11	1.14 ± 0.12	1.28 ± 0.15	1.03 ± 0.12	0.85 ± 0.09	0.93 ± 0.11
Diphosphate	0.16 ± 0.05	0.15 ± 0.03	0.32 ± 0.09	0.50 ± 0.12	0.55 ± 0.11	0.80 ± 0.14	0.40 ± 0.09	0.33 ± 0.10	0.45 ± 0.13
Glucoheptonate-1,4-lactone	1.09 ± 0.19	1.50 ± 0.27	1.18 ± 0.20	1.33 ± 0.18	1.00 ± 0.12	1.11 ± 0.15	0.93 ± 0.11	1.03 ± 0.18	1.12 ± 0.14
Glycerate	2.43 ± 0.23	4.16 ± 0.42	2.08 ± 0.19	1.41 ± 0.13	1.53 ± 0.20	1.16 ± 0.12	1.51 ± 0.17	1.52 ± 0.14	1.44 ± 0.14
2-Hydroxyglutarate	1.34 ± 0.24	1.47 ± 0.29	0.93 ± 0.15	1.29 ± 0.25	0.98 ± 0.17	0.95 ± 0.18	0.83 ± 0.20	1.11 ± 0.19	1.12 ± 0.18
2-Methylmalate	0.20 ± 0.08	0.23 ± 0.09	0.72 ± 0.19	2.53 ± 0.44	1.55 ± 0.27	2.48 ± 0.46	1.23 ± 0.27	1.00 ± 0.21	2.97 ± 0.54
2-Methylmalonate	0.35 ± 0.09	0.24 ± 0.06	1.37 ± 0.33	0.98 ± 0.18	1.38 ± 0.22	1.38 ± 0.42	0.77 ± 0.15	1.08 ± 0.20	0.88 ± 0.15
2-Methylserine	2.07 ± 0.21	2.25 ± 0.27	4.51 ± 0.61	6.49 ± 2.68	1.89 ± 0.22	1.41 ± 0.13	3.19 ± 1.05	2.30 ± 0.77	2.50 ± 0.26
Phosphate	0.99 ± 0.07	0.97 ± 0.08	0.87 ± 0.07	0.87 ± 0.07	0.99 ± 0.12	0.90 ± 0.08	0.89 ± 0.07	0.82 ± 0.06	0.96 ± 0.07

S6: Fold changes of all intracellular metabolites of *P. inhibens* DSM 17395 detected in the experiment "amino acid degradation". (Continued)

Metabolites	Fold change in abundance as compared to succinate grown cells								
	Trp	Phe	Met	Leu	Ile	Val	His	Lys	Thr
Phosphate monomethyl ester	2.27 ± 0.38	2.32 ± 0.31	1.42 ± 0.18	1.13 ± 0.17	1.55 ± 0.61	1.00 ± 0.13	1.07 ± 0.16	1.19 ± 0.16	1.06 ± 0.16
Putrescine	1.01 ± 0.11	3.13 ± 0.35	0.55 ± 0.04	1.72 ± 0.17	1.36 ± 0.14	1.19 ± 0.10	0.73 ± 0.08	0.51 ± 0.08	1.40 ± 0.12
Toluate	1.21 ± 0.21	0.84 ± 0.09	1.30 ± 0.12	0.89 ± 0.10	1.08 ± 0.10	1.25 ± 0.11	1.01 ± 0.12	1.07 ± 0.11	1.08 ± 0.09
Unidentified compounds									
NA66 (RI_1325)	1.24 ± 0.77	2.05 ± 0.56	1.77 ± 0.48	40.2 ± 40.2	11.3 ± 11.3	1.32 ± 1.73	2.26 ± 4.54	15.7 ± 15.7	2.93 ± 2.93
Unknown#1171.6-pin-mhe_002	0.55 ± 1.44	0.40 ± 1.06	1.03 ± 2.68	1.20 ± 3.15	1.10 ± 2.82	1.12 ± 2.85	1.62 ± 4.21	0.93 ± 2.46	1.09 ± 3.01
Unknown#1226.1-pin-mhe_004			0.74 ± 0.24	1.58 ± 0.24	2.92 ± 0.44	1.12 ± 0.20	1.71 ± 0.30	1.05 ± 0.25	1.70 ± 0.33
Unknown#1234.8-pin-mhe_005				x	x				
Unknown#1325.8-pin-mhe_007	0.95 ± 0.14	1.31 ± 0.22	1.67 ± 0.24	0.98 ± 0.22	0.85 ± 0.16	1.10 ± 0.13	0.86 ± 0.16	0.63 ± 0.13	0.86 ± 0.11
Unknown#1348.0-pin-mhe_009	5.30 ± 3.62	2.15 ± 1.35	0.55 ± 0.27	0.49 ± 0.25	0.44 ± 0.22	0.65 ± 0.32	0.55 ± 0.29	0.76 ± 0.53	0.41 ± 0.20
Unknown#1361.3-pin-mhe_010	0.45 ± 0.06	0.87 ± 0.10	1.10 ± 0.11	0.98 ± 0.11	0.67 ± 0.08	0.86 ± 0.11	1.12 ± 0.13	0.65 ± 0.09	1.12 ± 0.12
Unknown#1366.9-pin-mhe_011	1.13 ± 0.24	2.33 ± 0.46	1.22 ± 0.18	0.99 ± 0.16	0.63 ± 0.11	0.83 ± 0.12	1.08 ± 0.18	0.93 ± 0.21	1.10 ± 0.17
Unknown#1461.8-pin-mhe_015		x		x	x	x	x	x	x
Unknown#1586.9-pae-bth_039	0.29 ± 0.06	0.48 ± 0.07	0.34 ± 0.03	0.53 ± 0.07	0.89 ± 0.12	0.57 ± 0.06	1.06 ± 0.11	0.64 ± 0.10	0.85 ± 0.10
Unknown#1635.2-pin-mhe_031	2.45 ± 0.41	2.71 ± 0.41	1.31 ± 0.27	1.58 ± 0.35	1.08 ± 0.19	0.58 ± 0.11	1.04 ± 0.23	2.43 ± 0.39	1.50 ± 0.25
Unknown#1647.7-pae-bth_045		x	x	x	x	x	x	x	x
Unknown#1669.1-pin-mhe_033	0.27 ± 0.08	0.80 ± 0.14	1.00 ± 0.19	1.12 ± 0.18	0.68 ± 0.16	0.89 ± 0.18	1.14 ± 0.23	0.68 ± 0.13	1.26 ± 0.20
Unknown#1746.5-cgl-sst_058	1.97 ± 1.25	0.98 ± 0.43	1.30 ± 0.60	0.87 ± 0.40	1.09 ± 0.51	1.59 ± 0.81	1.13 ± 0.50	0.92 ± 0.40	1.42 ± 0.64
Unknown#1881.9-pin-mhe_041	1.67 ± 0.20	2.42 ± 0.28	1.39 ± 0.16	0.94 ± 0.13	0.91 ± 0.16	1.41 ± 0.14	1.02 ± 0.15	1.06 ± 0.13	0.85 ± 0.12
Unknown#1953.9-pin-mhe_025	2.12 ± 0.59	2.32 ± 0.60	3.02 ± 0.95	2.00 ± 0.60	1.54 ± 0.47	1.72 ± 0.51	1.47 ± 0.39	1.77 ± 0.47	1.43 ± 0.39
Unknown#2018.7-pin-mhe_028	0.49 ± 0.08	0.54 ± 0.09	0.66 ± 0.06	0.84 ± 0.08	0.79 ± 0.09	1.08 ± 0.09	0.84 ± 0.09	0.64 ± 0.08	0.63 ± 0.07
Unknown#2078.9-pin-mhe_042	1.21 ± 0.19	0.86 ± 0.23	0.85 ± 0.18	1.10 ± 0.21	0.56 ± 0.12	0.90 ± 0.17	0.93 ± 0.27	0.81 ± 0.13	0.77 ± 0.12
Unknown#2090.48-ypy-mse_021	1.38 ± 0.18	1.54 ± 0.20	1.41 ± 0.13	1.23 ± 0.12	1.45 ± 0.17	1.46 ± 0.15	1.18 ± 0.08	1.35 ± 0.12	0.85 ± 0.08
Unknown#2274.6-dsh-nbi_004	0.72 ± 0.15	0.93 ± 0.15	1.21 ± 0.17	1.45 ± 0.14	1.26 ± 0.20	1.13 ± 0.15	1.14 ± 0.10	1.14 ± 0.15	1.22 ± 0.15
Unknown#2329.3-pin-mhe_050	1.00 ± 0.12	1.34 ± 0.17	0.97 ± 0.12	0.74 ± 0.13	1.72 ± 0.24	1.44 ± 0.16	0.32 ± 0.11	0.64 ± 0.10	0.45 ± 0.08
Unknown#2334.1-pin-mhe_051	0.54 ± 0.29	0.74 ± 0.40	1.01 ± 0.53	1.49 ± 0.79	1.34 ± 0.70	0.71 ± 0.38	1.49 ± 0.78	0.75 ± 0.41	1.00 ± 0.52

Colour scale for fold changes:	<0.1	<0.2	<0.4	<0.67	0.67 – 1.5	>1.5	>2.5	>5.0	>10.0

S7: Significance of abundance changes of intracellular metabolites detected in the experiment "amino acid degradation".
Substrates: Trp, tryptophan; Phe, phenylalanine; Met, methionine; Leu, leucine; Ile, isoleucine; Val, valine; His, histidine; Lys, lysine; Thr, threonine.

Metabolites	p-values for abundance changes as compared to succinate grown cells								
	Trp	Phe	Met	Leu	Ile	Val	His	Lys	Thr
Amino acids and derivatives									
Alanine	4E-006	1E-006	5E-005	0.0019	1.0000	1.0000	0.9675	1.0000	0.0003
Asparagine	8E-005	0.4077	0.1446	0.6125	1.0000	1.0000	0.5899	1.0000	0.0009
Aspartate	0.0003	0.2966	0.0281	0.2488	1.0000	9E-005	0.0018	0.0394	1E-006
β-Alanine	0.0653	0.0084	0.005	0.2243	0.0237	0.3306	0.5599	0.0083	0.1259
Cysteine			0.0002						0.1721
Glutamate	0.0003	0.0002	0.0002	0.0103	1.0000	0.0042	1.0000	0.0008	1.0000
Glycine	0.0002	8E-007	0.036	0.0007	1.0000	0.4241	0.003	7E-005	0.0004
Homocysteine	0.0301	1.0000	0.0245	0.0012	1.0000	1.0000	0.012	0.0052	1.0000
Homoserine	0.0301	0.0055	0.6586	0.0215	0.524	0.8944	0.1468	0.001	0.8358
Isoleucine	0.1011	3E-005	1.0000	0.0005	0.1367	0.508	0.0052	0.0021	1.0000
Leucine	0.0019	0.0009	0.0002	1.0000	0.0056	0.0298	0.0009	0.0394	0.0476
Lysine	0.0094	0.0003	0.0056	0.0005	0.2405	0.0144	0.0041	0.9607	1.0000
Methionine	1E-006	0.0106	0.0002	0.0005	0.0006	0.0064	0.0073	0.0053	0.0006
N-Acetyl-glutamate	0.8551	0.0084	0.0007	1.0000	0.2022	0.8871	0.4431	0.0202	0.0007
Ornithine	0.7488	0.0002	1E-005	0.022	9E-006	0.0008	0.4276	0.2181	1.0000
Phenylalanine	3E-008	1E-006	1E-010	0.0005	0.0038	2E-006	1E-006	0.0005	0.0001
Proline	0.0002	0.0002	2E-008	0.0019	0.0007	0.0091	0.0012	0.0008	0.0008
Pyroglutamate	0.0394	0.6778	0.0146	1.0000	0.2022	0.0259	0.0191	0.7665	0.0414
Serine	0.0019	0.0166	0.0732	1.0000	0.0341	1.0000	1.0000	1.0000	1.0000
Threonine	0.0009	4E-006	0.0496	0.0007	1.0000	1.0000	1.0000	0.0008	0.0003
Tyrosine	0.0003	0.0002	3E-007	0.0012	1.0000	0.0542	1.0000	0.0366	1.0000
Valine	9E-008	3E-009	4E-009	0.0005	1.0000	0.0005	3E-007	3E-005	0.0006
Tryptophan degradation									
2-Aminobenzoate (anthranilate)	0.0003								
Phenylalanine degradation									
Phenylpyruvate		0.0002							0.7905
Methionine degradation									
2-Oxobutanoate			0.0002						
Isoleucine degradation									
3-Methyl-2-Oxopentanoate									

S7: **Significance of abundance changes of intracellular metabolites detected in the experiment "amino acid degradation".** (Continued)

Metabolites	p-values for abundance changes as compared to succinate grown cells								
	Trp	Phe	Met	Leu	Ile	Val	His	Lys	Thr
2-Oxoisovalerate									
Histidine degradation									
Urocanate							0.9003		
Lysine degradation									
2-Aminoadipate						0.0005		1.0000	0.1826
5-Aminopentanoate									
Cadaverine	0.3901	0.0003	0.0002	7E-005	0.0004	0.0032	0.8501	0.0005	0.1931
Glutarate	0.8127	1.0000	0.1801	0.1512	0.0006	1.0000	0.7849	0.0179	0.0009
Other compounds associated with amino acid metabolism									
Homogentisate		0.0002							
Hydantoin-5-propionate									
4-Hydroxyphenylacetate		0.0002	1.0000		0.4187	0.5411			
Phenylacetate		0.0004							
Shikimate-3-phosphate	0.8273	0.1332	0.0002	0.0009	0.0004	0.0005	0.0062	0.0107	0.0009
TCA Cycle									
2-Oxoglutarate	0.024	0.0033	0.1254	0.894	1.0000	1.0000	0.4861	1.0000	1.0000
Citrate	0.8273	0.8012	0.1112	0.8349	1.0000	1.0000	0.0035	3E-005	1.0000
Fumarate	0.0061	0.0002	0.0032	1.0000	0.1565	0.1372	0.4593	0.0014	0.8647
Malate	0.0004	0.0004	0.0005	1.0000	0.0341	0.1881	0.6181	0.0083	0.5511
Succinate	0.0023	2E-007	0.0389	0.0015	0.9395	0.2557	1.0000	0.0291	0.0021
Gluconeogenesis									
Dihydroxyacetone phosphate	0.0003	0.0036	0.0036	1.0000	0.7209	1.0000	0.9003	1.0000	0.003
Fructose	0.0009	0.0004	0.0828	1.0000	1.0000	0.4241	0.074	0.0743	0.8995
Fructose-1-phosphate	0.5765	0.6334	0.0316	1.0000	0.0213	0.0483	0.1468	0.7311	0.0916
Fructose-6-phosphate		0.2299	0.0036	1.0000	0.0885	0.1281	0.5835	0.0039	0.0509
Glucose	0.5227	0.2299	0.0513	1.0000	0.2442	0.34	0.6949	0.6662	0.6186
Glucose-6-phosphate	0.0128	1.0000	0.244	0.2195	0.6426	1.0000	0.1701	0.0453	1.0000
3-Phosphoglycerate	0.2256	0.5742	1.0000	0.7885	1.0000	1.0000	0.7849	1.0000	1.0000
Phosphoenolpyruvate	0.0083	0.0097	0.0059	1.0000	0.9415	0.8871	0.5599	0.4575	0.8647
Pyruvate	0.0003	3E-007	1.0000	0.0005	1.0000	0.9817	7E-005	0.0024	0.0063

S7: **Significance of abundance changes of intracellular metabolites detected in the experiment "amino acid degradation".** (Continued)

Metabolites	p-values for abundance changes as compared to succinate grown cells								
	Trp	Phe	Met	Leu	Ile	Val	His	Lys	Thr
Entner-Doudoroff pathway									
Gluconate / galactonate	0.1361	0.8687	0.4831	1.0000	0.2238	0.0005	0.0587	0.3357	0.0007
Gluconate-1,4-lactone	0.0019	0.2299	2E-008	0.0008	1E-007	0.0014	0.0083	0.0005	0.0003
Glucono-1,5-lactone	2E-005	0.9087	0.7316	0.0877	1.0000	0.5982	1.0000	1.0000	0.6604
Glyceraldehyde	0.8273	1.0000	0.761	1.0000	0.9144	1.0000	1.0000	0.0677	0.643
2-Keto-3-deoxy-gluconate (KDG)	0.0009	0.0055	0.0032	1.0000	0.9144	0.0298	0.5599	0.0268	0.9403
6-Phospho-gluconate	0.4536	0.2299	0.2559	0.7372	0.3804	0.9212	1.0000	1.0000	0.0408
Pentose phosphate pathway									
2-Deoxyribose		0.0082	0.2339	0.2488	1.0000		1.0000	1.0000	1.0000
Ribose-5-phosphate	0.7135	0.6899	1.0000	1.0000	0.2022	1.0000	1.0000	1.0000	1.0000
Xylose-1-phosphate	0.0428	0.0089	0.8271	1.0000	0.027	0.0585	0.8855	0.0346	0.1931
Xylulose-5-phosphate	1.0000	0.0616	0.0513	0.1259	1.0000	1.0000	1.0000	1.0000	0.1135
Other sugars and derivatives									
1,6-Anhydro-glucose	0.0003	2E-009	5E-012	0.0005	2E-010	4E-014	0.0008	9E-009	4E-005
1-*O*-Methyl-*β*-galactopyranoside	0.0027	0.0005	0.0032	1.0000	0.0137	0.4809	0.0083	0.0005	0.0003
Hexose	0.099	0.0167	0.4586	0.0005	0.0476	0.0483	5E-007	1E-008	5E-007
Arabinose	0.0023	2E-005	0.8982	1.0000	0.524	0.0277	1.0000	1.0000	1.0000
Galactose	0.0027	0.0048	0.0007	0.0513	0.001	0.2817	0.044	0.0009	0.0008
Lipid and phospholipid headgroup components									
Ethanolamine	0.6725	0.0263	0.1954	1.0000	0.005	0.5982	0.1468	0.1385	0.0731
Ethanolaminephosphate	0.0016	0.0055	0.5916	1.0000	0.0518	0.0111	0.808	0.0748	1.0000
Glycerol-3-phosphate	1.0000	1.0000	0.4531	0.0092	0.0028	0.6152	0.0004	0.8018	8E-008
Glycerophosphoglycerol	0.0209	0.179	0.0013	1.0000	0.0075	0.4241	0.0093	0.7311	0.0003
Octanoate ($C_{8:0}$)	0.6725	0.1645	0.0211	1.0000	0.1891	0.6216	0.0073	0.1297	1.0000
3-Hydroxydecanoate ($C_{10:0,\ 3\text{-}OH}$)	0.0008	0.1805	0.954	1.0000	0.0098	0.5388	0.0352	1.0000	1.0000
Dodecanoate ($C_{12:0}$)	5E-008	4E-005	0.0024	1.0000	0.5065	1.0000	1.0000	0.1319	0.0846
Hexadecanoate ($_{C16:0}$)	0.6725	0.4725	0.104	1.0000	0.0237	0.34	0.1701	0.0748	0.4453
1-Hexadecanol	0.0209	0.0075	0.306	1.0000	0.7995	0.1281	0.1592	0.3357	0.1501
Octadecanoate ($C_{18:0}$)	1.0000	1.0000	0.8438	0.0716	0.6688	0.3668	1.0000	1.0000	1.0000
9-Octadecenoate ($C_{18:1}$)	0.0805	0.0161	3E-009	7E-005	0.0004	0.1603	0.0012	0.9881	0.9558
Peptidoglycan components									
Alanyl-alanine	0.0023	0.0106	0.0573	1.0000	0.03	0.0111	0.6949	0.0512	0.0373
Glucosamine-6-phosphate		0.0893	0.1511	0.4465	0.0083	1.0000	0.0945	1.0000	1.0000

S7: **Significance of abundance changes of intracellular metabolites detected in the experiment "amino acid degradation".** (Continued)

Metabolites	p-values for abundance changes as compared to succinate grown cells								
	Trp	Phe	Met	Leu	Ile	Val	His	Lys	Thr
N-Acetyl-glucosamine	0.0005	0.0003	0.0009	1.0000	0.0451	1.0000	0.7658	0.8019	1.0000
Butanoates									
2-Aminobutanoate	0.0051	0.0106	0.2559	0.7141	0.4744	1.0000	0.7624	1.0000	0.0916
4-Aminobutanoate	1.0000	1.0000	2E-005	0.0017	0.0746	0.34	0.0276	0.0005	1.0000
3-Aminoisobutanoate	0.3005	0.059	0.761	1.0000	0.4047	0.954	0.074	0.7311	0.4807
2,4-Diaminobutanoate	1.0000	1.0000	0.018	1.0000	0.0642	1.0000	0.0048	1.0000	0.0006
2-Hydroxybutanoate	0.5227	1.0000	0.7268	0.5434	1.0000	0.8796	0.8501	1.0000	1.0000
3-Hydroxybutanoate	0.961	0.0002	0.1319	1.0000	0.0451	0.5694	0.0045	0.0239	0.0054
4-Hydroxybutanoate	0.0043	0.0072	0.2559	0.1391	1.0000	1.0000	0.4593	1.0000	0.1799
Nicotinamide metabolism									
Nicotinamide	1E-006	0.0019	0.0007	0.064	1.0000	1.0000	1.0000	0.2062	1.0000
Nicotinate	0.0009	0.0097	0.0211	1.0000	0.3232	0.8944	0.1592	0.0222	0.1655
Purines, pyrimidines and derivatives									
Adenine				1.0000	0.5806		0.9003	0.5807	0.484
Adenosine	0.0267	0.2299	0.8915	1.0000	0.8425	0.0165	0.2476	0.5649	0.5319
Cytosine	0.0005	0.0004	6E-007	0.064	0.446	0.6429	1.0000	0.0005	1.0000
4,5-Dihydroorotate	0.1516	0.0249	0.005	1.0000	0.027	0.5343	0.1315	0.1259	1.0000
Orotate	1.0000		5E-007	0.5434	1.0000	0.2534	0.0398	0.594	2E-011
Thymine	0.0003	0.3631	1.0000	0.0158	0.1121	0.001	0.0357	1.0000	0.0352
Uracil	0.0083	0.1348	1.0000	0.3292	1.0000	0.6164	1.0000	0.6463	1.0000
Uridine	0.0638	1.0000	1.0000	0.7211	1.0000	0.0077	1.0000	1.0000	0.5511
Others									
Benzoate	1.0000	1.0000	0.4873	1.0000	0.1284	6E-011	1.0000	0.0034	1.0000
Carbodiimide	0.9216	0.179	0.2797	1.0000	0.0709	0.0483	0.9675	0.5835	0.7647
Diphosphate	0.0004	0.0005	0.0036	1.0000	0.0709	0.34	0.1225	0.0061	0.0166
Glucoheptonate-1,4-lactone	0.9216	0.179	0.514	1.0000	0.9415	0.6984	0.5835	0.7675	0.5038
Glycerate	2E-006	1E-008	3E-006	0.0066	1.0000	1.0000	0.2241	0.0014	0.1065
2-Hydroxyglutarate	1.0000	0.0968	1.0000	0.2309	1.0000	1.0000	1.0000	1.0000	0.5038
2-Methylmalate	0.0267	0.0435	0.0462	0.0001	0.0187	0.0028	0.3595	0.8309	0.0006
2-Methylmalonate	0.0036	0.0006	0.6586	1.0000	0.2985	0.8796	0.3595	0.9607	0.5511
2-Methylserine	0.0002	0.0017	0.0002	1.0000	0.0009	0.2172	0.0021	0.0025	0.0003
Phosphate	1.0000	1.0000	0.0934	0.1997	1.0000	0.4809	1.0000	1.0000	1.0000

S7: **Significance of abundance changes of intracellular metabolites detected in the experiment "amino acid degradation".** (Continued)

Metabolites	p-values for abundance changes as compared to succinate grown cells								
	Trp	Phe	Met	Leu	Ile	Val	His	Lys	Thr
Phosphate monomethyl ester	0.0014	0.0004	0.0109	1.0000	0.8865	0.6216	0.5418	0.1385	0.5845
Putrescine	1.0000	0.0002	0.0002	0.0144	0.0111	1.0000	0.7656	0.0021	0.0839
Toluate	0.8127	1.0000	0.8996	0.5434	1.0000	1.0000	1.0000	1.0000	1.0000
Unidentified compounds									
NA66 (RI_1325)	1.0000	0.2073	0.2045	0.0128	0.1319	1.0000	0.4861	0.2382	0.0135
Unknown#1171.6-pin-mhe_002	0.5765	0.3639	0.715	1.0000	0.9314	0.7876	0.5418	0.6662	0.8358
Unknown#1226.1-pin-mhe_004			0.1954	0.0328	0.0006	1.0000	0.0251	0.5263	0.0509
Unknown#1234.8-pin-mhe_005									
Unknown#1325.8-pin-mhe_007	1.0000	1.0000	0.0036	0.8793	1.0000	1.0000	1.0000	0.1014	1.0000
Unknown#1348.0-pin-mhe_009	0.2046	0.0399	0.6586	1.0000	0.1565	0.1689	0.4276	0.0145	0.0509
Unknown#1361.3-pin-mhe_010	0.0005	0.2716	0.453	1.0000	0.0075	0.5694	0.4431	0.0129	0.3698
Unknown#1366.9-pin-mhe_011	0.8886	0.0019	0.0573	1.0000	0.0137	0.4809	0.7806	0.4315	0.4453
Unknown#1461.8-pin-mhe_015									
Unknown#1586.9-pae-bth_039	0.0003	0.0022	5E-007	0.0017	1.0000	0.0035	0.7849	0.5283	1.0000
Unknown#1635.2-pin-mhe_031	0.0007	0.0002	0.4238	1.0000	0.8648	0.0277	1.0000	0.0039	1.0000
Unknown#1647.7-pae-bth_045									
Unknown#1669.1-pin-mhe_033	0.0031	0.134	1.0000	0.7885	1.0000	1.0000	1.0000	1.0000	1.0000
Unknown#1746.5-cgl-sst_058	0.8273	0.0399	0.0281	1.0000	0.0805	0.0298	0.0587	0.1014	0.0274
Unknown#1881.9-pin-mhe_041	0.0031	0.0003	0.0192	1.0000	0.524	0.0146	0.941	0.6127	0.3941
Unknown#1954.3-pin-mhe_026	0.0071	0.004	0.0032	1.0000	0.0137	0.0146	0.0169	0.0129	0.0257
Unknown#2018.7-pin-mhe_028	0.0006	0.0013	0.0009	1.0000	0.0642	0.34	0.1701	0.0061	0.0025
Unknown#2078.9-pin-mhe_042	0.4912	0.2716	0.1954	1.0000	0.0098	0.34	0.2105	0.2142	0.0509
Unknown#2090.48-ypy-mse_021	1.0000	0.8915	0.0032	0.0786	1.0000	0.0064	0.0523	0.5467	1.0000
Unknown#2274.6-dsh-nbi_004	0.0505	1.0000	0.7894	0.2102	0.353	1.0000	1.0000	1.0000	0.3427
Unknown#2329.3-pin-mhe_050	1.0000	0.7468	0.4831	1.0000	0.0039	0.0542	0.0056	0.803	0.2932
Unknown#2334.1-pin-mhe_051	0.7908	0.134	0.0169	1.0000	0.013	0.2061	0.0083	0.402	0.0274
p-Values:						<0.0001	<0.001	<0.01	<0.05

underlined: t-test, Holm-Bonferroni correction

alternatively: Wilcoxon-Mann-Whitney Test, False Discovery Rate Control

S8: Intracellularly detected metabolites of *P. inhibens* DSM 17395 in the experiment "carbohydrate degradation".
Abbreviations: NAG, N-acetyl-glucosamine; MTL, mannitol; SUCR, sucrose; GLC, glucose; XYL, xylose; *, compound probably dephosphorylated during sample treatment; x, compound not detected in reference condition; XX, compound not detected in reference condition, but intense peak observed in test condition.

Metabolites	Fold change in metabolite abundance as compared to succinate grown cells					p-Values for abundance changes				
	NAG	MTL	SUCR	GLC	XYL	NAG	MTL	SUCR	GLC	XYL
Sugars and derivatives										
Hexoses										
1,6-Anhydro-glucose	1.46 ± 0.09	1.71 ± 0.09	0.84 ± 0.06	1.07 ± 0.08	1.23 ± 0.11	0.00015	0.00011	0.11588	0.31577	0.05948
6-Deoxy-mannose	13.0 ± 2.5	15.6 ± 2.1	4.07 ± 0.55	4.64 ± 0.63	15.0 ± 2.0	0.00025	0.00011	0.00112	0.00073	0.00018
Fructose	0.73 ± 0.05	8.27 ± 0.66	17.3 ± 1.7	2.21 ± 0.20	1.05 ± 0.12	0.00870	0.00016	0.00131	0.00039	0.91107
Fructose-6-phosphate	0.07 ± 0.06	0.02 ± 0.01	4.28 ± 2.15	4.30 ± 2.44	0.44 ± 0.36	0.1310754	0.1308055	0.0351274	0.1459156	0.4791699
Glucose	1.59 ± 0.07	2.00 ± 0.10	0.78 ± 0.04	1.04 ± 0.07	0.86 ± 0.05	3.5E-08	1.1E-09	0.01389	0.34174	0.03513
Glucose/Galactose/Mannose-6-P	0.03 ± 0.01	0.04 ± 0.02	0.16 ± 0.06	0.30 ± 0.12	0.14 ± 0.06	0.015791	0.0728393	0.428487	0.3770686	0.5050026
Glucose/Glucosamine/Sorbitol-6-P	0.03 ± 0.01	0.12 ± 0.08	0.66 ± 0.31	47.3 ± 25.7	0.33 ± 0.18	0.6641592	0.580338	0.0850328	0.0191952	0.6709364
Gluconate-1,4-lactone	0.91 ± 0.11	1.97 ± 0.22	1.44 ± 0.33	0.81 ± 0.09	1.13 ± 0.13	0.00015	0.00011	0.00112	0.00012	0.00018
Glucoheptonate-1,4-lactone (Heptose)	1.53 ± 0.12	0.70 ± 0.07	0.69 ± 0.06	0.56 ± 0.08	2.18 ± 0.38	0.00028	0.00645	0.02669	0.00066	0.02620
Glucosamine	0.49 ± 0.07		0.12 ± 0.02		0.12 ± 0.02	0.00105		0.01296		0.00080
Glucosaminate	XX	x	x	x	x					
N-Acetyl-glucosamine	12.0 ± 0.6	1.33 ± 0.16	1.69 ± 0.23	2.65 ± 0.29	1.36 ± 0.17	1.0E-10	0.04265	0.23790	0.00592	1.0000
N-Acetyl-mannosamine	x		x	x						
Glucuronate			3.35 ± 0.44	87.0 ± 17.6				0.01454	0.00015	
Mannitol	0.76 ± 0.14	19.9 ± 2.5	1.02 ± 0.09	0.47 ± 0.06	0.43 ± 0.03	0.03080	0.00011	0.47815	0.00256	0.00018
Pentoses / Pentose-Phosphate Pathway										
Arabinonate	9.34 ± 2.73	11.2 ± 2.0	4.25 ± 0.83	21.6 ± 12.3	110 ± 19.2	0.0645205	0.080547	0.0402735	0.3021725	0.0526444
Erythrose-4-phosphate	3.74 ± 2.99	2.75 ± 2.68	5.45 ± 5.20	0.48 ± 0.35	0.99 ± 0.93	0.0645205	0.8059139	0.5844601	0.679489	0.6709364
Ribonate	5.71 ± 2.13	13.6 ± 1.5	5.49 ± 0.95	8.90 ± 1.11	69.5 ± 9.3	0.0215946	0.0728393	0.0181589	0.0191952	0.0237982
Ribose	1.02 ± 0.05	2.30 ± 0.08	0.81 ± 0.07	0.89 ± 0.07	2.45 ± 0.11	1.0000	1.3E-13	1.0000	0.26492	1.6E-11
Xylose			x		XX					
Xylulose	0.81 ± 0.08	0.76 ± 0.07	0.52 ± 0.06	0.87 ± 0.10	0.87 ± 0.13	0.09208	0.01358	0.05173	1.0000	0.44062
Xylulose-/ Ribulose-5-phosphate	0.09 ± 0.06		0.05 ± 0.05	0.17 ± 0.11	1.00 ± 1.00	0.05960			0.78382	0.86521
Di-Saccharides										
Melibiose	x	x	x	x	x					
Sucrose			x							
α-D-Glucopyranosyl-(1,6)-mannitol		x								
α-D-Mannopyranosyl-(1,2)-*D*-mannopyranose		XX	x							

S8: Intracellularly detected metabolites of *P. inhibens* DSM 17395 in the experiment "carbohydrate degradation". (Continued)

Metabolites	Fold change in metabolite abundance as compared to succinate grown cells					p-Values for abundance changes				
	NAG	MTL	SUCR	GLC	XYL	NAG	MTL	SUCR	GLC	XYL
Entner-Doudoroff pathway										
Glucono-1,5-lactone *	4.70 ± 0.32	8.99 ± 0.57	9.83 ± 0.71	22.4 ± 2.3	4.99 ± 0.42	0.00015	0.00011	0.00112	0.00012	0.00018
Galactonate / Gluconate *	11.4 ± 1.8	4.62 ± 0.74	8.06 ± 1.26	26.0 ± 3.7	6.58 ± 1.34	2.0E-05	0.00030	4.0E-05	2.3E-07	0.01746
6-Phosphogluconate	0.24 ± 0.09	0.96 ± 0.37	5.05 ± 1.98	15.8 ± 6.0	0.17 ± 0.16	0.015791	0.51537	0.015791	0.0191952	0.0526444
2-Keto-3-deoxy-gluconate (KDG) *	30.5 ± 4.3	4.66 ± 2.49	1.87 ± 0.10	3.18 ± 0.28	2.05 ± 0.13	0.00020	0.00016	1.0E-07	0.00015	7.9E-07
Glyceraldehyde *	1.05 ± 0.13	0.75 ± 0.11	0.50 ± 0.07	0.64 ± 0.08	0.76 ± 0.09	0.74436	0.09832	0.00474	0.04120	0.34395
Dihydroxyacetone phosphate	1.68 ± 0.33	0.31 ± 0.15	0.39 ± 0.09	0.63 ± 0.17	0.60 ± 0.18	0.2040539	0.0761095	0.0181589	0.1700449	0.2691744
1,3-Dihydroxyacetone *	0.77 ± 0.04	0.95 ± 0.05	1.00 ± 0.06	1.12 ± 0.08	0.98 ± 0.05	0.00819	0.37593	1.0000	1.0000	1.0000
3-Phosphoglycerate	3.77 ± 0.44	1.58 ± 0.16	1.66 ± 0.23	8.75 ± 1.04	2.60 ± 0.31	0.00037	0.00226	0.14412	0.00029	0.00090
2-Phosphoglycerate	1.64	0.42	0.80	2.70		0.3634587	0.2186292	0.3089399	0.191776	
Phosphoenolpyruvate	1.95 ± 0.28	1.77 ± 0.24	1.27 ± 0.21	4.43 ± 0.66	1.84 ± 0.28	0.00245	0.00786	0.21103	0.00019	0.00912
Pyruvate	7.71 ± 1.29	3.62 ± 0.60	3.11 ± 0.54	3.84 ± 0.57	5.35 ± 0.77	0.00018	0.00011	0.00112	1.9E-06	2.8E-08
TCA Cycle										
Citrate	4.00 ± 0.58	1.28 ± 0.14	0.89 ± 0.15	5.06 ± 0.83	4.39 ± 0.72	0.00015	0.02385	0.61250	0.00012	0.00044
2-Oxoglutarate	1.90 ± 0.12	0.73 ± 0.05	0.60 ± 0.04	1.10 ± 0.11	1.31 ± 0.10	0.00015	0.00226	0.00135	0.26492	0.00443
Succinate	0.60 ± 0.06	0.30 ± 0.02	0.07 ± 0.01	0.13 ± 0.01	0.24 ± 0.02	0.00142	9.5E-10	9.8E-13	6.8E-12	1.1E-10
Fumarate	2.11 ± 0.20	0.71 ± 0.06	0.35 ± 0.03	0.37 ± 0.05	0.52 ± 0.05	0.00024	0.01203	0.00112	0.00012	0.00033
Malate	3.45 ± 0.35	0.48 ± 0.04	0.28 ± 0.03	0.34 ± 0.04	0.40 ± 0.04	2.2E-08	0.00043	0.00112	1.5E-05	9.0E-05
Amino acids and derivatives										
Alanine	4.21 ± 1.05	0.47 ± 0.12	0.05 ± 0.01	0.16 ± 0.04	0.27 ± 0.06	0.00039	1.0000	0.00112	0.00255	0.01326
Aspartate	0.13 ± 0.02	0.08 ± 0.01	0.05 ± 0.01	0.06 ± 0.01	0.03 ± 0	0.00015	0.00011	0.00112	0.00012	0.00018
β-Alanine	0.55 ± 0.03	0.44 ± 0.03	0.24 ± 0.01	0.28 ± 0.03	0.42 ± 0.02	0.00015	0.00011	0.00112	0.00012	0.00018
Glutamate	0.89 ± 0.09	0.75 ± 0.09	0.43 ± 0.05	0.70 ± 0.07	0.66 ± 0.07	0.6641592	0.2186292	0.015791	0.1093279	0.0489275
Glutamine	1.12 ± 0.17	1.48 ± 0.23	1.41 ± 0.14	1.33 ± 0.11	1.09 ± 0.09	0.42638	0.00316	0.49292	0.25900	1.0000
Glycine	0.76 ± 0.09	0.36 ± 0.03	0.20 ± 0.02	0.18 ± 0.02	0.23 ± 0.02	0.05008	3.8E-06	7.0E-08	0.00012	1.7E-07
Homoserine	1.16 ± 0.13	1.39 ± 0.20	1.23 ± 0.16	1.21 ± 0.33	3.02 ± 1.58	1.0000	1.0000	1.0000	1.0000	0.01959
Isoleucine	1.20 ± 0.27	1.27 ± 0.16	0.16 ± 0.02	0.77 ± 0.11	0.58 ± 0.08	0.59820	0.08867	0.00592	0.03256	0.02620
Leucine	1.05 ± 0.18	1.43 ± 0.14	0.24 ± 0.03	0.74 ± 0.09	0.56 ± 0.06	0.52612	0.00081	0.00112	0.02867	0.01326
Lysine	0.19 ± 0.06	0.42 ± 0.09	0.08 ± 0.02	0.21 ± 0.04	0.17 ± 0.05	0.015791	0.0728393	0.015791	0.0191952	0.0237982
Methionine	2.53 ± 0.35	0.31 ± 0.03	0.12 ± 0.01	0.26 ± 0.03	0.47 ± 0.05	0.00632	2.4E-07	0.00112	0.00012	6.7E-05
N,N-Dimethylglycine	1.02 ± 0.12	0.73 ± 0.08	1.38 ± 0.17	2.23 ± 0.28	1.29 ± 0.15	0.33716	0.01810	0.03253	0.00019	0.01326
N-Acetyl-glutamate	6.77 ± 0.41	0.78 ± 0.06		0.87 ± 0.07	1.08 ± 0.12	6.3E-14	0.29151		1.0000	0.91107
O-Acetyl-serine	18.6 ± 4.4	11.8 ± 3.9	0.91 ± 0.38	3.08 ± 0.67	11.5 ± 3.9	0.00015	0.00751	0.5844601	0.1700449	0.01326

S8: Intracellularly detected metabolites of *P. inhibens* DSM 17395 in the experiment "carbohydrate degradation". (Continued)

Metabolites	Fold change in metabolite abundance as compared to succinate grown cells					p-Values for abundance changes				
	NAG	MTL	SUCR	GLC	XYL	NAG	MTL	SUCR	GLC	XYL
Phenylalanine	0.91 ± 0.08	0.35 ± 0.03	0.13 ± 0.01	0.24 ± 0.03	0.37 ± 0.03	0.26021	0.00011	0.00112	0.00012	0.00018
Proline	0.57 ± 0.06	0.39 ± 0.04	0.06 ± 0.01	0.13 ± 0.02	0.27 ± 0.03	0.00125	0.00105	0.00112	0.00026	0.00119
Pyroglutamate	0.64 ± 0.11	0.91 ± 0.12	0.55 ± 0.07	0.70 ± 0.10	0.70 ± 0.12	1.0000	1.0000	0.02669	0.15101	1.0000
Serine	1.15 ± 0.15	0.41 ± 0.05	0.25 ± 0.03	0.33 ± 0.04	0.42 ± 0.05	0.84682	0.00027	0.00112	0.00012	0.00033
Threonine	1.17 ± 0.18	1.01 ± 0.10	0.31 ± 0.03	0.42 ± 0.06	0.74 ± 0.08	0.36543	0.90807	0.00112	0.00014	0.09520
Tyrosine	0.93 ± 0.07	0.72 ± 0.10	0.17 ± 0.03	0.43 ± 0.05	0.48 ± 0.10	0.5237063	0.0761095	0.015791	0.0191952	0.0213179
Valine	1.99 ± 0.30	1.64 ± 0.20	0.54 ± 0.07	0.62 ± 0.08	0.66 ± 0.08	0.01358	0.00011	0.09908	0.03256	0.05237
Organic acids										
2-Aminoadipate	0.36 ± 0.11	1.36 ± 0.36	0.08 ± 0.06	0.29 ± 0.11	0.71 ± 0.23	0.1275492	0.2965681	0.0181589	0.0951313	0.6709364
Benzoate	1.35 ± 0.22	1.74 ± 0.22	1.45 ± 0.19	1.76 ± 0.27	1.91 ± 0.26	0.14508	0.00093	0.01181	0.00513	0.00119
Erythronate	8.23 ± 0.88	2.70 ± 0.28	1.61 ± 0.21	2.90 ± 0.35	1.91 ± 0.24	0.00015	0.00011	0.03253	0.00014	0.00096
Glycerate	0.99 ± 0.07	1.98 ± 0.12	1.86 ± 0.11	2.21 ± 0.18	1.34 ± 0.07	0.84682	6.9E-08	4.1E-07	0.00097	0.00024
Glyoxylate	1.72 ± 0.05	1.31 ± 0.17	2.20 ± 0.30	5.33 ± 0.57	3.03 ± 0.31	0.0280729	0.2965681	0.0210547	0.0191952	0.0304541
2-Hydroxyglutarate	2.03 ± 0.26	0.44 ± 0.06	0.29 ± 0.04	0.19 ± 0.03	0.63 ± 0.08	0.00015	0.01175	0.00046	0.00190	0.43082
Iminodiacetate	31.1 ± 5.9	1.90 ± 0.36	0.77 ± 0.15	5.64 ± 1.17	2.13 ± 0.41	0.00015	0.00128	0.47815	0.00012	0.00044
Lactate	1.30 ± 0.32	0.33 ± 0.07	0.51 ± 0.13	0.42 ± 0.13	0.30 ± 0.07	0.96233	0.00030	0.09908	0.00793	0.00052
Maleate	2.53 ± 0.23	0.64 ± 0.22	0.42 ± 0.08	0.69 ± 0.25	0.52 ± 0.10	0.015791	0.3826504	0.015791	0.1700449	0.0213179
Malonate	x	x	x	x	x					
2-Methyl-malate	4.02 ± 0.26	2.59 ± 0.16	2.29 ± 0.15	4.20 ± 0.40	2.88 ± 0.20	7.4E-13	0.00011	4.3E-09	0.00014	0.00018
2-Methyl-serine	1.83 ± 0.13	2.81 ± 0.13	3.29 ± 0.17	1.27 ± 0.09	0.91 ± 0.06	2.7E-05	3.2E-14	1.5E-12	0.00145	1.0000
Nicotinamide	0.91 ± 0.53	1.03 ± 0.58	0.72 ± 0.38	0.86 ± 0.49	0.85 ± 0.45	0.8689045	1.0000	0.647778	1.00000	0.7382145
Nicotinate	0.39 ± 0.05	0.71 ± 0.10	0.58 ± 0.07	0.66 ± 0.06	0.42 ± 0.06	0.00033	0.03256	0.01384	0.00816	0.00063
Phenylacetate	0.39 ± 0.03	0.79 ± 0.08	0.88 ± 0.09	0.81 ± 0.08	0.59 ± 0.05	2.1E-06	1.0000	1.0000	1.0000	0.00052
Succinate-methylester	0.96 ± 0.11	1.34 ± 0.10	1.04 ± 0.09	1.29 ± 0.12	1.05 ± 0.09	1.0000	0.02100	1.0000	0.49383	1.0000
Tartrate	0.68 ± 0.15	1.59 ± 0.40	10.8 ± 2.2	169 ± 37	3.06 ± 0.68	0.42638	0.01058	0.00112	0.00012	0.00044
Threonate	2.59 ± 0.72	4.20 ± 0.77	29.6 ± 5.5	13.1 ± 2.6	2.64 ± 0.54	0.00151	0.00011	0.00112	0.00012	0.00104
Urea	0.98 ± 0.18	0.80 ± 0.34	0.26 ± 0.07	0.69 ± 0.18	0.27 ± 0.05	0.71081	0.48175	0.08503	0.26832	0.05264
Lipid and phospholipid headgroup components										
Ethanolamine	0.41 ± 0.05	0.23 ± 0.02	0.12 ± 0.02	0.19 ± 0.03	0.18 ± 0.02	0.00020	0.00011	0.00112	0.00012	0.00018
Ethanolaminephosphate	1.01 ± 0.17	0.09 ± 0.09	0.23 ± 0.04	0.36 ± 0.06	0.36 ± 0.05	0.9168149	0.2616974	0.0210547	0.0191952	0.0526444
Diethanolamine	6.30 ± 1.16	8.24 ± 1.30	2.19 ± 0.51	5.14 ± 0.82	7.85 ± 1.28	0.00015	0.00011	0.01717	0.00012	0.00018
Glycerol-3-phosphate	0.18 ± 0.02	0.11 ± 0.01	0.05 ± 0	0.12 ± 0.02	0.07 ± 0.01	0.00015	0.00011	0.00170	0.00012	0.00018
Glycerophosphoglycerol	0.05 ± 0.04	0.03 ± 0.02	0.09 ± 0.06	0.89 ± 0.52	0.07 ± 0.04	0.6104239	0.580338	0.824878	0.7760652	0.7963619
Octanoate ($C_{8:0}$)	0.67 ± 0.07	0.29 ± 0.03	0.27 ± 0.03	0.31 ± 0.03	0.25 ± 0.03	0.00361	0.00011	0.00112	0.00012	0.00018
3-Hydroxydecanoate ($C_{10:0,\ 3\text{-}OH}$)	0.57 ± 0.04	0.60 ± 0.06	0.67 ± 0.08	0.63 ± 0.05	0.52 ± 0.06	0.00013	0.00105	0.10814	0.00019	0.00044

S8: Intracellularly detected metabolites of *P. inhibens* DSM 17395 in the experiment "carbohydrate degradation". (Continued)

Metabolites	Fold change in metabolite abundance as compared to succinate grown cells					p-Values for abundance changes				
	NAG	MTL	SUCR	GLC	XYL	NAG	MTL	SUCR	GLC	XYL
Dodecanoate ($C_{12:0}$)	0.59 ± 0.05	1.13 ± 0.09	1.52 ± 0.16	1.52 ± 0.13	0.95 ± 0.09	0.00240	1.0000	0.06992	0.00217	0.59502
Dodecanol	0.44 ± 0.10	13.6 ± 3.7	11.5 ± 3.3	5.63 ± 2.31	4.75 ± 2.13	0.07662	0.00276	0.00842	0.07126	0.37877
Tetradecanoate ($C_{14:0}$)	0.36 ± 0.06	0.44 ± 0.08	0.25 ± 0.04	0.28 ± 0.05	0.41 ± 0.08	0.04895	0.01203	0.00828	0.00066	0.00615
Tetradecanol	0.79 ± 0.03	1.84 ± 0.12	1.69 ± 0.10	1.61 ± 0.12	1.28 ± 0.13	0.00039	0.00011	0.00112	0.00056	0.04024
Hexadecanoate ($C_{16:0}$)	0.71 ± 0.05	1.02 ± 0.08	0.83 ± 0.08	0.96 ± 0.10	1.12 ± 0.32	0.02643	1.0000	1.0000	1.0000	0.34395
Octadecanoate ($C_{18:0}$)	0.51 ± 0.08	1.11 ± 0.11	1.11 ± 0.13	0.80 ± 0.17	0.93 ± 0.16	0.00059	0.25355	0.41893	0.78527	0.46466
Octadecenoate ($C_{18:1}$)	0.29 ± 0.13	0.22 ± 0.08	0.80 ± 0.26	0.47 ± 0.15	0.20 ± 0.10	0.1563382	0.2186292	0.5844601	0.3770686	0.0720765
Butanoates										
2-Aminobutanoate	0.42 ± 0.06	0.16 ± 0.02	0.12 ± 0.02	0.19 ± 0.04	0.19 ± 0.05	0.00024	0.00011	0.00112	0.00012	0.00024
4-Aminobutanoate	0.81 ± 0.05	0.55 ± 0.04	0.21 ± 0.01	0.19 ± 0.01	0.46 ± 0.03	0.13779	2.3E-06	6.2E-13	0.00012	6.6E-09
3-Aminoisobutanoate	3.03 ± 0.16	0.29 ± 0.02	0.09 ± 0.01	0.20 ± 0.02	0.50 ± 0.04	0.00015	0.00011	0.00328	0.00012	0.00030
2-Hydroxybutanoate	0.82 ± 0.06	1.25 ± 0.10	1.16 ± 0.10	1.29 ± 0.11	1.06 ± 0.09	1.0000	0.75550	1.0000	0.52215	1.0000
3-Hydroxybutanoate	0.19 ± 0.03	0.29 ± 0.03	0.34 ± 0.04	0.29 ± 0.03	0.18 ± 0.02	4.4E-07	3.0E-06	1.2E-05	3.7E-06	2.1E-07
4-Oxobutanoate	0.80 ± 0.11	0.51 ± 0.05	0.36 ± 0.04	0.48 ± 0.05	0.59 ± 0.07	0.11677	0.00118	1.4E-05	0.00047	0.02187
Diamines and dipeptides										
Cadaverine	0.93 ± 0.15	1.17 ± 0.18	0.73 ± 0.12	1.36 ± 0.33	1.06 ± 0.18	0.6641592	0.51537	0.428487	0.2683235	0.9063486
Glycyl-glycine	0.92 ± 0.08	0.46 ± 0.07	0.06 ± 0.02	0.18 ± 0.03	0.71 ± 0.11	0.04389	0.00081	0.00170	0.00039	0.01010
Putrescine	0.99 ± 0.12	0.52 ± 0.07	0.12 ± 0.04	0.13 ± 0.02	0.53 ± 0.08	1.0000	0.01169	0.13538	2.1E-06	0.02843
Nucleosides and nucleobases										
Cytosine	0.35 ± 0.05	0.30 ± 0.07	0.06 ± 0.01	0.05 ± 0.01	0.33 ± 0.07	0.00105	0.00055	0.00016	0.00045	0.00595
Thymine	1.20 ± 0.06	0.94 ± 0.10	0.16 ± 0.03	0.22 ± 0.07	0.99 ± 0.09	0.14012	0.82479	5.2E-06	8.5E-06	1.0000
Uracil	0.66 ± 0.10	0.74 ± 0.12	0.66 ± 0.07	0.31 ± 0.06	0.55 ± 0.09	0.015791	0.2616974	0.0850328	0.0191952	0.0213179
Uridine	0.28 ± 0.26	2.11 ± 2.11	1.03 ± 1.03	0.27 ± 0.25	18.3 ± 16.8	0.3349823	0.2186292	0.8681263	0.3021725	0.0213179
Others										
Borate	0.67 ± 0.09	0.54 ± 0.11	2.18 ± 0.19	7.71 ± 0.90	1.75 ± 0.13	0.00497	0.00188	0.00112	0.00012	1.0E-06
Carbodiimide	0.69 ± 0.06	1.20 ± 0.06	0.85 ± 0.07	0.84 ± 0.10	0.90 ± 0.07	0.00361	0.00081	0.11588	0.11228	0.24743
Hydrogen sulfide	0.78 ± 0.06	0.82 ± 0.04	0.80 ± 0.05	0.51 ± 0.04	0.84 ± 0.05	0.01585	0.00105	0.01384	0.00012	0.01982
Phosphate	0.79 ± 0.11	0.88 ± 0.10	0.67 ± 0.09	0.69 ± 0.09	0.81 ± 0.10	0.05626	0.09832	0.13538	0.04120	0.08474
Phosphate monomethyl ester	0.88 ± 0.09	1.29 ± 0.12	1.36 ± 0.13	1.34 ± 0.11	1.11 ± 0.11	1.00000	0.01369	0.37782	0.10349	1.0000
Toluate	0.94 ± 0.12	1.41 ± 0.15	1.30 ± 0.15	1.41 ± 0.19	1.42 ± 0.15	0.74436	0.01576	0.03955	0.02152	0.01186

S8: Intracellularly detected metabolites of *P. inhibens* DSM 17395 in the experiment "carbohydrate degradation". (Continued)

Metabolites	Fold change in metabolite abundance as compared to succinate grown cells					p-Values for abundance changes				
	NAG	MTL	SUCR	GLC	XYL	NAG	MTL	SUCR	GLC	XYL
Unidentified compounds										
Unknown#1252.3-pin-mhe_006	1.16 ± 0.107	0.70 ± 0.053	0.36 ± 0.031	0.58 ± 0.049	0.71 ± 0.056	1.0000	0.00268	4.9E-07	0.00068	0.04914
Unknown#1361.3-pin-mhe_010	1.81 ± 0.208	0.94 ± 0.071	0.58 ± 0.043	0.51 ± 0.043	1.59 ± 0.13	0.00256	1.0000	0.00020	3.2E-05	0.00168
Unknown#1366.9-pin-mhe_011	1.31 ± 0.10	1.05 ± 0.061	0.89 ± 0.059	0.84 ± 0.065	1.56 ± 0.109	0.00711	0.18596	0.30950	0.04120	0.00040
Unknown#1651.8-pin-mhe_032	0.77 ± 0.782	2.67 ± 3.12	1.15 ± 1.183	7.47 ± 7.487	89.0 ± 89.1	0.26021	0.24252	1.00000	0.12714	0.13631
Unknown#1830.2-pin-mhe_038	0.59 ± 0.026	0.78 ± 0.035	0.34 ± 0.017	0.47 ± 0.029	0.58 ± 0.028	2.8E-08	0.00193	5.3E-13	1.0E-09	2.9E-08
Unknown#1856.7-pin-mhe_040	5.79 ± 5.789	3.49 ± 3.491	2.04 ± 2.055	9.85 ± 9.898	1.68 ± 1.68	0.14721	0.12714	0.16064	0.12714	0.15691
Unknown#1942.0-pin-mhe_022	x		x		x					
Unknown#1946.5-pin-mhe_024	x	x	x	XX	x					
Unknown#1955.0-pin-mhe_027	x	x	x	x	x					
Unknown#2135.2-pin-mhe_044	x		x		x					
Unknown#2139.6-pin-mhe_045		x	x	x						
Unknown#2477.7-pin-mhe_061					x					
Unknown#2545.5-pin-mhe_065					x					
Unknown#2836.5-pin-mhe_072		x								

Colour scale for fold changes:	n.det.	<0.1	<0.2	<0.4	<0.67	0.67 – 1.5	>1.5	>2.5	>5.0	>10.0

p-Value:	n.signif.	<0.05	<0.01	<0.001	<0.0001

underlined, p-value from t-test with Bonferoni Holms correction, otherwise from Wilcoxon-Mann-Whitney test with false discovery rate control

S9: Intracellularly detected metabolites in *P. inhibens* DSM 17395 during growth under ammonium limited conditions.
Symbols between sampling point represent significance of abundance changes; a legend is provided at the bottom of this table. Abbreviations: **x**, compound detected, but absent in reference condition, t_{30}; *, compound probably dephosphorylated during extraction; [1], Ornithine was improper detected and quantified; slightly higher abundant at beginning of cultivation, i.e. t_{15} and t_{20}.

Metabolites	Fold change in abundance as compared to reference condition (t_{30})								
	t_{15}	t_{20}	t_{25}	t_{30}	t_{40}	t_{50}	t_{60}	t_{75}	t_{90}
Amino acids and derivatives									
Alanine	3.34 ± 0.54	2.44 ± 0.44	1.10 ± 0.21	1	1.11 ± 0.23	0.92 ± 0.19	0.47 ± 0.17	0.02 ± 0.01	0.02 ± 0
Aspartate	5.78 ± 0.91	5.78 ± 0.79	0.55 ± 0.06	1	1.15 ± 0.14	1.65 ± 0.29	0.50 ± 0.15		
β-Alanine	3.35 ± 0.53	3.00 ± 0.34	1.57 ± 0.19	1	0.97 ± 0.10	0.44 ± 0.07	0.15 ± 0.05		
Glutamate	1.89 ± 0.20	1.84 ± 0.13	0.85 ± 0.09	1	1.21 ± 0.05	0.95 ± 0.08	0.33 ± 0.08	0.01 ± 0	0.00 ± 0
Glycine	1.63 ± 0.09	1.05 ± 0.06	1.32 ± 0.11	1	1.07 ± 0.07	0.37 ± 0.06	0.09 ± 0.03	0.00 ± 0	0.00 ± 0
Homoserine	1.70 ± 0.22	1.33 ± 0.14	0.91 ± 0.07	1	0.84 ± 0.06	0.94 ± 0.14	0.95 ± 0.09	1.25 ± 0.10	1.61 ± 0.15
Isoleucine	6.79 ± 1.35	9.81 ± 2.22	1.75 ± 0.42	1	1.39 ± 0.31	0.61 ± 0.11	0.02 ± 0.01	0.02 ± 0.01	0.06 ± 0.02
Leucine	14.8 ± 4.8	19.7 ± 7.2	3.50 ± 1.74	1	2.00 ± 1.09	0.74 ± 0.25	0.26 ± 0.10	0.91 ± 0.74	0.47 ± 0.15
Methionine	6.71 ± 0.77	3.96 ± 0.41	1.85 ± 0.20	1	1.46 ± 0.16	0.63 ± 0.10	0.52 ± 0.15		
N-Acetyl-glutamate	1.48 ± 0.47	1.63 ± 0.44	1.06 ± 0.21	1	1.43 ± 0.25	0.77 ± 0.18	0.38 ± 0.09		
N,N-Dimethylglycine	0.40 ± 0.06	0.44 ± 0.06	0.76 ± 0.11	1	1.38 ± 0.20	2.00 ± 0.28	0.63 ± 0.17	0.14 ± 0.04	
O-Acetyl-serine	14.3 ± 2.6	30.9 ± 3.2	1.67 ± 0.27	1	1.04 ± 0.09				
Ornithine [1]	x	x	x		x	x	x		
Phenylalanine	2.62 ± 0.48	2.05 ± 0.17	1.33 ± 0.12	1	4.36 ± 0.35	0.48 ± 0.04	0.07 ± 0.02		
Proline	3.28 ± 0.63	3.34 ± 0.76	1.26 ± 0.20	1	1.00 ± 0.25	0.53 ± 0.09	0.31 ± 0.07	0.02 ± 0	0.04 ± 0.01
Pyroglutamate	2.40 ± 0.29	2.14 ± 0.26	1.41 ± 0.15	1	1.08 ± 0.12	0.61 ± 0.10	0.25 ± 0.05	0.01 ± 0	0.01 ± 0
Serine	2.44 ± 0.53	2.35 ± 0.32	1.06 ± 0.19	1	1.47 ± 0.28	1.21 ± 0.17	0.39 ± 0.07	0.24 ± 0.14	
Threonine	3.76 ± 0.26	2.92 ± 0.19	1.27 ± 0.09	1	1.28 ± 0.09	0.61 ± 0.06	0.33 ± 0.07		
Valine	7.33 ± 0.76	4.37 ± 0.67	1.46 ± 0.12	1	0.86 ± 0.05	0.32 ± 0.02	0.13 ± 0.04	0.03 ± 0	0.06 ± 0
Diamines and dipeptides									
Glycyl-glycine	18.7 ± 2.3	10.8 ± 2.0	0.84 ± 0.17	1	3.17 ± 0.27	1.15 ± 0.24	0.20 ± 0.06		
Putrescine	11.4 ± 1.7	13.4 ± 1.0	1.61 ± 0.19	1	1.84 ± 0.11	0.58 ± 0.10	0.75 ± 0.18		
Sugars									
1,6-Anhydro-glucose	2.25 ± 0.24	1.98 ± 0.23	2.22 ± 0.31	1	1.06 ± 0.12	0.19 ± 0.03			0.61 ± 0.13
6-Deoxy-mannose	7.38 ± 0.38	11.4 ± 1.0	1.31 ± 0.08	1	1.51 ± 0.13	0.71 ± 0.05	0.68 ± 0.10	0.47 ± 0.03	0.74 ± 0.09
Arabinonate	0.63 ± 0.04	0.75 ± 0.04	1.60 ± 0.09	1	0.78 ± 0.04	0.33 ± 0.02	0.20 ± 0.01		
Erythrose/Threose	0.60 ± 0.12	0.70 ± 0.16	0.92 ± 0.21	1	0.88 ± 0.17	0.59 ± 0.12	0.53 ± 0.08	0.53 ± 0.10	0.66 ± 0.12
Galactarate	1.05 ± 0.26	2.19 ± 0.53	1.81 ± 0.27	1	0.96 ± 0.08	0.55 ± 0.09			
Gluconate *	0.41 ± 0.09	0.47 ± 0.11	1.53 ± 0.18	1	0.48 ± 0.03	0.20 ± 0.07	0.10 ± 0.04	0.01 ± 0	
Glucoheptonate-1,4-lactone	0.89 ± 0.06	0.91 ± 0.15	1.22 ± 0.09	1	0.98 ± 0.08	0.49 ± 0.08			

S9: Intracellularly detected metabolites in *P. inhibens* DSM 17395 during growth under ammonium limited conditions. (Continued)

Metabolites	Fold change in abundance as compared to reference condition (t_{30})								
	t_{15}	t_{20}	t_{25}	t_{30}	t_{40}	t_{50}	t_{60}	t_{75}	t_{90}
Gluconate-1,4-lactone	1.19 ± 0.40	0.64 ± 0.24	2.90 ± 0.90	1	0.50 ± 0.17	0.55 ± 0.17	1.40 ± 0.52	0.45 ± 0.17	0.24 ± 0.07
Glucuronate-3,6-lactone	1.68 ± 0.33	6.12 ± 1.56	2.03 ± 0.18	1	1.01 ± 0.08	0.08 ± 0.02	0.08		
N-Acetyl-glucosamine	1.74 ± 0.17	1.63 ± 0.19	2.65 ± 0.62	1	1.07 ± 0.08	0.75 ± 0.05			
Ribose/Xylose	1.02 ± 0.09	0.93 ± 0.08	1.00 ± 0.08	1	0.87 ± 0.06	0.80 ± 0.06	0.68 ± 0.05	0.54 ± 0.07	0.36 ± 0.06
Ribose/Xylose-5-phosphate	1.10 ± 0.26	0.64 ± 0.14	0.94 ± 0.17	1	0.94 ± 0.15	0.63 ± 0.29	0.45		
Entner-Doudoroff and Embden-Meyerhof-Parnas pathway									
Glucose	0.99 ± 0.06	0.88 ± 0.06	1.48 ± 0.12	1	0.56 ± 0.03	0.30 ± 0.02	0.20 ± 0.02	0.06 ± 0.01	0.04 ± 0
Hexose-6-phosphate		0.11 ± 0.04	0.74 ± 0.26	1	0.54 ± 0.18				
Glucono-1,5-lactone *	0.40 ± 0.08	0.37 ± 0.04	2.06 ± 0.30	1	0.26 ± 0.03	0.19 ± 0.02	0.18 ± 0.02	0.02 ± 0	
2-Keto-3-deoxy-gluconate (KDG) *	0.93 ± 0.10	0.52 ± 0.06	2.05 ± 0.17	1	1.44 ± 0.14	0.30 ± 0.05	0.16 ± 0.03		
Dihydroxyacetone phosphate	0.85 ± 0.15		1.08 ± 0.05	1	0.69 ± 0.04	0.41 ± 0.09			
1,3-Dihydroxyacetone *	1.02 ± 0.14	0.93 ± 0.15	1.52 ± 0.21	1	0.84 ± 0.11	0.65 ± 0.10	0.54 ± 0.07		
Fructose	0.88 ± 0.14	1.40 ± 0.15	1.49 ± 0.10	1	0.64 ± 0.14	0.35 ± 0.02	0.32 ± 0.03	0.12 ± 0.01	
Fructose-1-phosphate *		0.16 ± 0.06	0.76 ± 0.27	1	0.50 ± 0.16				
Fructose-6-phosphate		0.86	0.95 ± 0.12	1	0.55 ± 0.07				
3-Phosphoglycerate	0.29 ± 0.03	0.20 ± 0.03	0.71 ± 0.13	1	0.34 ± 0.03	0.53 ± 0.14	0.19 ± 0.09		
2-Phosphoglycerate	1.19 ± 0.13	0.99 ± 0.07	1.11 ± 0.09	1	0.82 ± 0.05	0.81 ± 0.09			
Phosphoenolpyruvate	1.50 ± 0.13	1.26 ± 0.09	1.32 ± 0.12	1	0.84 ± 0.05	0.62 ± 0.07			
Pyruvate	0.81 ± 0.15	0.39 ± 0.04	0.89 ± 0.13	1	0.94 ± 0.09	0.39 ± 0.07	0.14 ± 0.02	0.12 ± 0.02	0.18 ± 0.02
TCA cycle									
Citrate	0.90 ± 0.29	0.31 ± 0.10	0.93 ± 0.16	1	0.31 ± 0.05	0.43 ± 0.11	0.52 ± 0.18	0.41 ± 0.14	
2-Oxoglutarate	0.99 ± 0.13	0.68 ± 0.04	1.53 ± 0.10	1	1.35 ± 0.10	0.48 ± 0.05	0.31 ± 0.03		
Succinate	2.08 ± 0.27	2.41 ± 0.42	2.30 ± 0.39	1	1.43 ± 0.23	0.77 ± 0.14	0.29 ± 0.06	0.02 ± 0.01	0.09 ± 0.02
Fumarate	2.38 ± 0.35	2.36 ± 0.43	1.63 ± 0.22	1	1.43 ± 0.25	0.88 ± 0.14	0.30 ± 0.05	0.12 ± 0.02	0.14 ± 0.02
Malate	2.19 ± 0.28	1.28 ± 0.14	2.13 ± 0.20	1	1.75 ± 0.21	0.47 ± 0.06	0.12 ± 0.02		
Butanoates									
3-Aminoisobutanoate	4.20 ± 0.53	4.73 ± 0.46	1.49 ± 0.16	1	0.83 ± 0.09	0.54 ± 0.06	0.43 ± 0.08		
4-Aminobutanoate	9.28 ± 1.82	7.23 ± 0.99	1.37 ± 0.20	1	1.23 ± 0.17				
2-Hydroxybutanoate	1.39 ± 0.12	1.17 ± 0.07	1.09 ± 0.11	1	0.95 ± 0.07	0.82 ± 0.10	0.70 ± 0.07	0.80 ± 0.10	1.03 ± 0.10
3-Hydroxybutanoate	0.16 ± 0.02	0.18 ± 0.03	0.89 ± 0.08	1	1.08 ± 0.10	3.06 ± 0.31	3.77 ± 0.41	0.12 ± 0.02	0.07 ± 0.01
4-Oxobutanoate	1.43 ± 0.20	1.29 ± 0.17	1.18 ± 0.16	1	0.99 ± 0.14	0.68 ± 0.09	0.51 ± 0.08		
Lipid and phosphoplipid headgroup components									
Diethanolamine	5.50 ± 1.40	6.77 ± 1.14	1.70 ± 0.29	1	1.12 ± 0.16	0.99 ± 0.16	0.61 ± 0.15		

S9: Intracellularly detected metabolites in *P. inhibens* DSM 17395 during growth under ammonium limited conditions. (Continued)

Metabolites	Fold change in abundance as compared to reference condition (t_{30})								
	t_{15}	t_{20}	t_{25}	t_{30}	t_{40}	t_{50}	t_{60}	t_{75}	t_{90}
Ethanolamine	1.31 ± 0.15	0.76 ± 0.09	0.81 ± 0.22	1	0.74 ± 0.09	0.70 ± 0.11	0.39 ± 0.08	0.05 ± 0.01	0.07 ± 0.02
Glycerol-3-phosphate	0.65 ± 0.08	0.21 ± 0.02	0.81 ± 0.07	1	0.69 ± 0.06	0.38 ± 0.04	0.11 ± 0.02		
Glycerophosphoglycerol	0.35 ± 0.16	0.16 ± 0.04	0.39 ± 0.09	1	1.30 ± 0.28	0.82 ± 0.43			
Octanoate ($C_{8:0}$)	1.04 ± 0.34	0.53 ± 0.19	0.69 ± 0.24	1	0.58 ± 0.20	0.71 ± 0.23	0.74 ± 0.25	0.70 ± 0.24	0.83 ± 0.30
3-Hydroxydecanoate ($C_{10:0,\ 3\text{-}OH}$)	1.22 ± 0.15	0.86 ± 0.12	0.93 ± 0.14	1	0.82 ± 0.11	0.84 ± 0.15	0.65 ± 0.12	0.46 ± 0.07	0.56 ± 0.09
Dodecanoate ($C_{12:0}$)	1.33 ± 0.17	1.08 ± 0.16	1.01 ± 0.14	1	1.10 ± 0.28	0.97 ± 0.13	1.00 ± 0.14	1.07 ± 0.14	1.45 ± 0.18
Tetradecanoate ($C_{14:0}$)	1.34 ± 0.12	1.39 ± 0.12	1.29 ± 0.16	1	1.07 ± 0.20	0.71 ± 0.10	0.71 ± 0.08	0.63 ± 0.08	1.02 ± 0.07
Hexadecanoate ($C_{16:0}$)	1.30 ± 0.27	1.62 ± 0.33	1.48 ± 0.37	1	1.04 ± 0.22	0.54 ± 0.21	0.66 ± 0.24	0.74 ± 0.14	1.31 ± 0.26
Octadecanoate ($C_{18:0}$)	0.87 ± 0.20	1.00 ± 0.20	1.30 ± 0.31	1	1.03 ± 0.16	0.50 ± 0.28	0.39 ± 0.16	0.53 ± 0.11	1.13 ± 0.30
Octadecenoate ($C_{18:1}$)	1.27 ± 0.21	0.95 ± 0.20	1.00 ± 0.20	1	0.72 ± 0.12	0.75 ± 0.16	0.71 ± 0.18		
Nucleosides and nucleobases									
Cytosine	17.2 ± 5.8	12.8 ± 6.0	0.92 ± 0.18	1	1.29 ± 0.25	13.3 ± 5.9			
Thymine	3.57 ± 0.90	4.45 ± 1.15	1.33 ± 0.33	1	1.17 ± 0.33	0.73 ± 0.23	0.24 ± 0.06		
Uracil	3.67 ± 1.22	3.23 ± 1.15	1.09 ± 0.38	1	1.02 ± 0.39	0.55 ± 0.25	0.28 ± 0.11	0.37	
Organic acids									
5-Aminopentanoate	1.61 ± 0.20	1.54 ± 0.20	0.76 ± 0.09	1	3.38 ± 0.42	1.31 ± 0.21	0.98 ± 0.35		
Benzoate	1.24 ± 0.25	1.03 ± 0.21	1.22 ± 0.26	1	0.85 ± 0.16	0.97 ± 0.17	0.61 ± 0.11	0.75 ± 0.12	0.94 ± 0.14
Erythronate	1.02 ± 0.10	1.35 ± 0.15	1.40 ± 0.12	1	0.62 ± 0.05	0.38 ± 0.04	0.13 ± 0.01		
Glycerate	0.66 ± 0.10	0.61 ± 0.10	0.70 ± 0.11	1	0.52 ± 0.07	2.01 ± 0.38	2.51 ± 0.54	0.34 ± 0.04	0.48 ± 0.07
2-Hydroxyglutarate	0.66 ± 0.08	0.45 ± 0.04	1.50 ± 0.17	1	1.41 ± 0.14	0.38 ± 0.05	0.33 ± 0.08		
Iminodiacetate	4.30 ± 0.73	2.03 ± 1.12	2.67 ± 0.30	1	0.40 ± 0.04	0.21 ± 0.03	0.06		
Lactate	0.89 ± 0.22	0.63 ± 0.15	1.00 ± 0.31	1	1.15 ± 0.35	0.41 ± 0.13	0.50 ± 0.21	0.33 ± 0.10	0.47 ± 0.10
Malonate	1.07 ± 0.18	1.32 ± 0.20	1.24 ± 0.20	1	1.12 ± 0.19	0.73 ± 0.11	0.60 ± 0.09	0.76 ± 0.10	0.96 ± 0.13
2-Methyl-malate	0.89 ± 0.11	0.88 ± 0.12	0.75 ± 0.09	1	0.81 ± 0.10	0.57 ± 0.07	0.30 ± 0.03	0.21 ± 0.03	
2-Methyl-serine	1.09 ± 0.11	1.02 ± 0.11	1.20 ± 0.13	1	0.97 ± 0.14	1.19 ± 0.15	1.19 ± 0.21		
Nicotinamide	2.52 ± 0.86	2.59 ± 0.90	0.77 ± 0.10	1	0.63 ± 0.09	2.18 ± 0.70	1.36 ± 0.42		
Nicotinate	1.39 ± 0.13	1.39 ± 0.18	1.13 ± 0.15	1	5.60 ± 0.81	2.84 ± 0.33	0.77 ± 0.11		
Succinate-methylester	2.07 ± 0.23	2.19 ± 0.34	1.27 ± 0.19	1	1.04 ± 0.17	1.07 ± 0.13	1.03 ± 0.13	1.31 ± 0.13	1.69 ± 0.17
Tartrate	4.05 ± 0.49	13.7 ± 1.3	4.61 ± 0.53	1	1.27 ± 0.10	0.17 ± 0.02	0.05 ± 0		
Threonate	2.76 ± 0.42	5.08 ± 0.55	1.82 ± 0.16	1	0.97 ± 0.08	0.30 ± 0.02			
Others									
Borate	0.73 ± 0.22	3.68 ± 0.56	1.30 ± 0.23	1	2.60 ± 0.41	0.66 ± 0.34	0.05 ± 0.03	0.16 ± 0.04	0.38 ± 0.09
Diphosphate	1.40 ± 0.64	1.27 ± 0.54	1.49 ± 0.51	1	1.25 ± 0.52	0.44 ± 0.18	0.19 ± 0.06	0.22 ± 0.06	0.34 ± 0.10
Phosphate	1.22 ± 0.26	0.91 ± 0.17	1.09 ± 0.29	1	0.93 ± 0.17	0.69 ± 0.21	0.41 ± 0.09	0.16 ± 0.04	0.24 ± 0.05

S9: Intracellularly detected metabolites in *P. inhibens* DSM 17395 during growth under ammonium limited conditions. (Continued)

Metabolites	Fold change in abundance as compared to reference condition (t_{30})								
	t_{15}	t_{20}	t_{25}	t_{30}	t_{40}	t_{50}	t_{60}	t_{75}	t_{90}
Phosphate monomethyl ester	1.35 ± 0.25	1.14 ± 0.24	1.02 ± 0.19	1	0.81 ± 0.14	0.78 ± 0.14	0.85 ± 0.19		
Propane-1,2-diol	1.95 ± 0.39	1.74 ± 0.24	1.11 ± 0.18	1	1.08 ± 0.20	0.98 ± 0.17	0.86 ± 0.14	1.00 ± 0.14	1.78 ± 0.28
Toluate	1.62 ± 0.13	1.63 ± 0.17	1.20 ± 0.12	1	0.93 ± 0.09	0.83 ± 0.08	0.48 ± 0.06	0.35 ± 0.06	0.57 ± 0.06
Unidentified compounds									
Unknown#1004.0-pin-mhe_001	2.26 ± 0.33	1.40 ± 0.10	0.86 ± 0.10	1	1.09 ± 0.11	1.18 ± 0.14	0.61 ± 0.15	0.11 ± 0.01	0.15 ± 0.02
Unknown#1018.14-ppu-cja_002	1.48 ± 0.13	1.49 ± 0.09	1.08 ± 0.09	1	0.94 ± 0.07	0.91 ± 0.08	0.77 ± 0.05	0.70 ± 0.09	1.25 ± 0.12
Unknown#1093.67-ypy-mse_001	1.53 ± 0.18	1.70 ± 0.24	0.95 ± 0.17	1	1.32 ± 0.29	0.71 ± 0.24	0.29 ± 0.08	0.17 ± 0.03	0.33 ± 0.04
Unknown#1226.1-pin-mhe_004	1.02 ± 0.22	1.36 ± 0.29	1.04 ± 0.24	1	0.81 ± 0.18	1.02 ± 0.20	0.69 ± 0.13	0.24 ± 0.05	0.17 ± 0.03
Unknown#1361.3-pin-mhe_010	0.81 ± 0.08	0.86 ± 0.08	0.69 ± 0.07	1	0.94 ± 0.10	0.57 ± 0.05	0.24 ± 0.03	0.08 ± 0.01	0.09 ± 0.01
Unknown#1366.9-pin-mhe_011	1.42 ± 0.23	1.32 ± 0.22	1.00 ± 0.15	1	1.05 ± 0.19	0.89 ± 0.12	0.70 ± 0.11	0.73 ± 0.10	0.88 ± 0.12
Unknown#1392.1-pin-mhe_012	0.81 ± 0.37	1.73 ± 1.19	1.45 ± 0.70	1	4.72 ± 2.53	4.83 ± 2.18	11.4 ± 6.1	11.9 ± 5.8	18.0 ± 8.7
Unknown#1394.5-dsh-skl_001	1.39 ± 0.12	1.30 ± 0.09	1.16 ± 0.10	1	0.98 ± 0.08	0.89 ± 0.08	0.96 ± 0.07	1.03 ± 0.19	1.39 ± 0.12
Unknown#1586.9-pae-bth_039	2.04 ± 0.48	2.15 ± 0.45	1.23 ± 0.25	1	2.84 ± 0.55	1.45 ± 0.26	0.51 ± 0.13	0.58 ± 0.11	1.86 ± 0.37
Unknown#1594.3-pin-mhe_030	1.66 ± 0.17	1.10 ± 0.09	0.99 ± 0.08	1	1.42 ± 0.11	8.57 ± 0.69	12.9 ± 1.3	1.54 ± 0.24	1.68 ± 0.15
Unknown#1635.2-pin-mhe_031	1.34 ± 0.27	0.66 ± 0.17	1.41 ± 0.61	1	0.79 ± 0.19	0.74 ± 0.16	0.66 ± 0.16	0.59 ± 0.12	0.69 ± 0.18
Unknown#1651.8-pin-mhe_032	0.74 ± 0.08	3.84 ± 0.41	1.32 ± 0.13	1	1.78 ± 0.15	0.45 ± 0.03	0.27 ± 0.03		
Unknown#1811.9-pin-mhe_037	1.00 ± 0.67	0.86 ± 0.46	0.76 ± 0.36	1	1.59 ± 0.82	1.50 ± 0.75	2.90 ± 1.83	1.50 ± 0.77	2.36 ± 1.14
Unknown#1830.2-pin-mhe_038	1.62 ± 0.11	1.52 ± 0.09	1.26 ± 0.06	1	0.73 ± 0.03	0.56 ± 0.03	0.32 ± 0.02	0.25 ± 0.02	0.29 ± 0.06
Unknown#1836.1-pin-mhe_039	1.01 ± 0.31	2.79 ± 1.51	1.68 ± 0.71	1	6.23 ± 2.47	5.96 ± 2.10	12.0 ± 6.7	2.24 ± 1.43	6.12 ± 3.02
Unknown#1856.7-pin-mhe_040	0.91 ± 0.09	1.98 ± 0.15	1.52 ± 0.15	1	0.96 ± 0.06	0.37 ± 0.04	0.37 ± 0.03		
Unknown#1937.2-pin-mhe_021	1.74 ± 0.34	6.35 ± 1.77	1.99 ± 0.15	1	1.09 ± 0.08	0.19 ± 0.03			
Unknown#1944.9-pin-mhe_023	0.41 ± 0.08	0.64 ± 0.12	2.34 ± 0.54	1	0.31 ± 0.04	0.26 ± 0.04	0.18 ± 0.04		
Unknown#1954.3-pin-mhe_026	0.37 ± 0.08	0.42 ± 0.09	2.17 ± 0.42	1	0.27 ± 0.03	0.18 ± 0.03	0.14 ± 0.03		
Unknown#2018.7-pin-mhe_028	2.17 ± 1.38	2.62 ± 1.16	1.88 ± 0.83	1	1.05 ± 0.45	0.47 ± 0.29			
Unknown#2090.48-ypy-mse_021	1.09 ± 0.25	1.82 ± 0.31	1.22 ± 0.25	1	1.60 ± 0.27	0.98 ± 0.36	0.57		
Unknown#2139.6-pin-mhe_045	1.20 ± 0.35	1.14 ± 0.35	1.13 ± 0.34	1	1.17 ± 0.30	1.55 ± 0.41	2.48 ± 0.62	3.05 ± 0.78	4.23 ± 1.07
Unknown#2269.25-ypy-mse_027	1.27 ± 0.64	1.00 ± 0.24	1.48 ± 0.26	1	1.22 ± 0.19	0.50 ± 0.10			

Colour scale for fold changes: < 0.1 | < 0.2 | < 0.4 | < 0.67 | 0.67 – 1.5 | > 1.5 | > 2.5 | > 5.0 | > 10.0

Significance of abundance changes between sampling points; corrected p-Values from t-test (●) or Wilcoxon-Mann-Whitney test (◆): <0.0001 | <0.001 | <0.01 | <0.05

S10: Selected enzymes and proteins of *P. inhibens* DSM 17395.
If not indicated otherwise, E-values were obtained from EnzymeDetector, based on Swiss-Prot sequences. Abbreviations: Acc.-No., protein accession number; M, presumably multifunctional enzyme; S, Swiss-Prot sequence used for protein blast; T, TrEMBL sequence used for protein blast.

Locus Tag	Gene name	EC number	Enzyme/protein function	E-value	
Glycerol-phospho-lipids degradation					
PGA1_c02710	*ugpB*		*sn* -glycerol-3-phosphate-binding periplasmic protein [precursor]		
PGA1_c02730	*ugpE*		*sn* -glycerol-3-phosphate transport system permease		
PGA1_c02740	*ugpC2*	3.6.3.20	glycerol-3- phosphate- transporting ATPase	6.00E-171	
PGA1_c05210	*ugpC1*	3.6.3.20	glycerol-3- phosphate- transporting ATPase	9.00E-071	
PGA1_c05220	*ugpC*		putative sn-glycerol-3-phosphate import ATP-binding protein		
PGA1_c08240	*glpD*	1.1.5.3	glycerol-3-phosphate dehydrogenase	7.00E-143	
Fatty acids degradation / Beta oxidation					
PGA1_c12020	*fadJ*	1.1.1.35	3-hydroxyacyl-CoA dehydrogenase	3.00E-123	M
PGA1_c12020	*fadJ*	4.2.1.17	enoyl-CoA hydratase	3.00E-123	M
PGA1_c12020	*fadJ*	5.1.2.3	3-hydroxybutyryl-CoA epimerase	3.00E-123	M
PGA1_c12030	*fadA1*	2.3.1.16	acetyl-CoA C-acyltransferase	1.00E-080	M
PGA1_c12030	*fadA1*	2.3.1.9	acetyl-CoA C-acetyltransferase	3.00E-076	M
PGA1_c16990	*fadB1*	4.2.1.17	putative enoyl-CoA hydratase	6.00E-097	
PGA1_c17340	*acdA1*	1.3.8.1	short-chain acyl-CoA dehydrogenase	4.00E-080	M
PGA1_c17340	*acdA1*	1.3.99.12	2-methyacyl-CoA dehydrogenase		M
PGA1_c22180	*fadD1*	6.2.1.30	long-chain-fatty- acid-CoA ligase	2.00E-069	
PGA1_c29100	*fadH*	1.3.1.34	2,4-dienoyl-CoA reductase (NADPH)	0	
Fatty acids biosynthesis					
PGA1_c04640	*fabI*	1.3.1.9	enoyl-[acyl-carrier-protein] reductase	5.00E-105	
PGA1_c04650	*fabB*	2.3.1.41	3-oxoacyl-[acyl-carrier-protein] synthase	0	
PGA1_c04660	*fabA*	5.3.3.14	trans-2-decenoyl- [acyl- carrier protein] isomerase	9.00E-075	M
PGA1_c04660	*fabA*	4.2.1.59	3-hydroxyacyl-[acyl- carrier- protein] dehydratase	9.00E-075	M
PGA1_c11240	*fabH*	2.3.1.41	3-oxoacyl-[acyl-carrier-protein] synthase	0	
PGA1_c12600	*accC*	6.3.4.14	biotin carboxylase	0	
PGA1_c12600	*accC*	6.4.1.2	biotin carboxylase (Acetyl-CoA carboxylase subunit A)		
PGA1_c12610	*accB*		biotin carboxyl carrier protein of acetyl-CoA carboxylase		
PGA1_c16810	*fabI*	1.3.1.9	enoyl-[acyl-carrier- protein] reductase (NADH)	1.00E-146	
PGA1_c17930	*fabG*	1.1.1.100	3-oxoacyl-[acyl- carrier- protein] reductase	4.00E-094	
PGA1_c17940	*fabD*	2.3.1.39	[acyl-carrier- protein] *S*-malonyltransferase	7.00E-102	
PGA1_c30540	*accA*	6.4.1.2	acetyl-coenzyme A carboxylase carboxyl transferase subunit α	0	
PGA1_c31690	*accD*	6.4.1.2	acetyl-coenzyme A carboxylase carboxyl transferase subunit β	0	
Quorum sensing					
PGA1_262p02120		2.7.13.3	histidine kinase	0	
PGA1_262p02260		2.7.13.3	histidine kinase	1.00E-096	
PGA1_c03880	*luxR / pgaR*		transcriptional activator protein (LuxR)		
PGA1_c03890	*luxI / pgaI*		acyl-homoserine lactone synthase (LuxI) (BlastP: *Vibrio fischeri* (strain ATCC 700601). Acc.-No.: P35328)	3.00E-010	S
Nucleotide metabolism					
PGA1_c06670	*carA*	6.3.5.5	carbamoyl-phosphate synthase (glutamine-hydrolysing)	0	
PGA1_c12940	*adk2*	2.7.4.3	adenylate kinase	8.00E-091	
PGA1_c23900	*pyrG*	6.3.4.2	CTP synthase	0	
PGA1_c24560	*carB*	6.3.5.5	carbamoyl-phosphate synthase (large chain)	0	
Polyhydroxybutanoate (PHB) – metabolism					
PGA1_c03390	*phaB*	1.1.1.36	acetoacetyl-CoA reductase	1.00E-124	
PGA1_c03400	*phaA*	2.3.1.9	acetyl-CoA acetyltransferase	0	
PGA1_c20910	*phaR*		PHA synthesis repressor protein		
PGA1_c20920	*phaP*		granule associated protein (phasin)		
PGA1_c20930	*phaC*	2.3.1.-	poly(3-hydroxyalkanoate) polymerase		
PGA1_c20940	*phaZ*	3.1.1.75	poly(3-hydroxybutanoate) depolymerase		
Amino acid biosynthesis					
Aspartate / asparagine					
PGA1_c20300		2.6.1.1	aspartate transaminase / aspartate aminotransferase	1.00E-071	
PGA1_c21250		2.6.1.1	aspartate transaminase / aspartate aminotransferase	0	

S10: Selected enzymes and proteins of *P. inhibens* DSM 17395. (Continued)

Locus Tag	Gene name	EC number	Enzyme/protein function	E-value	
Cysteine / glycine / serine					
PGA1_c11870	*glyA*	2.1.2.1	glycine hydroxymethyl transferase	0	M
PGA1_c13950	*cysK*	2.5.1.47	cysteine synthase	1.00E-106	
PGA1_c17600		2.3.1.30	serine *O*-acetyltransferase	6.00E-040	
PGA1_c17690	*cysE*	2.3.1.30	serine *O*-acetyltransferase	3.00E-095	
PGA1_c36150	*serC*	2.6.1.52	phosphoserine aminotransferase	8.00E-163	
PGA1_c36160	*serB*	3.1.3.3	phosphoserine phosphatase	1.00E-050	
Histidine					
PGA1_c09230		3.6.1.31	phosphoribosyl-ATP diphosphatase	2.00E-054	
PGA1_c09330	*hisB*	4.2.1.19	imidazoleglycerol- phosphate dehydratase	1.00E-131	
PGA1_c14400	*cfa*	3.5.4.19	phosphoribosyl-AMP cyclohydrolase	9.00E-072	
PGA1_c17230	*tktA*	2.2.1.1	transketolase	0	
PGA1_c17910		5.3.1.16	1-(5-phospho ribosyl)- 5-[(5- phosphoribosylamino) carboxamide isomerase]	2.00E-130	
PGA1_c25240	*hisC*	2.6.1.9	histidinol-phosphate transaminase	0	
PGA1_c29870		2.4.2.17	ATP phosphoribosyl transferase	4.00E-107	
PGA1_c31190	*hisD4*	1.1.1.23	histidinol dehydrogenase	0	
Leucine					
PGA1_c26470	*leuA*	2.3.3.13	2-isopropylmalate synthase	0	
Tryptophan					
PGA1_c04860	*trpF*	5.3.1.24	phosphoribosyl anthranilate isomerase	6.00E-099	
PGA1_c04870	*trpB*	4.2.1.20	tryptophan synthase	0	
PGA1_c16860	*trpE*	4.1.3.27	anthranilate synthase	0	
PGA1_c16890	*trpD*	2.4.2.18	anthranilate phosphoribosyl transferase	0	
PGA1_c16910	*trpC*	4.1.1.48	indole-3-glycerol- phosphate synthase	9.00E-126	
Amino acid degradation					
Alanine / glycine / serine / threonine					
PGA1_78p00260	*lpdA2*	1.8.1.4	dihydrolipoyl dehydrogenase	1.00E-161	
PGA1_78p00280			putative sodium/alanine symporter		
PGA1_78p00290	*gcvT*	2.1.2.10	aminomethyl transferase	1.00E-105	
PGA1_78p00300	*gcvH2*		glycine cleavage system protein		
PGA1_78p00310	*gcvP*	1.4.4.2	glycine dehydrogenase (aminomethyl- transferring)	0	
PGA1_c04590		4.3.1.19	threonine ammonia-lyase	2.00E-046	
PGA1_c05560	*gcvH1*		glycine cleavage system protein		
PGA1_c07110			putative sodium/alanine symporter		
PGA1_c11870	*glyA*	2.1.2.1	glycine hydroxymethyl transferase	0	M
PGA1_c11870		4.1.2.48	low-specificity *L*-threonine aldolase	0	M
PGA1_c23770	*tdcG*	4.3.1.17	*L*-serine ammonia-lyase	6.00E-153	
PGA1_c25010		4.1.2.5	*L*-threonine aldolase (BlastP: *Candida albicans*. Acc.-No.: O13427)	3.00E-008	S
PGA1_c30420		1.4.1.1	alanine dehydrogenase	1.00E-139	
PGA1_c34320	*tdh*	1.1.1.103	threonine-3-dehydrogenase	0	
PGA1_c34330	*kbl*	2.3.1.29	glycine *C*-acetyltransferase / 2-amino-3-oxobutanoate_CoA ligase	2.00E-179	
PGA1_c34900	*ilva*	4.3.1.19	threonine ammonia-lyase / threonine dehydratase	3.00E-112	
Arginine / ornithine / proline / glutamate					
PGA1_c03800		4.1.1.17	ornithine decarboxylase	8.00E-048	
PGA1_c11650	*ldc*	4.1.1.17	lysine/ornithine decarboxylase	6.00E-039	
PGA1_c11750	*pitA*	1.5.5.2	proline dehydrogenase	0	M
PGA1_c11750	*pitA*	1.2.1.88	*L*-glutamate γ-semialdehyde dehydrogenase	0	M
PGA1_c14470	*speE*	2.5.1.16	spermidine synthase	1.00E-173	
PGA1_c16370	*arcA*	3.5.3.1	arginase	6.00E-124	
PGA1_c16390	*arcB*	4.3.1.12	ornithine cyclodeaminase	0	
Branched-chain amino acids (leucine, isoleucine, valine)					
PGA1_c06200	*scoB*	2.8.3.5	succinyl-CoA:3-oxoacid-CoA transferase, subunit B	6.00E-098	
PGA1_c06210	*scoA*	2.8.3.5	succinyl-CoA:3-oxoacid-CoA transferase, subunit A	1.00E-102	
PGA1_c10280	*ivd*	1.3.8.4	isopentanoyl-CoA dehydrogenase	3.00E-165	
PGA1_c10340	*mvaB*	4.1.3.4	hydroxymethylglutaryl-CoA lyase	3.00E-100	
PGA1_c10360	*mgh*	4.2.1.18	methylglutaconyl-CoA hydratase	2.00E-018	
PGA1_c11320		1.1.1.178	3-hydroxy-2- methylbutyryl-CoA dehydrogenase	3.00E-090	M

S10: Selected enzymes and proteins of *P. inhibens* DSM 17395. (Continued)

Locus Tag	Gene name	EC number	Enzyme/protein function	E-value	
PGA1_c12020	*fadJ*	1.1.1.35	fatty acid oxidation complex, α subunit	3.00E-123	M
PGA1_c12020	*fadJ*	4.2.1.17	fatty acid oxidation complex, α subunit	3.00E-123	M
PGA1_c17080		1.2.7.8	indolepyruvate ferredoxin oxidoreductase	1.00E-018	
PGA1_c17300	*mmsA*	1.2.1.18	malonate-semialdehyde dehydrogenase (acetylating)	3.00E-144	
PGA1_c17300	*mmsA*	1.2.1.27	methylmalonate-semialdehyde dehydrogenase	3.00E-151	
PGA1_c17340	*acdA1*	1.3.99.12	2-methyacyl-CoA dehydrogenase		
PGA1_c17350	*hibch*	3.1.2.4	3-Hydroxyisobutanoyl-CoA hydrolase	2.00E-064	
PGA1_c17360	*mmsB*	1.1.1.31	3-Hydroxyisobutanoate dehydrogenase	7.00E-079	
PGA1_c20500	*ldh*	1.4.1.9	leucine dehydrogenase	5.00E-103	
PGA1_c21510	*bhbA*	5.4.99.2	methylmalonyl-CoA mutase	0	
PGA1_c21540	*pccA*	6.4.1.3	propanonyl-CoA carboxylase, α subunit	0	
PGA1_c21600	*pccB*	6.4.1.3	propanonyl-CoA carboxylase, β subunit	0	
PGA1_c24490	*mce*	5.1.99.1	methylmalonyl-CoA epimerase	2.00E-052	
PGA1_c33180		2.3.1.9	acetyl-CoA acetyltransferase	3.00E-118	M
PGA1_c33180		2.3.1.16	acetyl-CoA C-acyltransferase	1.00E-083	M
PGA1_c34110	*ilvE*	2.6.1.42	branched-chain- amino-acid transaminase	6.00E-075	
PGA1_c34350	*phbA*	2.3.1.9	acetyl-CoA acetyltransferase	8.00E-160	M
PGA1_c34350		2.3.1.16	acetyl-CoA C-acyltransferase	8.00E-160	M
Various		1.2.1.3	aldehyde dehydrogenase (NAD+)		
Various		1.2.1.4	aldehyde dehydrogenase (NADP+)		
Histidine					
PGA1_c08740	*gluD*	1.4.1.3	glutamate dehydrogenase	6.00E-147	
PGA1_c36320	*hutU*	4.2.1.49	urocanate hydratase	0	
PGA1_c36330	*hutG*	3.5.1.68	*N*-Formylglutamate deformylase (BlastP: *Roseobacter denitrificans* Och 114. Acc.-No.: Q162E1)	4.00E-109	T
PGA1_c36340	*hutH*	4.3.1.3	histidine ammonia-lyase	0	
PGA1_c36350	*hutI*	3.5.2.7	imid azolonepropionase	0	
PGA1_c36360	*hutF*	3.5.3.13	formimino-glutamate deiminase *(BlastP: Pseudomonas fluorescens* BRIP34879. Acc.-No.: L7H3A0)	9.00E-128	T
?		1.14.13.-	oxygenase/hydroxylase		
Lysine					
PGA1_c03390	*phaB*	1.1.1.36	acetoacetyl-CoA reductase	1.00E-124	
PGA1_c03400	*phaA*	2.3.1.9	acetyl-CoA acetyltransferase	0	
PGA1_c09350		2.6.1.-	aminotransferase class-III		
PGA1_c11650	*ldc*	4.1.1.17	lysine/ornithine decarboxylase	6.00E-039	
PGA1_c12020	*fadJ*	1.1.1.35	Fatty acid oxidation complex, α subunit	3.00E-123	M
PGA1_c12020	*fadJ*	4.2.1.17	Fatty acid oxidation complex, α subunit	3.00E-123	M
PGA1_c15710	*gcdH*	1.3.8.6	glutaryl-CoA dehydrogenase	0	
PGA1_c27870		2.8.3.16	formyl-CoA transferase	2.00E-045	
PGA1_c27870		6.2.1.6	putative glutarate-CoA ligase (BlastP: *Renibacterium salmoninarum* ATCC 33209. Acc.-No.: YP_001623353)	6.00E-023	T
PGA1_c33040		1.2.1.-	aldehyde dehydrogenase	4.00E-144	
PGA1_c33640		1.2.4.4	3-methyl-2-oxobutanoate dehydrogenase (2-methylpropanoyl-transferring)	9.00E-041	
PGA1_c34400		2.6.1.-	aminotransferase class-III	3.00E-116	
PGA1_c36500	*fadJ / paaG*	4.2.1.17	enoyl-CoA hydtratase/reductase	4.00E-108	
PGA1_c36500		4.2.1.55	enoyl-CoA hydratase/isomerase		
Methionine					
PGA1_c16600	*mdeA*	4.4.1.11	methionine γ-lyase (BlastP: *Pseudomonas putida* .Acc.-No.: P13254)	0	
PGA1_c21510	*bhbA*	5.4.99.2	methylmalonyl-CoA mutase	0	
PGA1_c21540	*pccA*	6.4.1.3	propanonyl-CoA carboxylase, α subunit	0	
PGA1_c21600	*pccB*	6.4.1.3	propanonyl-CoA carboxylase, β subunit	0	
PGA1_c24490	*mce*	5.1.99.1	methylmalonyl-CoA epimerase	2.00E-052	
PGA1_c27800		1.4.3.16	*L*-aspartate oxidase	4.00E-161	
Phenylalanine					
PGA1_262p00800	*paaZ2*		Oxepin-CoA hydrolase	5.00E-110	M
PGA1_262p00800	*paaZ2*	1.17.1.7	3-oxo-5,6- dehydrosuberyl-CoA semialdehyde dehydrogenase	5.00E-110	M
PGA1_c01220		1.1.1.157	3-hydroxybutanoyl-CoA dehydrogenase	2.00E-146	M
PGA1_c01220 ?		1.1.1.35	3-hydroxyacyl-CoA dehydrogenase 3-hydroxyadipyl-CoA dehydrogenase		M
PGA1_c04040	*paaE*	1.14.13.149	ring 1,2- phenylacetyl-CoA epoxidase, subunit E (BlastP: *Escherichia coli* K12 – substrain MG1655. Acc.-No.: P76081)	9.00E-091	S

S10: Selected enzymes and proteins of *P. inhibens* DSM 17395. (Continued)

Locus Tag	Gene name	EC number	Enzyme/protein function	E-value	
PGA1_c04050	*paaD*	1.14.13.149	ring 1,2- phenylacetyl-CoA epoxidase, subunit D (BlastP: *Escherichia coli* SE11. Acc.-No.: YP_00229751)	1.00E-050	
PGA1_c04060	*paaC*	1.14.13.149	ring 1,2- phenylacetyl-CoA epoxidase, subunit C		
PGA1_c04070	*paaB*	1.14.13.149	ring 1,2- phenylacetyl-CoA epoxidase, subunit B (BlastP: *Escherichia coli* K12 –substrain MG1655. Acc.-No.: NP415907)	1.00E-039	S
PGA1_c04080	*paaA*	1.14.13.149	ring 1,2- phenylacetyl-CoA epoxidase, subunit A	3.00E-159	
PGA1_c04090	*paaJ*	2.3.1.223	3-oxo-5,6- didehydrosuberyl-CoA thiolase	0	
PGA1_c04090	*paaJ*	2.3.1.174	3-oxoadipyl-CoA thiolase	0	
PGA1_c04490	*iorAB*	1.2.7.8	indolepyruvate ferredoxin oxidoreductase	4.00E-017	
PGA1_c07610	*hpd*	1.13.11.27	4-hydroxyphenyl pyruvate dioxygenase	2.00E-117	
PGA1_c26800	*paaK1*	6.2.1.30	phenylacetate CoA ligase	0	
PGA1_c26810	*paaI*	3.1.2.-	thioesterase (3.1.2.-)		
PGA1_c26820	*paaG*	5.3.3.18	ring 1,2-epoxyphenylacetyl-CoA isomerase (oxepin-CoA forming) (BlastP: *Escherichia coli* K-12 – substrain MG1655. Acc.-No.: P77467)	2.00E-078	S
PGA1_c26830	*paaZ1*	3.3.2.12	oxepin-CoA hydrolase	0	M
PGA1_c26830	*paaZ1*	1.17.1.7	3-oxo-5,6- dehydrosuberyl-CoA semialdehyde dehydrogenase	0	M
PGA1_c29420	*tyrB*	2.6.1.57	aromatic amino acid aminotransferase	0	M
PGA1_c31390		4.1.1.28	aromatic-*L*- amino-acid decarboxylase	2.00E-104	M
PGA1_c31390		4.1.1.25	tyrosine decarboxylase	3.00E-109	M
PGA1_c36500	*fadJ / paaG*	4.2.1.17	enoyl-CoA hydtratase/reductase	4.00E-108	M
PGA1_c36500		4.2.1.55	enoyl-CoA hydratase/isomerase		M
Tryptophan					
PGA1_c09970	*kynA*	1.13.11.11	tryptophan 2,3-dioxygenase	7.00E-132	
PGA1_c09980	*kynU*	3.7.1.3	kynureninase	4.00E-134	
PGA1_c23440		6.2.1.32	2-aminobenzoate-CoA ligase (BlastP: *Azoarcus evansii*. Acc.-No.: AAL02077)	0	T
PGA1_c23450	*acdA2*	1.3.8.1	short-chain acyl-CoA dehydrogenase	5.00E-063	
PGA1_c23460			putative enoyl-CoA hydratase		
PGA1_c23480			3-hydroxyacyl-CoA dehydrogenase		
PGA1_c23490		1.14.13.40	2-aminobenzoyl-CoA monooxygenase/reductase (BlastP: *Azoarcus evansii*. Acc.-No.: AAL02063)	0	T
PGA1_c29640		3.5.1.9	Arylformamidase (BlastP: *Rhodobacter capsulatus* SB 1003. Acc.-No.: YP_003576584)	2.00E-078	T
Tyrosine					
PGA1_c00380		5.2.1.2	maleylacetoacetate isomerase	8.00E-071	
PGA1_c00430	*fah*	3.7.1.2	fumarylacetoacetase	1.00E-133	
PGA1_c00440	*hmgA*	1.13.11.5	homogentisate 1,2-dioxygenase	0	
PGA1_c07610	*hpd*	1.13.11.27	4-hydroxyphenylpyruvate dioxygenase	2.00E-117	
PGA1_c07610	*hpd*	1.13.11.27	4-hydroxyphenyl pyruvate dioxygenase	2.00E-117	
PGA1_c29420	*tyrB*	2.6.1.57	aromatic-amino-acid aminotransferase	0	M
PGA1_c29420	*tyrB*	2.6.1.5	tyrosine transaminase	9.00E-115	M
Glutamate metabolism / ammonium assimilation					
PGA1_c08740	*gluD*	1.4.1.3	glutamate dehydrogenase	6.00E-147	
PGA1_c18720	*glnA*	6.3.1.2	glutamine synthetase / glutamate-ammonia ligase	0	
PGA1_c36090	*gltD*	1.4.1.13	glutamate synthase (NADPH) small chain	0	
PGA1_c36100	*gtlB*	1.4.1.13	glutamate synthase (NADPH) large chain		M
PGA1_c36100	*gtlB*	2.6.1.16	glutamine-fructose-6-phosphate transaminase (isomerizing)		M
Urea cycle					
PGA1_c03450	*argH*	4.3.2.1	argininosuccinate lyase	0	
PGA1_c03450		2.3.1.1	amino-acid *N*-acetyltransferase	2.00E-128	
PGA1_c06670	*carA*	6.3.5.5	carbamoyl-phosphate synthase (glutamine- hydrolysing)	0	
PGA1_c16370	*arcA*	3.5.3.1	arginase	6.00E-124	
PGA1_c24220	*argF*	2.1.3.3	ornithine carbamoyltransferase	0	
PGA1_c24560	*carB*	6.3.5.5	carbamoyl-phosphate synthase large chain	0	
PGA1_c34920	*argG*	6.3.4.5	argininosuccinate synthase	0	
Carbohydrate degradation					
Transport					
PGA1_78p00530			putative Outer membrane protein		
PGA1_262p00430	*xylF*		xylose ABC transporter , periplasmic sugar-binding protein		
PGA1_262p00440	*xylH*		xylose ABC transporter , permease		

S10: Selected enzymes and proteins of *P. inhibens* DSM 17395. (Continued)

Locus Tag	Gene name	EC number	Enzyme/protein function	E-value	
PGA1_262p00450	*xylG*		xylose ABC transporter, ATP-binding protein		
PGA1_c07860	*aglE*		alpha-glucoside ABC transporter, periplasmic sugar-binding protein		
PGA1_c07870	*aglF*		alpha-glucoside ABC transporter, permease		
PGA1_c07880	*aglG*		alpha-glucoside ABC transporter, permease		
PGA1_c07900	*aglK*		alpha-glucoside ABC transporter, permease		
PGA1_c10290			outer membrane protein		
PGA1_c13180	*smoK*		mannitol ABC transporter, ATP-binding protein		
PGA1_c13190			mannitol ABC transporter, permease		
PGA1_c13200			mannitol ABC transporter, permease		
PGA1_c13210			mannitol ABC transporter, periplasmic sugar-binding protein		
PGA1_c25180			outer membrane protein-like protein		
PGA1_c27930			*N*-Acetylglucosamine ABC transporter, permease		
PGA1_c27940			*N*-Acetylglucosamine ABC transporter, permease		
PGA1_c27950			*N*-Acetylglucosamine ABC transporter, permease		
PGA1_c27970			*N*-Acetylglucosamine ABC transporter, ATP-binding protein		
Peripheral carbohydrate degradation					
PGA1_c05420	*glk*	2.7.1.2	glucokinase	9.00E-019	
PGA1_c07890	*aglA*	3.2.1.20	α-glucosidase		
PGA1_c12950	*acs*	6.2.1.1	Acetyl-coenzymeA synthetase	0	
PGA1_c13160	*mtlK*	1.1.1.67	mannitol 2-dehydrogenase	1.00E-166	
PGA1_c13170	*polS*	1.1.1.14	*L*-iditol 2-dehydrogenase / sorbitol dehydrogenase	2.00E-130	
PGA1_c14000	*xylA*	5.3.1.5	xylose isomerase	0	
PGA1_c14010	*xylB*	2.7.1.17	xylulose kinase	9.00E-133	
PGA1_c17230	*tktA*	2.2.1.1	transketolase	0	
PGA1_c27880	*nagA*	3.5.1.25	*N*-acetyl-glucosamine-6-phosphate deacetylase	2.00E-078	
PGA1_c27890	*nagB*	2.6.1.16	glutamine- fructose-6- phosphate transaminase (isomerizing)	4.00E-039	
PGA1_c27890	*nagB*	3.5.99.6	glucosamine-6-phosphate deaminase (BlastP: *Ruegeria sp.* TW15. Acc.-No.: WP_010439364)	3.00E-148	T
PGA1_c27910	*nagK*	2.7.1.59	*N*-acetylglucosamine kinase (BlastP: *Roseobacter denitrficans* Och 114. Acc.-No.: YP_682036)	2.00E-048	T
PGA1_c27980	*pgi*	5.3.1.9	glucose-6-phosphate isomerase / Phosphoglucose isomerase	0	
PGA1_c28020	*frk*	2.7.1.4	fruktokinase	2.00E-069	
Pentose phosphate pathway					
PGA1_c04170	*rpe*	5.1.3.1	ribulose-phosphate 3-epimerase	5.00E-135	
PGA1_c05780	*tal*	2.2.1.2	transaldolase	2.00E-146	
PGA1_c10730	*rpiB*	5.3.1.6	ribose-5-phosphate isomerase B	6.00E-039	
PGA1_c17230	*tktA*	2.2.1.1	transketolase	0	
PGA1_c23740	*rpiA*	5.3.1.6	ribose-5-phosphate isomerase A	1.00E-165	
Entner-Doudoroff pathway and Embden-Meyerhof Parnas pathway					
PGA1_c02770	*gpmI*	5.4.2.12	2,3-bisphosphoglycerate-independent phyosphoglycerate mutase	0	
PGA1_c06970	*pykA*	2.7.1.40	pyruvate kinase	1.00E-163	
PGA1_c11420	*eno*	4.2.1.11	phosphopyruvate hydratase	0	
PGA1_c15170	*pgl*	3.1.1.31	6-phosphogluconolactonase	2.00E-031	
PGA1_c17530	*pgk*	2.7.2.3	phosphoglycerate kinase	0	
PGA1_c27490	*gap*	1.2.1.12	glyceraldehyde-3-phosphate dehydrogenase	1.00E-155	
PGA1_c27990	*zwf2*	1.1.1.49	glucose-6-phosphate-1-dehydrogenase	0	
PGA1_c28000	*edd*	4.2.1.12	phosphogluconate dehydratase	0	
PGA1_c28010	*eda*	4.1.3.16	4-hydroxy-2- oxoglutarate aldolase	6.00E-061	M
PGA1_c28010	*eda*	4.1.2.14	2-dehydro-3-deoxy- phosphogluconate aldolase	6.00E-061	M
Pyruvate dehydrogenase complex					
PGA1_c17390	*lpdA1*	1.8.1.4	dihydrolipoyl dehydrogenase	0	
PGA1_c17550	*pdhA*	1.2.4.1	pyruvate dehydrogenase (acetyl- transferring) / pyruvate dehydrogenase, E1 α subunit	2.00E-159	
PGA1_c17560	*pdhB*	1.2.4.1	pyruvate dehydrogenase (acetyl- transferring) / pyruvate dehydrogenase, E1 β subunit	0	
PGA1_c17570	*pdhC*	2.3.1.12	dihydrolipoyllysine- residue acetyltransferase / pyruvate dehydrogenase, E2	2.00E-144	
TCA cycle					
PGA1_c03550	*lpd2*	1.8.1.4	dihydrolipoyl dehydrogenase	0	
PGA1_c03590	*sucA*	2.3.1.61	2-oxoglutarate dehydrogenase, E1 / dihydrolipoyllysine- residue succinyltransferase	1.00E-170	

S10: Selected enzymes and proteins of *P. inhibens* DSM 17395. (Continued)

Locus Tag	Gene name	EC number	Enzyme/protein function	E-value	
PGA1_c03600	*sucB*	1.2.4.2	2-oxoglutarate dehydrogenase, E2	0	
PGA1_c03610	*sucD*	6.2.1.5	succinyl-CoA ligase [ADP-forming], subunit α	5.00E-160	
PGA1_c03630	*sucC*	6.2.1.5	succinyl-CoA ligase [ADP-forming], subunit β	0	
PGA1_c03650	*mdh*	1.1.1.37	malate dehydrogenase	0	
PGA1_c03740	*sdhC*		succinate dehydrogenase, cytochrome b 556 subunit		
PGA1_c03750	*sdhD*		succinate dehydrogenase hydrophobic membrane		
PGA1_c03760	*sdhA*	1.3.5.1	succinate dehydrogenase, flavoprotein subunit	0	
PGA1_c03780	*sdhB*	1.3.5.1	succinate dehydrogenase, iron-sulfur subunit	5.00E-169	
PGA1_c13520	*fumC*	4.2.1.2	fumarate hydratase class II	0	
PGA1_c16970	*gltA1*	2.3.3.1	citrate synthase (BlastP: *Escherichia coli* K12. Acc.-No.: P0ABH7)	0	S
PGA1_c18830	*acnA*	4.2.1.3	aconitate hydratase	0	
PGA1_c28340	*Icd*	1.1.1.42	isocitrate dehydrogenase [NADP]	0	
Gluconeogenesis					
PGA1_c08640	*glpx*	3.1.3.11	fructose-1,6-bisphosphate class 2	1.00E-087	M
PGA1_c08640	*glpx*	3.1.3.37	sedoheptulose- bisphosphatase	4.00E-073	M
PGA1_c10230	*glmS*	2.6.1.16	glutamine- fructose-6- phosphate transaminase (isomerizing)	0	
PGA1_c17250	*gapB*	1.2.1.59	glyceraldehyde-3-phosphate dehydrogenase 2 (BlastP: *Bacillus subtilis* strain 168. Acc-No.: O34425)	1.00E-104	S
PGA1_c20650	*tpiA*	5.3.1.1	triosephosphate isomerase	9.00E-119	
PGA1_c23910	*fda*	4.1.2.13	fructose-bisphosphate aldolase class 1	5.00E-119	
Anaplerotic reactions					
PGA1_c01140	pckA	4.1.1.49	phosphoenolpyruvate carboxykinase (ATP)	0	
PGA1_c03650	mdh	1.1.1.37	malate dehydrogenase	0	
PGA1_c03650	mdh	1.1.1.82	malate dehydrogenase (NADP+)	2.00E-077	
PGA1_c09420	pyc	6.4.1.1	pyruvate carboxylase	0	
PGA1_c34990		1.1.1.40	malate dehydrogenase (oxaloacetate- decarboxylating) (NADP+)	0	
Ethylmalonyl-CoA pathway					
PGA1_c01110		1.3.8.-	putative 2-mehtylfumaryl-CoA dehydrogenase (BlastP: *Rhodobacter sphaeroides* 2.4.1. Acc.-No.: Q3J5V7)	0	T
PGA1_c03390	*phaB*	1.1.1.36	acetoacetyl-CoA reductase	1.00E-124	
PGA1_c03400	*phaA*	2.3.1.9	acetyl-CoA C-acetyltransferase	0	
PGA1_c03710	*mch*	4.2.1.148	2-methylfumaryl-CoA hydratase	0	
PGA1_c03870	*ccr*	1.3.1.86	crotonyl-CoA reductase	0	
PGA1_c09900	*glcB*	2.3.3.9	malate synthase	0	
PGA1_c21510	*bhbA*	5.4.99.2	methylmalonyl-CoA mutase	0	
PGA1_c21540	*pccA*	6.4.1.3	propanonyl-CoA carboxylase, α subunit	0	
PGA1_c21600	*pccB*	6.4.1.3	propanonyl-CoA carboxylase, β subunit	0	
PGA1_c24490	*mce*	5.1.99.1	methylmalonyl-CoA epimerase	2.00E-052	
PGA1_c30490	*mcl1*	4.1.3.24	β-methylmalyl-CoA lyase	0	
PGA1_c36500	*fadJ / paaG*	1.1.1.35	enoyl-CoA hydtratase/reductase		
PGA1_c36500	*fadJ / paaG*	4.2.1.17	enoyl-CoA hydtratase/reductase	4.00E-108	
?			putative 2-methylfumaryl-CoA mutase		
C_4-carboxylates					
PGA1_c13520	*fumC*	4.2.1.2	fumarate hydratase class II	0	
PGA1_c17990		4.1.1.73	tartrate decarboxylase	1.00E-138	M
PGA1_c17990		1.1.1.93	tartrate dehydrogenase	1.00E-138	M
PGA1_c17990		1.1.1.83	*D*-malate dehydrogenase (decarboxylating)	3.00E-142	M
PGA1_c27490	*gap*	1.2.1.12	glyceraldehyde-3-phosphate dehydrogenase	1.00E-155	

Danksagung

Zur Entstehung dieser Arbeit haben viele Personen beigetragen, bei denen ich mich an dieser Stelle herzlich bedanken möchte. Zunächst möchte ich mich bei meinen Mentor Herrn Prof. Dr. Dietmar Schomburg bedanken, an diesem spannenden Thema arbeiten zu dürfen, sowie für die hilfreichen Diskussionen in allen Phasen dieser Arbeit. Außerdem danke ich Herrn Prof. Dr. Ralf Rabus für die Übernahme des Zweitgutachtens und die fachliche Unterstützung meiner Arbeit. Bei Herrn Prof. Dr. Dieter Jahn möchte ich mich für die Übernahme des Vorsitzes der Prüfungskommission bedanken.

Ein großer Dank gebührt meinen Kooperationspartnern aus der Arbeitsgruppe von Prof. Rabus für die gute Zusammenarbeit an *Phaeobacter*, insbesondere danke ich Dr. Hajo Zech, Dr. Katharina Wiegmann und Sebastian Koßmehl für die Bereitstellung von Proben und die fachlichen Diskussionen. PD Dr. Jörn Petersen und seinem Team danke ich für die Bereitstellung der Plasmid-cured *Phaeobacter* Stämme.

Weiterhin möchte ich mich bei Dr. Meina Neumann-Schaal für das Korrekturlesens meiner Arbeit bedanken. Christian Nieke danke ich für die Weiterentwicklung des MetaboliteDetectors. Zudem danke ich Sabine Kaltenhäuser für die unermüdliche Instandhaltung der GC-MS Systeme, sowie Katrin Müller für die Analyse der Coenzym A Derivate. Für die vielen Diskussionen zur Klärung Roseobacter-spezifischen Fragestellungen möchte ich mich insbesondere bei Nelli Bill, Sarah Kleist, Sabine Will und Dr. Kerstin Schmidt-Hohagen bedanken.

Ein großer Dank gebührt allen aktuellen und ehemaligen Mitarbeitern der Arbeitsgruppe, insbesondere dem Laborteam für die gute Atmosphäre, fachlichen Diskussionen und Hilfestellung, sowie der sozialen Zerstreuung.

Zuletzt möchte ich mich bei meiner Familie und meinen Freunden für die Unterstützung und Motivation während meiner Doktorarbeit danken. Meinen Bruder Martin danke ich für die Bereitschaft Teile meiner Arbeit Korrektur zu lesen.